



ALUMIDE® TOOLING FOR LIMITED PRODUCTION PLASTIC INJECTION MOULDING

JACQUES COMBRINCK

Thesis submitted in fulfilment of the requirements of the degree

DOCTOR OF ENGINEERING: MECHANICAL

in the

Department of Mechanical and Mechatronics Engineering
Faculty of Engineering and Information Technology

at

Central University of Technology, Free State

Promotor: Dr JG van der Walt (D Tech: Mechanical Engineering)

Co-promotor: Prof DJ de Beer (D Tech: Mechanical Engineering)

Co-promotor: Mr GJ Booyesen (M Tech: Mechanical Engineering)

Bloemfontein

2018

DECLARATION

I, JACQUES COMBRINCK (ID number), (Student number), do hereby declare that this research project submitted to Central University of Technology, Free State for the Degree **DOCTOR OF ENGINEERING: MECHANICAL**, is my own independent work; and complies with the Code of Academic Integrity, as well as other relevant policies, procedures, rules and regulations of Central University of Technology, Free State; and has not been submitted before to any institution by me or any other person in fulfilment (or partial fulfilment) of the requirements for the attainment of any qualification.



SIGNATURE OF STUDENT

10 May 2018

DATE

ABSTRACT

Existing techniques for the production of conventional steel tooling for plastic injection moulding are expensive and time consuming. The result is that many new products often do not advance beyond the prototype stage. This thesis describes an investigation into the possibility of using laser-sintered Alumide[®] (an aluminium-filled polyamide material) in a novel approach as an alternative process for producing rapid tooling inserts for the injection moulding process.

Alumide[®] material properties and process parameters, such as heat capacity, accuracy and surface roughness, required for injection moulding applications, were examined. To reduce internal stresses during the manufacturing process of Alumide[®] inserts, which could result in warpage, the inserts need to be shelled. For shelled inserts to withstand the injection pressures occurring during an injection moulding cycle, they need to be backfilled. A suitable backfilling material as well as a suitable wall thickness for the shelled Alumide[®] inserts was determined.

Injection moulding trials conducted with Alumide[®] inserts showed that conformal cooling channels inside the inserts have an influence on the cooling of the inserts. During the trials, cooling channels underneath the cavities of the Alumide[®] inserts collapsed due to injection pressures of the molten polymer. To prevent cooling channels from collapsing during an injection moulding cycle, a suitable distance between the cavity surface and a cooling channel was ascertained.

To determine the durability of Alumide[®] inserts for the injection moulding process, a geometrical product was developed and Alumide[®] inserts were manufactured for injection moulding trials. Two hundred geometrical parts were manufactured from Alumide[®] inserts using Polypropylene (PP) and Acrylonitrile-Butadiene-Styrene (ABS) with minimal wear on the inserts. Injection moulding trials conducted with Polycarbonate (PC) and Polyamide 6 (PA 6) resulted in significant wear during the first few injection moulding cycles. From these trials, it was concluded that polymer materials with process parameters similar to PP and ABS can be used with Alumide[®] inserts for the injection moulding process.

A limited production run for an electrical enclosure was conducted with Alumide[®] inserts. Two sets of inserts were manufactured and injection mould trials with PP and ABS were

conducted. Two hundred parts were manufactured from each set of inserts using PP and ABS, without significant wear to the inserts. Production with the ABS material was continued and 2500 parts were manufactured from the Alumide[®] inserts with deformation occurring to the fixed side insert (cavity) and minimal wear to the moving side insert (punch).

A manufacturing cost and time comparison between Alumide[®] inserts, tool steel and aluminium inserts (manufactured through conventional manufacturing techniques), additive manufactured inserts (through the Direct Metal Laser Sintering (DMLS) and PolyJet processes) and parts manufactured directly from additive manufacturing processes (rapid manufacturing), were conducted. From the comparisons, it was evident that Alumide[®] inserts are the most cost-effective manufacturing process to produce limited run plastic injection moulded parts.

*I dedicate this work to my daughter, Annabelle,
who is the joy of my life.*

*I also thank our Lord for providing me with the
strength and perseverance to complete this work.*

ACKNOWLEDGEMENTS

I wish to acknowledge the following persons and institutions for their contributions whilst I was working on this research project:

- Funding support from the South African Research Chairs Initiative of the Department of Science and Technology and National Research Foundation of South Africa (Grant № 97994) and the Collaborative Program in Additive Manufacturing (Contract № CSIR-NLC-CPAM-15-MOA-CUT-01).
- I wish to express my gratitude to my promoters for their endless support and guidance I received during this research project.
- The staff of the Centre for Rapid Prototyping and Manufacturing (CRPM) for their support during the research project.
- Hanren Precision Engineering for their assistance during the injection moulding trials.
- My colleagues at the Mechanical and Mechatronics Engineering Department of Central University of Technology, Free State for their support and interest in my progress during the project.
- Lastly, to my wife and family – for all the encouragement and support I received from them during the project.

PUBLICATIONS

J. Combrinck; G.J. Booysen; J.G. van der Walt; D.J. de Beer, Limited run production using Alumide® tooling for the plastic injection moulding process, South African Journal for Industrial Engineering. vol.23 no.2, Pretoria, 2012.

Table of Contents

DECLARATION.....	i
ABSTRACT	ii
ACKNOWLEDGEMENTS.....	v
PUBLICATIONS.....	vi
LIST OF TABLES	x
LIST OF FIGURES.....	xi
ABBREVIATIONS	xvii
1 INTRODUCTION	1
1.1 Introduction	1
1.2 Problem statement	2
1.3 Aim of study	2
1.4 Hypothesis	3
1.5 Objectives	3
1.6 Methodology.....	3
1.7 Limitations of study.....	5
1.8 Original contribution to the field of study	5
1.9 Flow diagram of study	6
2 PRODUCT DEVELOPMENT	7
2.1 Introduction	7
2.2 Drive behind product development.....	7
2.2.1 Increased global competition	8
2.3 Plastic product development	8
2.4 Classification of plastics	10
2.5 Thermoplastic product development process.....	13
2.5.1 Thermoplastic product design process	13
2.6 Injection mould development process	16
2.7 Manufacturing of plastic injection moulds.....	19
2.8 Injection moulding process.....	20
2.8.1 Injection moulding machine	21
2.8.2 Injection moulding cycle.....	22
2.9 Conclusion	25
3 ADDITIVE MANUFACTURING AND RAPID TOOLING	26

3.1	Introduction	26
3.2	AM workflow	26
3.2.1	Creation of a 3D CAD model	27
3.2.2	Conversion of CAD model to a STL file format	27
3.2.3	Pre-processing of an STL file.....	28
3.2.4	Construction of physical part.....	29
3.2.5	Cleaning and finishing of the AM part	29
3.3	AM technologies.....	29
3.3.1	SLS process	31
3.4	AM applications	32
3.5	AM advantages and limitations	33
3.6	Rapid tooling	34
3.7	RT techniques	35
3.7.1	Indirect tooling	35
3.7.2	Direct tooling.....	36
3.7.3	RT advantages and limitations.....	38
3.8	Hybrid tooling	42
3.9	Applications of RT and hybrid tooling	43
3.10	Alumide® as an RT alternative	44
3.11	Conclusion	45
4	EXPERIMENTAL APPROACH AND RESULTS	46
4.1	Introduction	46
4.2	Phase 1: Alumide® material properties and process parameters	47
4.2.1	Alumide® tensile strength.....	47
4.2.2	Specific heat capacity of Alumide®	50
4.2.3	Accuracy of Alumide® products	51
4.2.4	Surface roughness of Alumide® products	54
4.3	Phase 2: Mould preparation for injection moulding trials	57
4.3.1	Steel bolster preparation.....	58
4.3.2	Alumide® insert preparation	59
4.3.3	Backfilling of Alumide® inserts.....	65
4.3.4	Machining of Alumide® inserts.....	66
4.3.5	Mould assembly.....	67
4.4	Phase 3: Injection moulding trials.....	69
4.4.1	Draft angle experiment	70

4.4.2	Geometrical mould experiment.....	73
4.4.3	Cooling channel experiments.....	78
4.4.4	Geometrical experiment with oval cooling channels	88
4.4.5	Geometrical V2 experiment	91
5	CASE STUDY: INDUSTRIAL APPLICATION OF ALUMIDE® INSERTS	123
5.1	Enclosure mould.....	123
5.1.1	Procedure	124
5.1.2	Results.....	128
5.1.3	Discussion	139
5.2	Comparisons between different manufacturing processes.....	141
5.2.1	Time and cost comparison of geometrical parts	142
5.2.2	Time and cost comparison of enclosure parts	144
5.2.3	Time and cost comparison of tractor wheel parts	146
5.2.4	Discussion	149
6	CONCLUSION AND FUTURE WORK.....	150
6.1	Conclusions and recommendations	150
6.2	Future work	156
	REFERENCES.....	158

LIST OF TABLES

<i>Table 3.1 Summary of properties of some direct and indirect rapid tooling techniques [91].</i>	40
<i>Table 3.2 Comparison between RT and conventional mould-manufacturing techniques [34, 89].</i>	43
<i>Table 3.3 Material properties of Alumide® [108].</i>	45
<i>Table 4.1 UTS results obtained from Alumide® tensile test pieces.</i>	49
<i>Table 4.2 Surface roughness of Alumide® test products after polishing and machining operations.</i>	56
<i>Table 4.3 Time and cost comparisons between solid and shelled Alumide® parts.</i>	60
<i>Table 4.4 Properties of the possible backfilling materials.</i>	61
<i>Table 4.5 Deviation of the measuring points for different wall thickness test pieces.</i>	64
<i>Table 4.6 Deviation between the scan and the CAD data of Alumide® inserts with cooling channels 3 to 8 mm from the cavity surface.</i>	84
<i>Table 4.7 Deviation between the scan and CAD data of Alumide® inserts with cooling channels 5 to 10 mm from the cavity surface.</i>	86
<i>Table 4.8 SIGMASOFT® simulations results for the heat removed and maximum mould temperatures of an Alumide® insert with oval and round cooling channels.</i>	87
<i>Table 4.9 Injection moulding process parameters used during the manufacturing of geometrical parts from PP.</i>	96
<i>Table 4.10 Injection moulding process parameters used during the manufacturing of geometrical parts from ABS.</i>	100
<i>Table 4.11 Injection moulding process parameters used during the manufacturing of geometrical parts from PC.</i>	106
<i>Table 4.12 Injection moulding process parameters used during the manufacturing of geometrical parts from PA 6.</i>	113
<i>Table 5.1 Injection moulding process parameters used during the manufacturing of enclosure parts from PP.</i>	128
<i>Table 5.2 Injection moulding process parameters used during the manufacturing of enclosure parts from ABS.</i>	132
<i>Table 5.3 Time and cost comparison of different manufacturing techniques and the cost per product for geometrical parts.</i>	142
<i>Table 5.4 Time and cost comparison of different manufacturing techniques and the cost per product for the enclosure part.</i>	144
<i>Table 5.5 Time and cost comparison for different manufacturing techniques and the cost for 200 sets of the tractor wheel parts.</i>	147
<i>Table 5.6 Cost comparison of the different manufacturing techniques to produce 1000 parts.</i>	149
<i>Table 6.1 Alumide® design rules for limited IM production runs.</i>	155

LIST OF FIGURES

Figure 1.1 Flowchart of the composition of the thesis. _____	6
Figure 2.1 Reduction in different product's life cycles during the past fifty years [12]. _____	7
Figure 2.2 Global and European plastic production from 2007 to 2016 [21]. _____	9
Figure 2.3 Plastic material consumption in South Africa from 2005 to 2016 [22]._____	10
Figure 2.4 Classification of plastics [25]._____	11
Figure 2.5 Product geometries adjusted for the different thermoplastic materials to obtain the same strength [32]. _____	14
Figure 2.6 Schematic illustration of the product development process adapted from [15]. _____	15
Figure 2.7 Flow chart of the mould design process adapted from [38]. _____	17
Figure 2.8 Main components of a typical injection mould. _____	18
Figure 2.9 Three axis CNC milling machine. _____	19
Figure 2.10 A typical plunge EDM machine with its main components. _____	20
Figure 2.11 Main components of an injection moulding machine. _____	21
Figure 2.12 Plasticisation of the polymer melt from solid granules or pellets. _____	22
Figure 2.13 Injection and packing of mould cavities. _____	24
Figure 2.14 Ejection stage of the plastic part. _____	24
Figure 3.1 Flow diagram of the AM manufacturing workflow. _____	26
Figure 3.2 An STL file representation of a CAD model, showing the triangular facets. _____	27
Figure 3.3 AM process categories based on the classification by the ASTM F42 Technical Committee and the state of the unprocessed material. _____	30
Figure 3.4 Schematic of the Selective Laser Sintering process. _____	32
Figure 3.5 Stair step effect on curved and inclined surfaces on AM parts. _____	34
Figure 4.1 Representation of the four-phased approach to determine the feasibility of Alumide® inserts for injection moulding applications. _____	46
Figure 4.2 Schematic representation of experiments conducted during Phase 1. _____	47
Figure 4.3 Different build orientations used to manufacture tensile test pieces in Alumide®. _____	48
Figure 4.4 MTS Criterion™ Model 43 tensile testing machine used to conduct the tensile testing of the Alumide® test pieces. _____	48
Figure 4.5 Heat capacity values of Alumide® at different temperatures showing the extrapolated intersection point from the baseline curves. _____	51
Figure 4.6 Accuracy results of a cranio-plate press tool prototype. _____	52
Figure 4.7 Accuracy results of a female half of a press tool. _____	53
Figure 4.8 Accuracy results of the male half of a press tool. _____	53
Figure 4.9 Comparison of the stair step effect on a surface with a 1° and 45° incline. _____	54
Figure 4.10 Products used during the surface roughness experiment, (A) 3° surface angle and (B), 45° surface angle. _____	55
Figure 4.11 Position and direction of surface roughness measurements taken on the surface angle of the test products. _____	56

Figure 4.12 Schematic representation of Phase 2. _____	58
Figure 4.13 Dimensions and components of the steel bolster used during the IM trials. _____	58
Figure 4.14 Mould components of the steel bolster with machined pockets, O-ring grooves and ejector pin holes. _____	59
Figure 4.15 Unfilled Alumide® test pieces with varying wall thicknesses. _____	63
Figure 4.16 Test pieces filled with EPO 4030 with measuring points indicated. _____	64
Figure 4.17 Location of the measuring points on the test pieces. _____	64
Figure 4.18 Shelled Alumide® insert showing the rib feature along the cavity and internal features. _____	65
Figure 4.19 Backfilled Alumide® insert showing the formation of air bubbles on the surface. _____	66
Figure 4.20 Alumide® insert with machined rear and outer surfaces as well as drilled and reamed ejector pin holes. _____	67
Figure 4.21 Assembled Alumide® inserts and steel bolster with temperature probes connected. _____	68
Figure 4.22 Portable computer with DAQ interface software connected to the temperature probes. _____	68
Figure 4.23 Schematic representation of experiments conducted during Phase 3. _____	69
Figure 4.24 Dimensions and CAD model of the draft angle part used in the draft angle mould experiment. _____	71
Figure 4.25 Alumide® inserts with four draft angle parts in each insert. _____	71
Figure 4.26 Shelled Alumide® insert with a conformal cooling channel. _____	72
Figure 4.27 CAD representation of a conformal cooling channel showing the centre line radius of 9 mm used to assist with the un-sintered powder removal. _____	72
Figure 4.28 Wear on the gate features which deliver molten material to the cavities during an IM cycle. _	73
Figure 4.29 Dimensions and CAD model of the different geometrical features included in the part to be manufactured. _____	74
Figure 4.30 Layout of the conformal cooling channels avoiding mould features such as screw and ejector pin holes. _____	75
Figure 4.31 Stair step effect visible on the geometrical features of the Alumide® insert in the as-built form. _____	76
Figure 4.32 Polished Alumide® inserts. _____	76
Figure 4.33 Sectioned Alumide® insert indicating the deformation of the cavity surface onto the cooling channels. _____	77
Figure 4.34 Drawings of the rectangular parts used to determine the optimal distance a cooling channel needs to be positioned from a cavity surface. _____	78
Figure 4.35 An Alumide® insert showing the arrangement of the three rectangular parts and the conformal cooling channel. _____	79
Figure 4.36 Layout of the fixed and moving halves of the Alumide® inserts with Ø 8 mm conformal cooling channels placed at 3, 4, 5, 6, 7 and 8 mm respectively, from a cavity surface. _____	79
Figure 4.37 Layout of the fixed and moving halves of the Alumide® inserts with oval cooling channels placed at 3, 4, 5, 6, 7 and 8 mm respectively from the cavity surface. _____	80
Figure 4.38 Location of heat sensing probes inside the fixed and moving halves of Alumide® inserts. _____	81

<i>Figure 4.39 Mould temperature graph for the moving insert with cooling water interruption.</i>	81
<i>Figure 4.40 Mould temperature graph for the fixed insert with cooling water interruption.</i>	82
<i>Figure 4.41 Ruptured surface of the round cooling channel 3 mm from the surface (A) and the deformed surface of the cavity with a cooling channel 4 mm from the surface (B).</i>	83
<i>Figure 4.42 Results of a comparison between scan data and the CAD file of an insert indicating the maximum deformation of the cavity surface.</i>	83
<i>Figure 4.43 Deformed surface of a cavity with an oval cooling channel 3 mm (A) and 4 mm from the surface (B).</i>	84
<i>Figure 4.44 Layout of the redesigned fixed and moving halves of Alumide® inserts with a 8 mm diameter conformal cooling channels placed at 5, 6, 7, 8, 9 and 10 mm, respectively from the cavity surfaces.</i>	85
<i>Figure 4.45 Layout of the redesigned fixed and moving halves of Alumide® inserts with oval cooling channels placed at 5, 6, 7, 8, 9 and 10 mm respectively, from the cavity surfaces.</i>	85
<i>Figure 4.46 Model used during the heat flow simulation with varying distance of the round and oval cooling channels from the cavity.</i>	87
<i>Figure 4.47 Positions of Alumide® pin features broken off during the IM trial.</i>	89
<i>Figure 4.48 Wear of geometrical features close to the injection point.</i>	90
<i>Figure 4.49 Results of the SIGMASOFT® flow analysis for the geometrical part showing the flow path of the molten material during the filling of the mould cavity.</i>	91
<i>Figure 4.50 Dimensions and CAD model of the redesigned geometrical part.</i>	92
<i>Figure 4.51 Results of the SIGMASOFT® flow analysis for the redesigned geometrical part showing the flow path of the molten material during the filling of the mould cavity.</i>	93
<i>Figure 4.52 Layout of the oval conformal cooling channels avoiding insert features such as screw and ejector pin holes.</i>	93
<i>Figure 4.53 Insert features where the maximum temperatures occur for the fixed (A) and moving (B) Alumide® inserts after the 20th IM cycle, according to SIGMASOFT® virtual moulding software.</i>	94
<i>Figure 4.54 Stair step effect visible on features of the redesigned geometrical insert in the as-built form of the fixed and moving inserts.</i>	95
<i>Figure 4.55 Machined and polished Alumide® insert with steel pins for producing hole features.</i>	95
<i>Figure 4.56 Fixed half of the Alumide® insert after 200 IM cycles using PP.</i>	96
<i>Figure 4.57 Temperatures of the fixed half Alumide® insert using PP after the 20th IM cycle, according to SIGMASOFT® virtual moulding software.</i>	97
<i>Figure 4.58 Moving half of the Alumide® insert after 200 IM cycles using PP. Figures A and B are enlargements of the encircled regions of the insert.</i>	98
<i>Figure 4.59 Temperatures of the moving half Alumide® insert using PP after the 20th IM cycle, according to SIGMASOFT® virtual moulding software.</i>	99
<i>Figure 4.60 Text features and knife-edge corners without any wear after 200 IM cycles using PP.</i>	99
<i>Figure 4.61 Scan results of the moving and fixed Alumide® inserts after 200 IM cycles using PP.</i>	100
<i>Figure 4.62 Fixed half of the Alumide® insert after 200 IM cycles using ABS.</i>	101

<i>Figure 4.63 Temperatures of the fixed half Alumide® insert using ABS after the 20th IM cycle, according to SIGMASOFT® virtual moulding software.</i>	101
<i>Figure 4.64 Moving half of the Alumide® insert after 200 IM cycles using ABS. Figures A and B are enlargements of the encircled regions of the insert.</i>	102
<i>Figure 4.65 Temperatures of the moving half Alumide® insert using ABS after the 20th IM cycle, according to SIGMASOFT® virtual moulding software.</i>	103
<i>Figure 4.66 Sectioned view of a CAD model showing the wear of the mould feature as well as the location of the measured, reference and wear values of the IM part.</i>	103
<i>Figure 4.67 Wear of the uncooled insert feature from the first to the 200th IM cycle.</i>	104
<i>Figure 4.68 Insert temperatures of the moving half Alumide® insert during the 6th (A) and 7th (B) IM cycle, according to SIGMASOFT® virtual moulding software.</i>	105
<i>Figure 4.69 Text features and knife-edge corners without any wear after 200 IM cycles using ABS.</i>	105
<i>Figure 4.70 Scan results of the moving and fixed Alumide® inserts after 200 IM cycles using ABS.</i>	106
<i>Figure 4.71 Fixed half of the Alumide® insert after 180 IM cycles using PC. Figures A and B are enlargements of the encircled regions of the insert.</i>	107
<i>Figure 4.72 Temperatures of the fixed half Alumide® insert using PC after the 5th IM cycle, according to SIGMASOFT® virtual moulding software.</i>	108
<i>Figure 4.73 Graphical representation of the wear progression of a geometrical feature from the fixed half of the Alumide® insert from an IM trial with PC material.</i>	109
<i>Figure 4.74 Moving half of the Alumide® insert after 180 IM cycles using PC. Figures A and B are enlargements of the encircled regions of the insert.</i>	110
<i>Figure 4.75 Temperatures of the moving half Alumide® insert using PC after the 5th IM cycle, according to SIGMASOFT® virtual moulding software.</i>	111
<i>Figure 4.76 Graphical representation of the wear progression of geometrical features from the moving half of the Alumide® insert from an IM trial with PC material.</i>	112
<i>Figure 4.77 Wear occurring on text features and knife-edge corners after 180 IM cycles with PC material.</i>	113
<i>Figure 4.78 Fixed half of the Alumide® insert after 150 IM cycles using PA 6. Figures A and B are enlargements of the encircled regions of the insert.</i>	114
<i>Figure 4.79 Temperatures of the fixed half Alumide® insert using PA6 after the 10th IM cycle, according to SIGMASOFT® virtual moulding software.</i>	115
<i>Figure 4.80 Alumide® material bonded to the polyamide 6 and torn from the Alumide® insert during the ejection of the part.</i>	116
<i>Figure 4.81 Graphical representation of the wear progression of a geometrical feature from the fixed half of the Alumide® insert from an IM trial with PA 6 material.</i>	117
<i>Figure 4.82 Moving half of the Alumide® insert after 150 IM cycles using PA 6. Figures A and B are enlargements of the encircled regions of the insert.</i>	118
<i>Figure 4.83 Temperatures of the moving half Alumide® insert using PA6 after the 10th IM cycle, according to SIGMASOFT® virtual moulding software.</i>	119

<i>Figure 4.84 Graphical representation of the wear progression of a geometrical feature from the moving half of the Alumide® insert from an IM trial with PA 6 material.</i>	120
<i>Figure 4.85 Wear of text features and knife-edge corners after 150 IM cycles with PA 6 material.</i>	121
<i>Figure 5.1 Schematic representation of Phase 4.</i>	123
<i>Figure 5.2 Dimensions and CAD model of the enclosure part.</i>	124
<i>Figure 5.3 CAD models of the Alumide® inserts consisting of a single part cavity.</i>	124
<i>Figure 5.4 Conformal cooling channel design for the enclosure inserts avoiding mould features such as screw and ejector pin holes.</i>	125
<i>Figure 5.5 Geometrical features of the moving half insert with temperatures more than the melting temperature of Alumide®.</i>	126
<i>Figure 5.6 Stair step effect visible on features of enclosure insert in the as-manufactured form. A and B show the stair step effect on the fixed insert and C and D on the moving inserts.</i>	127
<i>Figure 5.7 Machined and polished enclosure insert with ejector pin holes and steel pins inserted for the manufacturing of hole features.</i>	127
<i>Figure 5.8 Positions of the four points where measurements were taken on the enclosure parts.</i>	128
<i>Figure 5.9 Alumide® inserts after 200 IM cycles using PP. C and D show the features where wear occurred.</i>	129
<i>Figure 5.10 Temperatures of the moving half enclosure insert using PP material after the 20th IM cycle, according to SIGMASOFT® virtual moulding software.</i>	130
<i>Figure 5.11 Wall thickness deviation of enclosure parts manufactured from Alumide® inserts using PP.</i>	130
<i>Figure 5.12 Temperatures of the fixed half enclosure insert using PP material after the 20th IM cycle, according to SIGMASOFT® virtual moulding software.</i>	131
<i>Figure 5.13 Scan results of the fixed (A) and moving (B) Alumide® inserts after 200 IM cycles using PP.</i>	132
<i>Figure 5.14 Alumide® inserts after 200 IM cycles using ABS. Figures A to D show the features where wear occurred.</i>	133
<i>Figure 5.15 Temperatures of the moving half enclosure insert using ABS material after the 20th IM cycle, according to SIGMASOFT® virtual moulding software.</i>	134
<i>Figure 5.16 Graphical representation of the wear progression from 5th to the 200th IM cycle.</i>	135
<i>Figure 5.17 Fixed half of the Alumide insert showing the delamination of the cavity surface after 2500 IM cycles using ABS.</i>	136
<i>Figure 5.18 Wall thickness deviation of enclosure parts manufactured from Alumide® inserts using ABS.</i>	136
<i>Figure 5.19 Temperatures of the fixed half enclosure insert using ABS material after the 20th IM cycle, according to SIGMASOFT® virtual moulding software.</i>	137
<i>Figure 5.20 Graphical representation of the wear progression from 200th to the 2500th IM cycle.</i>	138
<i>Figure 5.21 Scan results of the fixed (A) and moving (B) Alumide® inserts after 2500 IM cycles using ABS.</i>	139
<i>Figure 5.22 Holes on the cavity surface of the Alumide® insert causing a coarse surface finish on the parts manufactured from ABS and PP.</i>	140

Figure 5.23 Magnified image (150 magnification) of laser-sintered Alumide® material showing the aluminium particles enclosed by the polyamide material. _____ 140

Figure 5.24 The aluminium particles and polyamide material, as manufactured by AM techniques (A), and after machining operations on the Alumide® surface (B). _____ 141

Figure 5.25 Cost comparison for the different manufacturing processes to manufacture one to two hundred geometrical parts. _____ 143

Figure 5.26 Break-even plot between Alumide® and RM manufacturing processes for the geometrical part. _____ 144

Figure 5.27 Cost comparison for the different manufacturing processes to manufacture one to two hundred enclosure parts. _____ 145

Figure 5.28 Break-even plot between Alumide® and RM manufacturing processes for the enclosure part. _____ 146

Figure 5.29 Dimensions and CAD model of the tractor wheel components used in the time and cost comparison. _____ 147

Figure 5.30 Cost comparison for the different manufacturing processes to manufacture one to two hundred sets of tractor wheel parts. _____ 148

Figure 5.31 Break-even plot between Alumide® and RM manufacturing processes for the tractor wheel part. _____ 148

ABBREVIATIONS

2D:	Two-dimensional
3D:	Three-dimensional
ABS:	Acrylonitrile-Butadiene-Styrene
AM:	Additive Manufacturing
ASA:	Acrylic-styrene-acrylonitrile
ASTM:	American Society for Testing and Materials
CAD:	Computer Aided Design
CNC:	Computer Numerical Control
CRPM:	Centre for Rapid Prototyping and Manufacturing
CSIR:	Council for Scientific and Industrial Research
CUT:	Central University of Technology, Free State
DMLS:	Direct Metal Laser Sintering
DSC:	Differential Scanning Calorimetry
EDM:	Electro Discharging Machining
EOS:	Electro Optical Systems GmbH
HDPE:	High Density Polyethylene
HIPS:	High Impact Polystyrene
HSM:	High Speed Machining
IM:	Injection moulding
LS:	Laser sintering
PA:	Polyamide
PC:	Polycarbonate
PE:	Polyethylene
POM:	Polyoxymethylene (Acetal)
PP:	Polypropylene
PS:	Polystyrene
PVC:	Polyvinylchloride
RM:	Rapid Manufacturing
RT:	Rapid Tooling
RTV:	Room Temperature Vulcanized
SAN:	Styrene-Acrylonitrile
STL:	Standard Triangulation Language
SLS:	Selective Laser Sintering
TPE:	Thermoplastic Elastomers
TPE-A:	Thermoplastic Polyamide Elastomers
TPE-O:	Thermoplastic Polyolefin Elastomers
TPE-S:	Styrenic Thermoplastic Elastomers
TPE-V:	Thermoplastic Vulcanisation Elastomers
UTS:	Ultimate Tensile Strength
UV:	Ultraviolet

1 INTRODUCTION

1.1 Introduction

Product development is a set of activities that transforms a concept into a product or service that is usable for the marketplace. Innovative companies use product development to increase demand or even create entirely new markets through innovative product design. In today's technology-driven marketplace, new products are essential for the survival of a company [1]. The complete process of developing a new product is filled with uncertainties and the risks involved are substantial. New product development seems to be widely acknowledged as a necessary evil [2].

Almost every product used daily consists of some if not all plastic components. The successful design of plastic products is a challenge for product development teams and contains financial risks to a company. The plastic industry is one of the world's fastest-growing industries, ranked as one of the few billion dollar industries of the world. Plastics have transitioned from a "cheap" alternative for metal and glass to the material of choice, providing unique properties and significant cost savings [3]. The plastic industry is also important in enabling growth in industries such as automotive, aerospace, electrical, electronic, construction, food and beverage.

Most of these plastic parts are produced by the plastic injection moulding (IM) process [4]. For every plastic part to be produced, a mould must be custom-designed and manufactured which can easily cost tens to hundreds or thousands of Rand. This can be several thousand times the unit cost of the plastic part manufactured through the mould. The process of designing and manufacturing a mould as well as the production of the first plastic part can easily take up to 20 weeks. The economical manufacturing of plastic parts depends upon the characteristics of the plastic material and the influence it has on the part design, mould manufacturing and production processes [5].

Due to the high cost of conventional tooling, most new product developments never realise because they are too risky to manufacture. When conventional tooling is removed from the equation, it becomes more feasible to introduce new products in small quantities which can then be used to investigate their possible market potential [6]. The design to production time for new components continues to decrease, thus the long lead times of manufacturing

production tooling conventionally becomes an obstacle in responding to customer demands [7]. This has led to the development of Rapid Tooling (RT) technologies. RT is based on Additive Manufacturing (AM) technologies for quickly manufacturing prototypes or production tooling inserts directly from Computer Aided Design (CAD) data by selectively adding material layer upon layer [8].

1.2 Problem statement

Existing techniques for the production of conventional steel tooling for plastic IM are expensive and in some instances, time consuming. Therefore, many new plastic parts developments do not advance beyond the prototype stage, since product developers do not want to take the risk of investing a large amount of money in IM tooling for a product that may not succeed commercially. A prototype of the product can be produced through AM which can be used for evaluation; however, there are a limited number of materials that can be processed through AM. Sometimes parts need to be manufactured in an end-use material, such as for mechanical testing or clinical trials, which may not be possible through AM. A new RT process needs to be developed that is able to produce a limited number of plastic IM parts at a reduced cost and time in order to evaluate the product before money is invested in conventional steel tooling for production.

1.3 Aim of study

The aim of this research was to investigate the possibility of using Laser Sintering (LS) of Alumide[®] (an aluminium-filled polyamide material) as an alternative process for producing RT inserts. This is a novel use of the material, with initial IM experiments performed by researchers at Central University of Technology (CUT), Free State as early as 2006. It was found that Alumide[®] inserts can be manufactured in about 30% of the time that it will take to produce the same size DMLS inserts, and the material cost of Alumide[®] is about four times less than that of DMLS material. Considering these two factors, it becomes viable to produce the entire product's geometry using only Alumide[®] inserts in bolsters.

1.4 Hypothesis

Alumide[®] can be used successfully as a RT medium in a plastic IM mould. This technique is likely to reduce the cost of tooling for limited production of injection-moulded parts for evaluation purposes.

1.5 Objectives

The objectives for this research study were as follows:

- Conduct a literature review on polymer consumption, the IM process, manufacturing through IM as well as existing AM processes and RT techniques.
- Investigate the mechanical properties of Alumide[®].
- Determine the effect of cooling channels inside an Alumide[®] insert.
- Determine the durability of Alumide[®] inserts in tooling applications.
- Determine the suitability of Alumide[®] inserts for processing different polymer materials through IM.
- Conduct manufacturing time and cost comparisons between Alumide[®], DMLS, PolyJet, and conventionally manufactured inserts as well as parts manufactured through AM.

1.6 Methodology

The methodology to determine if Alumide[®] can be used as a tooling medium for plastic IM was as follows:

- **Determine Alumide[®] material properties and part properties**
Material properties such as mechanical strength and thermal conduction were investigated and verified with experiments. Products manufactured from Alumide[®] were measured and compared to CAD drawings to determine the accuracy of the manufactured components. Surface roughness, due to the stair steps caused by the layer-by-layer manufacturing of the process, was measured and different finishing techniques were compared to improve the surface finish.

- **Investigate suitable shelling thickness and backfill material for Alumide® inserts**

Shelling of the Alumide® insert reduces warpage during the manufacturing process of the insert. It can also reduce the building cost and time to manufacture the insert. During the IM process inserts are subjected to high injection pressures and temperatures as molten material is forced into the mould cavities. The shelled Alumide® inserts need to be backfilled so that they will not collapse when subjected to this injection pressures. A suitable backfill material needed to be identified that could withstand the temperatures and pressures occurring during an IM cycle. An optimal shelling wall thickness that would not deform during the backfilling process and provide sufficient strength and support to internal mould features during the AM manufacturing process had to be determined, while still ensuring that the insert could be manufactured cost-effectively.

- **Effect of cooling channels inside an Alumide® insert**

The effectiveness of a cooling channel inside an IM mould depends upon its ability to transfer heat from the cavity surface to the cooling water flowing through the cooling channel. This depends upon the heat transfer coefficient of the insert material as well as the distance of the cooling channel from the cavity surface. Experiments were conducted to determine the minimum distance a cooling channel needs to be positioned from a cavity surface of an Alumide® insert to prevent deformation during an IM cycle. The heat removed by a cooling channel from a cavity surface was simulated for an Alumide® insert through virtual moulding software.

- **Determine the durability of Alumide® inserts in tooling applications**

IM trials with Alumide® inserts containing different geometrical features were conducted to determine the wear of these features during a production run. The maximum number of parts that could be manufactured from an Alumide® insert was also determined through a production run.

- **Evaluate suitability of Alumide® inserts for processing different polymers through IM**

IM trials were conducted to determine the suitability of Alumide® inserts with polymers which have different processing temperatures and parameters.

- **Evaluate cost and time comparisons**

The differences between the manufacturing costs and time spent manufacturing inserts using conventional methods; DMLS, PolyJet, rapid manufacturing and Alumide[®], were compared to determine the feasibility of Alumide[®] inserts for limited production runs.

1.7 Limitations of study

- Due to the high cost of Alumide[®] powder (R750 per kg), only a limited number of inserts could be produced through the AM process for experimental work.
- Only conformal cooling channels with round and oval geometries with a cross-sectional area the same as an 8 mm diameter cooling channel were used in Alumide[®] inserts during IM trials.
- Due to cost constraints, only PP, ABS, PC and PA 6 IM materials were used during IM trials with Alumide[®] inserts.
- Due to the high cost to scan and compare the Alumide[®] inserts with the CAD models by a 3rd party, only a limited number of scans and comparisons during the study could be conducted.

1.8 Original contribution to the field of study

This research study investigated the novel approach of using Alumide[®], developed for the manufacturing of AM prototypes, as a medium to manufacture IM inserts. With Alumide[®], IM inserts can be produced in a shorter lead time and cheaper than inserts manufactured through conventional manufacturing techniques. This will reduce the cost and time to market of products thus improving the idea to product success rate for new product developments.

1.9 Flow diagram of study

The composition of the thesis is represented in Figure 1.1 through a flowchart.

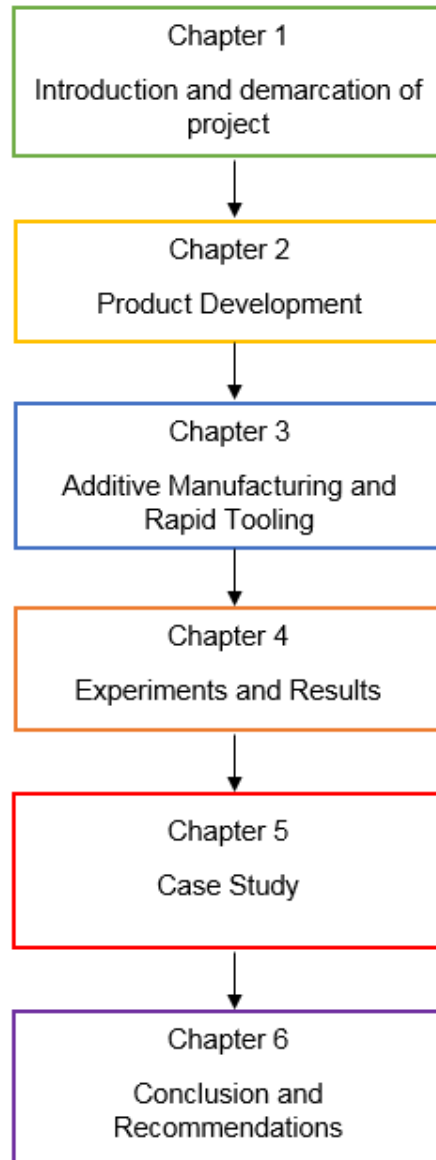


Figure 1.1 Flowchart of the composition of the thesis.

2 PRODUCT DEVELOPMENT

2.1 Introduction

To remain competitive in the marketplace, product development is essential for the survival of a company [9]. A successful new product can result in profits and growth, while an unsuccessful product can lead to market and financial losses to a company [10, 11].

2.2 Drive behind product development

The drive behind new product development can be initiated by the following [12]:

- **Technological advances.** Advances in technology provide an opportunity to improve existing products [13].
- **Changing customers' needs.** The market for products is changing regularly, as the consumers' preferences, needs and wants are changing. Customers expect new products with significant improvements more frequently [14].
- **Shortening product life cycles.** Shortening of a product's life cycle is due to technological advances and changing demands of the market. A product's life cycle has decreased by a factor of about four over the past fifty years, as shown in Figure 2.1. This renders the product obsolete, necessitating a new product development.

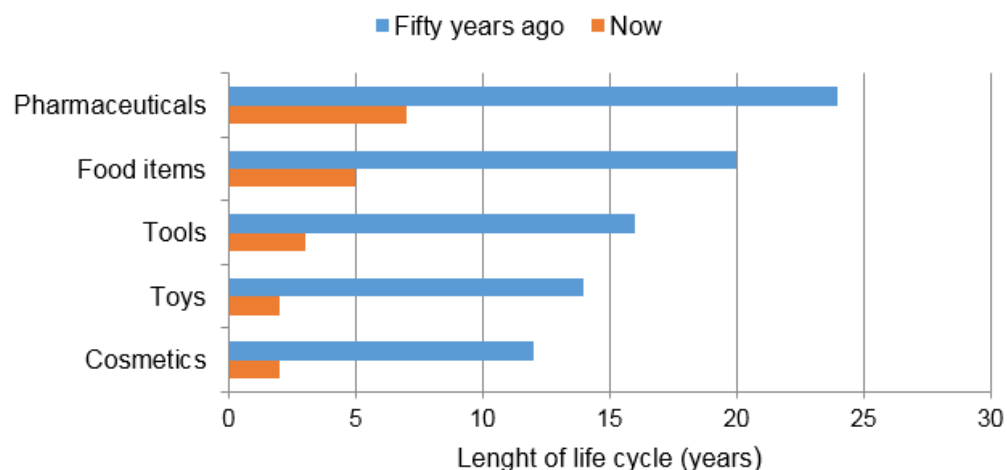


Figure 2.1 Reduction in different product's life cycles during the past fifty years [12].

2.2.1 Increased global competition

The globalisation of markets has created significant opportunities for the product developer but it has also increased the competitiveness in the marketplace. Important factors to be competitive in the market place are speed and change. Markets and technology are changing more rapidly than before. The ability to introduce new products into the market ahead of the competition, within the window of opportunity, is important to be a successful competitor. The main advantages are [12]:

- **Competitive advantage.** The ability to respond to customers' needs and changing markets, faster than the competition, is important to be successful.
- **Fewer surprises.** The ability to respond quickly to market changes should be considered as an opportunity rather than a threat. Reducing the lead times of a product development process decreases the possibility that the market conditions will change as the development proceeds.
- **Higher profitability.** Speed to market may improve a product's success by increasing market acceptance. The quicker a company can launch a new product the more certainty the company has of predicting customer preferences, thus creating a product concept customers find attractive [15].

2.3 Plastic product development

More than 70% of components in consumer products are manufactured using plastic materials [16]. There are more than 120 000 plastic materials available, each with unique material properties [17]. Replacing metallic products with plastic products resulted in an increased demand for engineering plastic materials internationally. Engineering plastics is the fastest growing sector in the plastics industry [18]. More and more applications are being found for the plastics industry to manufacture products compared to traditionally used materials such as steel and aluminium [18]. Since the 1970's, the global production of plastics has increased nearly 9 times compared to 4.5 times for aluminium and 2.5 times for steel [19].

Plastic materials can be used as a suitable replacement for metallic products due to the following characteristics [17]:

- Less weight compared to similar size metallic product.

- Lower material cost.
- Economical mass production [18].
- Specific electrical, isolative features.
- Easier part joining.
- Products can be manufactured with a specific colour during the manufacturing process.
- Corrosion resistance [18].

From 2005 until 2015, global plastic production increased annually. The plastic industry has an important role in the global economy since other industries depend on plastic products to generate income and continue to function. During 2013, the plastic industry was one of the biggest contributors to the European Union manufacturing sector [20]. Global production of plastics during 2016 increased to 335 million tons, a 3.8% increase from 2015 [21]. Figure 2.2 illustrates the European and global plastics production from 2007 to 2016.

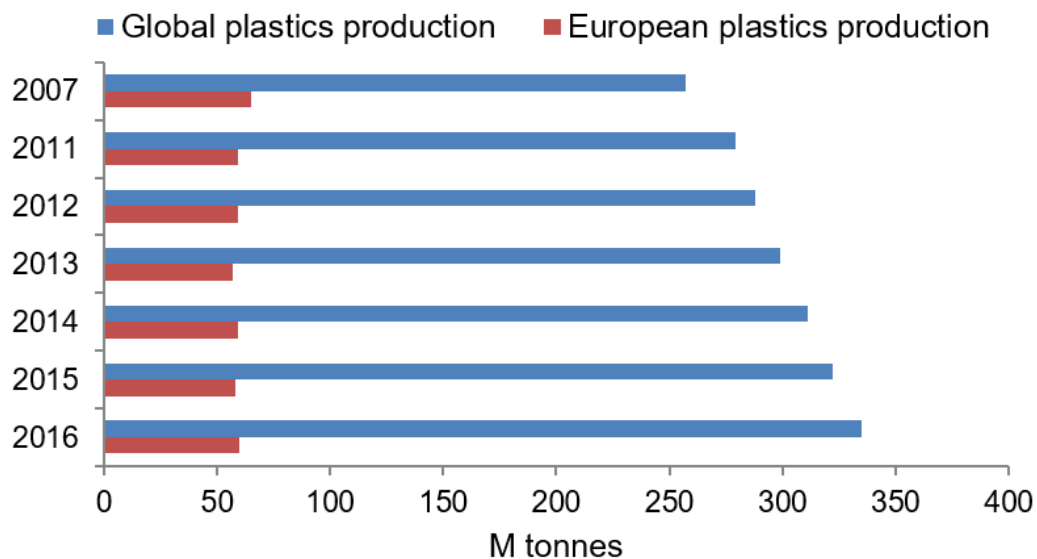


Figure 2.2 Global and European plastic production from 2007 to 2016 [21].

Data released by Plastics South Africa shows that the plastic consumption in South Africa increased at a steady rate from 2005 to 2016. Figure 2.3 indicates the annual consumption of polymer materials in South Africa from 2005 to 2016 [22].

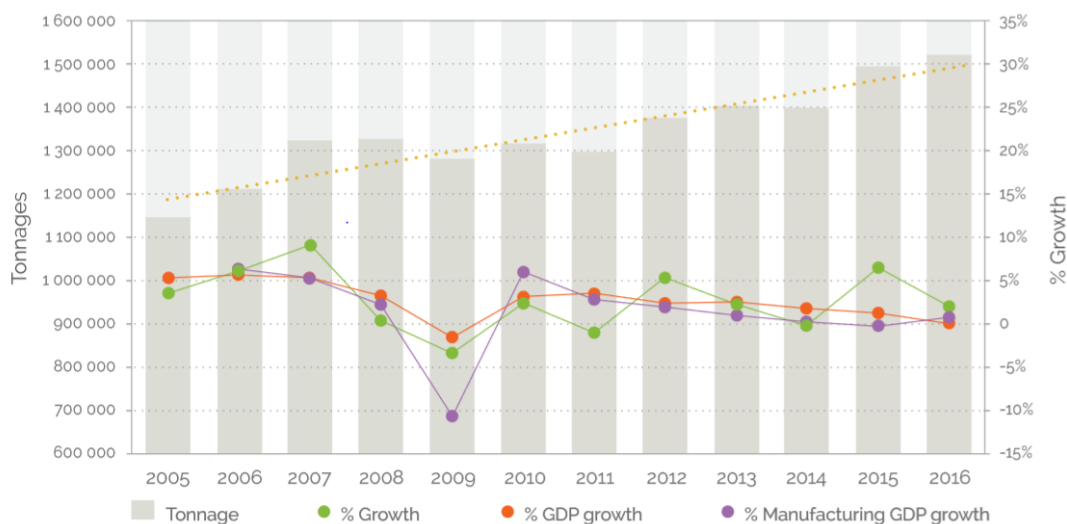


Figure 2.3 Plastic material consumption in South Africa from 2005 to 2016 [22].

2.4 Classification of plastics

Plastics describe a compound of polymers and different additives. Polymers consist of molecules with a high molecular weight. These large molecules are called macromolecules. The macromolecular structures of a polymer are generated synthetically or through natural processes. The basic structure of polymer materials is determined by its macromolecule structure, which consists of a repeating sequence of monomer units. Monomer units consist mainly of carbon (C) and hydrogen (H) atoms. Besides carbon and hydrogen, elements such as nitrogen (N), oxygen (O), sulphur (S), fluorine (F) and chlorine (Cl) can also be found in a monomer unit [23]. The type of element, their placing and proportion in the monomer unit differentiate one polymer material from another, each with its own unique physical and rheological properties.

Additives are added to plastics to alter or improve certain properties such as mechanical, physical or chemical. Examples of additives that can be added are processing stabilisers, ultraviolet (UV) stabilisers, reinforcements, flame retardants and colourants [24].

The macromolecular structures as well as the temperature-dependant physical properties differentiate plastic materials into four main groups, as illustrated by Figure 2.4 [25]:

- Thermoset polymers
- Elastomers
- Thermoplastic polymers
- Polymer compounds

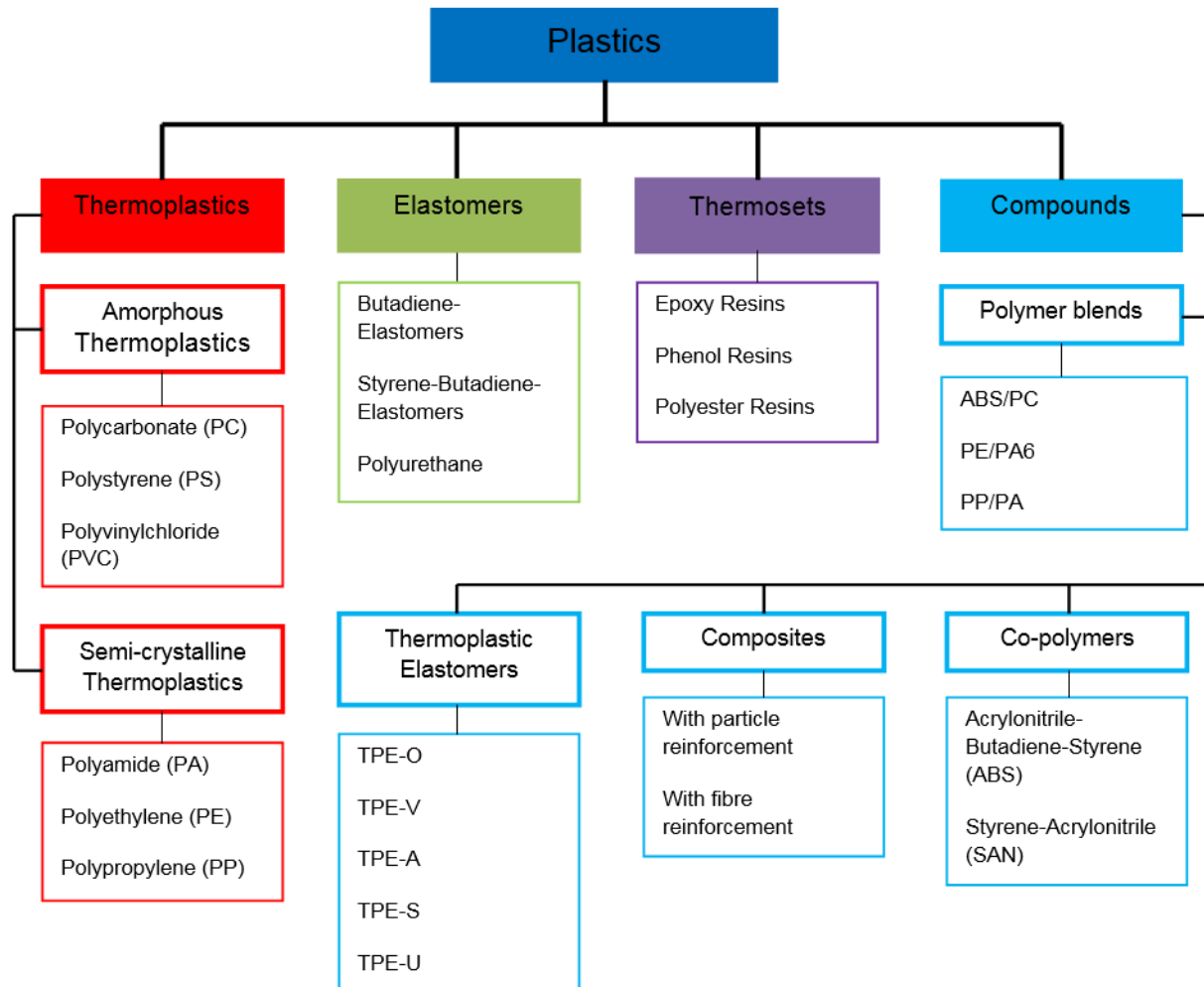


Figure 2.4 Classification of plastics [25].

Thermoset polymers

Thermosets are polymers that chemically react during processing to form irreversible cross-linked bonds between the macromolecular structures. Thermoset polymers are usually stronger than thermoplastic polymers after processing. Thermoset products are formed through a combination of heat and pressure. Due to the cross-linked bond, thermoset product's mechanical strength and elasticity is not temperature dependant, thus it cannot be remelted and reused. A typical application for thermoset products is where high strength and/or high heat resistance as well as chemical resistance are required [26].

Elastomers

Elastomers are plastic materials which consist of wide, netlike, cross-linked bonds between the molecules. Elastomers cannot be remelted without the degradation of the molecular structure. Above the glass transition temperature of an elastomer, the elastomer is soft elastic. Below its glass transition temperature, the elastomer becomes hard elastic to brittle [27].

Polymer compounds

Polymer compounds are composed of different polymers to achieve specific material properties such as high elasticity or fatigue strength [25].

Thermoplastic polymers

Thermoplastic polymers consist of individual polymer chains. These types of polymer soften and flow when heated. While heated, the material can be injected into a mould [28]. The material hardens during a cooling process and retains the shape of the mould it is injected into. Due to this processing characteristic, thermoplastic polymers can be injection moulded and extruded. Because there are not any cross-links created during processing, thermoplastic polymers can be reground and reused [29].

Thermoplastic polymers are also classified by their crystalline or amorphous state. Semi-crystalline and amorphous polymers have different characteristics. Semi-crystalline polymers have more stiffness and increased toughness compared to amorphous polymers. Semi-crystalline polymers have better flow characteristics, which is an advantage when filling thin-walled sections of a mould. Semi-crystalline polymers generally have better chemical resistance, greater stability at higher temperatures and better creep resistance compared to amorphous polymers. Amorphous polymers have better impact strength, less mould shrinkage and part warpage in comparison with crystalline materials [27].

Thermoplastic polymers are the most used polymer material due to their lower cost and relatively lower processing conditions compared to thermoset polymers. More than one third of all thermoplastic materials are injection moulded, and more than half of all polymer processing equipment used are IM machines [5].

2.5 Thermoplastic product development process

The reasons to design products made out of thermoplastic is either to create new products or to create something similar to an existing product which is better and more appealing to the consumer or more economical to produce [30]. Since thermoplastic product design and mould design are inter-dependant, it is necessary for both product and mould design engineers to understand the thermoplastic product development process and the role of mould design and mould making [31].

2.5.1 Thermoplastic product design process

The basic stages for a thermoplastic product design are as follows [32]:

- **Defining end use requirements.** The product development process starts with a complete and thorough definition of the product specifications and the end use requirements.
- **Create preliminary concept.** After the end use requirements for the product have been specified, the product development team will develop initial concept sketches of the product.
- **Material selection.** Material selection is accomplished by choosing a material that is best suited for the end use requirements of the product.
- **Design for the selected material.** Because there are differences in the properties of the individual polymer materials, there will also be a change in the product geometries associated with each of the different materials. Figure 2.5 shows product geometries for three different materials (Polyamide 66 {PA 66}, Polypropylene {PP} and High Density Polyethylene {HDPE}), designed for the same application. Because of the different material properties of the individual materials, the geometry has to be adjusted to obtain the same required strength.

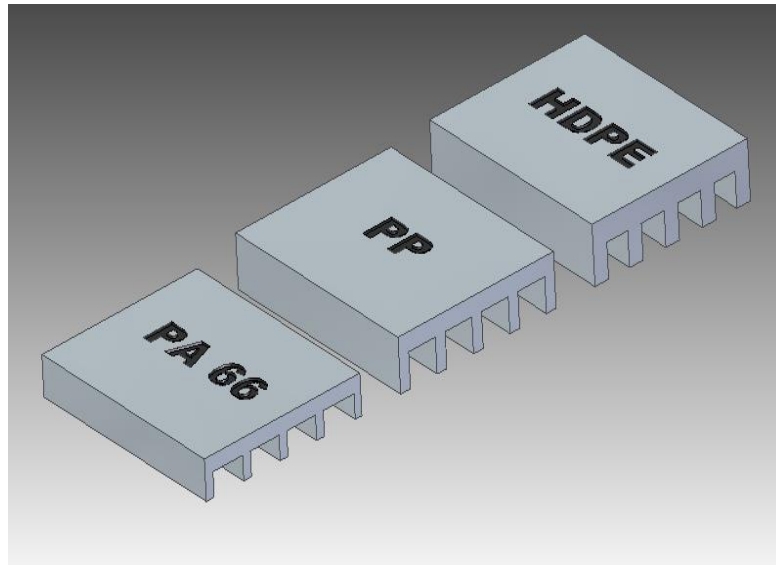


Figure 2.5 Product geometries adjusted for the different thermoplastic materials to obtain the same strength [32].

- **Design for manufacturability.** The designer must design the product with geometries that are mouldable. Factors such as radii, draft angles and surface texturing must be considered.
- **Prototyping.** The final product design is usually prototyped to evaluate the manufacturability and performance capabilities. Mould simulation software can predict and assist in the mould filling, weld line appearance, warpage, sink marks, etc. AM techniques can produce physical models of the product quickly and provide models for communication, verification, ergonomics, and fit and functionality before the IM tool is built [33].
- **Tooling.** Tooling for the IM process is a very important phase in the product development cycle. Creating IM tooling for the production of components represents one of the most time consuming and costly phases in the development of new products [34]. The operations and consequences of filling the mould, packing, cooling and demoulding have to be considered during the design process. Otherwise unforeseen problems may make it necessary to modify the mould, thereby incurring extra costs and prolonging the development time [23].
- **Production.** Once the production tools are completed, first-off samples are manufactured through an IM process. After approval, production of the product commences.

Figure 2.6 illustrates the product development cycle from an idea to the manufacturing of the new product. It also illustrates the different options that exist for the IM tooling fabrication for the new product.

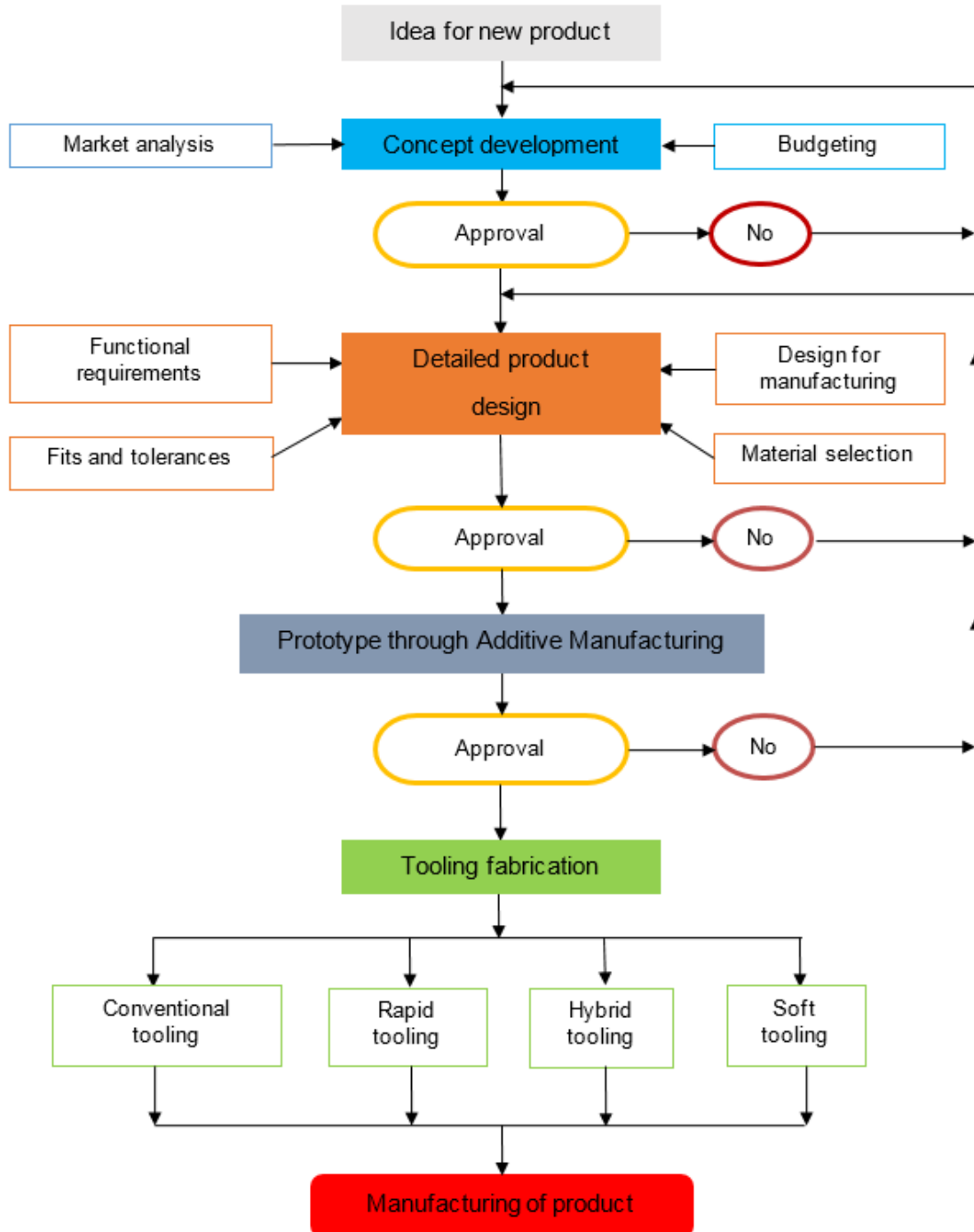


Figure 2.6 Schematic illustration of the product development process adapted from [15].

2.6 Injection mould development process

Injection mould design is very important, because it influences the quality and the economics of the moulded part. Injection moulds need to be manufactured to the highest precision since the moulded part's appearance, shape, size and strength are influenced by the quality of the moulds. Injection moulds must also be reliable during the production process and repeatedly create parts of the same standard. Repeatability and the lifespan of an injection mould are determined by the mould material used, heat treatment of the mould components, as well as the machining operations during the manufacturing of the mould [35].

While designing a thermoplastic part, the IM process must also be considered. This has an influence on the quality of the moulded parts as well as the efficiency obtained during the moulding process [36]. When designing a thermoplastic part, considerations should be given to the following:

- **Wall thickness.** Non-uniform wall thickness can cause dimensional problems, warpage and sink marks. If greater strength or stiffness is required at certain areas of the part, it is more economical to use ribs than to increase the wall thickness. Thicker parts also need a longer cooling time, thus increasing the cycle time of the parts [37].
- **Fillets and radii.** Sharp internal corners and notches are leading causes of plastic component failure. Most of the polymers are notch-sensitive and the increased stress at the notch can result in crack formation. It is easier to machine a corner with a radius compared to producing a sharp corner which requires secondary operations, thus increasing the cost of the mould manufacturing process [5].
- **Draft angles.** The surfaces of the parts need to be tapered in the direction of mould separation to assist during the ejection of the part [15].
- **Undercuts.** Undercuts are formed by using split cavity moulds, collapsible cores or sliding cores that retracts as the mould opens. Sliding cores add to the complexity of the tool design as well as the manufacturing time and cost of a mould [5].
- **Surface finish requirements.** Injection-moulded thermoplastic parts can have a variety of surface finishes, from a highly polished surface to a textured finish. The choice of surface finish is normally based on cosmetic considerations. A textured

surface can also assist to hide sink marks or parting lines. The smoother the surface finish, the easier the part will be ejected from the mould [15].

During the mould design process, it is sometimes required to redesign a previously designed feature to suit the specifications of the moulded part and to obtain the most economical method to manufacture a mould. The mould design process is illustrated in Figure 2.7 [15, 38].

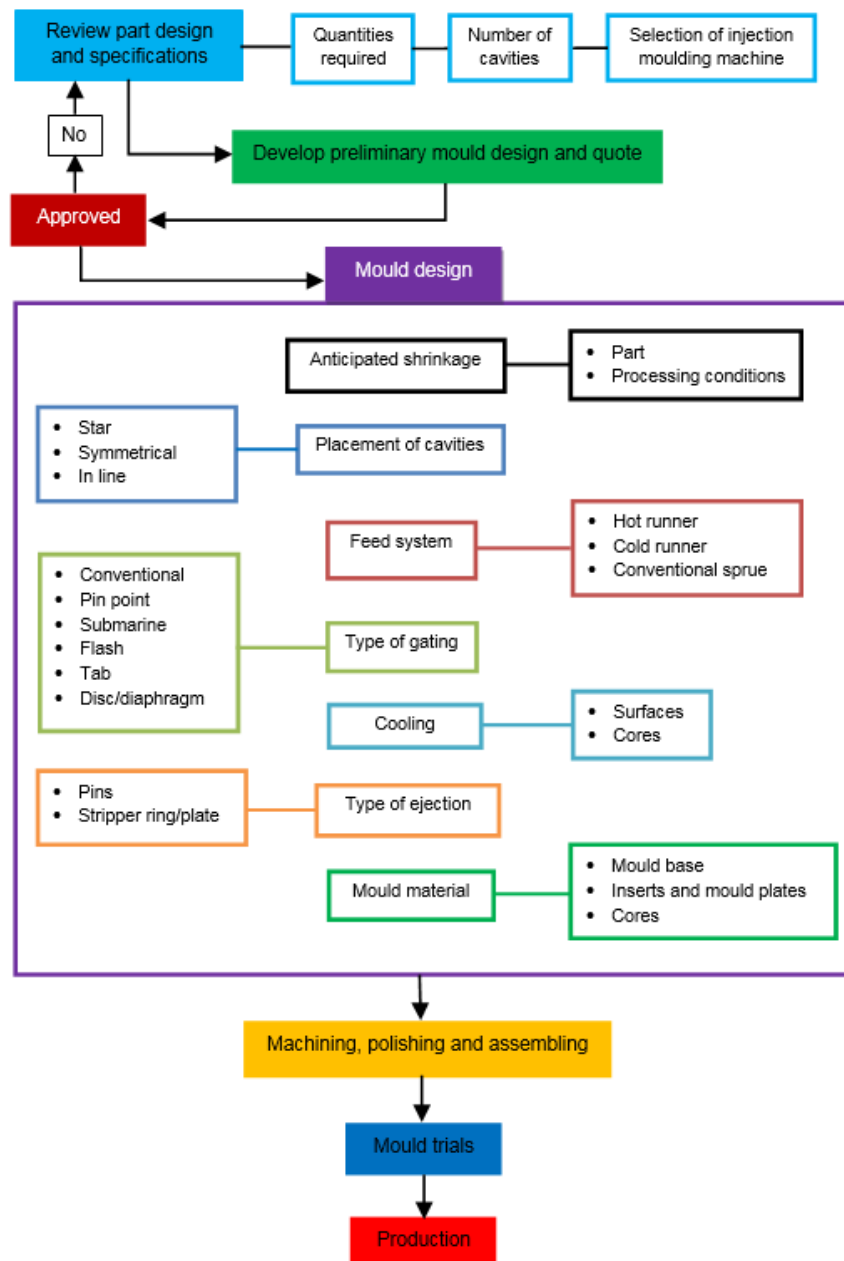


Figure 2.7 Flow chart of the mould design process adapted from [38].

After the mould has been machined, polished and assembled, it undergoes moulding trials to verify the basic functionality of the mould. Moulded parts are sampled and assessed according to the specifications [15]. If everything is approved, the mould is ready to go into production.

Figure 2.8 illustrates the main components of an injection mould. Many of the mould components have been standardised and can be easily ordered by catalogue, such as guide pins and bushes, sprue bushes, ejector pins etc.

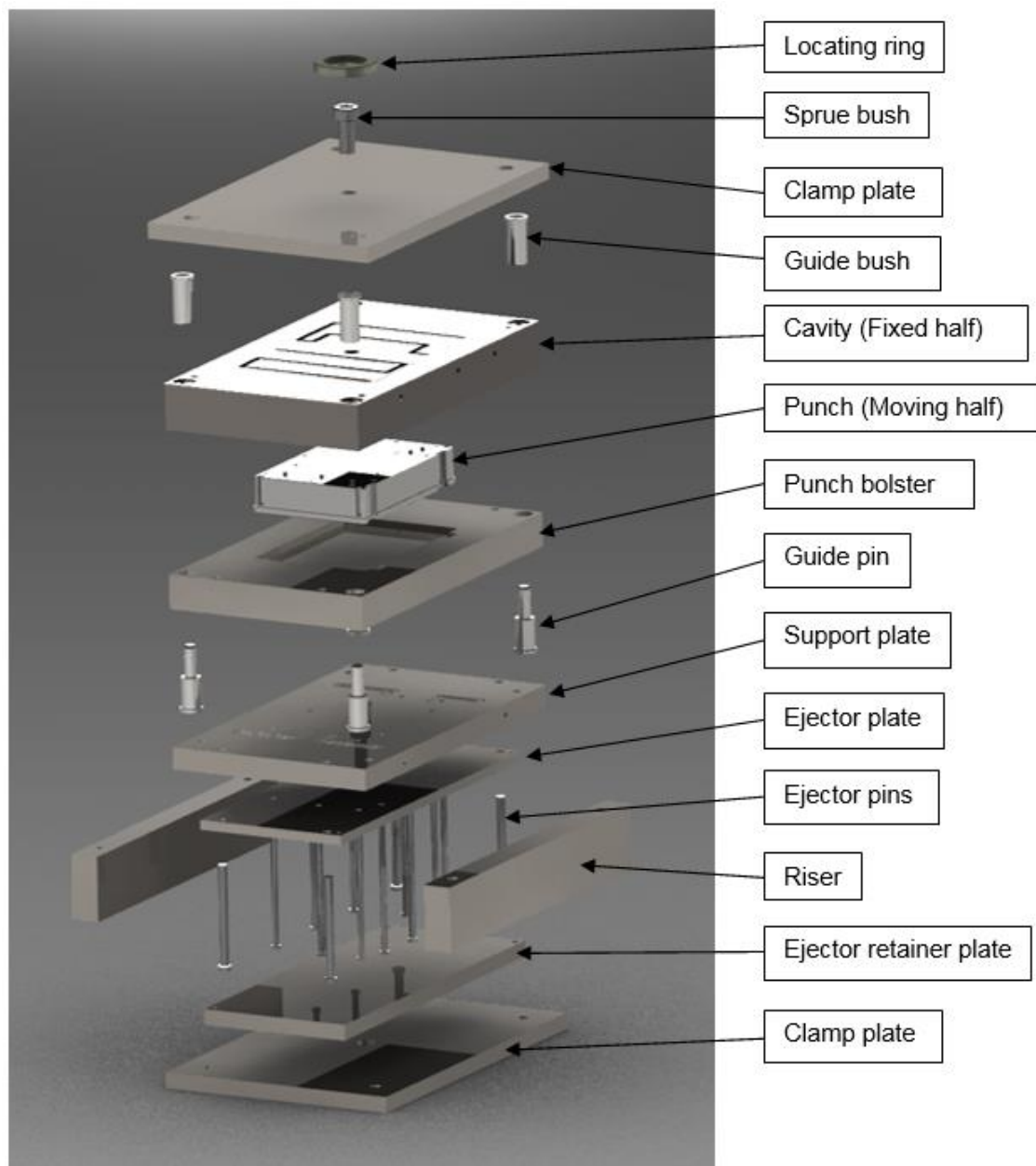


Figure 2.8 Main components of a typical injection mould.

2.7 Manufacturing of plastic injection moulds

High-precision, high-quality injection moulds can be manufactured through conventional manufacturing methods such as CNC machining. IM manufacturing is a highly labour intensive process and these moulds are not mass-produced items. Mould manufacturers must be able to meet close dimensional tolerances within tight time schedules to be economically competitive. Mistakes can be very costly and time consuming to correct.

Almost all injection moulds are manufactured by machining operations, mostly by CNC milling machines. Other manufacturing operations include CNC turning and Electrical Discharge Machining (EDM). These manufacturing operations must machine the cavities and cores so that very little post-processing operations, such as manual polishing, is required [35].

Figure 2.9 and Figure 2.10 show a typical three axis CNC milling machine and a plunge EDM machine used during the manufacturing of injection moulds.

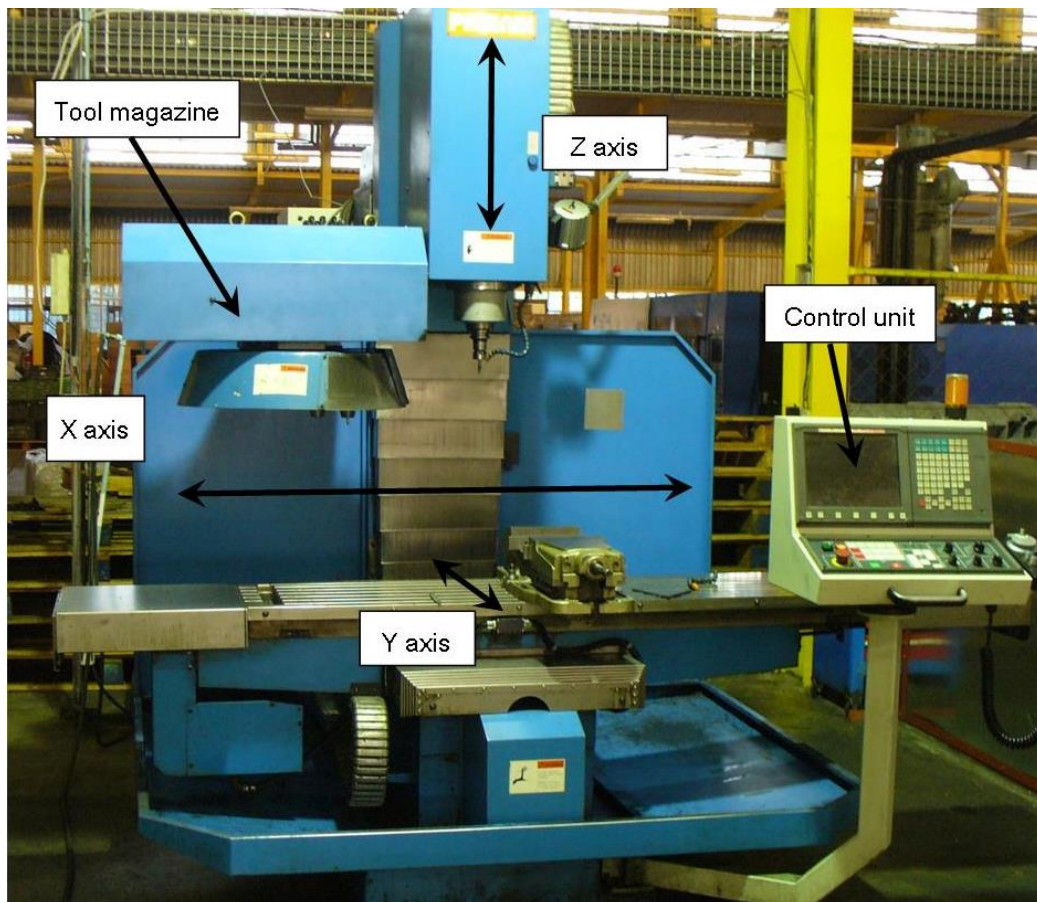


Figure 2.9 Three axis CNC milling machine.

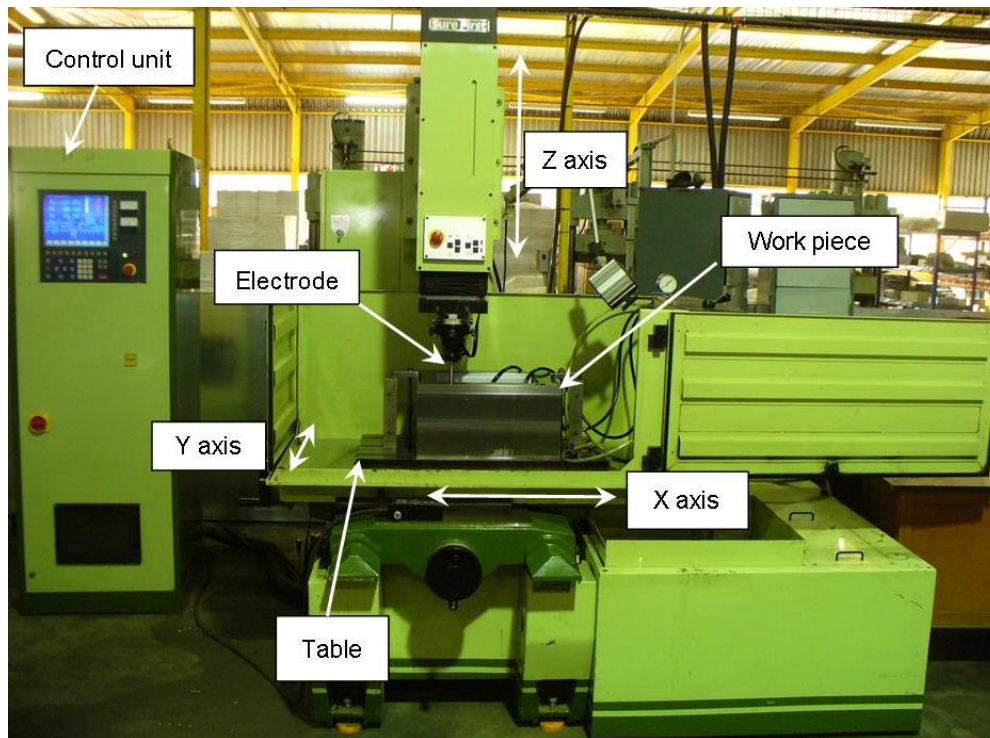


Figure 2.10 A typical plunge EDM machine with its main components.

2.8 Injection moulding process

The IM process can mass-produce thermoplastic parts with complex shapes to precise tolerances and dimensions at a high efficiency with a low cost per product [39]. The demand for injection-moulded parts continues to increase annually, because the process is the most efficient to economically produce large numbers of identical precision parts [40].

Some advantages of the IM process:

- An injection-moulded part can replace an assembly of products [41].
- The part can be manufactured with the required surface finish and colour, eliminating secondary operations [41].
- Compared to metals such as steel, an injection-moulded part has a lower mass, good strength-to-weight ratio and can include specific physical properties (e.g. corrosion-resistant properties) [3].
- The IM process is fast and well-automated [42].

- The waste (e.g. the runner system) of the process can be recycled, reducing the polymer material waste to a minimum [42].

Disadvantage of the IM process:

- The biggest disadvantage of the IM process is the very high initial capital outlay for the moulds and IM machines [3].

Some factors that can influence the IM process are the type of polymer material used, the material used to manufacture the injection moulds, the shape of the part to be manufactured and the type of IM machine to manufacture the parts [43].

2.8.1 Injection moulding machine

An IM machine consists of the following components, as illustrated in Figure 2.11 [44]:

- Clamping mechanism
- Plasticising and injection unit

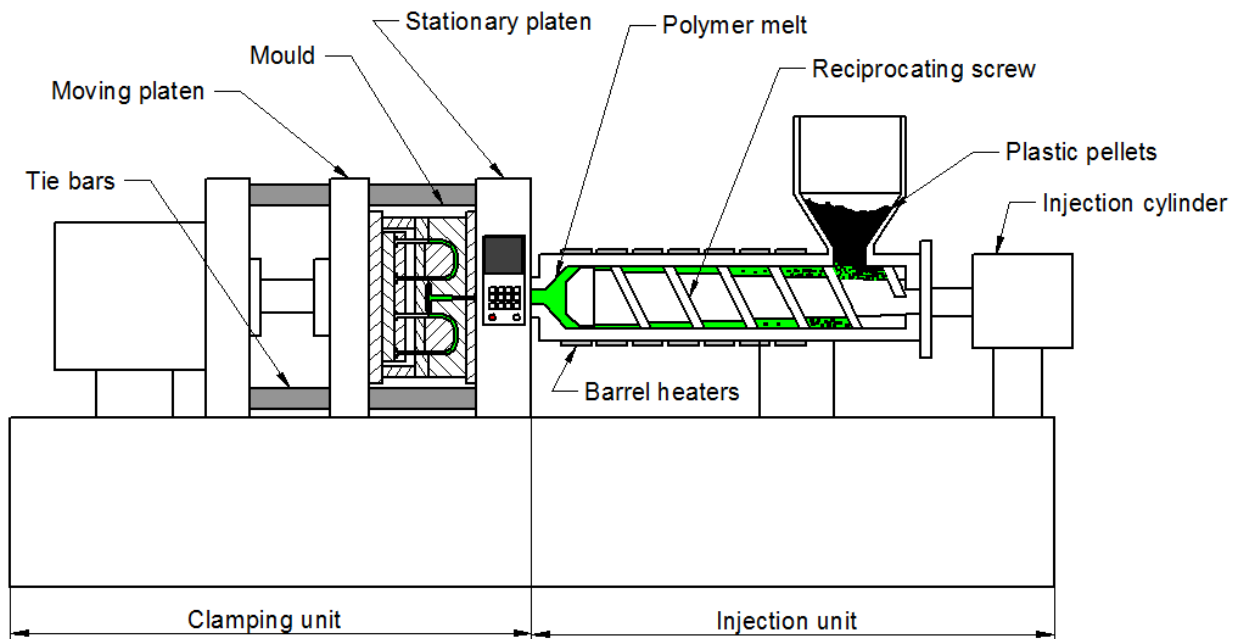


Figure 2.11 Main components of an injection moulding machine.

Clamp force and shot size are used to identify the size of an IM machine. Other machine parameters include the injection rate, injection pressure, screw design and the opening between the tie bars [45].

2.8.2 Injection moulding cycle

During the IM cycle, the IM machine converts granular or pelleted raw thermoplastic material into moulded parts through plasticisation, injection, packing, cooling and ejection stages.

The injection moulding cycle consists of the following stages [15]:

- **Plasticisation stage.** During this stage, the polymer melt is plasticised from solid granules or pellets through the combined effect of heat conduction from the heated barrel and internal viscous heating caused by molecular deformation with the rotation of an internal screw. This stage is illustrated in Figure 2.12.

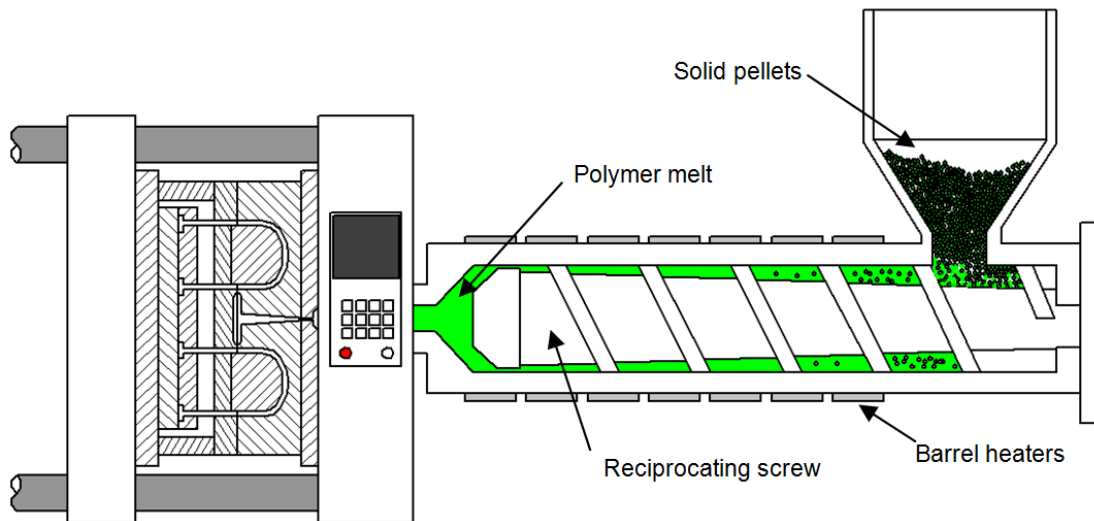


Figure 2.12 Plasticisation of the polymer melt from solid granules or pellets.

- **Injection stage.** During the injection stage, polymer melt is forced from the barrel of the moulding machine into the mould. The injection phase is characterised by high filling rates as well as high shear rates. Convection of the melt is the main means of heat transfer. Due to the high injection speed, heat may also be generated by viscous dissipation. Viscous dissipation depends on both the viscosity and deformation rate of the material.

The mould, at a lower temperature than the polymer melt, causes solidification of the polymer melt. Heat is removed from the melt through conduction from the mould wall to the cooling system. This results in a thin layer of solidified material being formed. Depending on the flow rate of the melt, this frozen layer can increase in

thickness thereby restricting the flow of the incoming melt. This has a significant impact on the pressure required to fill the mould. Some factors influencing the injection pressure inside a mould cavity are:

- Resistance in the runners and the gates [44].
- Temperature of the polymer melt [46].
- Viscosity of the polymer [45].
- Distance the polymer melt must flow from the gates to fill the part [45].
- Geometry of the cavity to be filled. Thin walls require more clamp force to hold the mould closed during the filling stage because higher pressure is required to fill the cavity [45].
- Rheology of the polymer melt [5].

The clamping unit needs to apply enough clamping force on the mould to keep it closed during the injection stage because the injection pressure acting on the internal surfaces of the cavity space tends to open the mould at the parting plane [44]. When the total space in the cavity is filled, the injection phase is completed but pressure is maintained by the moulding machine. This begins the packing stage [39].

- **Packing stage.** After the mould cavity is filled with the polymer melt, the packing stage forces additional material into the mould cavity to compensate for shrinkage during cooling [47]. During the packing stage, heat is transferred through conduction from the part to the mould; thus the frozen layer's thickness continues to increase. At some stage the gate will freeze, isolating the cavity from the pressure applied by the moulding machine. This begins the cooling stage [39]. Figure 2.13 illustrates the injection and packing stages of the mould cavities.

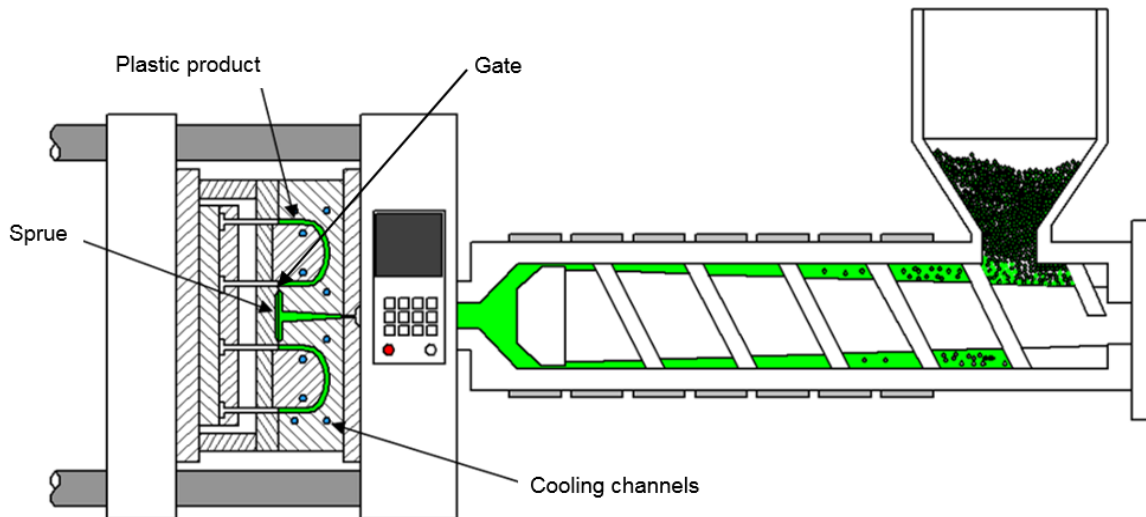


Figure 2.13 Injection and packing of mould cavities.

- **Cooling stage.** This stage provides time for the polymer to solidify through the conduction of heat to the cooling channels and become sufficiently rigid to be ejected out of the mould cavity.
- **Ejection stage.** When the part is sufficiently solidified, the mould opens and the part is ejected from the mould cavity by ejector pins inside the mould. This stage is illustrated in Figure 2.14.

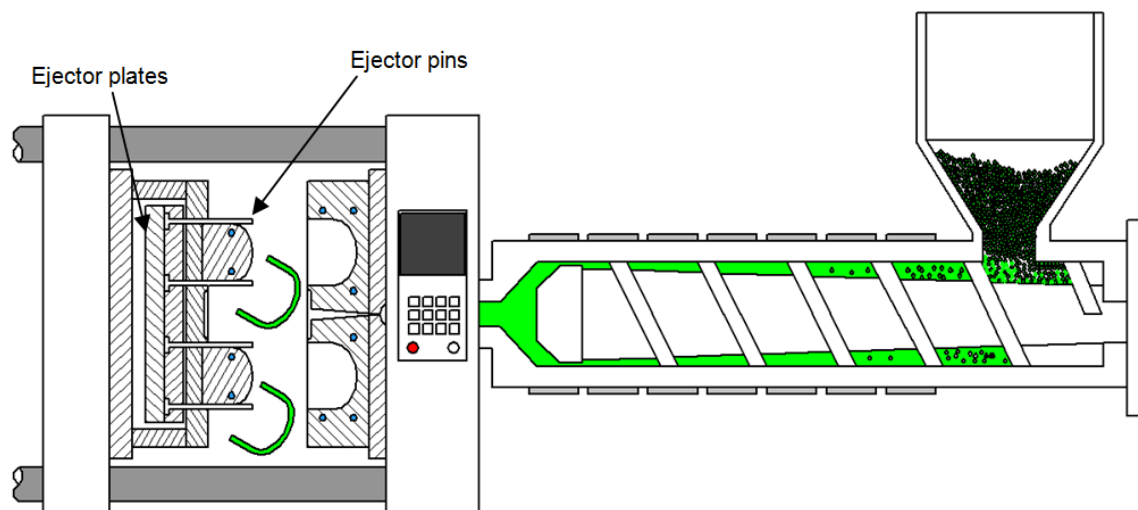


Figure 2.14 Ejection stage of the plastic part.

2.9 Conclusion

This chapter presented reasons for developing a new product and the different development stages that are necessary to successfully introduce a new polymer part to the market. For each new polymer part development, a mould needs to be designed and manufactured to mass-produce the part through the IM process.

From this chapter it can be deduced that due to the high cost to manufacture plastic injection moulds, most new products that are developed for manufacturing through the IM process do not reach the commercialisation stage. Global competitiveness is increasing the demand on mould manufacturers to reduce the lead time and costs of injection moulds in order to be competitive in the market place. A possible solution to these problems is to produce inserts that are suitable for use in the IM process through AM.

3 ADDITIVE MANUFACTURING AND RAPID TOOLING

3.1 Introduction

Since AM was introduced in the late 80's, it has become an important part of the product development process in many industries [48]. The American Society for Testing and Materials (ASTM) International Committee F42 on Additive Manufacturing Technologies defines AM as: “The process of joining materials to make objects from 3D model data, usually layer upon layer, as opposed to subtractive manufacturing technologies” [49].

AM prototype parts can be quickly produced for validation, measurement and in some cases, actual trials [50]. Parts that may be difficult or even impossible to manufacture by conventional manufacturing methods can often be manufactured through AM technologies. Companies that apply AM technologies during the product development stage are able to compete more effectively with other competitors in the marketplace [51]. AM can be a major cost- and time-saver as it allows the designer and manufacturer to see what a part will look like at an early development stage. It also allows design changes or product cancellations when such decisions are least expensive, particularly with highly complex designs [50].

3.2 AM workflow

The various steps to create an AM part, from a three-dimensional (3D) CAD model to a physical part are illustrated in Figure 3.1 [52].

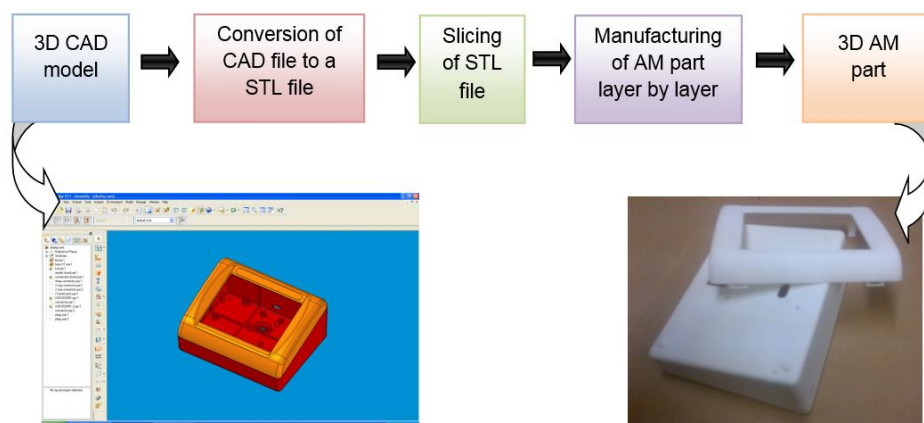


Figure 3.1 Flow diagram of the AM manufacturing workflow.

3.2.1 Creation of a 3D CAD model

The part to be built is first created using CAD software. Parts should be designed in such a way that they are easy and inexpensive to manufacture, a method referred to as design for manufacturing. A small change to the product design could have a significant impact on the cost, time and success of a project.

3.2.2 Conversion of CAD model to a STL file format

3D CAD data is converted into the Standard Triangulation Language (STL) data format. This is the standard data format used by most AM machines. In the STL file format, the surface of the solid is approximated by triangular facets. Each triangular facet is identified by a line perpendicular to the triangle with a length of one (a unit normal) and by three corners (vertices). The normal and each vertex are specified by three coordinates resulting in triangular facets which define the surface of a 3D model. Each facet is part of the boundary between the interior and the exterior of the model [53].

STL files are not an exact representation of the CAD model because triangular facets are generated over the surface of the model. Increasing the number of triangles improves the triangular approximation but increases the STL file size. Figure 3.2 illustrates a 3D CAD model in the STL file format.

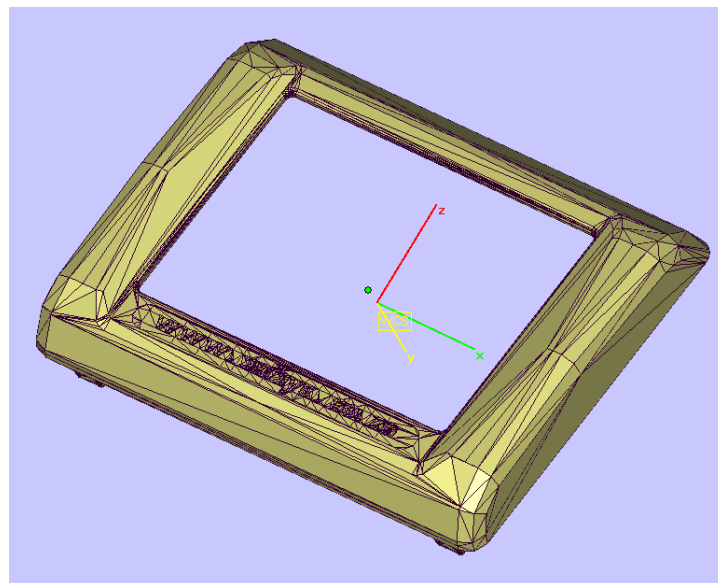


Figure 3.2 An STL file representation of a CAD model, showing the triangular facets.

The following should be considered during the conversion of files to the STL format:

- If a CAD model is converted to an STL file format with a very low resolution, it will result in large faceting of the triangular facets. This will result in an inaccurate part being manufactured.
- If the CAD data has numerous unstitched surfaces, these will cause errors when converting to the STL format. Time-consuming fixing of the STL file is then necessary before the file can be used to manufacture an AM part.
- The measurement units of the STL file should not differ from that used during the designing process in the CAD software.

3.2.3 Pre-processing of an STL file

Pre-processing of the part file to be manufactured is required before the file can be sent to the AM machine. The virtual model in STL format is sliced into thin virtual slices by dedicated software such as EOS RP-Tools. The most important criteria that should determine part orientation in the building process of a part on AM systems are:

- **Surface quality.** The surface quality of a part is estimated by analysing the surface roughness of an inclined surface and the contact area of the support structures used during the building process [54]. A better surface quality results in a more accurate representation of the part.
- **Support structures.** Support structures are required in most of the AM processes to support overhangs and thin walls while the part is built. Support structures result in rough surfaces on the part after removal, requiring finishing operations to improve the quality of the surfaces [55].
- **Build time.** Build time is an important factor in building a part. If the same part is orientated differently, the build time varies since it is largely dependent on the height of the part or the number of slices. It can also differ in terms of the number of support structures needed [54].
- **Part cost.** The longer the build time, the more expensive the part will be [54].

3.2.4 Construction of physical part

The part is built one layer at a time using different materials and binding mechanisms depending upon the AM process. Between the layers, the platform on which the part is built (build platform) is lowered by a predetermined increment, after which another layer of material is deposited or spread (depending upon the AM process), over the previous layer. The process then repeats until all the layers of the entire model have been fabricated.

3.2.5 Cleaning and finishing of the AM part

Post-processing includes the removal of the part from the AM machine, and depending upon the AM processes, removing of support structures. Some photosensitive materials need to be fully cured before the part can be used.

3.3 AM technologies

There are a large number of AM technologies available on the market. Different users have different requirements for manufacturing a part using an AM machine. These requirements can vary in terms of build materials available, manufacturing time and cost as well as the required accuracy and surface finish of the part [52, 56].

The ASTM F42 Technical Committee classifies AM technologies into seven different AM process categories [57]. These seven categories can also be characterised according to the state of the unprocessed material (liquid, powder or solid), used during the AM manufacturing process of a part [58]. Figure 3.3 illustrates the different AM process categories as well as the relevant AM technologies for each category [59].

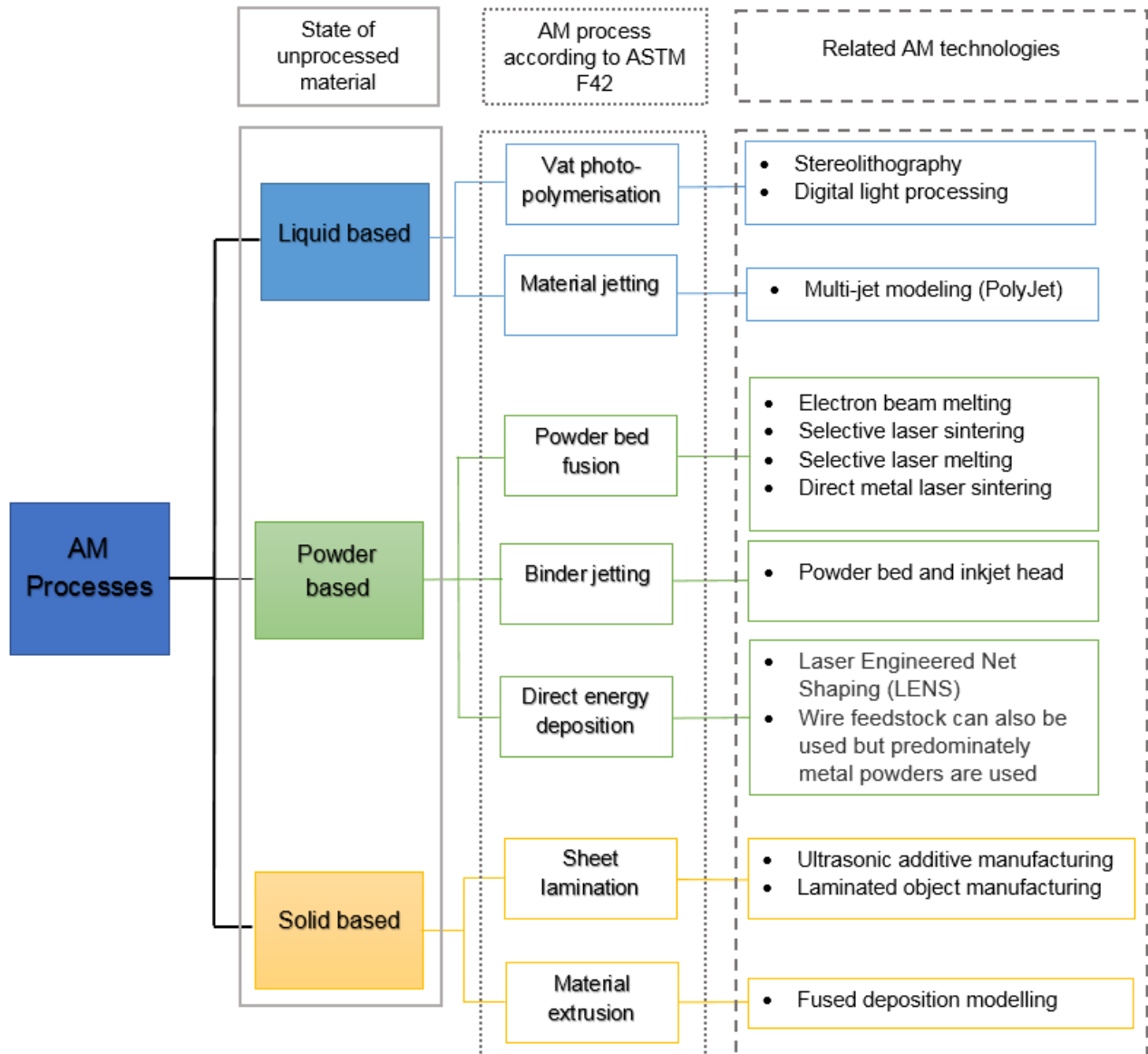


Figure 3.3 AM process categories based on the classification by the ASTM F42 Technical Committee and the state of the unprocessed material.

An overview of the different AM processes according the classification by the ASTM F42 Technical Committee, are as follow [60]:

- **Vat photo-polymerisation.** A liquid photopolymer inside a vat is selectively cured by light-activated polymerisation.
- **Material jetting.** Droplets of material (photopolymer or wax) are deposited selectively to produce a layer.

- **Binder jetting.** A liquid binding agent is selectively deposited to join powder particles.
- **Directed energy deposition.** Focused thermal energy (from a laser, electron beam, or plasma arc) is used to fuse materials by melting as they are being deposited.
- **Sheet lamination.** Sheets of material are bonded together to create an object.
- **Material extrusion.** Material is selectively dispensed through a nozzle to produce a layer.
- **Powder bed fusion.** A thermal energy source, such as a laser or electron beam, selectively fuses area of powder inside a powder bed.

The Selective Laser Sintering (SLS) process is one type of the powder bed fusion process. This process is used during this study and an explanation of this process is as follows:

3.3.1 SLS process

The SLS process manufactures parts by sintering powdered material, layer upon layer. Some of the materials that can be sintered include polymers (e.g. polyamides, polystyrene and polypropylene), metals (e.g. stainless steel, titanium, CoCrMo and maraging steel) and sand [61].

LS of polymer materials

The SLS process for polymers is conducted inside an enclosed chamber filled with nitrogen gas, which minimises the oxidation and degradation of the powder during processing. The powder inside the enclosed chamber is heated to a few degrees below the melting temperature of the material before manufacturing commences. This is to minimise the temperature difference between the sintered and un-sintered powder which reduces warpage of the model during the build due to non-uniform thermal expansion and contraction. The heating of the powder also reduces the energy required from the laser during the sintering process. The powdered material is sintered by a laser that selectively scans the surface of the powder bed to create a two-dimensional (2D) shape. The build platform then moves down the distance equal to one layer of the model. A new layer of powder is laid down and levelled using a recoating device. The next 2D profile is traced by

the laser, bonding it to the previous layer below. The SLS build process is illustrated in Figure 3.4.

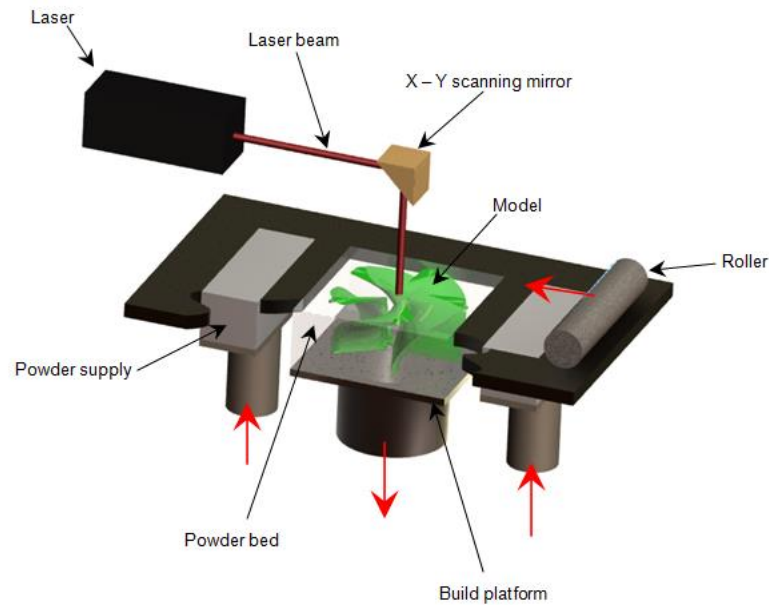


Figure 3.4 Schematic of the Selective Laser Sintering process.

This process continues until a 3D part is created. The powder that is not sintered acts as a supporting medium which eliminates the need to manufacture supports during the build process and the subsequent need for removal of supports during post-processing. A cool-down period is required to allow parts to uniformly cool down to a temperature where they can be handled and exposed to ambient temperature and atmospheric conditions. If the parts and powder are prematurely exposed to the ambient temperature and atmosphere, the powder may degrade in the presence of oxygen, and the parts may warp due to uneven thermal shrinkage. After the parts are removed from the powder bed, the un-sintered powder is cleaned off the parts, and if necessary, further finishing operations are performed [6, 62].

3.4 AM applications

Manufacturing companies using AM technologies indicated that functional models as well as fit and assembly applications are some of the most popular applications of AM parts [51]. AM applications in industry include:

- Visual aids for design engineers. AM models assist in solving design issues quickly during the product design process, and with less misinterpretation [63].
- Presentation models.
- Ergonomic studies of a design [63, 64].
- Conceptual mock-ups of product packaging [64].
- Fit and function [64].
- Requesting quotes [63].
- Patterns for moulds and castings [65].
- Visual aid for toolmakers [63]. Design issues can be resolved prior to the manufacturing of tooling.
- Rapid tooling (RT) processes [66].

AM parts are also used as an alternative to normal manufacturing techniques for metallic, ceramic or polymer components in many industrial applications such as mould inserts, automotive components and aerospace parts [67].

3.5 AM advantages and limitations

Some of the AM advantages are:

- Physical prototypes can be manufactured quickly [68].
- Almost unlimited complex geometries can be manufactured [68].
- Physical objects made by AM are used mainly as prototypes or models for other production procedures [68].
- AM can be used to manufacture a master pattern from which rapid tools could be created [69].
- The possible combination of different materials within the same model [66].
- AM prototype manufacturing processes offer time and cost advantages over conventional prototyping technologies [66].

Limitations of the AM process:

- **Layer thickness:** All AM parts have a characteristic stair step texture which is most obvious on curved and inclined surfaces, as illustrated in Figure 3.5 [69]. The stair step texture varies depending upon the layer thickness and the surface angle of an AM part. The surface roughness of an AM part depends upon the stair step texture; therefore, post-processing such as sanding is required to improve the surface finish of an AM produced part [70].

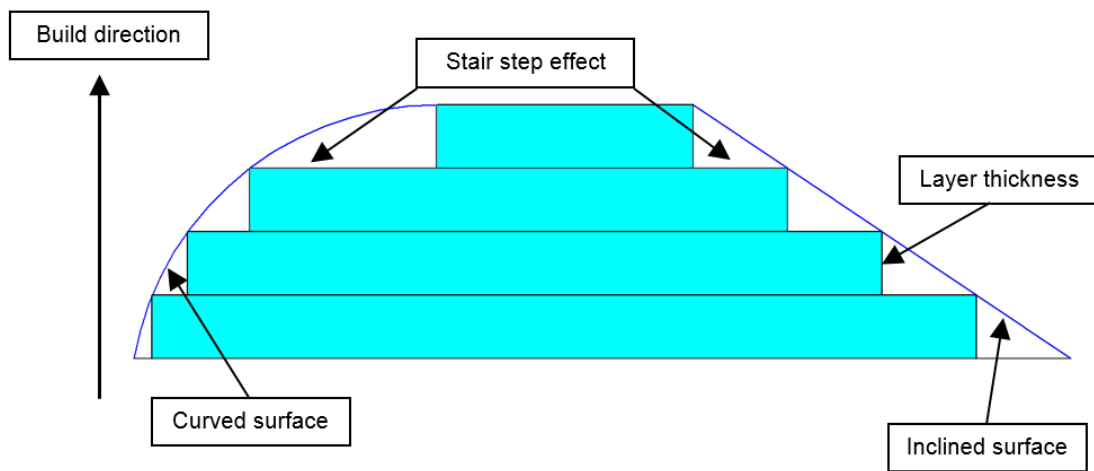


Figure 3.5 Stair step effect on curved and inclined surfaces on AM parts.

- **Part accuracy:** In some AM processes, overhangs and isolated regions need support structures. Normally when the supports are removed from the fabricated model, there is a surface roughness that affects the overall part accuracy [69].
- **Part size:** The working envelope of an AM machine restricts the maximum dimensions of a part. Some models require the manufacturing of parts in sections that can fit into the machine [69].
- **Mechanical properties:** The mechanical properties of an AM part may not be the same as that of a part manufactured through conventional processes (forming, IM, etc.) [68, 71] and can often be non-isotropic.

3.6 Rapid tooling

The demand for quicker ways of making technical prototypes manufactured in the correct material, using the appropriate production method (such as IM), have led to RT techniques

using AM technologies [72]. For example, these prototypes are used in the motor industry to test noise levels and the durability of components. The available design-to-production time for new components continues to decrease. Thus, the long lead times of manufacturing production tooling conventionally become more of a barrier in responding to customer demand [7].

RT defines mould-making processes that can create tools quickly and with minimum direct labour. RT includes tool manufacturing techniques that apply additive, subtractive, and pattern-based processes. RT can be applied in a variety of applications from IM to casting and sheet metal stamping operations.

The main reasons for developing RT technologies are [73]:

- Increase in design capabilities.
- Increase in product variety.
- Demand for shortened time to market.
- Decrease in production quantities.
- Reduction in tooling time and costs.

The potential of RT, as described above, led to tremendous interest in RT solutions for product design and manufacturing. Whether RT is used for prototyping, limited run, or production tooling, it provides an opportunity to reduce the time and cost of product development [74, 75].

3.7 RT techniques

RT techniques that use AM can be divided into two groups, namely indirect and direct tooling.

3.7.1 Indirect tooling

Indirect tooling includes pattern-based methods where a tool is cast from an AM product that represents the part to be manufactured. An example of indirect tooling is room temperature vulcanized (RTV) silicone rubber moulding.

Normally, the pattern used to produce this type of indirect tooling is manufactured through an AM process. Preparation of the first half of the mould begins by securing the pattern in oil-based clay or other building materials and constructing the parting line. Silicone moulding material is poured around the pattern and allowed to cure. A vacuum can be applied to either the RTV moulding material before pouring or the tooling assembly after pouring to remove air bubbles from the silicone RTV material. After the silicone has cured, the second half of the mould is prepared and poured. Once the second half has cured, the pattern is removed and the mould is prepared for use. RTV tooling can be used to mould small to medium quantities of parts out of a large variety of urethane, epoxy, or other polymer materials. RTV tooling can typically be used to manufacture small quantities of parts before replacement tooling becomes necessary. The tool life of RTV tooling depends upon the casting material, accuracy, finish requirements and the complexity of the part geometry [76].

3.7.2 Direct tooling

Direct tooling is a method where the complete mould or mould inserts are manufactured directly through an AM process. Direct tooling normally uses metal-based laser melting AM technologies to manufacture moulds and mould inserts. Metal-based laser melting technologies can produce mould inserts out of materials such as stainless steel, cobalt, chromium, maraging steel, titanium and alloy blends. These inserts can be used in an injection mould to manufacture products in the desired production material [77].

Direct and indirect RT techniques can be further subdivided into two groups, namely soft tooling and hard tooling.

Soft tooling

Soft tooling is a low-cost method used for low-volume production. Materials which have a low-hardness level, such as silicones, epoxies, low-melting-point alloys, etc., are used to manufacture moulds [78].

Hard tooling

Hard tooling is used for higher production volumes and uses materials with a higher hardness levels such as maraging steel. Hard tooling methods produce moulds/inserts that can be used in the IM process, which results in a better quality and larger quantity of products produced [79].

PolyJet rapid tooling

PolyJet printing using Objet™ 3D printers is a liquid-based material jetting process that deposits layers of liquid photopolymer. Once a layer of material is deposited onto the build platform, a UV light attached to the print head immediately cures it. The solidified layer is immediately ready to be built upon. Printing takes place according to 2D slice file images of the CAD part. Once a layer is completed, the printing platform is lowered by one layer thickness and the next 2D slice of the part is printed. This process is repeated until the part is completed. An advantage of the process is that the print head can print multi-material in one build including a water-based support material to support overhanging structures. This can be removed by dissolving in water after printing.

The PolyJet process, using Objet™ RGD 515 digital ABS, can successfully produce RT moulds for the IM process to fill the gap between soft tooling and AM prototypes [80]. RT inserts manufactured by the PolyJet process are suited for 25 to 100 IM parts, depending upon the IM material used and the complexity of the mould [81]. IM trials with the following materials have been conducted with PolyJet moulds using air to cool the moulds between each IM cycle:

- PE.
- PP.
- PS.
- ABS.
- Thermoplastic elastomer (TPE).
- PA.
- Acetal or Polyoxymethylene (POM).
- Polycarbonate-ABS blend.

- Glass-filled polypropylene or glass-filled resin.

The advantages of RT moulds manufactured through the PolyJet process are:

- Once fully cured, moulds can immediately be placed into IM equipment [80].
- RT moulds can produce prototypes from the same material that is specified for use in the final product [80, 81].
- Lower costs compared to conventional tooling [81].
- Mould inserts can be produced with conformal cooling due to the full density (non-porous) characteristics of a PolyJet manufactured part.

The disadvantages of RT moulds manufactured through the PolyJet process are [80, 81]:

- The RT moulds are not able to withstand extended periods of high temperatures and pressures typically occurring during an IM process, reducing the lifespan of the moulds.
- Only suitable for production runs up to 100 IM parts.
- Due to the layered AM manufacturing process, small steps occur on the surface resulting in surfaces not being completely smooth or polished.
- Size limitations of the mould due to printing size limitations.
- Low glass transitioning temperature of the PolyJet inserts, between 47 and 53 °C.
- Lengthened cycle time required to allow mould surface to cool down between each IM cycle.

3.7.3 RT advantages and limitations

Some of the advantages of RT are:

- Shortening of the tooling lead time [74].
- Lower cost of tooling due to the shortened lead time [82].
- Functional test of parts in early design stage is possible. Due to the shortened lead time, many engineers prefer to produce parts for functional tests leading to a phase where most of the faults are corrected before production [83].
- Automation. Many of the RT processes can build tooling inserts 24 hours a day, seven days per week [84].

- Building multiple cavity/core sets [84].
- Can produce inserts with conformal cooling channels. Conventional methods can only drill cooling channels in a straight line whereas conformal cooling allows cooling channels to flow through an insert in a pattern that conforms to the shape of the cavity. Conformal cooling channels can remove heat more efficiently and uniformly from the mould resulting in reduced cycle times, lower part costs and improved quality of the part manufactured [86, 87, and 88].

Some of the limitations of RT are:

- Accuracy: Direct tooling processes have a tolerance of approximately 0.05 mm to 0.127 mm. To obtain the same accuracy as with conventional methods (e.g. CNC milling machines), inserts must be manufactured as near net shapes and post-machined with CNC milling machines [89].
- Cost-effectiveness: The cost of AM materials and equipment means that a high overhead is associated with most RT techniques [85].
- Size limitations: Many of the RT methods are limited to the size of inserts that can be created.
- Tool life: Most of the RT techniques have a limited tool life due to the materials the cavity inserts are manufactured from.
- During the AM process, parts may move and distort [90].

Some of the direct and indirect RT techniques, with their advantages and disadvantages, are summarised in Table 3.1 [91].

Table 3.1 Summary of properties of some direct and indirect rapid tooling techniques [91].

Process	RT technique	Materials available for part manufacturing	Achievable part quantities	Advantage	Disadvantage
RTV silicone rubber	Indirect	Urethanes Epoxies Acrylics	10 to 50	Mould inexpensive to manufacture.	Expensive per part cost. Limited tool life. Limited manufacturing materials can be used Accuracy.
Sprayed metal	Indirect	Thermoplastic	50 to 100's	Conformal cooling possible. Manufacturing of large parts possible.	Limited tool life. Accuracy. Geometrical part limitations such as narrow slots.
Aluminium filled epoxy	Indirect	Thermoplastic	100's for complex parts 1000's simple parts	Least expensive mould for the manufacturing of thermoplastic parts.	Long cycle time. Limited tool life. Accuracy.
PolyJet printing	Direct	Thermoplastic	25 to 100	Fully dense parts. Conformal cooling possible.	Long cycle time. Limited tool life.

Process	RT technique	Materials available for part manufacturing	Achievable part quantities	Advantage	Disadvantage
Electron beam melting	Direct	Thermoplastic Metals	More than 250000 using IM process	Fully dense parts. Conformal cooling possible.	Limited part size. Requires finishing operations.
Direct metal deposition	Direct	Thermoplastic Metals	More than 250000 using IM process	Polishable. Repair or modify existing moulds. Conformal cooling possible.	Requires finishing machining operations. Geometric limitations on overhangs.
Direct metal laser sintering (DMLS)	Direct	Thermoplastic Metals	More than 250000 using IM process	Conformal cooling possible.	Surface finishing. May require finishing machining operations.
CNC Aluminium tooling	Direct	Thermoplastic	More than 250000 using IM process	Accuracy. Surface finish.	Expensive for complex parts.

3.8 Hybrid tooling

Global competitiveness is increasing the pressure on the manufacturing process of injection moulds to reduce lead times and cost and for increased part quality [78]. Conventional manufacturing methods, such as CNC machining, are able to manufacture high-precision, high-quality injection moulds. Some of the limitations of this process are:

- This process is costly due to the high level of human interface needed to generate CNC programs [92].
- Rough machining of cavities and cores is time consuming and costly [92].
- Machining constraints, for example fixed order of machining operations, such as roughing, semi-finishing, and finishing are required [93].
- Cutting tools limitations such as the length of cutters. Some machining operations may require special tooling at an additional cost [93].
- Complex geometries are time consuming to manufacture, such as thin walls and sharp corners. These usually require additional machining operations [93].

AM is able to produce inserts that are suitable for use in the IM process. AM processes do not require human interface during the manufacturing stage and they can manufacture inserts with complex geometries as well as internal features, such as conformal cooling channels [93, 94]. During the tool design for AM, the characteristics and design specifications of the part needs to be considered to ensure the quality of the manufactured part [95]. The biggest concern of the AM process is to keep the cost down. The two factors that have the greatest influence on cost are build time and volume. The larger the volume, the longer the manufacturing operation and the more expensive the process will be [94].

By combining the advantages of AM and the CNC machining processes, it is possible to create a tool that optimises the manufacturability, cost and lead time [96]. Hybrid tooling, based on AM technologies, combines the design flexibility of AM with the precision and productivity of conventional manufacturing techniques. This deviation from traditional machining and manufacturing processes encourages the use of AM-based tooling when components of a mould are intricate and highly detailed. Each component of the mould is evaluated separately to determine the best manufacturing process. Geometries of the mould that are complex and time consuming to machine as well as regions that cannot be accessed by conventional methods, can be manufactured using AM (e.g. DMLS) [96, 97].

This enables the manufacturing of parts that would be extremely difficult to produce through conventional manufacturing methods at a competitive cost [98], and internal features, such as conformal cooling, can also be included in the tool design [94]. AM used in association with more traditional processes (e.g. EDM or HSM) reduces the time required to manufacture moulds [99,100]. A mould can be manufactured as several parts simultaneously. Each part is manufactured separately with a chosen process. Afterwards, the mould is assembled to obtain a multi-part tool called “a hybrid tool”, using AM technologies [101].

Important strengths and limitations of RT techniques and conventional mould-manufacturing methods for injection moulding inserts are summarised in Table 3.2.

Table 3.2 Comparison between RT and conventional mould-manufacturing techniques [34, 89].

Operation/procedure	Rapid Tooling	Conventional tooling
Fabrication time and cost	Not affected by complexity.	Affected by complexity.
Accuracy and surface finish	Good accuracy and acceptable surface finish.	Highly accurate and excellent surface finish.
Modifications made to mould	Easily implemented.	Moderate to difficult implementation.
Tooling life	Small or medium volume capability. High volume possible through materials such as Maraging Steel MS1 steel.	High-volume capability.
Tooling types	Rapid soft, hard tools.	Hard tools.

3.9 Applications of RT and hybrid tooling

Some applications and advantages of RT and hybrid tooling are:

- They can be used for development tooling and low-volume production tooling [102].
- Parts that are produced through RT/hybrid tooling are manufactured from the same material that is used during the final production of the part [103].

- Customers are able to test their product in the marketplace before production tooling is manufactured. Feedback from the market can result in tooling modifications. Alterations to the production tooling can be expensive and time consuming.
- The revenue created by RT/hybrid tooling production can fund the manufacturing of multi-cavity production tooling [104].
- They can assist in assembly lines where manual assembly workers can be familiarised with the product and assembly robots can be programmed. This can result in changes that can simplify and reduce the cost of assembly before production tooling is finalised.
- Medical products can be manufactured in the correct material. This is especially important during the product approval stage, e.g. when the part must undergo clinical trials.

3.10 Alumide® as an RT alternative

This research investigated the possibility of using laser-sintered Alumide® as an alternative material for producing RT inserts. Using Alumide® for this application is a novel use of the material with initial IM experiments performed by researchers at CUT, Free State in 2006 [105,106]. RT inserts for the IM process were manufactured by the CRPM for an industry partner of CUT (Technimark). Although parts were successfully produced, there were a number of uncertainties during the process which justified further investigation of using Alumide® as an alternative RP process [107].

Alumide® is an aluminium-filled nylon material that produces a metallic-looking, non-porous component which can withstand temperatures of about 170 °C. A typical application of Alumide® is the manufacture of stiff parts with a metallic appearance for applications in the automotive industry, for illustrative models and for jig manufacture. Alumide® can be finished by grinding, polishing or coating. An additional advantage is that very little tool wear occurs during machining operations such as milling, drilling or turning of the material [107]. Some Alumide® material properties are summarised in Table 3.3.

Table 3.3 Material properties of Alumide® [108].

Property	Value
Density of laser sintered part	1.36 g/cm ³
Tensile modulus	3800 MPa
Ultimate tensile strength	48 MPa
Flexural modulus	3600 MPa
Flexural strength	72 MPa
Shore D hardness	76
Melting point	172 to 180 °C
Heat deflection temperature	177.1 °C
Vicat softening temperature	169 °C
Heat conductivity (170 °C)	0.5 to 0.8 W / m K

3.11 Conclusion

This chapter presented the different AM technologies and the advantages and limitations of AM processes. One of the main limitations of the AM process is its inadequacy to produce products manufactured in the correct material due to the limited number of materials that can be processed by AM technologies. This has led to the development of RT techniques using AM technologies, to provide a means to produce tooling quicker and cheaper than conventional mould manufacturing techniques, to produce IM parts in the correct material.

From this chapter it can be concluded that the advantage of RT is the direct manufacture of parts which offer high functionality and close-to-series properties and performance. Alumide® inserts can be used as a RT medium to produce parts through the IM process. Alumide® inserts can be manufactured in a shorter time compared to what it would take to produce the same size DMLS inserts, and the material cost of Alumide® is less than that of the DMLS material. Considering these two factors, it is possible to produce the entire part's geometry using only Alumide® inserts in bolsters, thereby making conventionally machined inserts (such as aluminium) in a hybrid tool unnecessary. By combining the advantages of AM and CNC machining processes, it is possible to create a rapid tool that optimises manufacturability, cost and lead time of tooling for the IM process.

4 EXPERIMENTAL APPROACH AND RESULTS

4.1 Introduction

To determine the feasibility of Alumide® tooling inserts for IM applications, a four-phased experimental approach was decided upon for this study. Figure 4.1 illustrates the four-phased approach schematically.

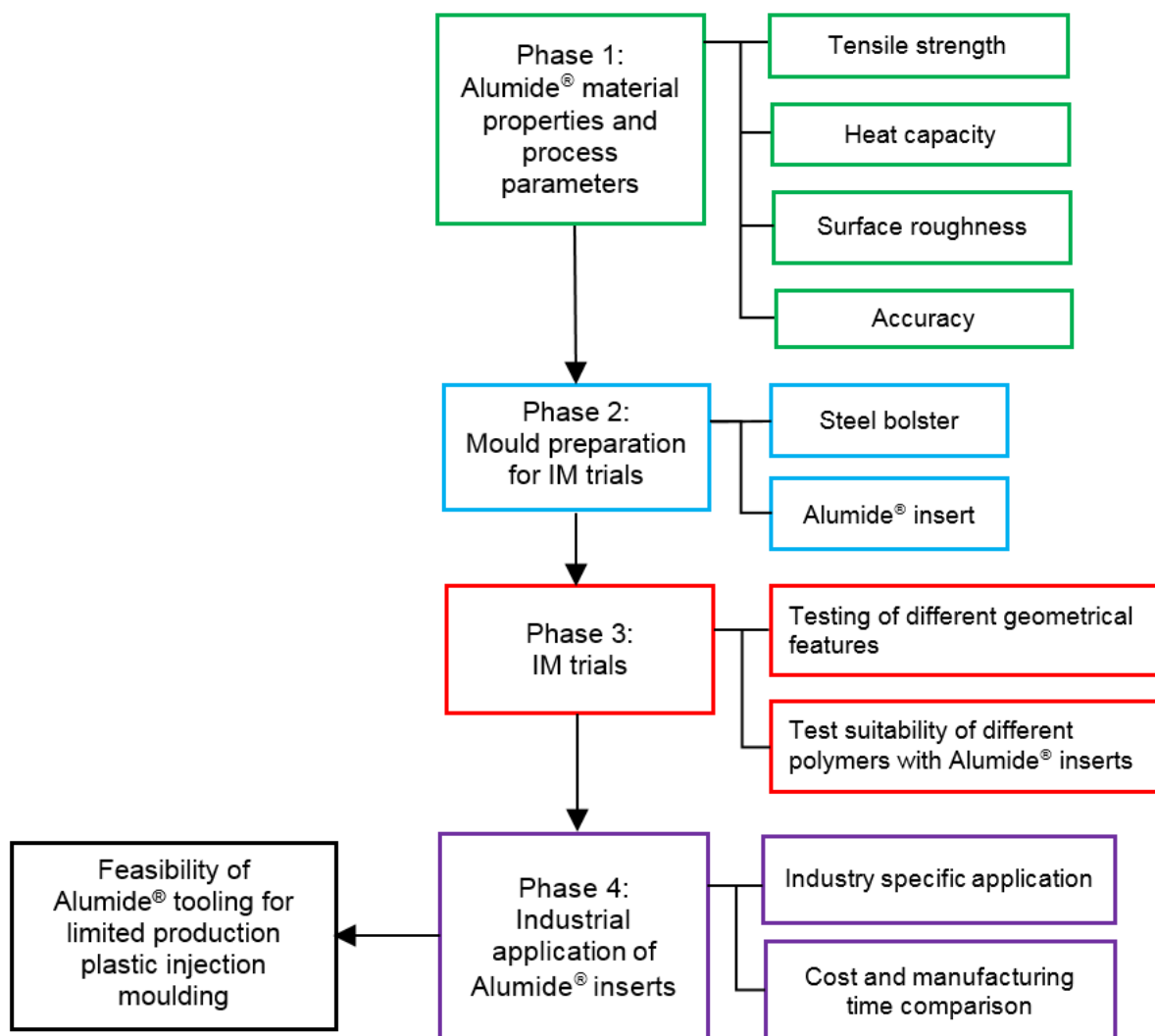


Figure 4.1 Representation of the four-phased approach to determine the feasibility of Alumide® inserts for injection moulding applications.

Alumide® test pieces and inserts used in the four phases were manufactured through an EOS P380 LS machine using standard process parameters. The four phases of the study are described in detail in the following sections.

4.2 Phase 1: Alumide® material properties and process parameters

This phase examined and verified some of the mechanical material properties of LS Alumide®. Limited data are available from the original equipment supplier (EOS) regarding material properties of LS Alumide® and material properties such as specific heat capacity, need to be obtained for design optimisation of the Alumide® inserts through finite element analysis. The layout of the experiments conducted during Phase 1 is schematically shown in Figure 4.2.

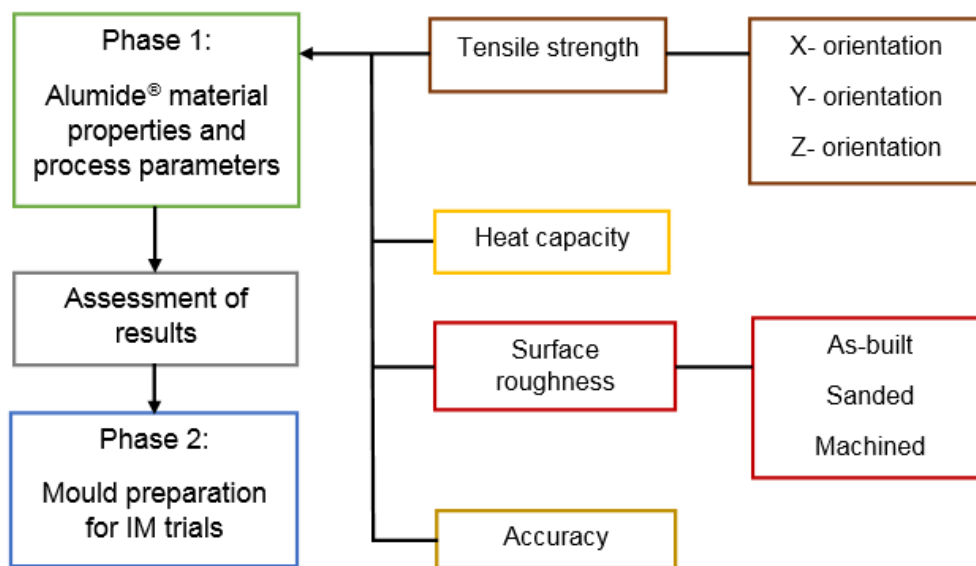


Figure 4.2 Schematic representation of experiments conducted during Phase 1.

4.2.1 Alumide® tensile strength

Aim

The aim of this experiment was to determine which build orientation would result in the highest Ultimate Tensile Strength (UTS) of an Alumide® product.

Procedure

Alumide® tensile test pieces orientated in the X, Y and Z directions inside the build volume of an EOS P380 LS machine, were manufactured using standard build parameters. The different build orientations of the tensile test pieces are shown in Figure 4.3.

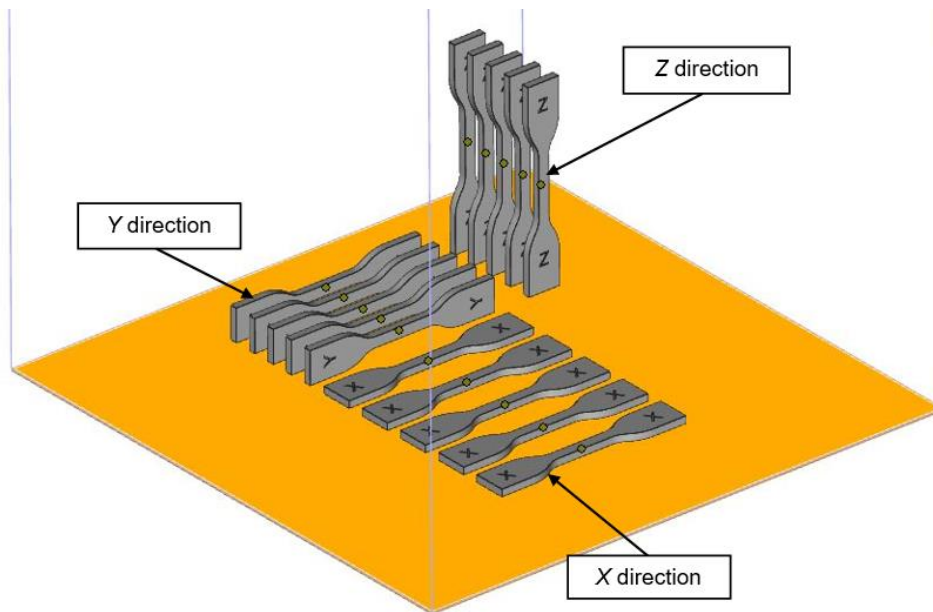


Figure 4.3 Different build orientations used to manufacture tensile test pieces in Alumide®.

Tensile strength tests were performed on test pieces manufactured according to ISO 527-1 specifications, using a calibrated MTS Criterion™ Model 43 tensile testing machine, as shown in Figure 4.4.



Figure 4.4 MTS Criterion™ Model 43 tensile testing machine used to conduct the tensile testing of the Alumide® test pieces.

Results

The UTS results obtained from the tensile testing of the Alumide[®] test pieces are summarised in Table 4.1. From the results it can be concluded that the build orientation has a significant influence on the UTS of an Alumide[®] test piece. Test pieces manufactured in the Z direction generally showed lower UTS compared to test pieces manufactured in the X and Y directions. This can be explained by how effectively one sintered layer is “bonded” to the previous one as well as the cross-sectional area of the sintered layers.

Table 4.1 UTS results obtained from Alumide[®] tensile test pieces.

Test piece number	Build orientation		
	X	Y	Z
	UTS (MPa)	UTS (MPa)	UTS (MPa)
1	44.72	43.31	41.89
2	44.56	42.91	40.45
3	44.64	43.15	41.66
4	44.72	43.20	41.78
5	44.60	42.95	41.37
Average	44.65	43.10	41.43

Discussion

From Table 4.1 it can be seen that the largest value of the UTS occurs with samples manufactured in the X direction. The values obtained for UTS from this experiment were less than the value of 48 MPa for Alumide[®] provided by the supplier (Table 3.3) of the material, namely EOS [108]. During the AM process, standard build parameters and settings were used as specified by EOS. To validate the parts manufactured by the EOS P380 LS machine (which is annually calibrated and serviced by EOS), tensile test pieces were manufactured using polyamide PA 2200 material and tested using the same

MTS Criterion™ tensile testing machine used for the Alumide® test pieces. The average UTS for the PA 2200 test pieces in the Y direction was 45.2 MPa and for the X direction 48.4 MPa. The results of the PA 2200 test pieces in the X direction were within 48 MPa, as specified by EOS for PA 2200 [109]. From the results obtained using the PA 2200 test pieces, it can be concluded that the P380 LS machine manufactured AM parts according to EOS specifications.

4.2.2 Specific heat capacity of Alumide®

Aim

The aim of this experiment was to obtain the specific heat capacity values for Alumide®. These values are not provided by the supplier and are required for heat flow simulation when Alumide® is used in an IM tooling application.

Procedure

Alumide® samples produced through AM were tested at the Council for Scientific and Industrial Research (CSIR), National Centre for Nanostructured Materials. The specific heat capacity was determined through the Differential Scanning Calorimetry (DSC) method using a TA Instruments DSC Q2000 V24.10 device. During the test, three Alumide® samples, weighing about 6.2 mg, each were exposed to heating at a rate of 10 °C/min in a nitrogen atmosphere. After cooling, the samples were exposed to a second heating cycle.

Results

The average heat capacity results for the second heating cycle are shown in Figure 4.5, with the peak value of the graph indicating the melting point of Alumide®. This occurs at 177.2 °C which compares favourably to the manufacturer's specified value of 172 to 180 °C. The intersection point between the extrapolated baseline curve and the linear section of the ascending peak slope results in the onset temperature of the melting phase [110]. From the graph, this temperature occurs at 169.4 °C which corresponds to the Vicat softening point of 169 °C, as indicated in the material data sheet for Alumide®.

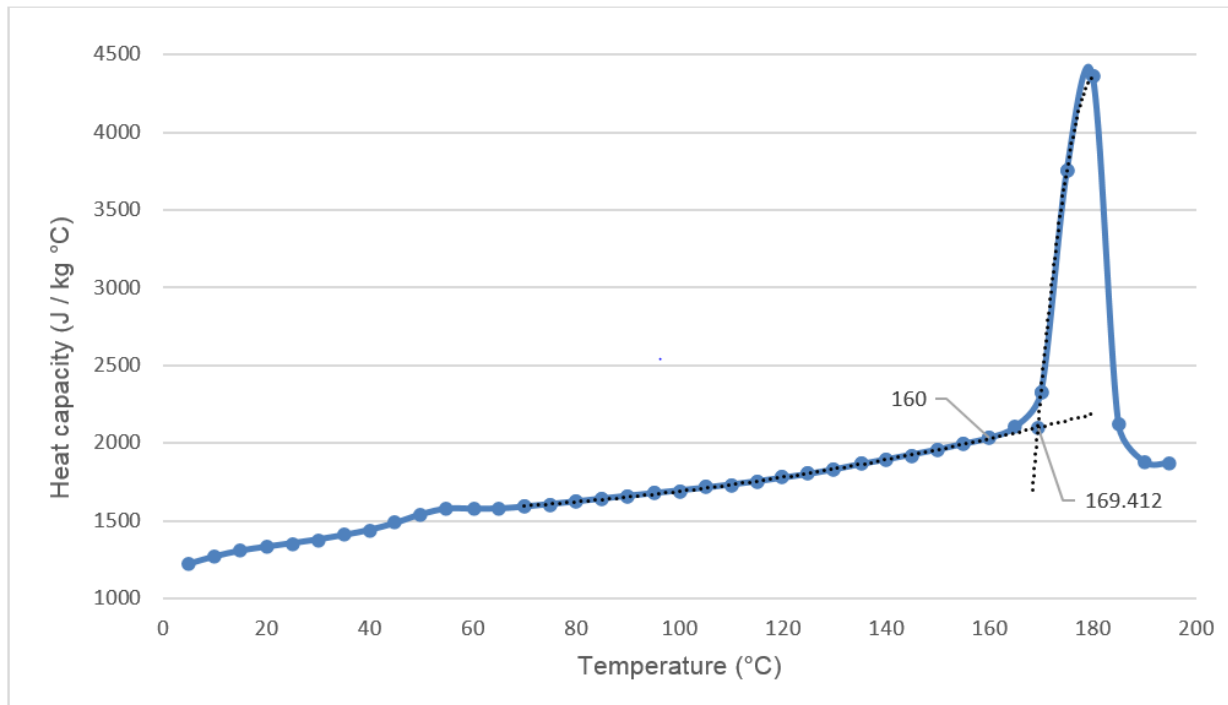


Figure 4.5 Heat capacity values of Alumide® at different temperatures showing the extrapolated intersection point from the baseline curves.

Discussion

From Figure 4.5 it can be concluded that Alumide® starts to soften at the extrapolated intersection point at a temperature of 169 °C. During the IM process, the Alumide® inserts will deform at this temperature due to the injection pressure of the molten polymer. The maximum useful operating temperature of Alumide® inserts for IM applications can be taken as 160 °C, which is the value before the curve starts to deviate from the baseline before the onset of the melting phase, as shown in Figure 4.5. From the heat capacity test results, it is apparent that the polyamide component of Alumide® is the main influence on the heat capacity properties of the Alumide® material.

4.2.3 Accuracy of Alumide® products

Aim

The aim of this experiment was to determine the accuracy of the LS process using Alumide® powder.

Procedure

Products manufactured from Alumide® through the LS process were scanned with a Renishaw touch probe scanner to determine the accuracy of the manufactured products. The scan data was compared to the CAD data of the products.

Results

Figure 4.6 shows a press tool for a cranio-plate prototype. A titanium plate was to be pressed over the Alumide® insert using hydroforming technology. The deviation across the surface of the tool was found to be within a -0.05 to 0.052 mm range when compared to the original CAD of the tool.

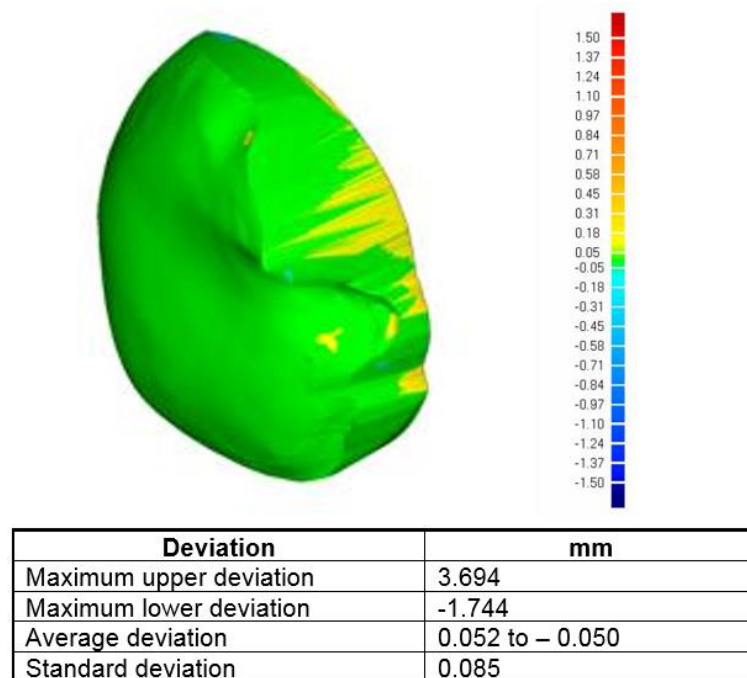
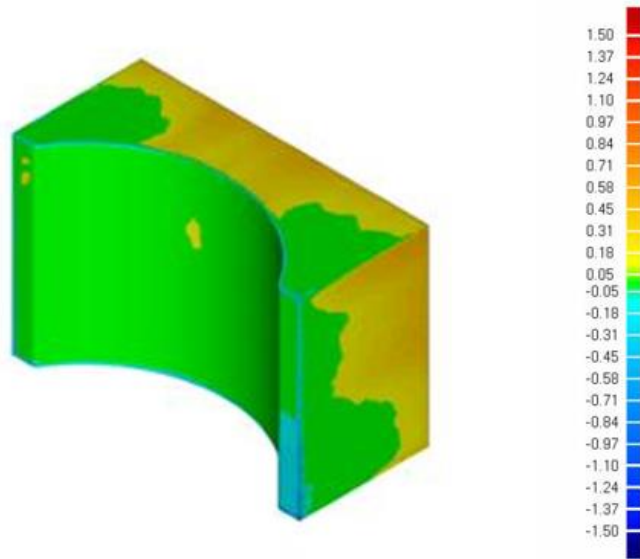


Figure 4.6 Accuracy results of a cranio-plate press tool prototype.

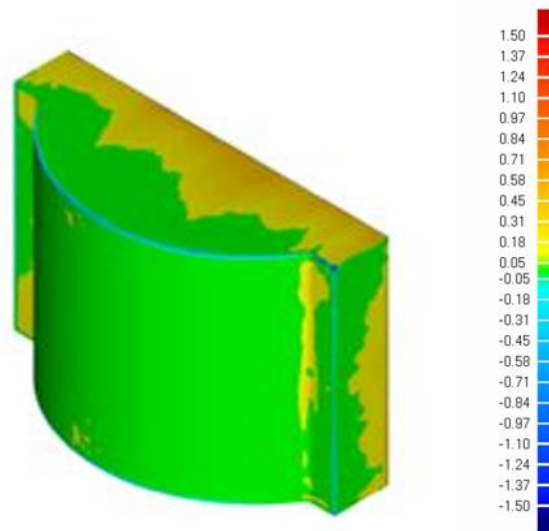
Figure 4.7 shows a design of a female part of a press tool that was tested at CUT to determine the spring-back of an aluminium plate when pressed between the two halves of the Alumide® tool. The deviation across the surface of the press tool shown in Figure 4.7 was between -0.063 to 0.107 mm.



Deviation	mm
Maximum upper deviation	0.644
Maximum lower deviation	-3.023
Average deviation	0.107 to -0.063
Standard deviation	0.104

Figure 4.7 Accuracy results of a female half of a press tool.

Figure 4.8 shows a design of the male part of the same press tool that was to be tested at CUT. The deviation indicated in Figure 4.8 across the surface of the press tool was between -0.043 to 0.087 mm.



Deviation	mm
Maximum upper deviation	0.688
Maximum lower deviation	-1.814
Average deviation	0.087 to -0.043
Standard deviation	0.089

Figure 4.8 Accuracy results of the male half of a press tool.

Discussion

From these results it can be concluded that an accuracy of up to 0.1 mm can be achieved with the LS process of Alumide[®], which is sufficiently accurate for it to be used to manufacture inserts for the IM process according to the DIN 16742 standard for plastic mouldings.

4.2.4 Surface roughness of Alumide[®] products

The characteristic stair step texture of AM processes on curved and inclined surfaces can result in rough surfaces, unsuitable for IM applications. The effect is less prominent on surfaces with a small incline compared to surfaces with a steep incline. Figure 4.9 illustrates the difference between the stair step effect on a surface with a 1° and 45° incline, for a layer thickness of 0.15 mm, typically used to manufacture Alumide[®] parts.

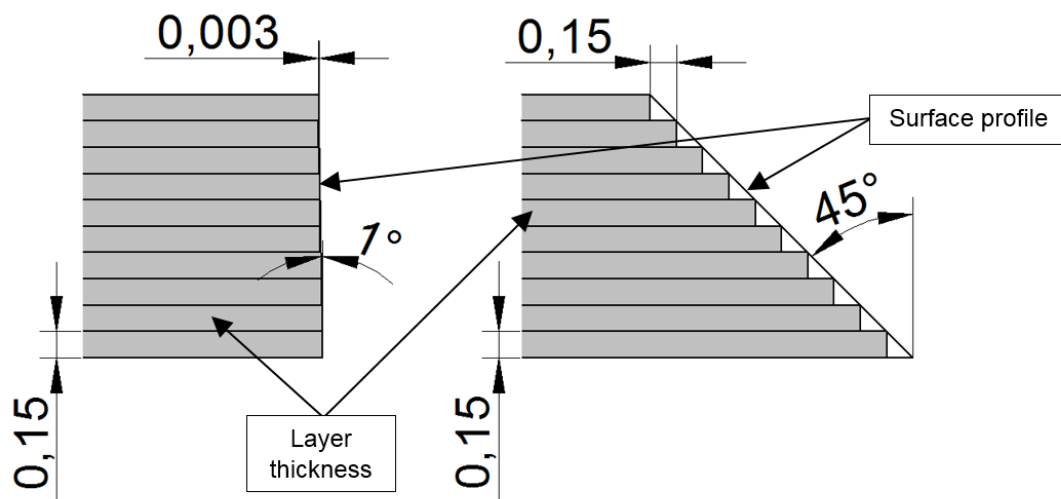


Figure 4.9 Comparison of the stair step effect on a surface with a 1° and 45° incline.

Aim

The aim of this experiment was to determine the effect of different finishing techniques to improve the surface finish of an Alumide[®] product.

Procedure

Two products, as shown in Figure 4.10 A and B, with surface angles of 3° and 45° respectively were designed for this experiment. A 3° surface angle was decided upon since it represents the recommended smallest draft angle range of 1 to 5° for plastic parts

manufactured through IM. Because of the layer-by-layer manufacturing process of AM, a surface angle of 45° results in the most significant stair step texture and was therefore also included in the experiment.

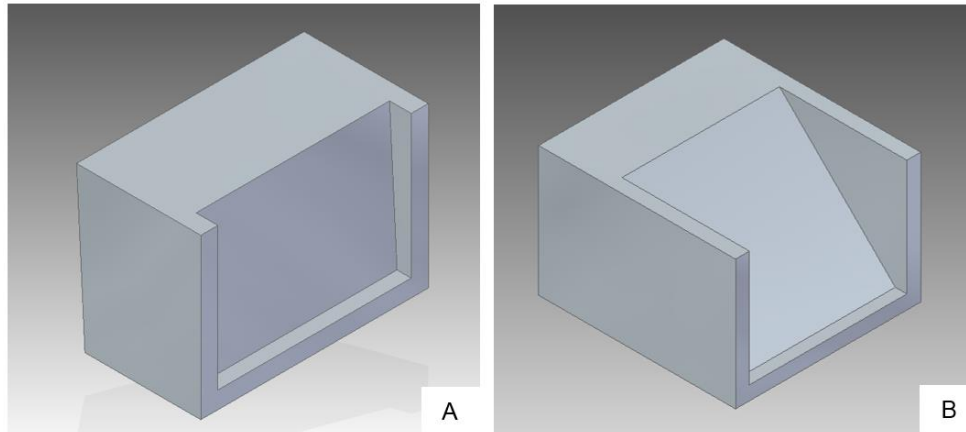


Figure 4.10 Products used during the surface roughness experiment, (A) 3° surface angle and (B), 45° surface angle.

Three sets of Alumide[®] products were manufactured through an EOS P380 LS machine. One set was machined with a 3 mm ball nose cutter using a Dahlih 720 CNC milling machine with the following machining parameters:

- Spindle speed of 6000 revolutions per minute.
- Feed rate of 800 mm per minute.
- Cut increment of 0.25 mm in the Z direction between each machining pass.

The second set was polished with 320 grit sandpaper followed by 400 grit sandpaper and the third set was kept as manufactured. The surface roughness of each set was measured using a Mitutoyo SURFTEST SJ-210 surface roughness measuring device. The surfaces of the products were positioned such that they were parallel to the axis of movement of the stylus. This ensured that the stylus was in proper contact with the surface to be measured. The surface roughness was measured at three positions across the build direction of the layers, as shown in Figure 4.11.

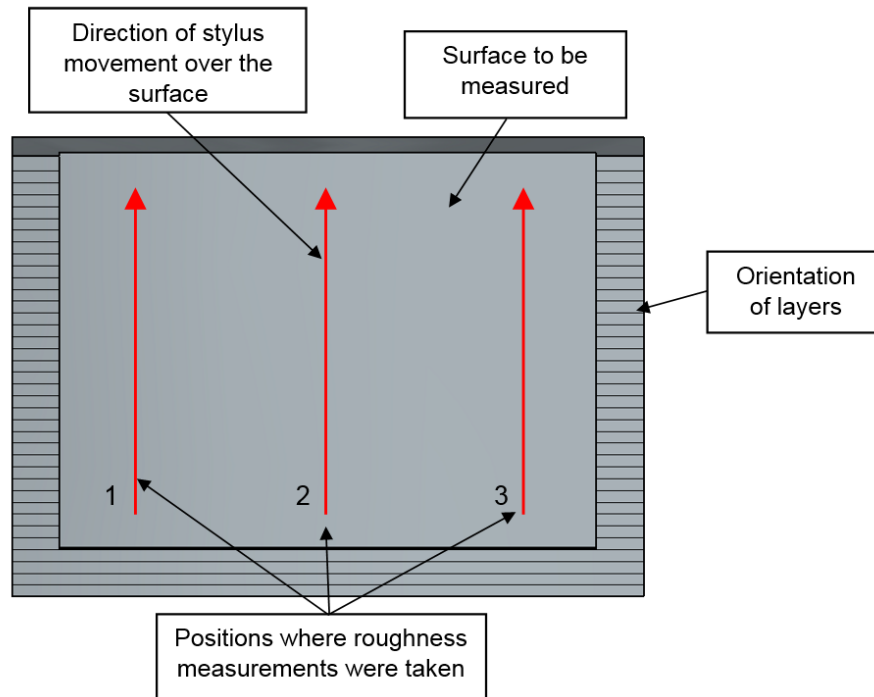


Figure 4.11 Position and direction of surface roughness measurements taken on the surface angle of the test products.

Results

The values of the surface roughness obtained for each surface is summarised in Table 4.2.

Table 4.2 Surface roughness of Alumide[®] test products after polishing and machining operations.

	R _a value as grown	R _a value polished	R _a value machined
3° surface angle	16.495	3.573	1.729
	16.500	3.680	1.737
	16.387	3.715	1.754
	16.469	3.735	1.747
	16.517	3.726	1.749
	16.507	3.662	1.731
	Average	16.479	3.682
45° surface angle	22.034	6.083	3.160
	22.075	6.108	3.150
	22.037	6.214	3.152
	22.133	6.282	3.151
	21.977	6.400	3.147
	22.017	6.169	3.164
	Average	22.046	6.209

Discussion

From the results it is apparent that surface finishing techniques, such as polishing and machining, have a significant effect on the surface roughness of an Alumide[®] product. A rough surface finish could cause molten polymer to bond to the Alumide[®] insert during an IM cycle. This will increase the demoulding forces required to eject a part from an Alumide[®] insert, which could result in damage to the part as well as the Alumide[®] insert.

The surface roughness values obtained from polishing and machining operations compare favourably to a C-2 surface finish, according to the international standard for surface roughness values from the Society of Plastic Industry. According to this standard, a C-2 surface finish is obtained after polishing a steel mould with a 400 grit polishing stone. This surface finish reduces the demoulding forces required to eject the part from the insert during an IM cycle.

From these results it is recommended that an Alumide[®] insert should at least be polished by means of sanding before it is used in an IM process. To maintain accurate dimensions of an Alumide[®] insert, at least 0.11 mm extra material need to be added to the surfaces of the insert. This extra material is required for the removal the stair step texture by sanding on inclined surfaces with a layer thickness of 0.15 mm, as shown in Figure 4.9. If a machined surface finish is required, extra material also needs to be added to the surfaces of the insert during the design of the insert. This extra material will be removed during the machining process while still maintaining accurate dimensions of the Alumide[®] insert.

4.3 Phase 2: Mould preparation for injection moulding trials

During Phase 2, pockets, ejector pin holes and cooling channels were machined into a steel bolster. Post-processing operations (for example backfilling) on the Alumide[®] inserts were completed before machining operations commenced. The machined bolster and Alumide[®] inserts were assembled and fitted into an IM machine to perform mould trials. The layout of Phase 2 is schematically presented in Figure 4.12.

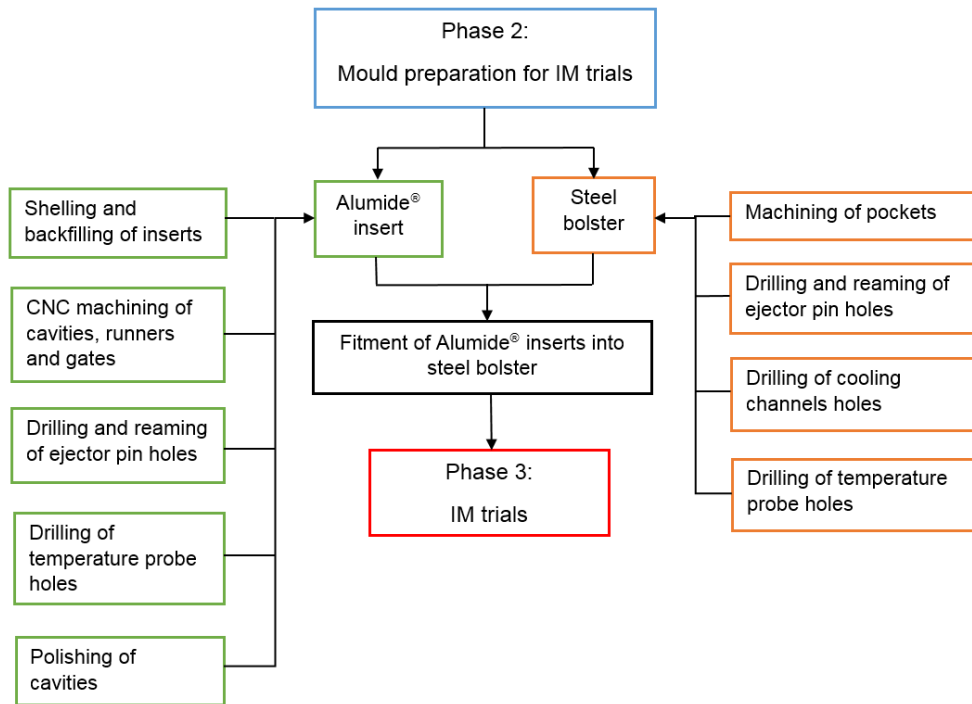


Figure 4.12 Schematic representation of Phase 2.

4.3.1 Steel bolster preparation.

A standard steel bolster for IM applications was purchased from a local supplier. Pockets for the Alumide® inserts were machined into the bolster using a Dahlih 720 CNC milling machine. Holes for ejector pins, temperature probes and cooling channels were also machined into the bolster. The dimensions and the components of the steel bolster are shown in Figure 4.13.

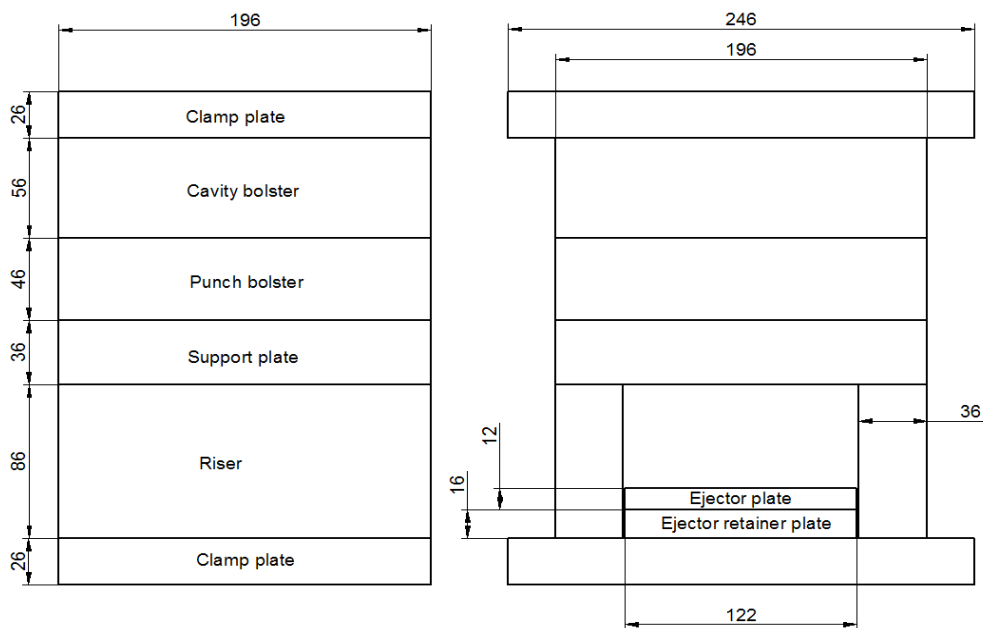


Figure 4.13 Dimensions and components of the steel bolster used during the IM trials.

The same outer dimensions (length, width and thickness) were used for all the Alumide[®] inserts during this study. The same bolster could then be utilised for all the IM trials. The inlet and outlet positions of the cooling channels were also maintained for each insert. Figure 4.14 shows the pockets, O-ring grooves and the ejector pin holes machined into the components of the steel bolster.

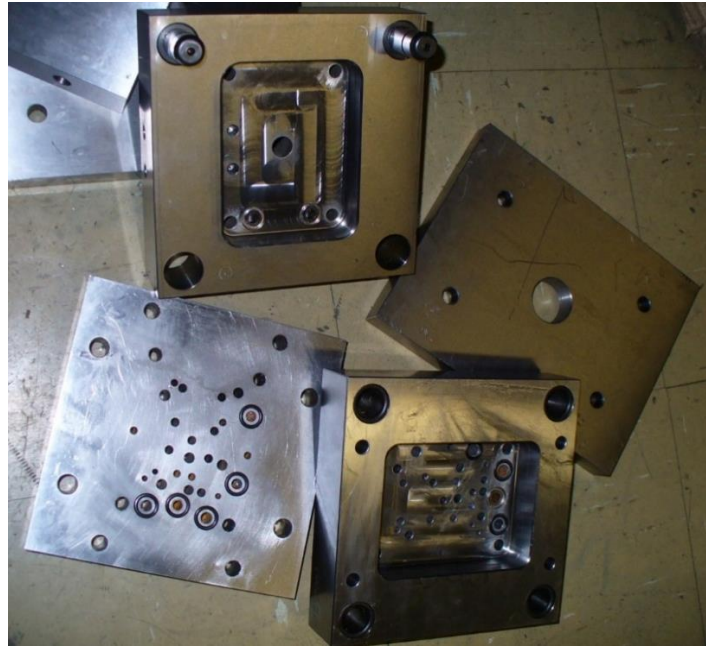


Figure 4.14 Mould components of the steel bolster with machined pockets, O-ring grooves and ejector pin holes.

4.3.2 Alumide[®] insert preparation

Shelling of Alumide[®] inserts

Significant internal stresses are induced in Alumide[®] parts during the AM LS process with an increase in stress as the volume of the part increases. These stresses can result in warpage of the insert during the AM manufacturing stage [111]. A method to overcome this problem is to shell the parts.

Table 4.3 compares the manufacturing time and cost of a solid and shelled Alumide[®] insert for three different part dimensions. From Table 4.3 it can be observed that shelling of inserts with small dimensions, does not influence the manufacturing time and cost of the insert. As the dimensions of the part increase, the manufacturing time and cost of the shelled insert is less than the solid part with the same dimensions. From these results it

can be concluded that shelling can also reduce the manufacturing costs and time of an Alumide® insert, since less material is used and it can be produced in a shorter time frame.

Table 4.3 Time and cost comparisons between solid and shelled Alumide® parts.

Part dimensions	Manufacturing time	Manufacturing cost
50 x 30 x 40 (solid)	2 h 46	R 6226.83
50 x 30 x 40 (shelled)	2 h 46	R 6226.83
130 x 100 x 40 (solid)	3 h 15	R 6412.17
130 x 100 x 40 (shelled)	2 h 56	R 6290.20
200 x 150 x 40 (solid)	4 h 46	R 6995.83
200 x 150 x 40 (shelled)	3 h 58	R 6688.03

During the IM process, Alumide® inserts inside a mould cavity are subjected to high injection pressures and temperatures as the molten plastic is forced into the mould cavities. The shelled Alumide® inserts need to be backfilled so that they will not collapse when subjected to these injection pressures.

Possible backfilling materials

A supplier of epoxy resin casting materials in South Africa suggested the following two materials as a possible backfilling solution:

- Axson EPO 4030
- Alwa-Mould D

Axson EPO 4030

Applications for this material are thermoforming moulds, polyurethane foam moulds and RIM injection moulds. Some of the material's characteristics are:

- Low viscosity.
- Good heat exchange.
- Fillers can be added (aluminium).
- Low shrinkage.
- Easily machineable.

Alwa-Mould D

Alwa-Mould D is a two-component resin based on methacrylate which is filled with aluminium for the production of moulds. A self-induced exothermic process cures the resin after addition of a hardener. Applications for this material are vacuum forming moulds, holding fixtures, models for digitising and duplicating, prototype moulds for blow moulding and compression moulding moulds. Some of the material's characteristics are:

- Very low linear shrinkage.
- Dimensional stability under heat.
- Easily machineable.
- Low viscosity.

Properties of backfilling materials

Properties of the possible backfilling materials are summarised in Table 4.4.

Table 4.4 Properties of the possible backfilling materials.

	AXSON EPO 4030	ALWA-MOULD D
Cost	R 100 / kg	R 140 / kg
Temperature resistance	120 °C	145 °C
Demoulding time	Up to 24 hours	± 50 min
Pot life	140 – 180 min (25 °C)	17 – 20 min (21 °C)
Hardness	84 -85 SHORE D	86 SHORE D
Compressive strength	90 MPa	80 - 90 MPa
Coefficient of thermal expansion	$55 \cdot 10^{-6} \text{ K}^{-1}$	$612 \cdot 10^{-6} \text{ K}^{-1}$
Shelf life	18 months	12 months
Linear shrinkage	0.08 %	± 0.1 %

Selection of a suitable backfilling material

To select a suitable backfilling material for Alumide[®] inserts, the following criteria were considered:

- It must be quick and easy to use. A time consuming/difficult process results in a labour-intensive operation that will increase the cost of the backfilling procedure.
- It must be able to withstand the injection pressures of the IM process (compression forces).
- It must be able to withstand the temperatures that occur during the IM process.
- It must be easily machineable. Features such as ejector pin holes need to be machined into the backfilling material.
- The material must be readily available in South Africa.
- It must be cost-effective.
- It must have a reasonable pot life. This will assist when the material needs to be slowly poured into the back of the insert, to avoid the forming of air pockets.

The negative aspect of Axson's EPO 4030 is its long demoulding time (up to 24 hours). This will lengthen the delivery time of the backfilled Alumide[®] inserts to a client. Alwa-Mould D's negative aspect is that during the casting and curing process, reaction peak temperatures of up to 130 °C can be reached. During the casting process, when the exothermic process peaks, the material will have a large linear expansion. The material's manufacturer advises that during this process the mould's ends should be released to allow for this expansion. The high exothermic temperature and linear expansion property of Alwa-Mould D during the curing process therefore render this material unsuitable as a backfilling material for Alumide[®] inserts. The high temperature together with the expansion forces will permanently deform the Alumide[®] insert.

Despite the long demoulding time of Axson EPO 4030, it is preferable to Alwa-Mould D as backfilling material suitable for Alumide[®] inserts. This material does not show any significant temperature rise during the mixing and curing process.

Deformation during the backfilling process

Experiments were conducted to determine a suitable shell wall thickness for an Alumide[®] insert that will not deform when filled with EPO 4030. Test pieces with the same

cavity volume, but with varying wall thickness, were manufactured. Figure 4.15 shows the unfilled test pieces with the different wall thicknesses.

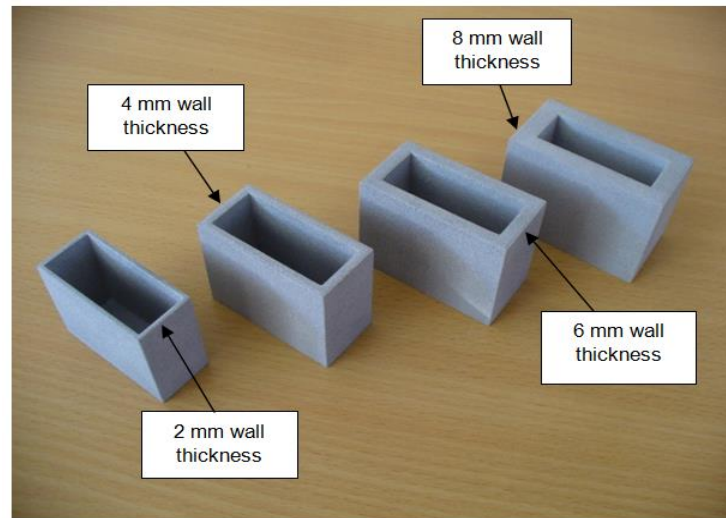


Figure 4.15 Unfilled Alumide® test pieces with varying wall thicknesses.

EPO 4030 was mixed according to the manufacturer's specifications, as indicated on the data sheet. The mixing ratio was:

- Resin.
- Hardener: 10% of resin weight.

The mixture was slowly poured into the cavities to minimise the forming of air pockets. Measurements were taken on the test pieces using a Mitutoyo micrometer before the cavities were filled with the EPO 4030. These measuring points were marked on the test pieces in order to measure at the same position after the cavities were filled, as shown in Figure 4.16.

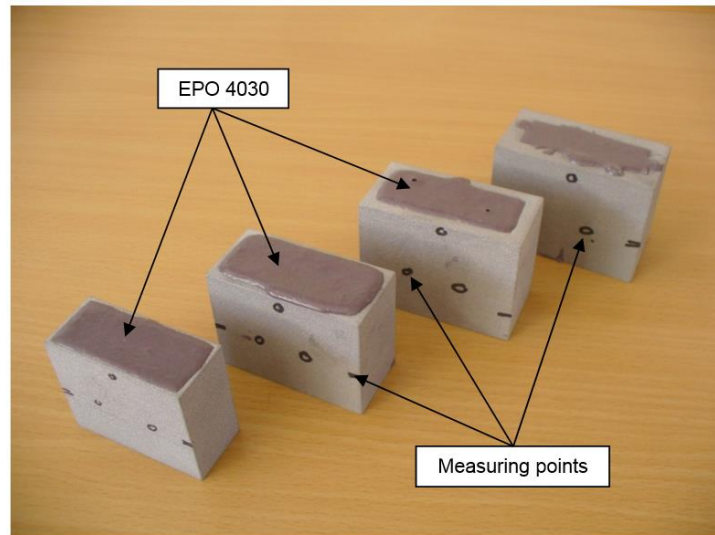


Figure 4.16 Test pieces filled with EPO 4030 with measuring points indicated.

Figure 4.17 indicates the location of the points where the measurements were taken schematically.

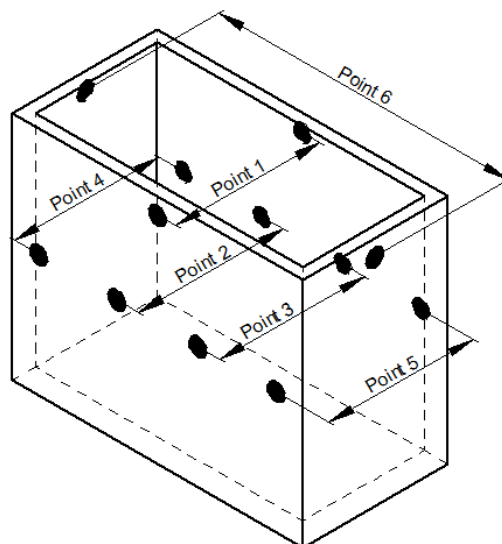


Figure 4.17 Location of the measuring points on the test pieces.

The deviation from the measurements taken before the filling of the test pieces, are summarised in Table 4.5.

Table 4.5 Deviation of the measuring points for different wall thickness test pieces.

Wall thickness	Deviation at measuring point					
	1	2	3	4	5	6
2 mm	0.04 mm	0.02 mm	0.03 mm	0.0 mm	0.0 mm	0.03 mm
4 mm	0.01 mm	0.01 mm	0.02 mm	0.0 mm	0.0 mm	0.01 mm
6 mm	0.0 mm	0.0 mm	0.0 mm	0.01 mm	0.0 mm	0.0 mm
8 mm	0.0 mm	0.0 mm	0.0 mm	0.0 mm	0.0 mm	0.01 mm

Discussion

From Table 4.5 it can be concluded that EPO 4030 resin does not significantly influence the dimensions of an Alumide[®] insert during the backfilling process. There are slight measurement deviations on the test pieces with two and four millimetre wall thickness, while the deviation on thicker walls is so small that it can be considered as negligible. From the results of Table 4.5 it can be concluded that an Alumide[®] insert with a wall thickness of more than 4 mm can be backfilled with EPO 4030 resin without any significant deformation occurring.

4.3.3 Backfilling of Alumide[®] inserts

The same outer dimensions (129.5 mm x 99.5 mm) of the Alumide[®] inserts were used during this study for fitment of different inserts into the same steel bolster. Alumide[®] inserts were manufactured without the holes for ejector pins, runners and gates. They were only manufactured with the shelled shape of the cavity and the conformal cooling channels, as shown in Figure 4.18. A wall thickness of 5 mm was used to shell the insert. This resulted in sufficient strength for internal features to prevent breakage and deformation during handling and backfilling. A rib along the edge of the cavity and features inside the cavity that needed to be backfilled, were added to the insert. This was to make provision for the meniscus effect occurring during the casting and curing of the backfilling resin.

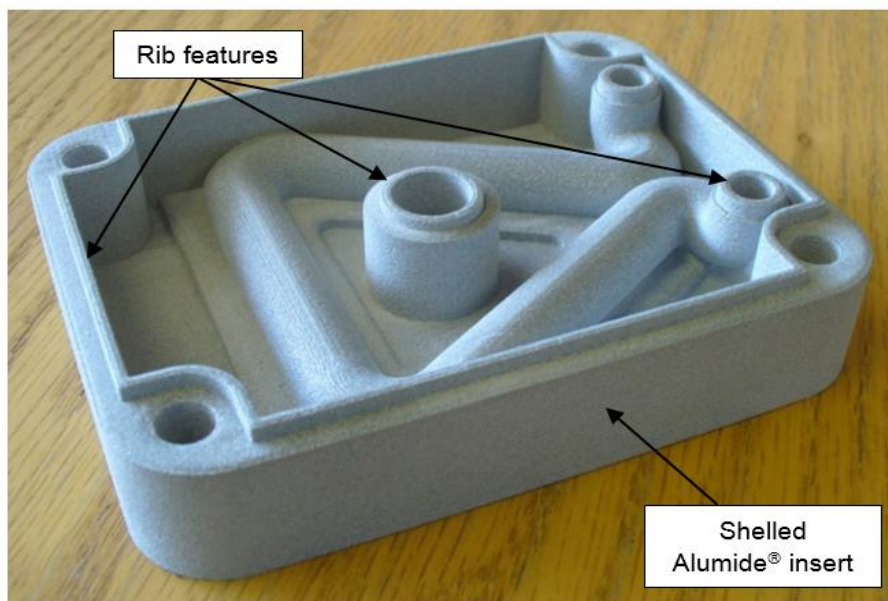


Figure 4.18 Shelled Alumide[®] insert showing the rib feature along the cavity and internal features.

Before the backfilling process commenced, all the powder inside the conformal cooling channels and the shelled cavity had to be removed. EPO 4030 resin was mixed according to the manufacturer's specification and slowly poured into the shelled cavities to avoid the formation of air bubbles. Air bubbles that formed rose to the surface of the cast epoxy during the curing phase of the resin, as shown in Figure 4.19.

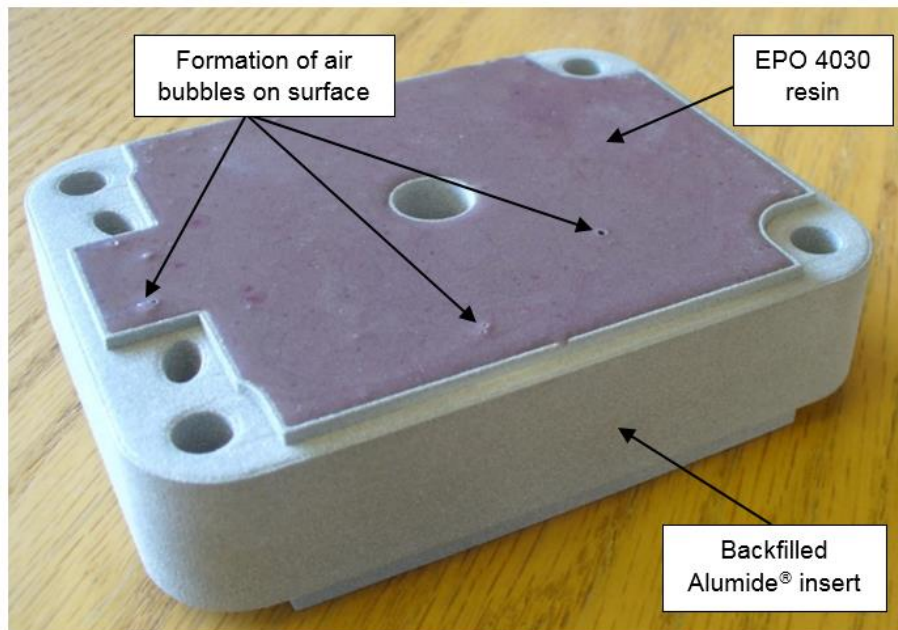


Figure 4.19 Backfilled Alumide[®] insert showing the formation of air bubbles on the surface.

4.3.4 Machining of Alumide[®] inserts

After the resin had cured, the sides and the rear surface of the insert were machined to obtain flat surfaces. A flat rear surface is required to avoid water leakage from the O-rings around the cooling channels' inlet and outlet holes. An uneven surface can also result in the deformation of the inserts when subjected to the clamping and injection pressures during a typical IM cycle. During the machining process, the air bubbles which had formed on the surface during the casting process were removed.

Ejector pin holes were not included in the design of the Alumide[®] inserts before the AM manufacturing process. These features need to be accurate to prevent molten polymer from leaking through between the holes and the ejector pins. Therefore, the ejector pin holes were only drilled and reamed into the insert after the backfilling process. Runners and gates were also machined into the cavities to obtain a smooth surface, improving the

flow of the molten polymer into the cavities. Figure 4.20 shows a machined Alumide[®] insert with ejector pin holes.

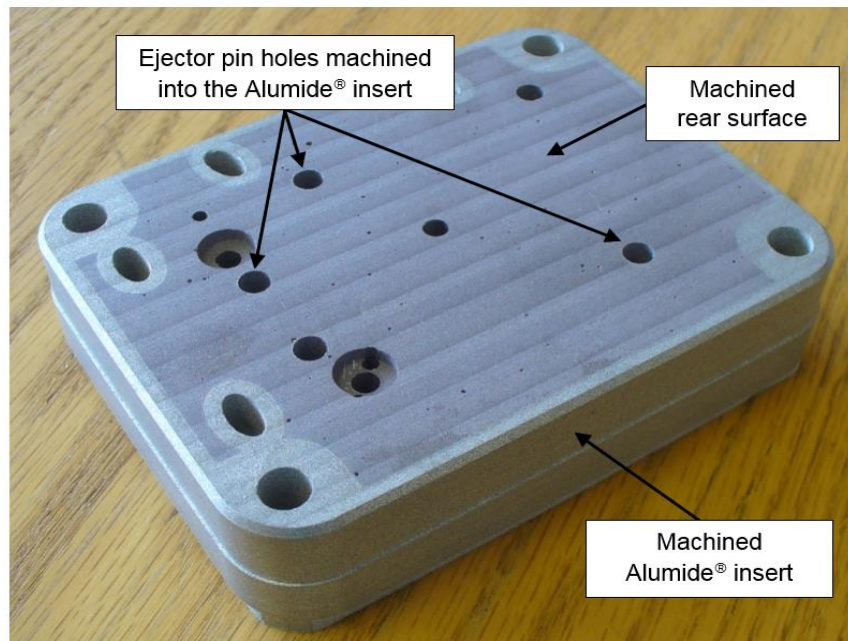


Figure 4.20 Alumide[®] insert with machined rear and outer surfaces as well as drilled and reamed ejector pin holes.

Depending upon the required surface finish, the cavities were lightly polished by sanding using 320 and 400 grit sandpaper. This was to reduce the surface roughness of the cavities caused by the stair step effect of the AM process, as described under Section 4.2.4. Surfaces requiring a polished finish were machined using a CNC milling machine. A 0.5 mm layer of material was added in the design to all the surfaces requiring machining after the build process. This provided enough material for a finishing cut and to still be within the required dimensions for the insert. Extra material (0.2 mm) was also added to the shut-off faces on the insert. The shut-off faces were then machined to the correct size to obtain a flat surface for the two halves of the insert to seal. The same finishing procedure was applied to all the Alumide[®] inserts used during the study.

4.3.5 Mould assembly

The machined Alumide[®] inserts were fitted into the steel bolster with ejector pins inserted. The mould assembly was fitted in a Haixing HXF 268 IM machine and temperature probes were inserted into the mould. Experiments were performed with water as a cooling medium

through the cooling channels. The temperature of the water was controlled by an industrial water chiller unit.

Temperature readings were taken inside the moulds using thermistor probes with a resistance of 10 K Ω . Readings from the probes were captured using a data acquisition DAQ NI-USB 6009 device from National Instruments, and an interface software program developed by the Research Group in Evolvable Manufacturing Systems in the Department of Electrical, Electronic and Computer Engineering, at CUT. Figure 4.21 shows the placement of the probes and Figure 4.22 illustrates the interface software and the portable computer connected to the DAQ device to collect the temperature readings during the IM trials.

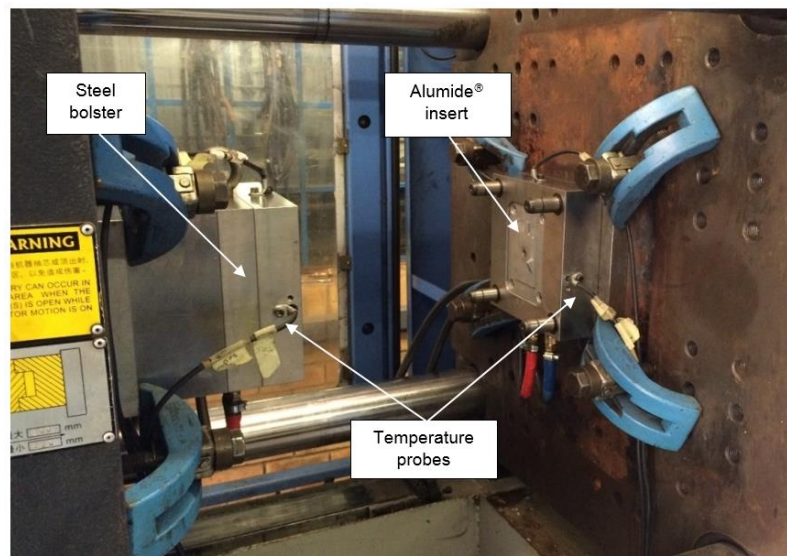


Figure 4.21 Assembled Alumide® inserts and steel bolster with temperature probes connected.

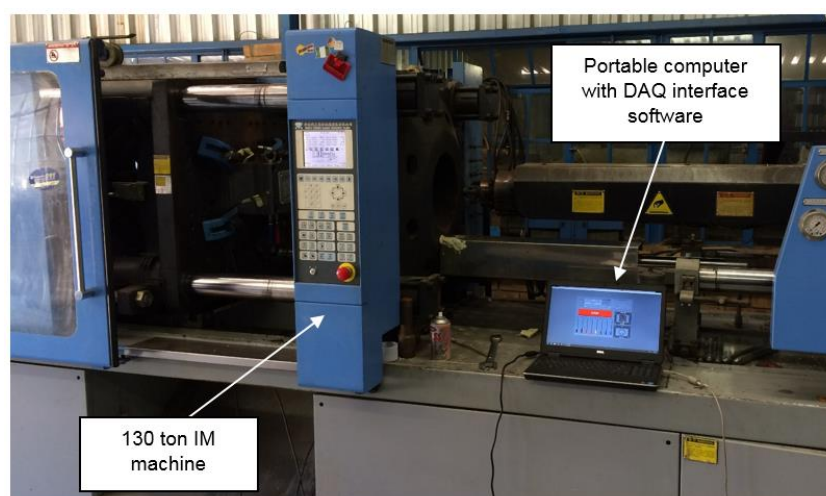


Figure 4.22 Portable computer with DAQ interface software connected to the temperature probes.

4.4 Phase 3: Injection moulding trials

During Phase 3, Alumide® inserts were manufactured and prepared for IM trials, as described during Phase 2. Experiments conducted with the Alumide® inserts were to determine the feasibility of using Alumide® inserts for IM applications. The layout of the experiments conducted during Phase 3 is schematically shown in Figure 4.23.

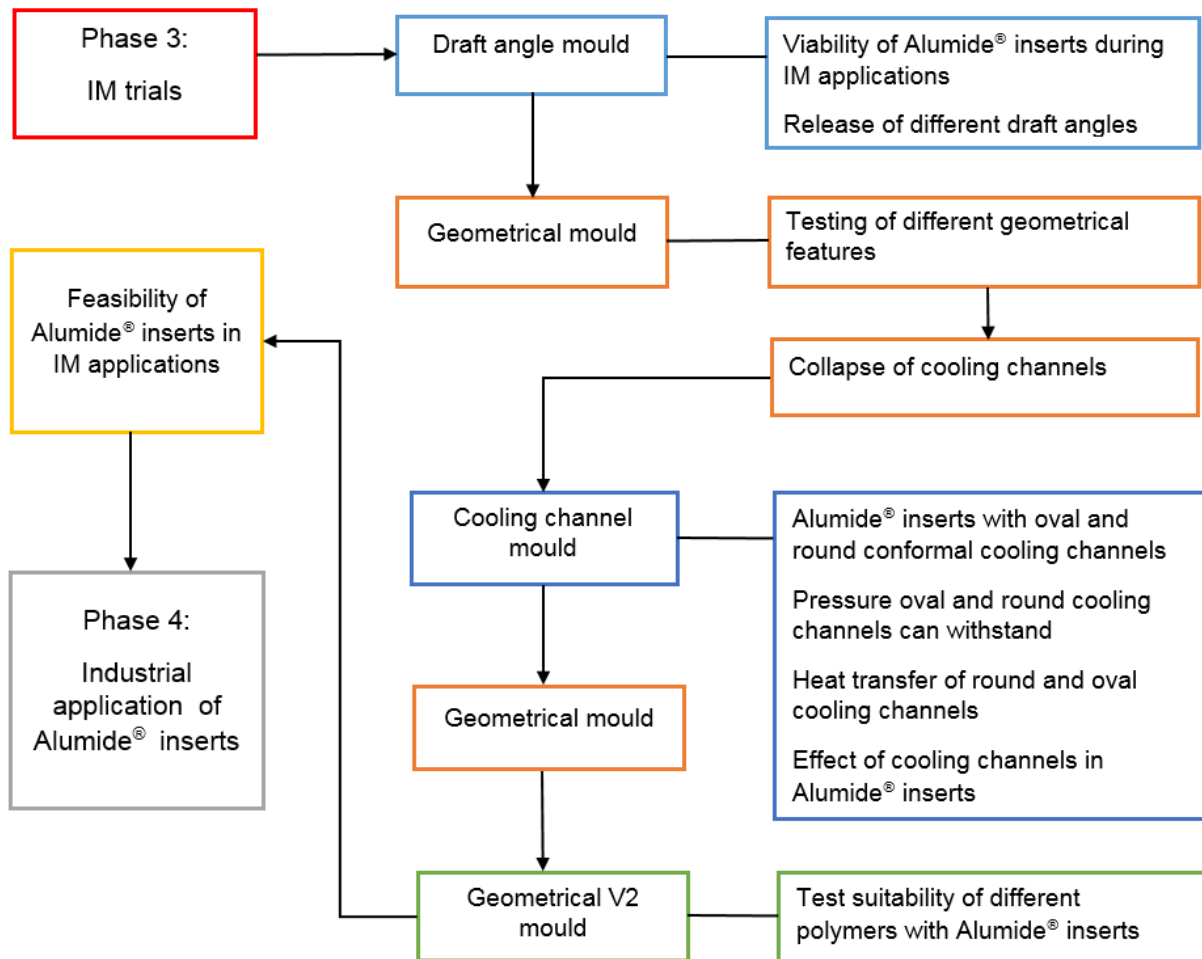


Figure 4.23 Schematic representation of experiments conducted during Phase 3.

Polypropylene (PP) was used during all the experiments due to its ease of mouldability and a minimum mould temperature range of 20 to 68 °C. It is also extensively used in appliance and consumer products and it is one of the most used polymer materials globally.

To test the suitability of using different IM polymers with an Alumide® insert, PP and the following polymers were used:

- Acrylonitrile-Butadiene-Styrene (ABS) has a melt temperature similar to PP and a minimum mould temperature range of 25 to 80 °C. ABS is extensively used for electrical enclosures as well as automotive and consumer products. These industries often require functional prototypes for testing and verification purposes.
- Polycarbonate (PC) was used to determine the influence of a polymer material with a high melt temperature injected into an Alumide[®] insert. The recommended melt temperature of PC is 300 °C. Due to the high melt temperature, PC requires a higher mould temperature than PP and ABS. The recommended minimum mould temperature range for PC is 70 to 120 °C.
- Polyamide 6 (PA 6) was used to determine the effect of injecting a polyamide material into Alumide[®], which is an aluminium-filled polyamide material. PA 6 has a melt temperature similar to PP and ABS, but requires a higher minimum mould temperature range of 70 to 110 °C.

4.4.1 Draft angle experiment

Aim

The aim of the draft angle experiment was to determine:

- The capability of the Alumide[®] and backfilling material to withstand the pressures and temperatures experienced during an IM cycle.
- The wear on the Alumide[®] insert (such as the ejector pins holes machined into the backfilled insert).
- If parts with different draft angles will release from a lightly polished Alumide[®] insert.

Procedure

Minimum recommended and mostly used draft angles for injection moulded components were applied to the part for this trial. Eight parts with the same outer dimensions but with different draft angles of 1°, 2°, 3°, 4°, 5°, 6°, 7° and 10° respectively, (as shown in Figure 4.24) were designed.

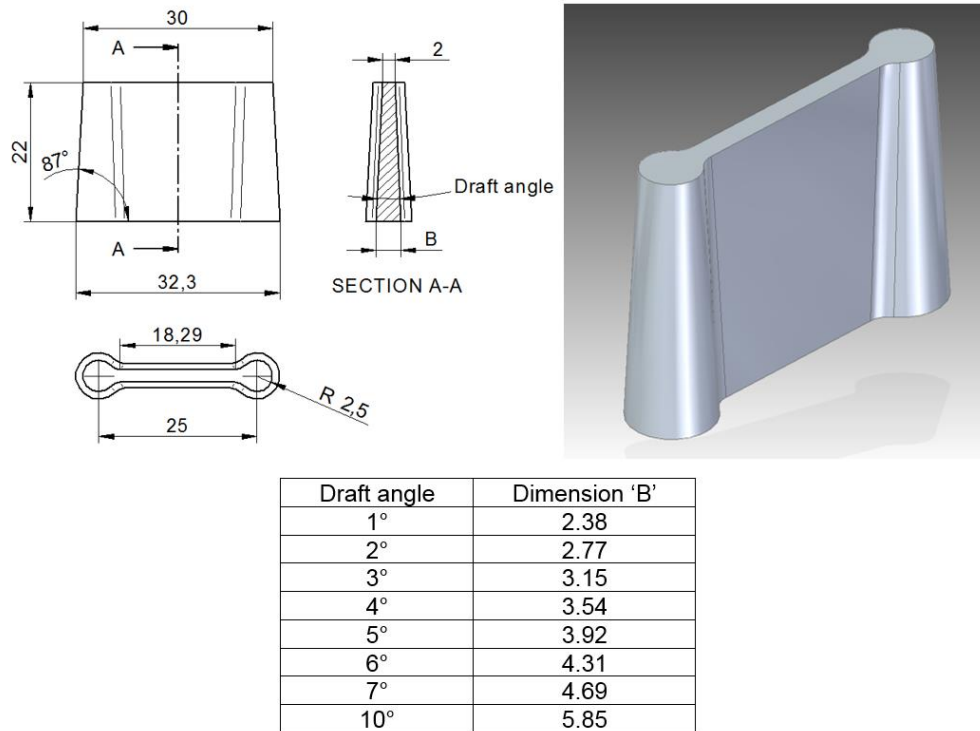


Figure 4.24 Dimensions and CAD model of the draft angle part used in the draft angle mould experiment.

Two Alumide® inserts were manufactured containing four of the draft angle parts per insert, as shown in Figure 4.25 A & B.

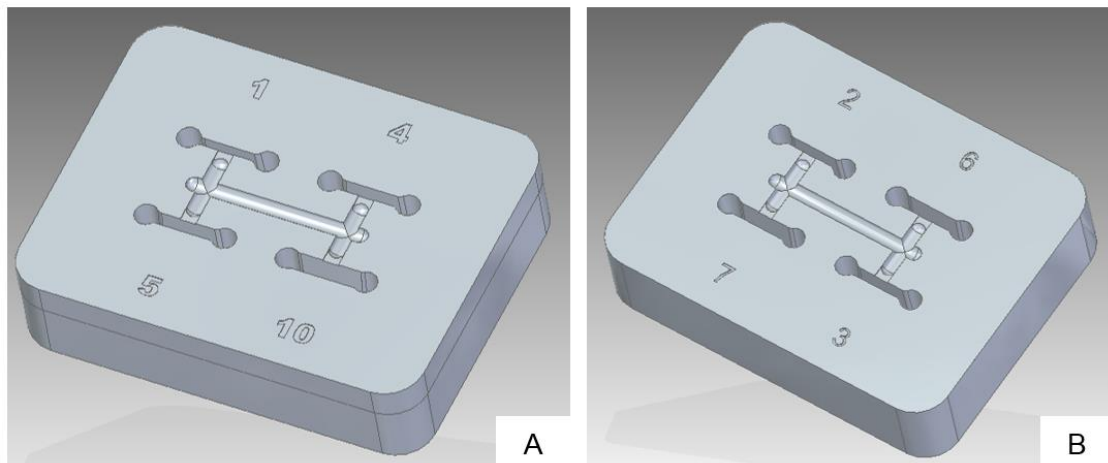


Figure 4.25 Alumide® inserts with four draft angle parts in each insert.

Conformal cooling channels were included in the Alumide® insert design. The inserts were shelled to reduce the building time and volume of the inserts before they were manufactured. Figure 4.26 shows a CAD model of the shelled insert with the conformal

cooling channel. The conformal cooling channel was placed at a minimum distance of 3 mm from the cavity surface.

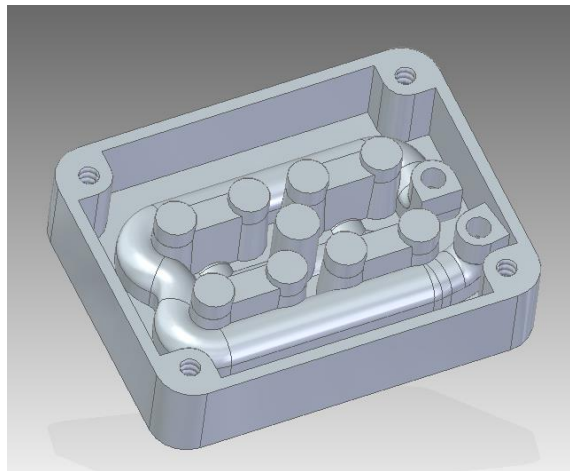


Figure 4.26 Shelled Alumide[®] insert with a conformal cooling channel.

A centre line radius of 9 mm for the conformal cooling channel was used for ease of removal of the un-sintered powder from the cooling channel, as shown in Figure 4.27.

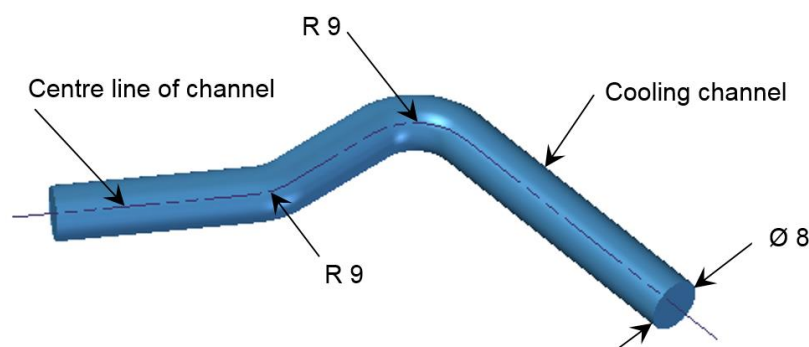


Figure 4.27 CAD representation of a conformal cooling channel showing the centre line radius of 9 mm used to assist with the un-sintered powder removal.

The Alumide[®] inserts were backfilled and machined as discussed in Section 4.3.3. The cavities were lightly polished by sanding using 320 and 400 grit sandpaper. The Alumide[®] inserts were mounted into the steel bolster and IM trials were conducted using PP.

Results

PP parts were manufactured from the Alumide[®] inserts with a cycle time of 54.1 seconds. All the different draft angle parts ejected from the cavities without any difficulties. After 100 parts were manufactured, the trial was ended and the Alumide[®] inserts were inspected for wear and deformation. The only wear noticed on the inserts was at the gate regions, as shown in Figure 4.28.

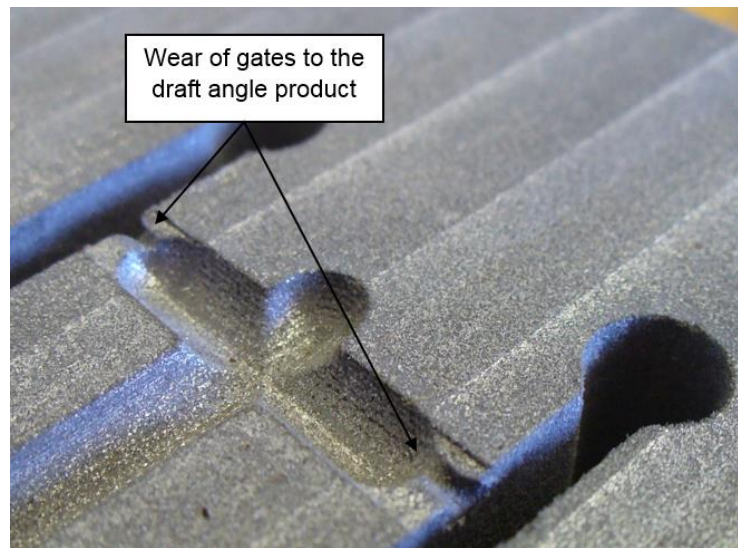


Figure 4.28 Wear on the gate features which deliver molten material to the cavities during an IM cycle.

The Alumide[®] and backfilled material was able to withstand the pressures and temperatures experienced during the limited run production. No wear (in the form of flashing) was observed at the ejector pin holes.

Discussion

Ejection from draft angles as small as one degree, included draft angle, is possible from an Alumide[®] mould with the surfaces lightly polished, providing the mould is designed with ejector pins close to these features.

4.4.2 Geometrical mould experiment

Aim

The aim of this experiment was to determine:

- The durability of different geometrical features, for example, knife-edge corners, which normally require secondary operations (such as EDM) to manufacture using conventional methods. Features which are complex and time consuming to manufacture using conventional manufacturing processes were also included in the insert design. These features included engraving, sharp internal corners and ribs with a height five times the nominal wall thickness.
- Durability of Alumide® cores to produce hole features in a part.
- The wear in regions of an Alumide® insert that cannot be cooled sufficiently due to mould constraints, such as screw holes and ejector pin features.

Procedure

A part with a wall thickness of 2 mm and outer dimensions of 91.2 x 61.2 mm² was designed with different geometrical features. These features included ribs with a thickness of 2 mm and a height of 10 mm as well as text features (engraving) 6.15 mm wide and 0.5 mm thick. One set of engraving was extruded outward and another set was extruded into the part. Boss features with internal hole diameters of 3, 4 and 5 mm respectively, were included to determine the durability of an Alumide® pin feature required to manufacture the hole of a boss feature. Figure 4.29 shows a CAD model and a part drawing indicating the dimensions of the different geometrical features.

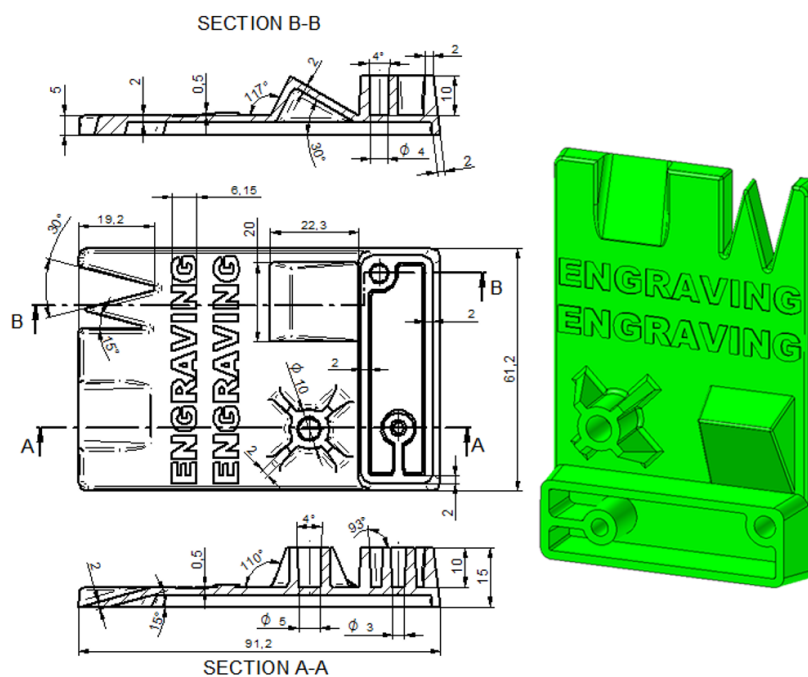


Figure 4.29 Dimensions and CAD model of the different geometrical features included in the part to be manufactured.

Round conformal cooling channels with a diameter of 8 mm were included into the Alumide[®] insert design. The conformal cooling channels were positioned to obtain the best possible cooling while avoiding mould features such as screw and ejector pin holes, as shown in Figure 4.30. A centre line radius of 9 mm for the conformal cooling channels was used for ease of removal of the un-sintered powder from the cooling channels, as shown in Figure 4.27. The inserts were shelled to reduce the building time and volume. The conformal cooling channels were placed at a minimum distance of 3 mm from the cavity surface. The inlet and outlet positions of the conformal cooling channels were placed at locations matching the cooling channel holes of the steel bolster.

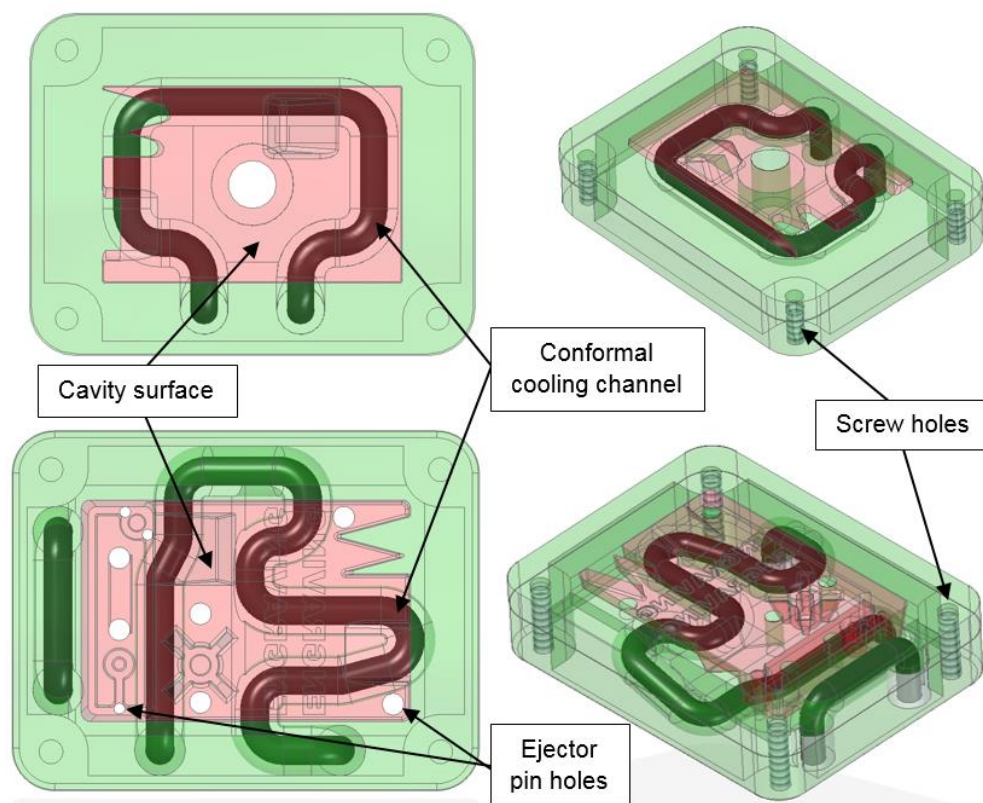


Figure 4.30 Layout of the conformal cooling channels avoiding mould features such as screw and ejector pin holes.

The cavity and punch of the inserts were polished to remove the stair step effect of features resulting from the AM build process, which could cause bonding of the molten polymer material to the Alumide[®] insert. Figure 4.31 shows some of the geometrical features in the as-built form with the stair step effect visible on these features.

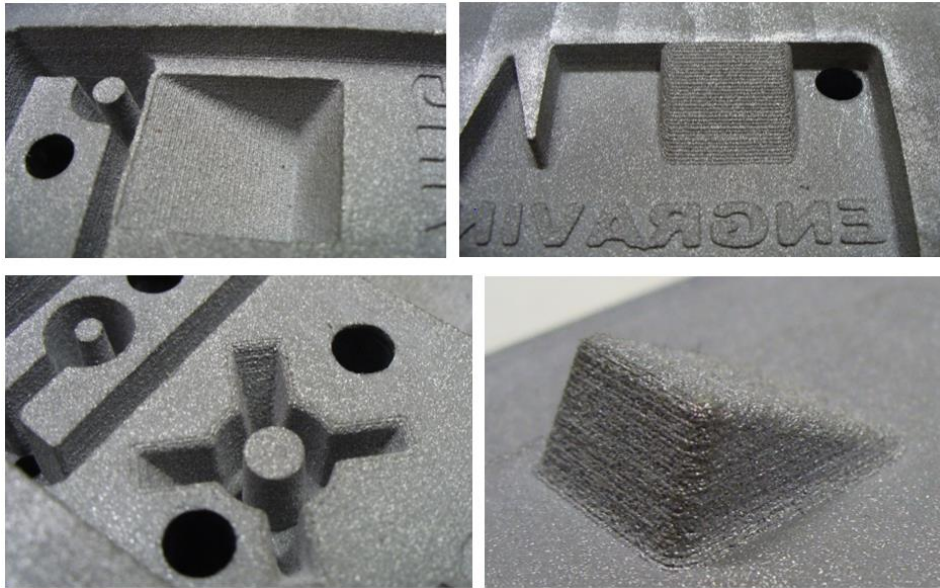


Figure 4.31 Stair step effect visible on the geometrical features of the Alumide® insert in the as-built form.

After backfilling and machining operations, the Alumide® inserts were polished by sanding using 320 and 400 grit sandpaper to remove the stair step effect on the geometrical features. Figure 4.32 shows the polished Alumide® inserts. The Alumide® inserts were mounted into the steel bolster and IM trials were conducted using PP.

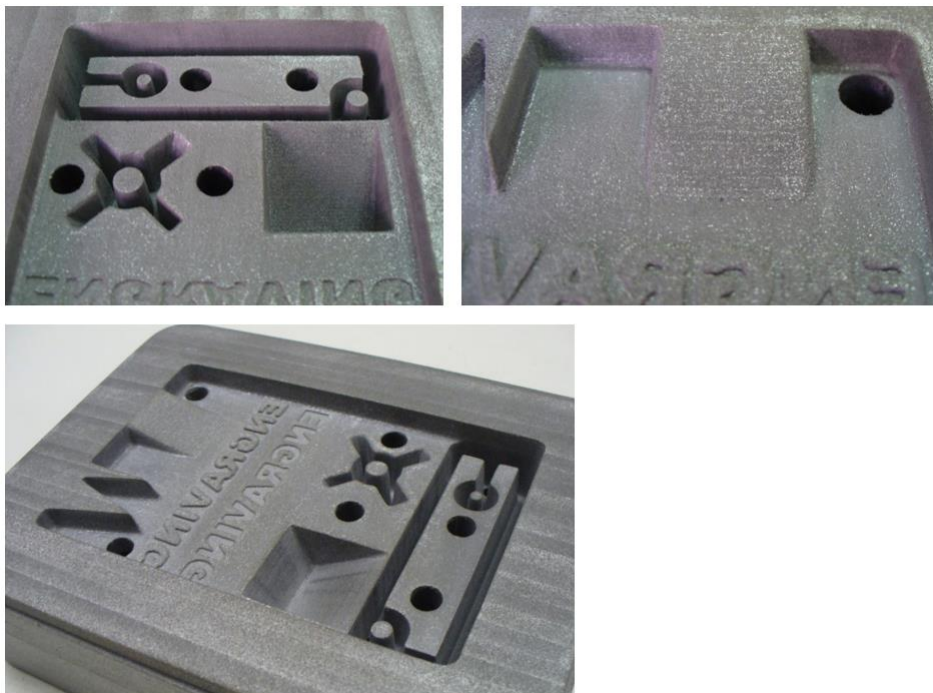


Figure 4.32 Polished Alumide® inserts.

Results

After the first few IM cycles, it was observed that the cavity surface was deforming into the cooling channels. The trial was stopped and the inserts were removed from the bolster and inspected.

Discussion

Due to the larger surface area and thinner wall thickness of the part (compared to the first trial), a greater injection pressure was required to fill the cavity. With the heat of the molten polymer and the injection pressure, the Alumide® material started to soften which resulted in the cavity surface deforming where the cooling channels were located, as shown in Figure 4.33.

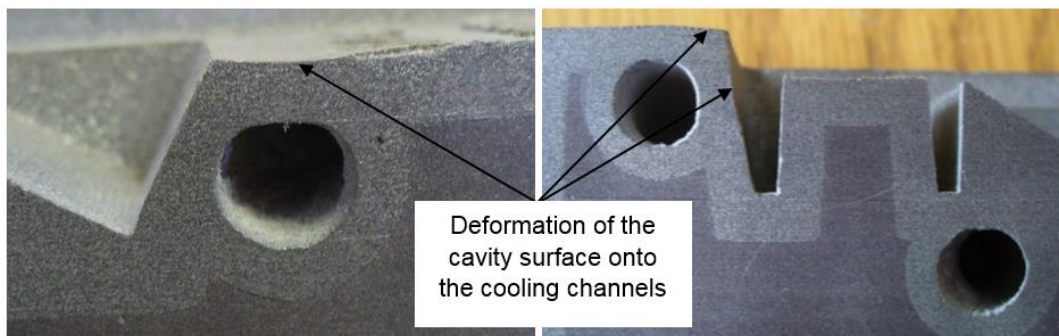


Figure 4.33 Sectioned Alumide® insert indicating the deformation of the cavity surface onto the cooling channels.

Deformation of the cavity surface only occurred in the areas where the cooling channels were located and not where the Alumide® was supported by the EPO 4030 backfilling material.

From these results the minimum wall thickness between the cavity surface and the cooling channels had to be determined while still providing adequate cooling to the Alumide® insert.

Due to the short IM trial, it was not possible to determine the durability of the geometrical features included in the Alumide® insert.

4.4.3 Cooling channel experiments

Aim

The aim of these experiments was to determine:

- The extent to which cooling channels inside an Alumide® insert influence the temperature of the insert during the IM process.
- The distance a cooling channel must be positioned from a cavity surface to prevent deformation occurring during injection.
- Heat transfer from a cavity to a cooling channel for an Alumide® insert.

Procedure

Rectangular parts, with outer dimensions of 50 mm x 20 mm and thicknesses of 2 and 3.5 mm respectively, were designed for this experiment. IM trials were conducted on the parts to determine the effect of the additional heat content on the 3.5 mm part compared to the 2 mm part on the inserts. Figure 4.34 shows the product drawings of the rectangular parts.

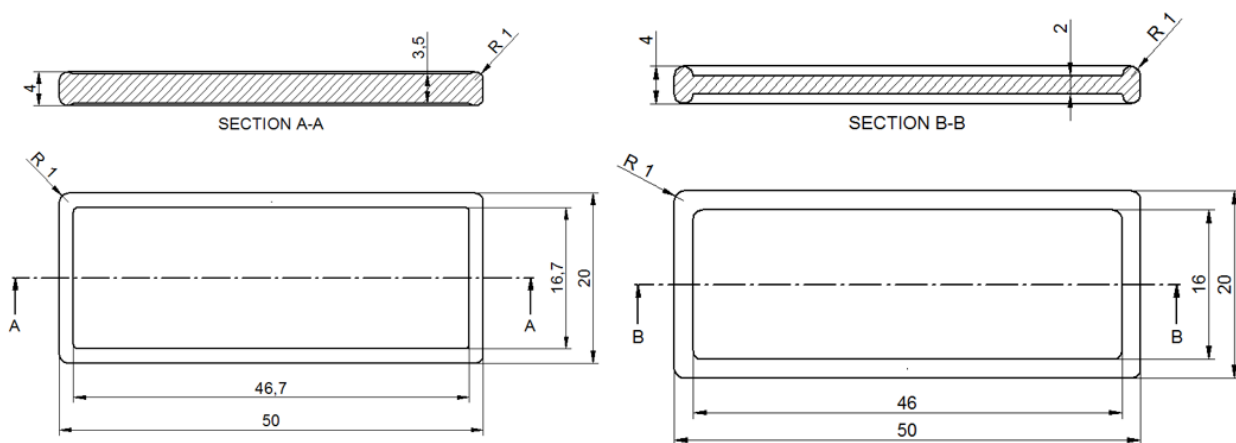


Figure 4.34 Drawings of the rectangular parts used to determine the optimal distance a cooling channel needs to be positioned from a cavity surface.

Three rectangular parts were positioned in the Alumide® insert, as shown in Figure 4.35. The inlet and outlet positions of the conformal cooling channels were placed at locations matching the cooling channel holes of the steel bolster.

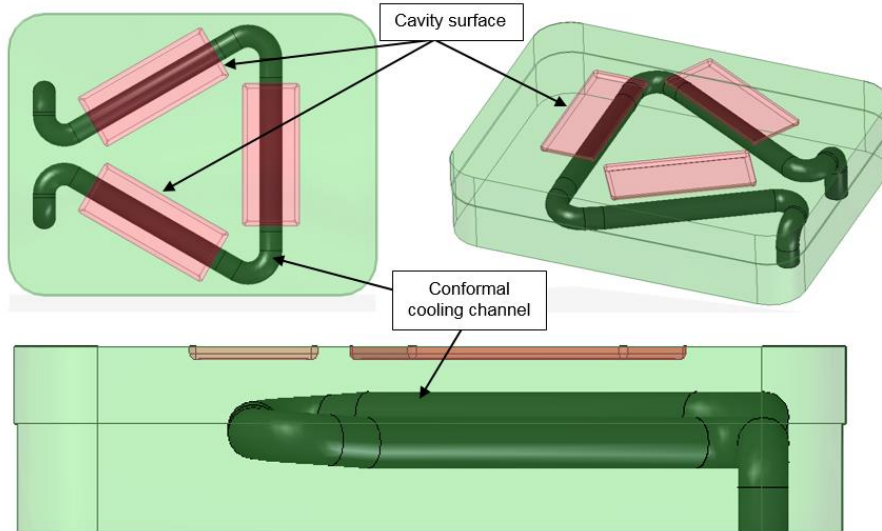


Figure 4.35 An Alumide® insert showing the arrangement of the three rectangular parts and the conformal cooling channel.

Two sets of inserts were manufactured. One set was designed with a round cooling channel, 8 mm in diameter. This shape and size of cooling channel is commonly used in conventional steel tooling. A 8 mm diameter cooling channel also improves the ease of removal of the un-sintered powder from the cooling channels. The distance from the cooling channel to the cavity surface was varied from 3 to 8 mm with 1 mm increments for the fixed and moving halves, as shown in Figure 4.36.

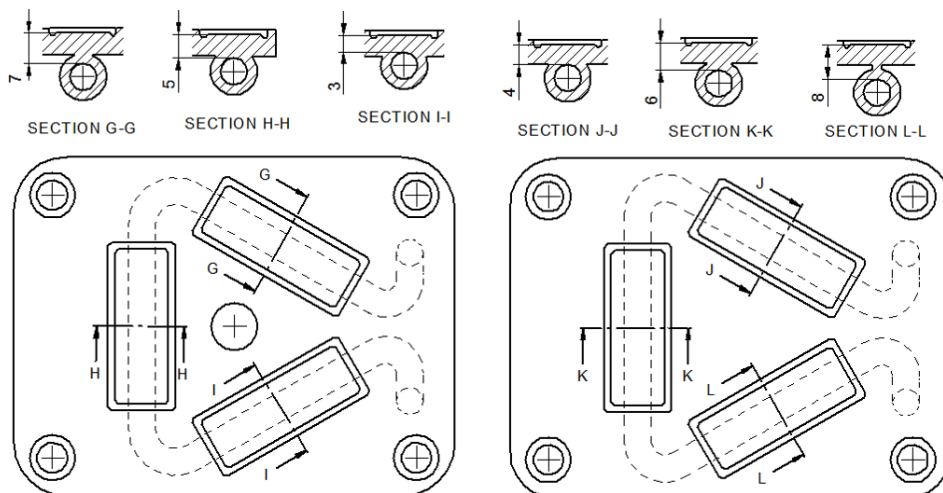


Figure 4.36 Layout of the fixed and moving halves of the Alumide® inserts with \varnothing 8 mm conformal cooling channels placed at 3, 4, 5, 6, 7 and 8 mm respectively, from a cavity surface.

The second set of inserts was designed with oval cooling channels, with primary and secondary axis dimensions of 10.6 mm and 6 mm, respectively. This oval cooling channel

has the same cross-sectional area as a 8 mm diameter cooling channel. Similar to the round cooling channels, the distances from the oval cooling channels to the cavity surfaces were varied from 3 mm to 8 mm with 1 mm intervals for the fixed and moving halves, as shown in Figure 4.37.

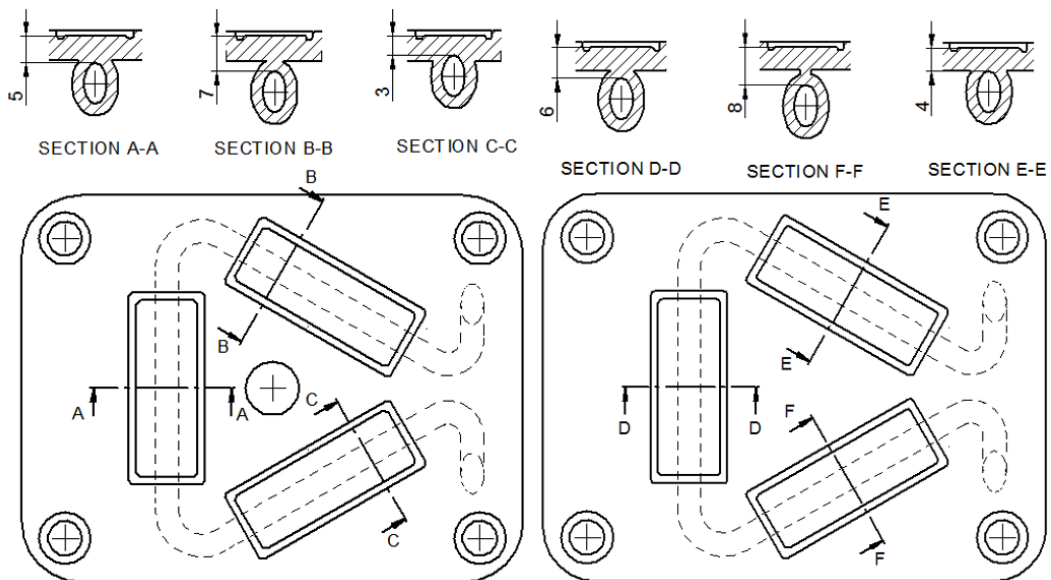


Figure 4.37 Layout of the fixed and moving halves of the Alumide® inserts with oval cooling channels placed at 3, 4, 5, 6, 7 and 8 mm respectively from the cavity surface.

Extra material was designed onto the cavity surfaces that once machined would result in perfectly flat reference surfaces. The Alumide® inserts were mounted into the steel bolster and IM trials were conducted using PP.

After the mould trials, the inserts were scanned with a Kreon Ace 7 axes measuring arm with a Solano Blue laser scanner. The scan data was compared to the CAD files of the Alumide® inserts using Geomagic® Qualify inspection software.

Results

- i. To determine the influence of cooling channels inside an Alumide® insert, the water supply to the cooling channels was closed during an IM trial. The temperature of the Alumide® inserts were recorded with temperature probes inside the inserts. Figure 4.38 shows the position of the probes inside the fixed and moving halves of the Alumide® inserts.

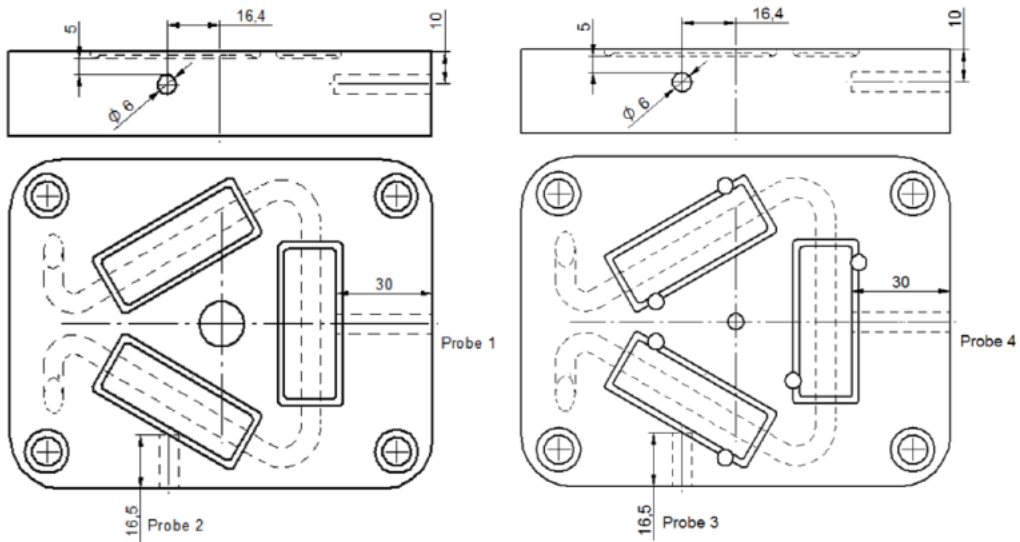


Figure 4.38 Location of heat sensing probes inside the fixed and moving halves of Alumide® inserts.

The mould was run for approximately 2000 seconds (25 IM cycles) to obtain steady state thermal conditions before the water supply to the mould was closed. After approximately 5160 seconds (1 h 26 min), the water supply to the mould was reopened. Figures 4.39 and 4.40 show plots of the mould temperatures for the fixed and moving halves of the Alumide® inserts.

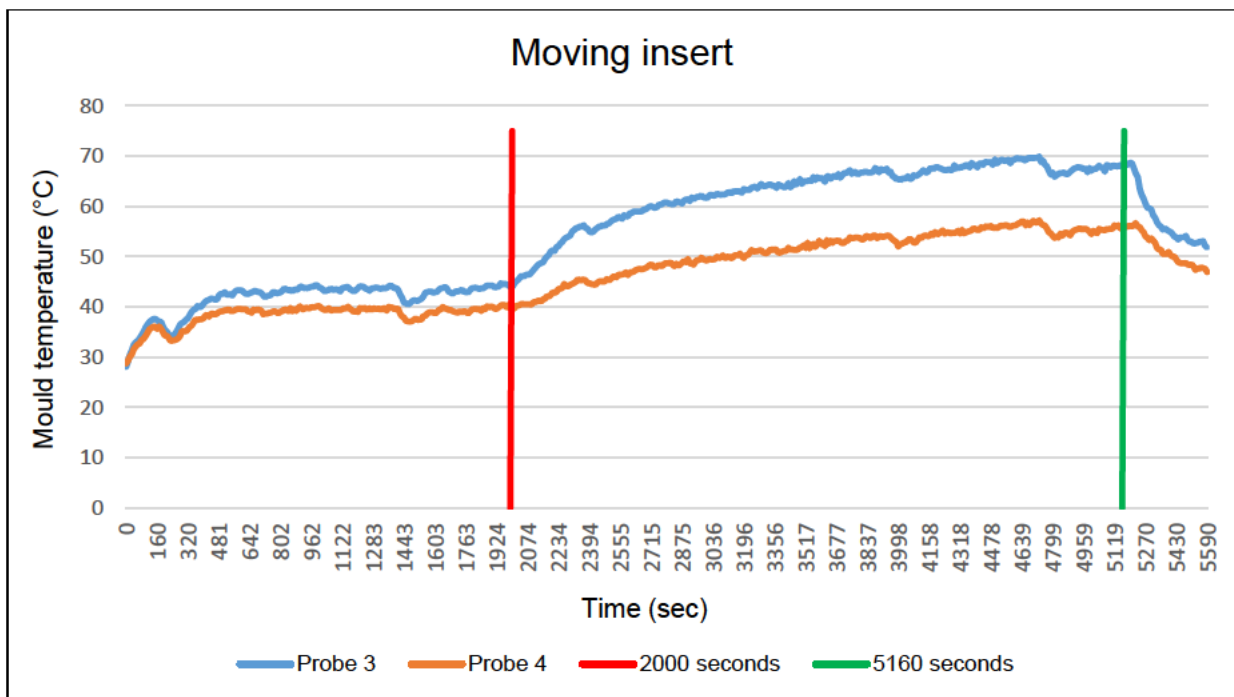


Figure 4.39 Mould temperature graph for the moving insert with cooling water interruption.

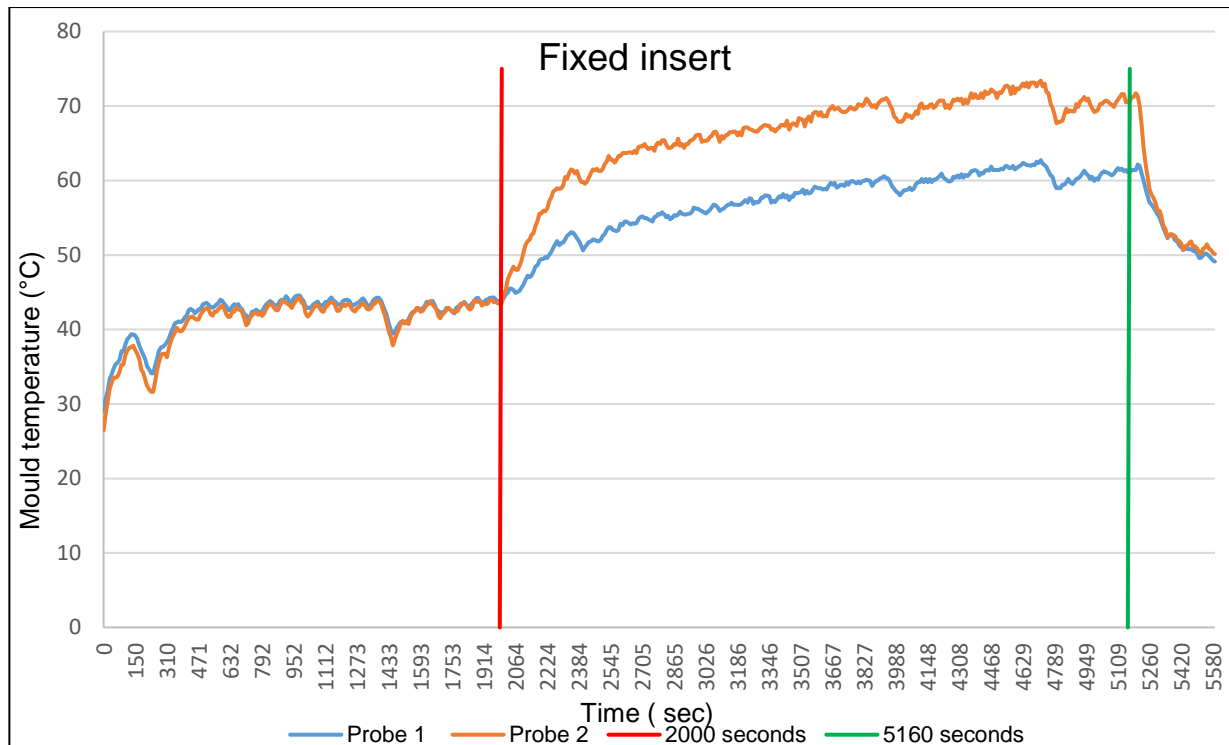


Figure 4.40 Mould temperature graph for the fixed insert with cooling water interruption.

From Figures 4.39 and 4.40 it can be seen that in both the fixed and moving inserts, the mould temperature increased after 2000 seconds when the water supply was closed. The mould temperature increased until the cooling water supply was reopened after 5160 seconds. After the water supply was reopened to the cooling channels, the insert temperatures started to decrease.

- ii. An IM trial of the Alumide[®] insert with the 2 mm thick part cavity, using round cooling channels, was conducted using PP material. A cycle time of 44.9 seconds was recorded with an injection pressure of 3.5 MPa. After 100 IM cycles, no deformation of the cavity surfaces was observed.

Alumide[®] inserts with the 3.5 mm thick part cavity and round cooling channels were placed into the bolster and the IM trial was repeated with the same processing parameters, using PP material. After the 13th IM cycle, the cavity with a cooling channel 3 mm from the surface ruptured. Significant deformation also occurred on the surface of the cavity with a cooling channel 4 mm from the surface. Figure 4.41 shows the ruptured surface of the cavity with a cooling channel 3 mm from the surface and the deformation of the cavity with a cooling channel 4 mm away.

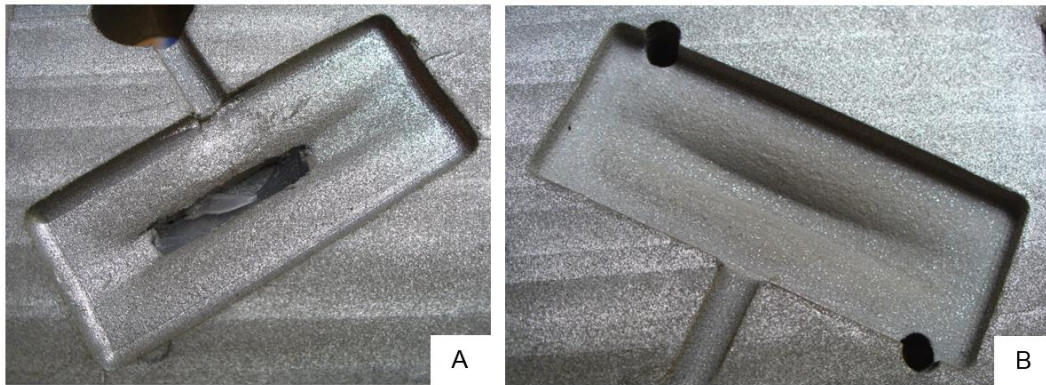


Figure 4.41 Ruptured surface of the round cooling channel 3 mm from the surface (A) and the deformed surface of the cavity with a cooling channel 4 mm from the surface (B).

The deformation of the cavity surfaces was measured with the Kreon laser scanning arm and the results compared to the CAD design of the insert, as shown in Figure 4.42. The deviation between the scan data and the CAD data is indicated in a colour scale. Regions with the smallest deviation are indicated in green while regions with the largest deviation are indicated in dark blue or red. Data points on the surfaces of the cavities were selected to indicate the maximum deviation for each cavity.

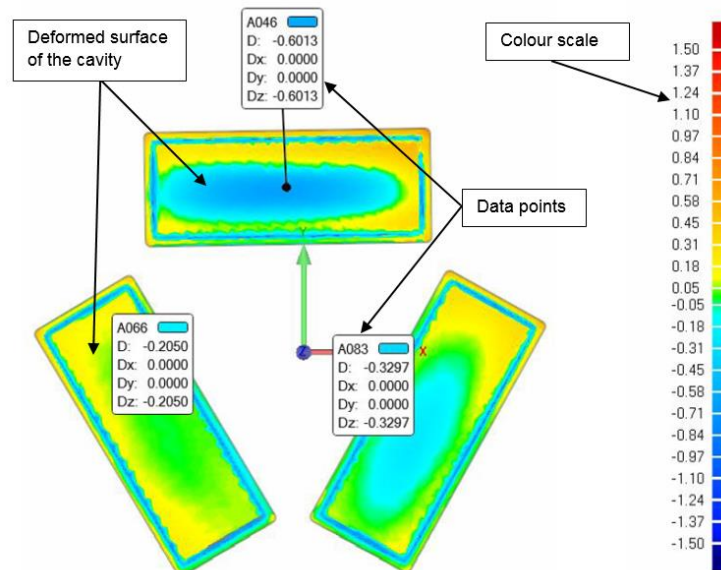


Figure 4.42 Results of a comparison between scan data and the CAD file of an insert indicating the maximum deformation of the cavity surface.

The trial was repeated with Alumide® inserts designed with the 3.5 mm thick part cavity and oval cooling channels. The injection pressure was gradually increased until deformation was observed at 6 MPa on the cavity surfaces. The surfaces were scanned

with the Kreon laser scanning arm and compared to the CAD data. Noticeable deformation was observed on the surfaces with cooling channels 3 mm and 4 mm from the cavity, as shown in Figure 4.43.

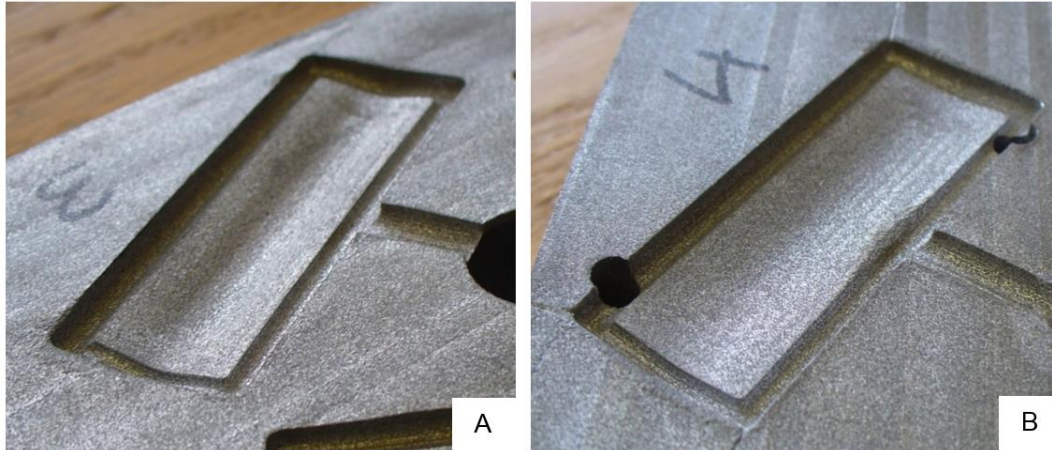


Figure 4.43 Deformed surface of a cavity with an oval cooling channel 3 mm (A) and 4 mm from the surface (B).

The deviation between the scan and CAD data for Alumide[®] inserts with cooling channels 3 to 8 mm from the cavity surface are summarised in Table 4.6.

Table 4.6 Deviation between the scan and the CAD data of Alumide[®] inserts with cooling channels 3 to 8 mm from the cavity surface.

Cooling channel profile	Distance from cavity surface (mm)	Part thickness (mm)	Deviation (mm)	Injection pressure (MPa)
Round (Ø8 mm)	3	3.5	Blow through	3.5
Round (Ø8 mm)	4	3.5	3.60	3.5
Round (Ø8 mm)	5	3.5	0.70	3.5
Round (Ø8 mm)	6	3.5	0.54	3.5
Round (Ø8 mm)	7	3.5	0.40	3.5
Round (Ø8 mm)	8	3.5	0.24	3.5
Oval (10.8 x 6)	3	3.5	1.98	6
Oval (10.8 x 6)	4	3.5	1.20	6
Oval (10.8 x 6)	5	3.5	0.21	6
Oval (10.8 x 6)	6	3.5	0.16	6
Oval (10.8 x 6)	7	3.5	0.11	6
Oval (10.8 x 6)	8	3.5	0.07	6

iii. The Alumide® inserts had to be redesigned since the cooling channels 3 and 4 mm from the cavity surface, caused a large deformation. Round and oval cooling channels, with distances of 5 mm to 10 mm from the cavity surface in 1 mm increments, were designed and manufactured, as shown in Figures 4.44 and 4.45. Only inserts with a part thickness of 3.5 mm were considered because the inserts with the 2 mm part did not deform as easily as the inserts with a 3.5 mm part thickness under the same injection pressure.

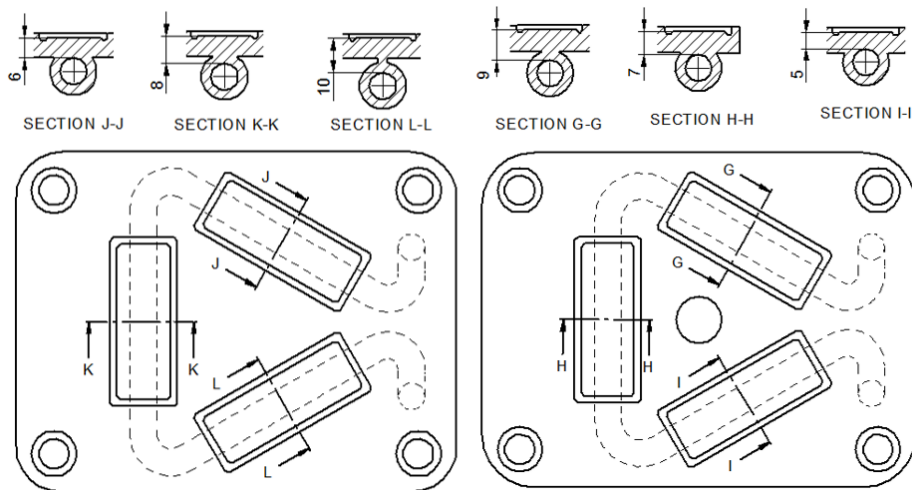


Figure 4.44 Layout of the redesigned fixed and moving halves of Alumide® inserts with a 8 mm diameter conformal cooling channels placed at 5, 6, 7, 8, 9 and 10 mm, respectively from the cavity surfaces.

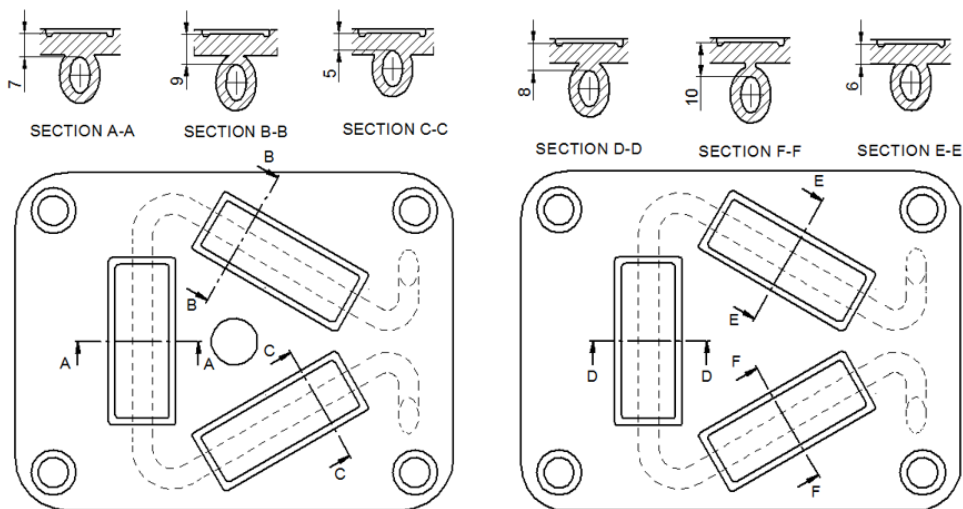


Figure 4.45 Layout of the redesigned fixed and moving halves of Alumide® inserts with oval cooling channels placed at 5, 6, 7, 8, 9 and 10 mm respectively, from the cavity surfaces.

During IM trials, the redesigned insert with the round cooling channels deformed at an injection pressure of 3.5 MPa while the oval cooling channels did not deform under the same injection pressure. The injection pressure was gradually increased until

deformation was observed at 8 MPa. The cavity surfaces of the inserts with round and oval cooling channels were scanned and compared to the CAD data. The deviation between the scan and CAD data with cooling channels 5 to 10 mm from the cavity surface are summarised in Table 4.7.

Table 4.7 Deviation between the scan and CAD data of Alumide[®] inserts with cooling channels 5 to 10 mm from the cavity surface.

Cooling channel profile	Distance from cavity surface (mm)	Part thickness (mm)	Deviation (mm)	Injection pressure (MPa)
Round (Ø8 mm)	5	3.5	0.60	3.5
Round (Ø8 mm)	6	3.5	0.43	3.5
Round (Ø8 mm)	7	3.5	0.33	3.5
Round (Ø8 mm)	8	3.5	0.26	3.5
Round (Ø8 mm)	9	3.5	0.21	3.5
Round (Ø8 mm)	10	3.5	0.11	3.5
Oval (10.8 x 6)	5	3.5	0.36	8.0
Oval (10.8 x 6)	6	3.5	0.23	8.0
Oval (10.8 x 6)	7	3.5	0.17	8.0
Oval (10.8 x 6)	8	3.5	0.10	8.0
Oval (10.8 x 6)	9	3.5	0.08	8.0
Oval (10.8 x 6)	10	3.5	0.03	8.0

iv. SIGMASOFT[®] virtual moulding simulation software was used to simulate the heat flow from a cavity to a cooling channel for an Alumide[®] insert. During a previous postgraduate study conducted at CUT on Alumide[®] tooling, SIGMASOFT[®] was successfully implemented as simulation software that accurately simulates IM temperatures which compare favourably to actual experimental Alumide[®] mould temperatures measured during IM trials [106]. A part 50 x 50 mm² with a thickness of 2.5 mm was used in the simulation. The distance between a cooling channel and the cavity surface was varied from 5 mm to 10 mm with 1 mm increments, as indicated by dimension “D” for an oval cooling channel and dimension “E” for a round cooling channel as shown in Figure 4.46.

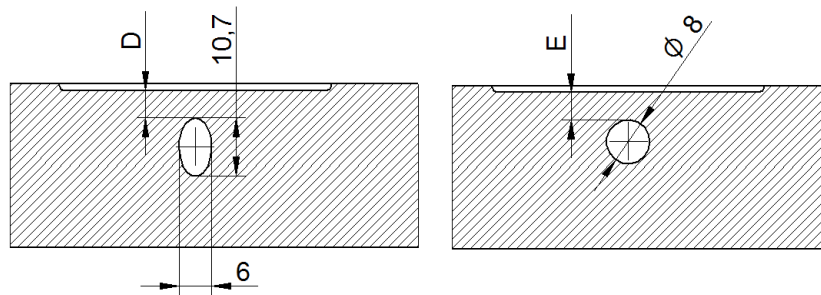


Figure 4.46 Model used during the heat flow simulation with varying distance of the round and oval cooling channels from the cavity.

ABS material with an injection melt temperature of 250 °C and an initial mould temperature of 20 °C, with a cycle time of 90 seconds, was applied to the simulation. SIGMASOFT® virtual moulding simulation results were obtained at the 20th injection moulded cycle, when the mould would be very close to a thermal steady state. The heat removed and the maximum mould temperatures with an oval and a round cooling channel at a certain distance from the cavity surface, as predicted by the simulation software, are summarised in Table 4.8.

Table 4.8 SIGMASOFT® simulations results for the heat removed and maximum mould temperatures of an Alumide® insert with oval and round cooling channels.

Distance from cavity (mm)	Round profile				Oval profile			
	Heat removed from cavity (J)	% Decrease in heat removal	Maximum mould temperature (°C)	% Increase in mould temperature	Heat removed from cavity (J)	% decrease in heat removal	Maximum mould temperature (°C)	% Increase in mould temperature
5	624.97	-	94.70	-	615.70	-	96.91	-
6	606.32	3.0 %	97.05	2.5 %	594.55	3.4 %	99.16	2.3 %
7	587.80	3.1 %	99.32	2.3 %	571.54	3.9 %	101.35	2.2 %
8	569.12	3.2 %	101.52	2.2 %	555.29	2.8 %	103.38	2.0 %
9	552.46	2.9 %	103.59	2.0 %	538.26	3.1 %	105.30	1.9 %
10	532.67	3.6 %	105.50	1.8 %	520.02	3.4 %	107.10	1.7 %

From Table 4.8 it can be observed that an oval cooling channel is able to remove a similar quantity of heat from the cavity compared to a round cooling channel 1 mm closer to the cavity surface. The maximum mould temperature of an oval cooling channel is also similar to the maximum value of a round cooling channel 1 mm closer to the cavity surface. From

Table 4.8 it can also be observed that for every 1 mm a round or oval cooling channel is further from the cavity surface, the heat removed from the cavity decreases by approximately 3 %, while the maximum mould temperature increases by approximately 2 %.

Discussion

From Figures 4.39 and 4.40 it can be concluded that conformal cooling channels had an effect on the mould temperatures of an Alumide[®] insert during the IM trials. Without cooling, the mould temperature increased by approximately 30 °C within 3160 seconds. This additional heat with the injection pressure can result in premature deformation of Alumide[®] inserts, reducing the usable lifespan.

Results from Table 4.6 indicate that cooling channels need to be a minimum distance of 5 mm from a cavity surface. Cooling channels 3 and 4 mm from the cavity surface deformed significantly under injection pressures. Results from Table 4.6 and 4.7 also indicate that oval cooling channels are able to withstand twice as high injection pressures compared to a round cooling channel, due to its geometrical shape.

Results from Table 4.8 indicate that an oval cooling channel removes less heat (about 2.3 %) from an insert compared to a round cooling channel at the same distance from a cavity surface. This results in about 2 °C higher mould temperature compared to a round cooling channel. Results from Table 4.6 and 4.7 show that a higher injection pressure is more likely to cause deformation than a slightly higher (about 2 °C) insert temperature.

From these results it is recommended that oval cooling channels, 5 mm from the cavity surface, should be used for Alumide[®] inserts with an injection pressure in the region of 3.5 MPa. For injection pressures in the region of 6 to 8 MPa, an oval cooling channel 9 mm from the cavity surface should be considered for minimal deformation as shown in Table 4.7.

4.4.4 Geometrical experiment with oval cooling channels

The experiment, as described in Section 4.4.2, was repeated with oval conformal cooling channels to prevent deformation of the cavity surface.

Aim

The aim of this experiment remained the same as stated in Section 4.4.2.

Procedure

A fill simulation analysis using SIGMASOFT® software was conducted to determine the injection pressure required to fill the cavity. Results from the analysis indicated that an injection pressure of 3.8 MPa was required to fill the cavity. Oval conformal cooling channels spaced 5 mm from the cavity surface were used in the design of the insert. Apart from the cooling channel design, the same procedure was followed as described in Section 4.4.2.

IM trials were conducted using PP material with an injection pressure of 4 MPa.

Results

During the fifth IM cycle, the 4 mm diameter pin broke from the insert. The 5 mm diameter pin broke after the 9th IM cycle and the 6 mm diameter pin after the 11th IM cycle. The trial was continued until the 24th IM cycle to determine if the cooling channels were able to withstand the injection pressure. Figure 4.47 shows the Alumide® insert with the positions where the pins features were broken from the insert.

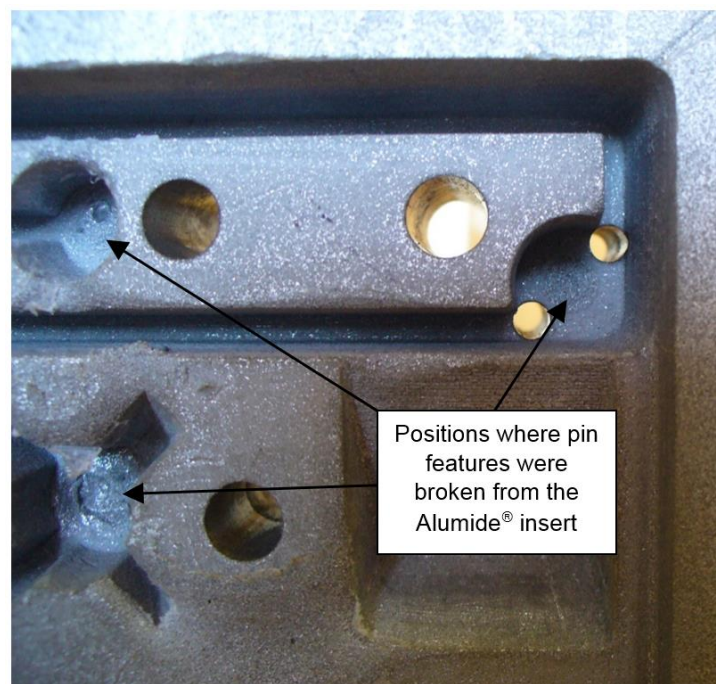


Figure 4.47 Positions of Alumide® pin features broken off during the IM trial.

Discussion

The hole features of the bosses manufactured from Alumide[®] broke off during the first few IM cycles. This resulted in large cavities where molten PP accumulated during injection. These cavities retained heat and resulted in increased wear on the Alumide[®] inserts. Steel pins inserted into the Alumide[®] inserts should be used for hole features instead of pins manufactured from Alumide[®] to overcome this problem.

No deformation of the cavity surface into the cooling channels occurred. From these results it can be concluded that oval cooling channels 5 mm from the cavity surface are able to withstand injection pressures of around 4 MPa without deformation.

Due to the short IM trial, it was not possible to determine the durability of geometrical features included in the Alumide[®] insert design. However, it was observed that there was significant wear to the geometrical features close to the injection point, as shown in Figure 4.48.

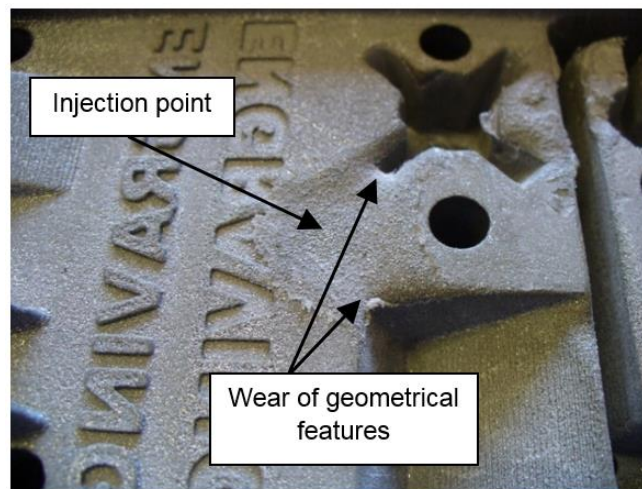


Figure 4.48 Wear of geometrical features close to the injection point.

The close proximity of the geometrical features to the injection point resulted in a continuous flow of molten polymer (from the IM machine's barrel at a nozzle temperature of 220 °C) over these features as the cavity filled. Figure 4.49 A to D shows the flow path of the molten polymer during the filling of the cavity as predicted by SIGMASOFT[®] IM simulation software. Figure 4.49 A shows the flow path of the molten polymer after 10 % filling of the cavity, B 20 %, C 40 % and D 80 %. Figure 4.49 A indicates that after 10 % filling of the cavity the molten polymer started to fill the geometrical features close to the

injection point. The flow of the molten polymer resulted in a higher mould temperature at regions near the injection point. The sharp-edged corners of the geometrical features were softened by the high temperature, causing it to wear. As these corners wore, the thickness of these features increased. This resulted in more material accumulating, increasing the temperature which accelerated the rate of wear.

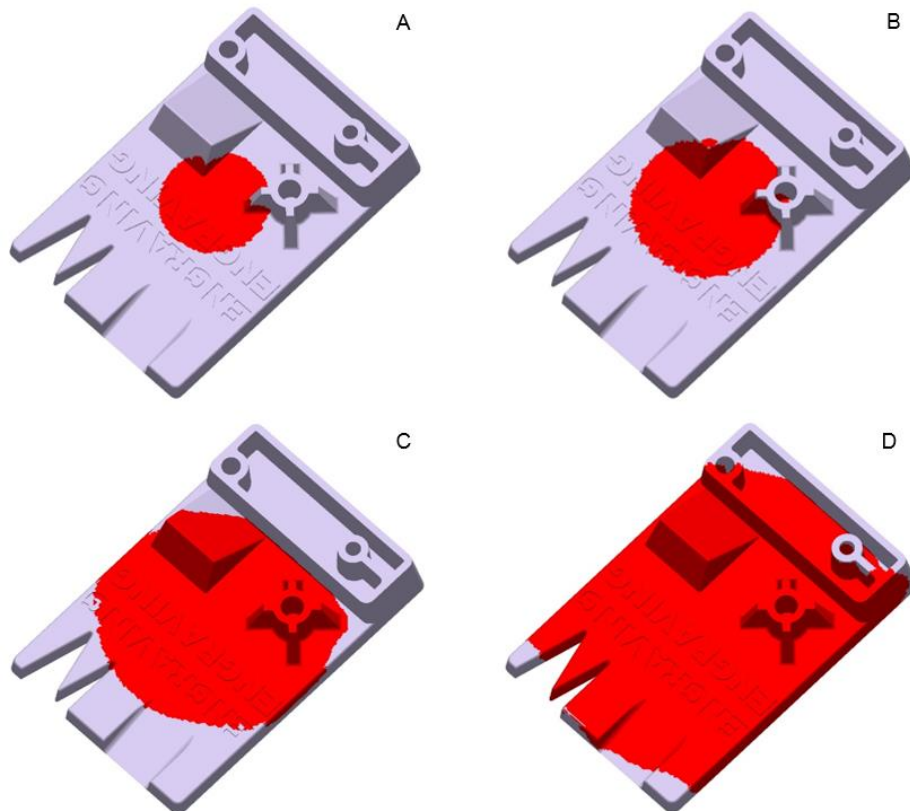


Figure 4.49 Results of the SIGMASOFT® flow analysis for the geometrical part showing the flow path of the molten material during the filling of the mould cavity.

4.4.5 Geometrical V2 experiment

Aim

The aim of this experiment was to determine:

- The durability of different geometrical features of an Alumide® insert.
- The wear in regions of an Alumide® insert that cannot be cooled sufficiently due to mould constraints such as screw holes and ejector pins.
- The suitability of different polymer materials for use with an Alumide® insert. IM trials were conducted using PP, ABS, PC and PA6.

Procedure

Due to the wear of features close to the injection point, the geometrical test part was redesigned with geometrical features repositioned further from the injection point. Figure 4.50 shows a CAD model and a product drawing of the redesigned part, indicating the dimensions and placement of the geometrical features.

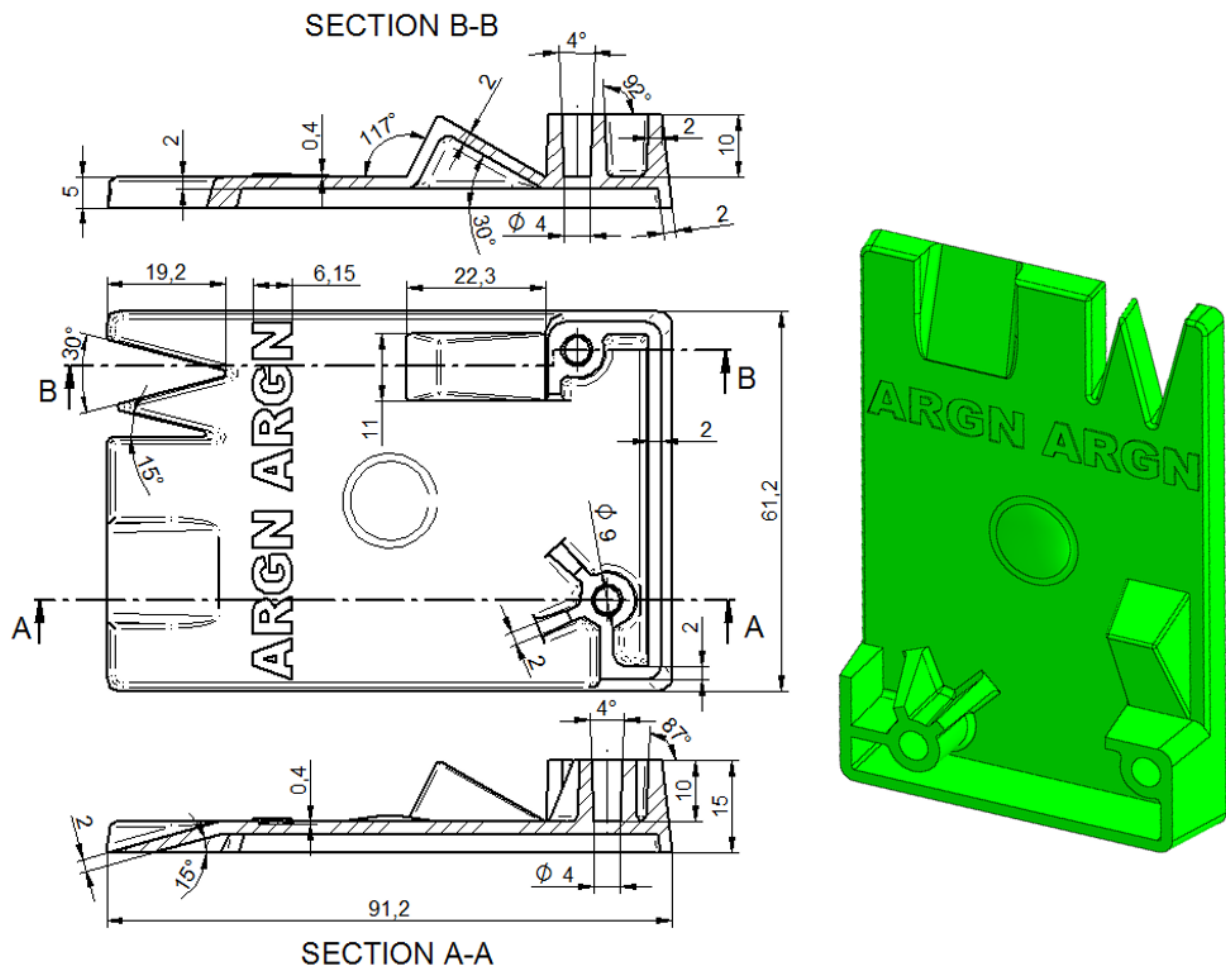


Figure 4.50 Dimensions and CAD model of the redesigned geometrical part.

Figure 4.51 A to D shows the flow path of the molten polymer of the redesigned geometrical part, as predicted by SIGMASOFT® IM simulation software. Figure 4.51 A shows the flow path of the molten polymer after 10 % filling of the cavity, B 20 %, C 40 % and D 80 %. Compared to Figure 4.49 A, the redesigned geometrical features only start to fill after 20 % and 40 % filling, as shown in Figure 4.51 B and C respectively.

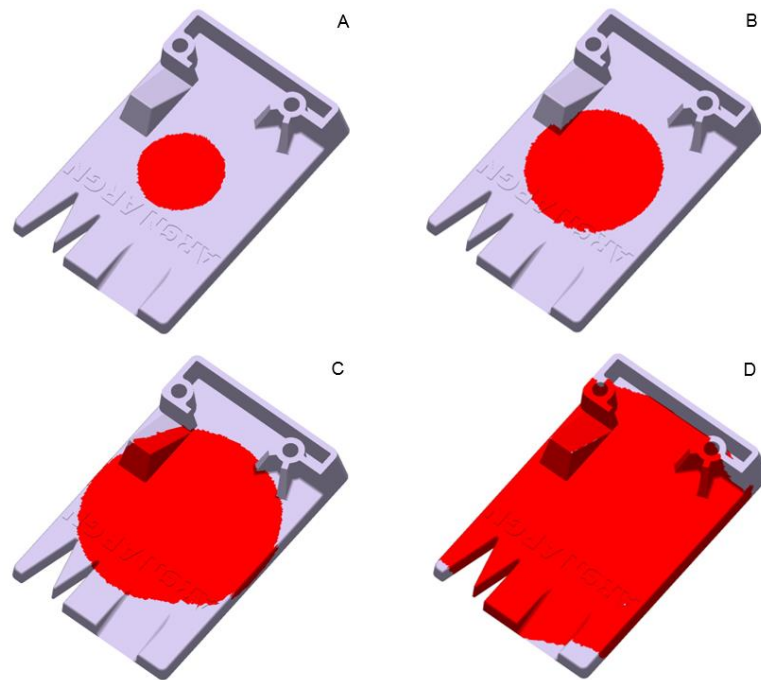


Figure 4.51 Results of the SIGMASOFT® flow analysis for the redesigned geometrical part showing the flow path of the molten material during the filling of the mould cavity.

Oval conformal cooling channels, 5 mm from the cavity surface, were included into the Alumide® insert design. The conformal cooling channels were positioned to obtain the best possible cooling while avoiding insert features such as screw and ejector pin holes, as shown in Figure 4.52. The inlet and outlet positions of the conformal cooling channels were placed at locations matching the cooling channel holes of the steel bolster.

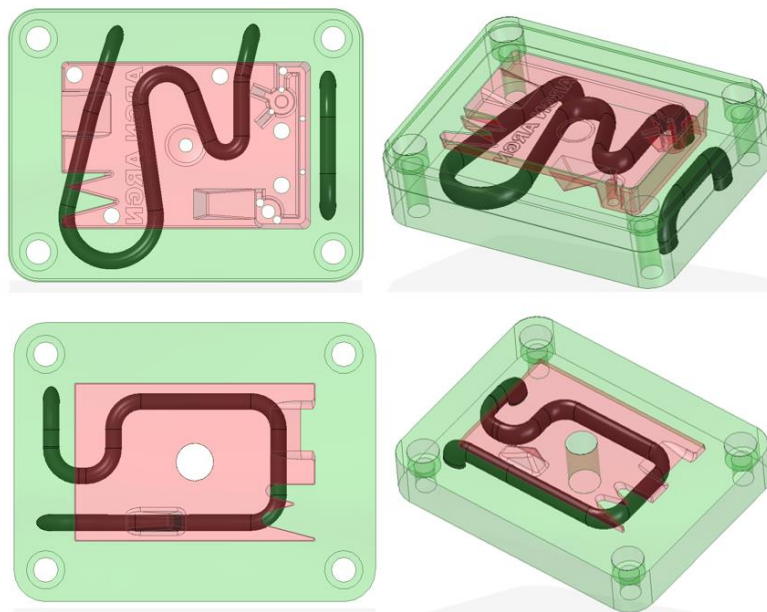


Figure 4.52 Layout of the oval conformal cooling channels avoiding insert features such as screw and ejector pin holes.

SIGMASOFT® IM simulation software was used to predict the temperatures of the Alumide® inserts after the 20th IM cycle, when the mould would have been at a thermal steady state. The temperature profiles as well as the maximum insert temperatures were obtained for the fixed and moving inserts, as shown in Figure 4.53.

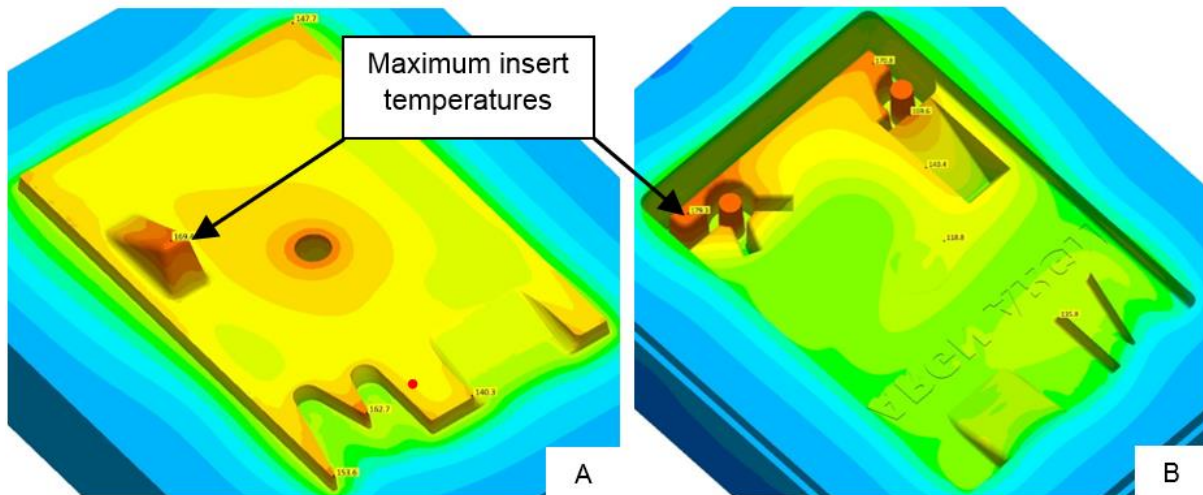


Figure 4.53 Insert features where the maximum temperatures occur for the fixed (A) and moving (B) Alumide® inserts after the 20th IM cycle, according to SIGMASOFT® virtual moulding software.

The insert features shown in Figure 4.53 where the maximum temperatures occurred, could not be cooled sufficiently due to their size and insert constraints. These insert features were not altered to determine the influence the higher insert temperature would have on the rate of wear.

After backfilling and machining operations, the Alumide® inserts were polished by sanding using 320 and 400 grit sandpaper to remove the stair steps resulting from the manufacturing process on the geometrical features. Figure 4.54 A and B show the geometrical features in the as-built form of the fixed insert, and Figure 4.54 C and D show the moving insert with the stair step effect visible on the features.

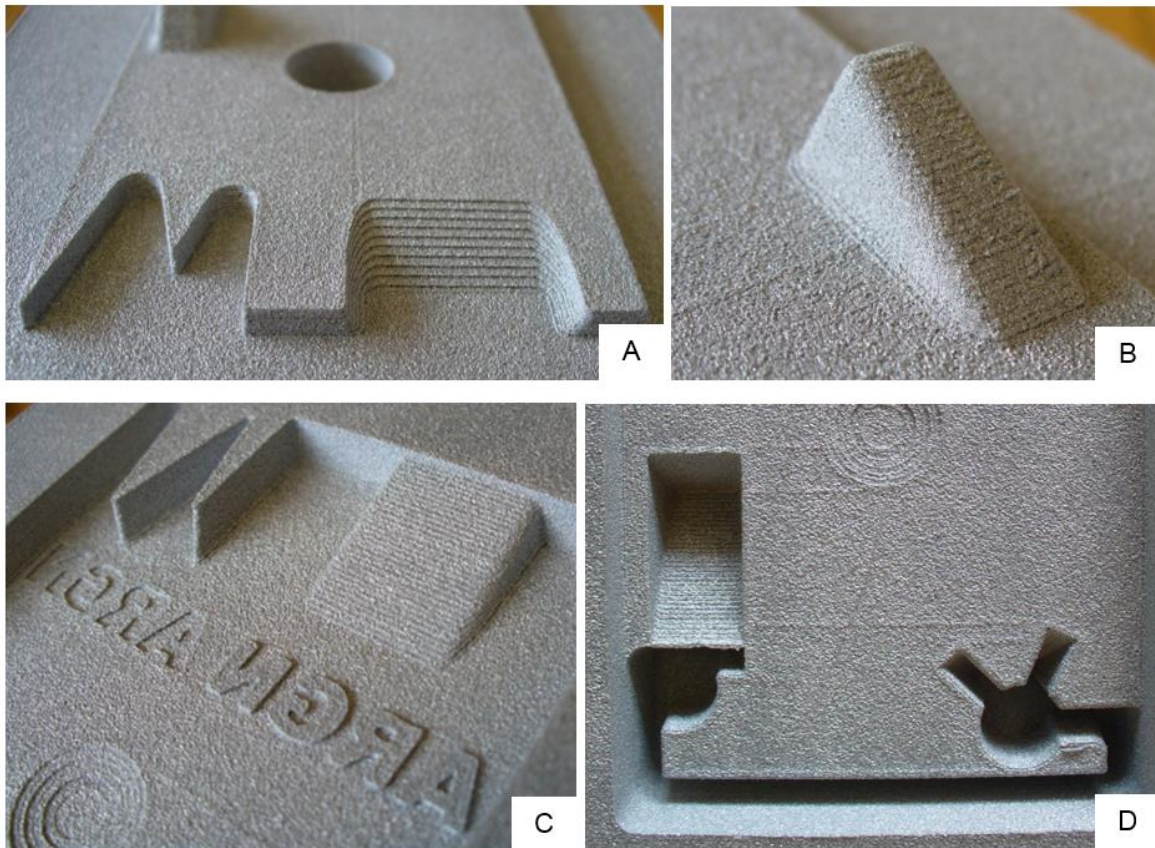


Figure 4.54 Stair step effect visible on features of the redesigned geometrical insert in the as-built form of the fixed and moving inserts.

Figure 4.55 shows the machined and polished Alumide[®] insert with steel pins inserted for producing hole features in the injection moulded parts. This post-processing procedure was repeated for the four sets of inserts used during this experiment.

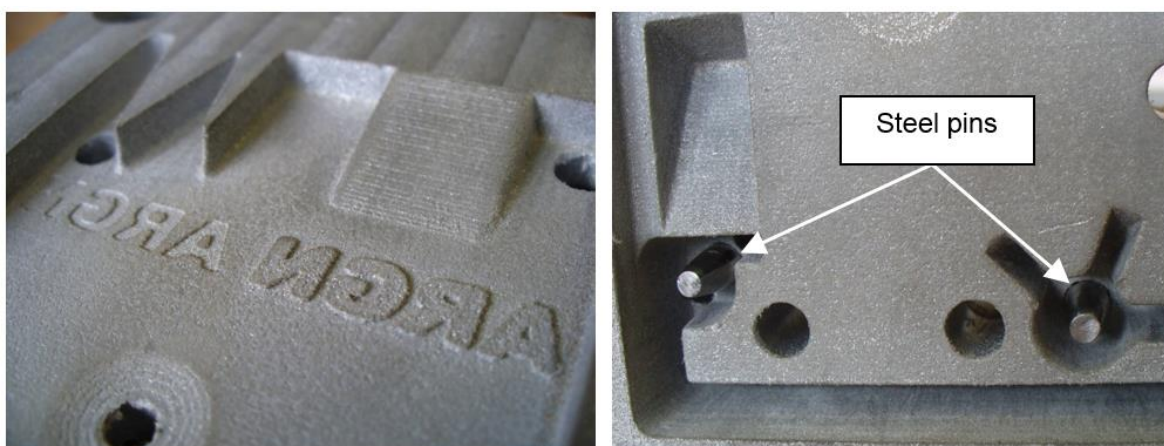


Figure 4.55 Machined and polished Alumide[®] insert with steel pins for producing hole features.

Results

i. Geometrical mould trial with PP

The process parameters used during the trial with PP are summarised in Table 4.9.

Table 4.9 Injection moulding process parameters used during the manufacturing of geometrical parts from PP.

Material preparation	None
Injection pressure	4 MPa
Nozzle temperature	220 °C
Cycle time	45 seconds
Mould cooling	Water temperature controlled by a chiller unit set at 7 °C

200 IM cycles were completed without any noticeable wear on the Alumide[®] inserts. Figure 4.56 shows the fixed half of the Alumide[®] insert after 200 IM cycles.

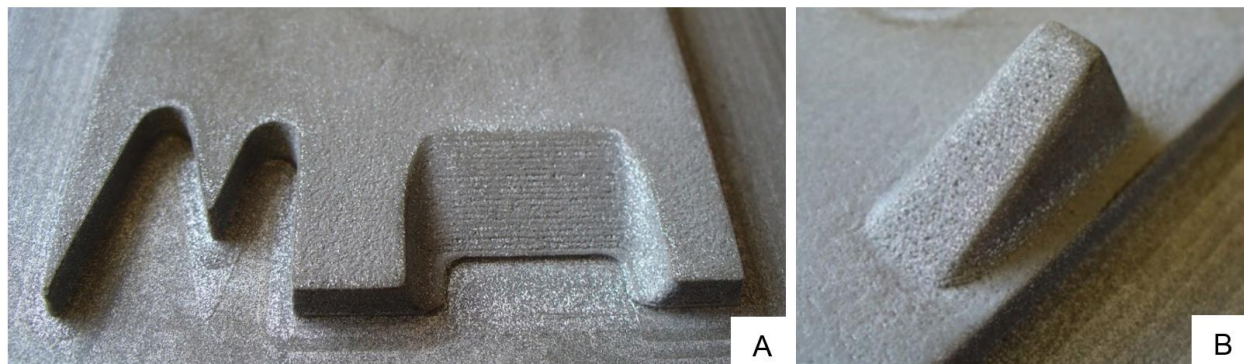


Figure 4.56 Fixed half of the Alumide[®] insert after 200 IM cycles using PP.

Results from SIGMASOFT[®] virtual moulding software indicated that the insert feature, shown in Figure 4.56 B, had a temperature of 169.4 °C after the 20th IM cycle, as shown in Figure 4.57. Because this temperature is less than the melt temperature of 177 °C for Alumide[®], obtained from the results in Section 4.2.2, the features shown in Figure 4.55 A and B did not have noticeable wear.

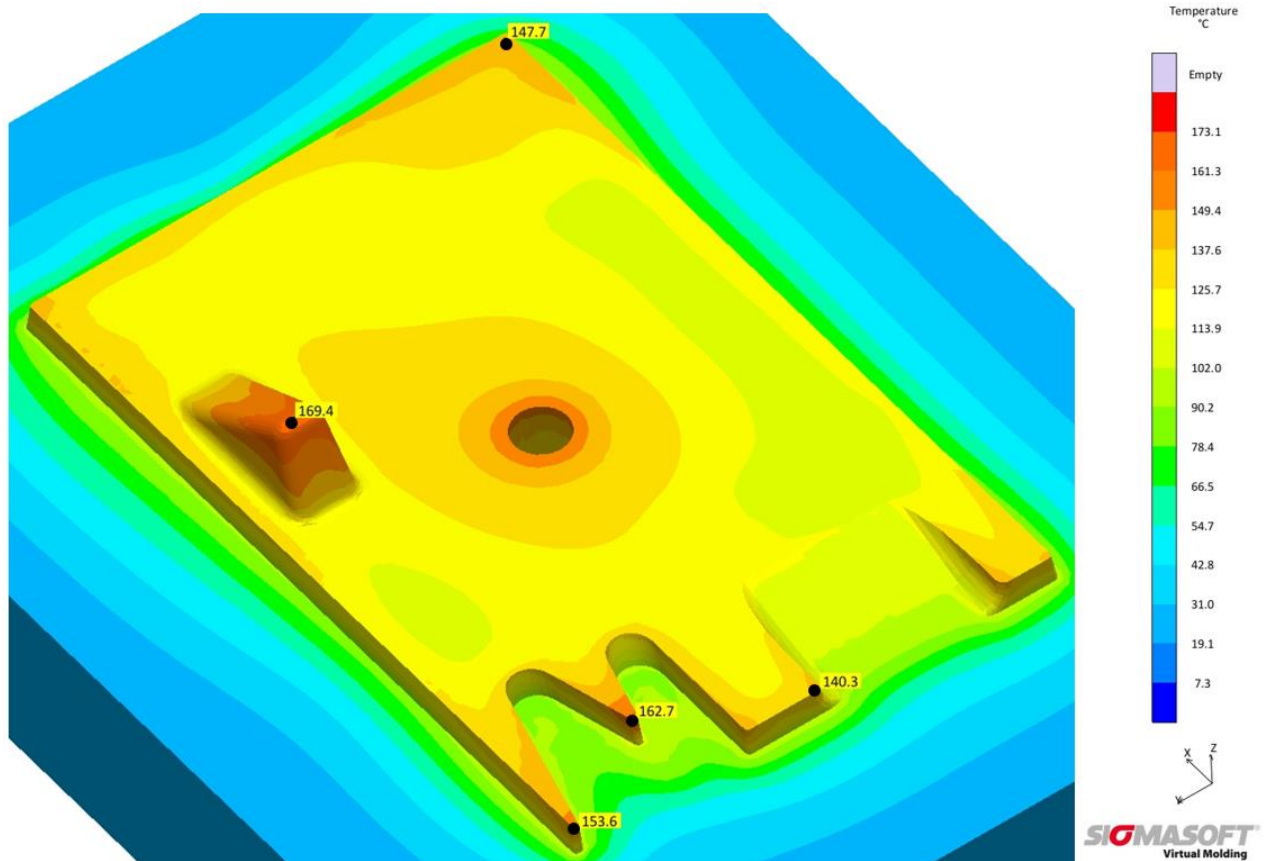


Figure 4.57 Temperatures of the fixed half Alumide[®] insert using PP after the 20th IM cycle, according to SIGMASOFT[®] virtual moulding software.

Figure 4.58 shows the moving half after 200 IM cycles. The insert feature shown in Figure 4.58 A did not wear but started to delaminate. This feature could not be cooled sufficiently due to its size and mould constraints. The knife-edge corner shown in Figure 4.58 B did not show any signs of wear.

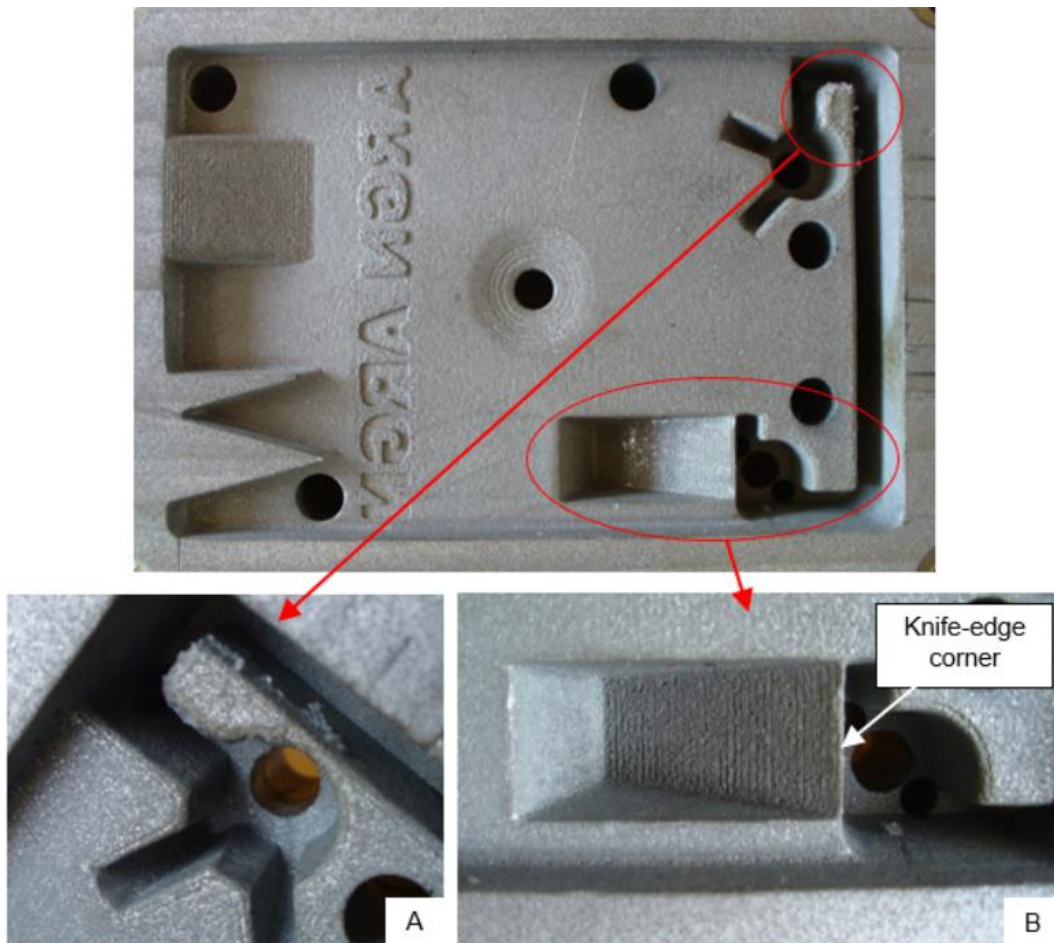


Figure 4.58 Moving half of the Alumide® insert after 200 IM cycles using PP. Figures A and B are enlargements of the encircled regions of the insert.

Results from SIGMASOFT® virtual moulding software indicated that the insert feature shown in Figure 4.58 A had a temperature of 179.3 °C after the 20th IM cycle, as shown in Figure 4.59. This temperature is slightly more than the melt temperature of 177 °C for Alumide®. This slightly higher temperature could have caused the delamination of the Alumide® insert feature shown in Figure 4.58 A.

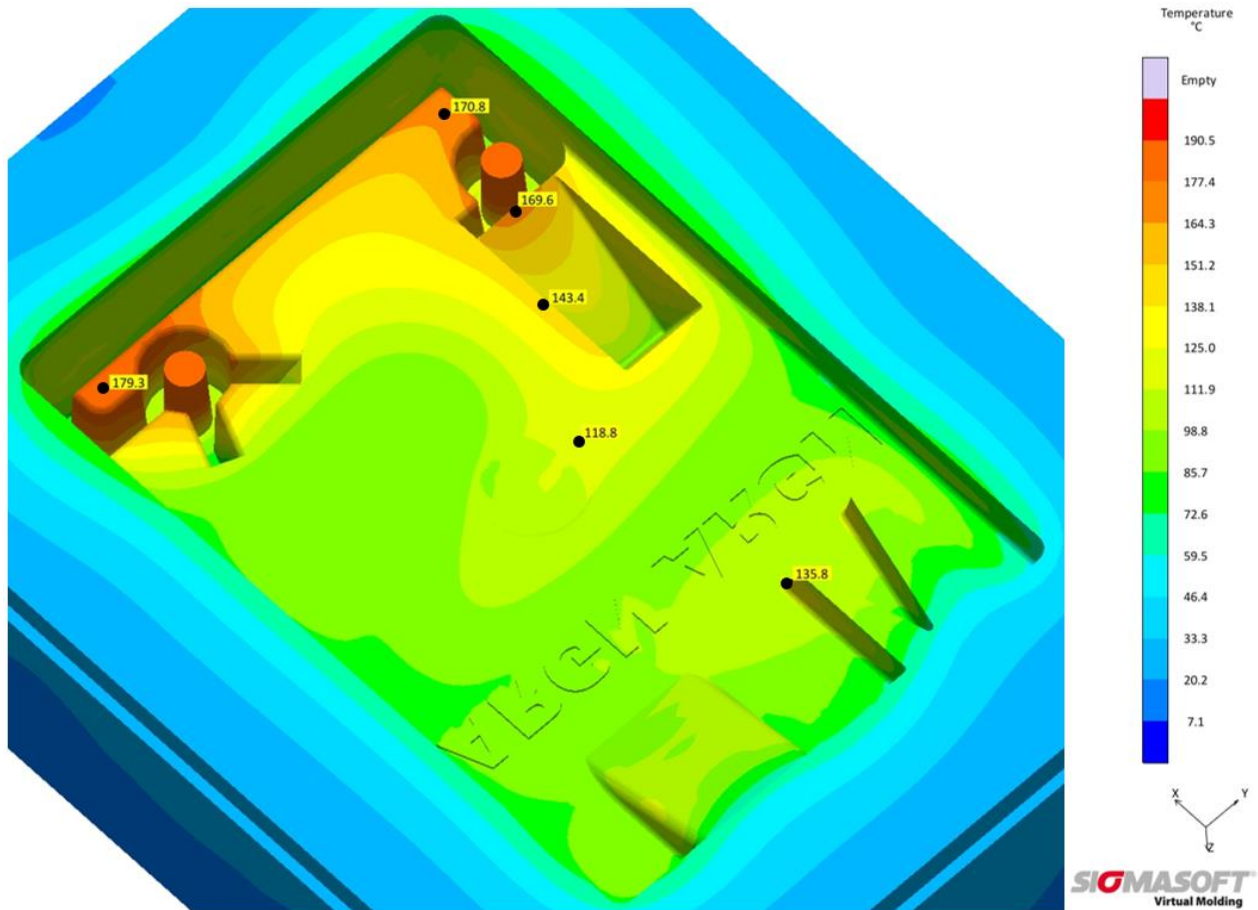


Figure 4.59 Temperatures of the moving half Alumide® insert using PP after the 20th IM cycle, according to SIGMASOFT® virtual moulding software.

No noticeable wear was observed on the text features and the knife-edge corners after 200 IM cycles, as shown in Figure 4.60.



Figure 4.60 Text features and knife-edge corners without any wear after 200 IM cycles using PP.

The Alumide® inserts were scanned after 200 IM cycles using the Kreon scanning arm and compared to the CAD data of the inserts using Geomagic® Qualify software. The deviation between the scan and the CAD data was consistently about 0.2 mm. Due to budget constraints, it was not possible to scan and compare the inserts to the CAD data before the IM trials commenced. Therefore this deviation could be from material removed during the polishing of the inserts. From the scan results, as shown in Figure 4.61, there were no geometrical features with a deviation value larger than 0.5 mm. This shows that there was no significant wear on the Alumide® inserts after 200 IM cycles.

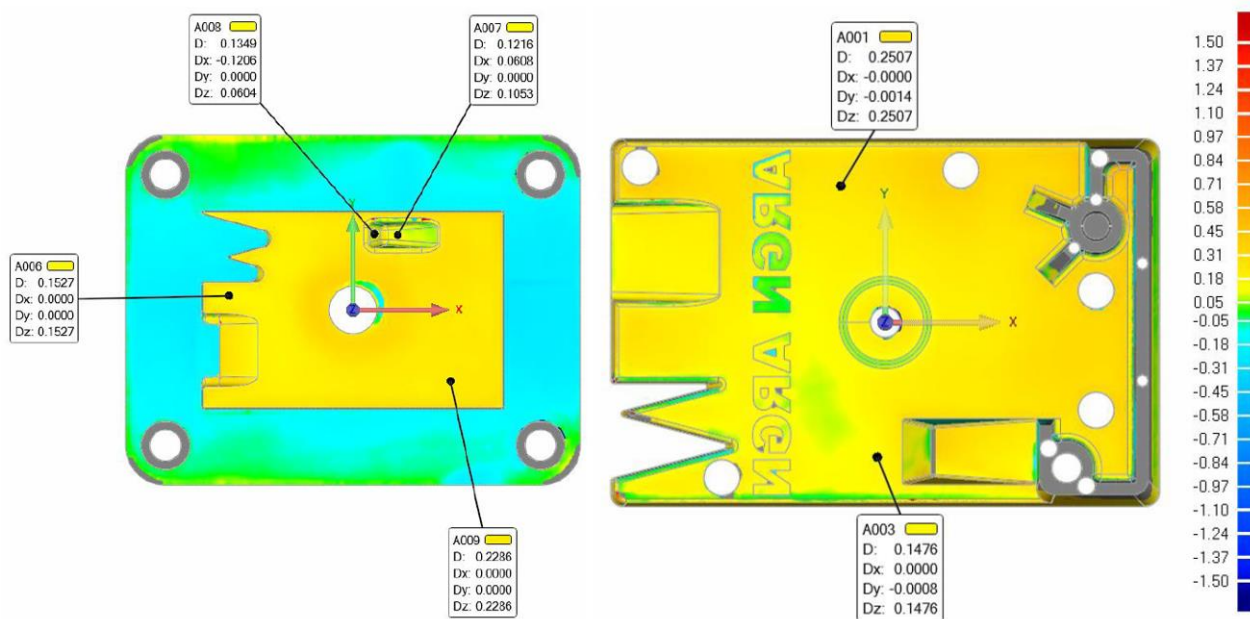


Figure 4.61 Scan results of the moving and fixed Alumide® inserts after 200 IM cycles using PP.

ii. Geometrical mould trial with ABS

The process parameters used during the trial with ABS are summarised in Table 4.10.

Table 4.10 Injection moulding process parameters used during the manufacturing of geometrical parts from ABS.

Material preparation	Material dried for 2 hours at 82 °C
Injection pressure	4 MPa
Nozzle temperature	230 °C
Cycle time	47 seconds
Mould cooling	Water temperature controlled by a chiller unit set at 7 °C

200 IM cycles were completed without any noticeable wear on the fixed half of the Alumide® insert, as shown in Figure 4.62. Due to the higher processing temperature of

ABS, the cycle time was increased to allow for solidification of the part before ejection from the mould.

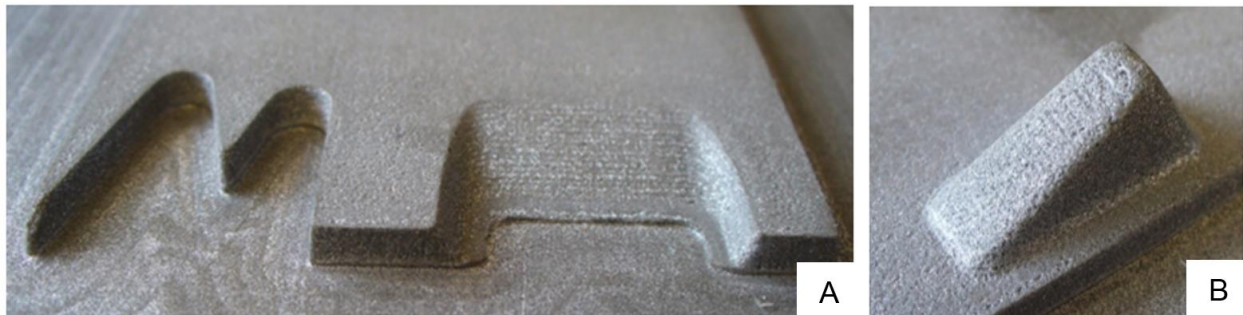


Figure 4.62 Fixed half of the Alumide[®] insert after 200 IM cycles using ABS.

SIGMASOFT[®] simulation, results (shown in Figure 4.63) indicated an insert temperature of 179.1 °C after the 20th IM cycle for the feature shown in Figure 4.62 B. This temperature is slightly higher than the melt temperature of Alumide[®], causing minor wear to the top corners of the feature shown in Figure 4.62 B.

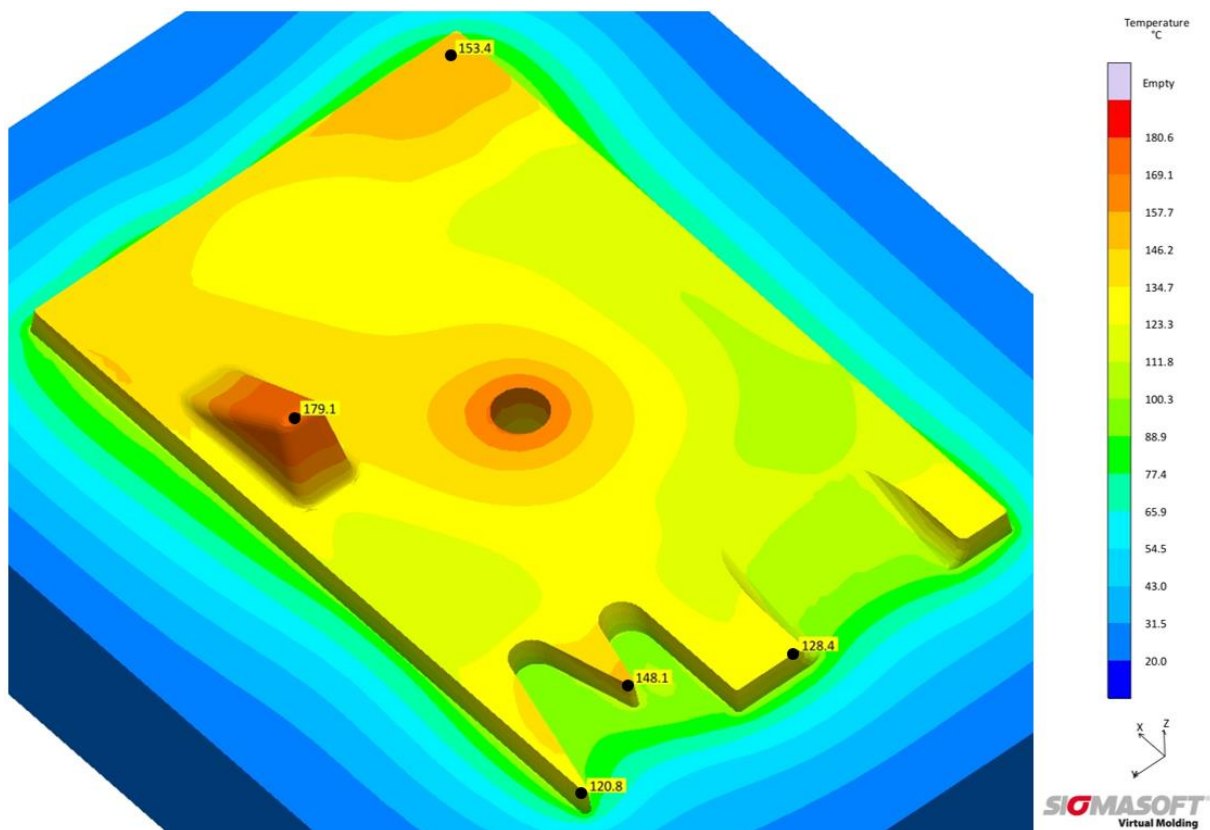


Figure 4.63 Temperatures of the fixed half Alumide[®] insert using ABS after the 20th IM cycle, according to SIGMASOFT[®] virtual moulding software.

Figure 4.64 shows the moving half after 200 IM cycles. The insert feature shown in Figure 4.64 A started to wear after the 10th IM cycle. Wear of this feature continued until the 100th IM cycle after which it remained constant until the trial was ended. This feature could not be cooled sufficiently due to its size and mould constraints. The knife-edge corners shown in Figure 4.64 B also started to wear.

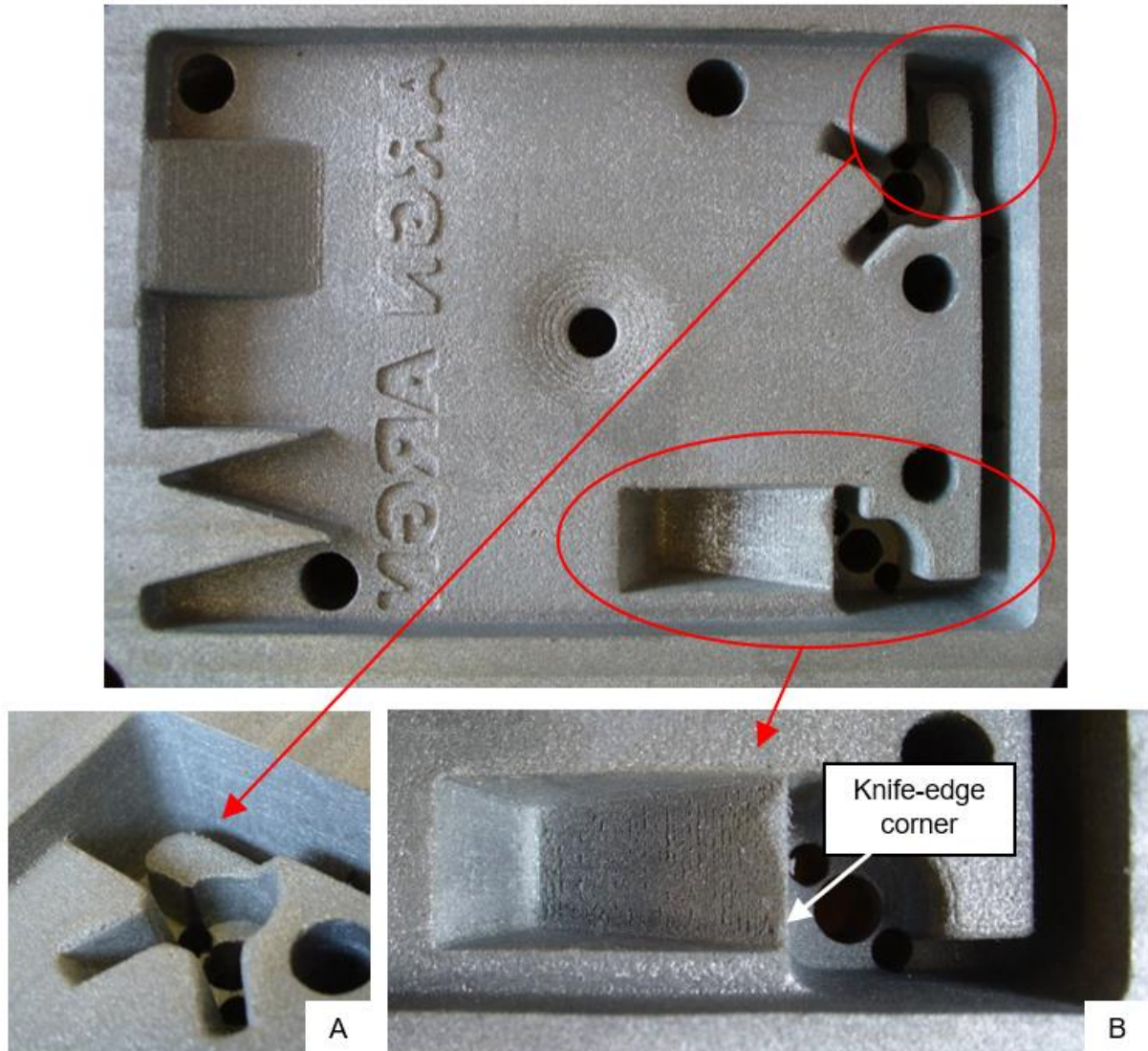


Figure 4.64 Moving half of the Alumide[®] insert after 200 IM cycles using ABS. Figures A and B are enlargements of the encircled regions of the insert.

SIGMASOFT[®] simulation results shown in Figure 4.65 indicated an insert temperature of 211.5 °C after the 20th IM cycle for the feature shown in Figure 4.64 A, and 204.7 °C for the feature shown in Figure 4.64 B. These temperatures exceeded the melt temperature of Alumide[®], resulting in the wear of these features.

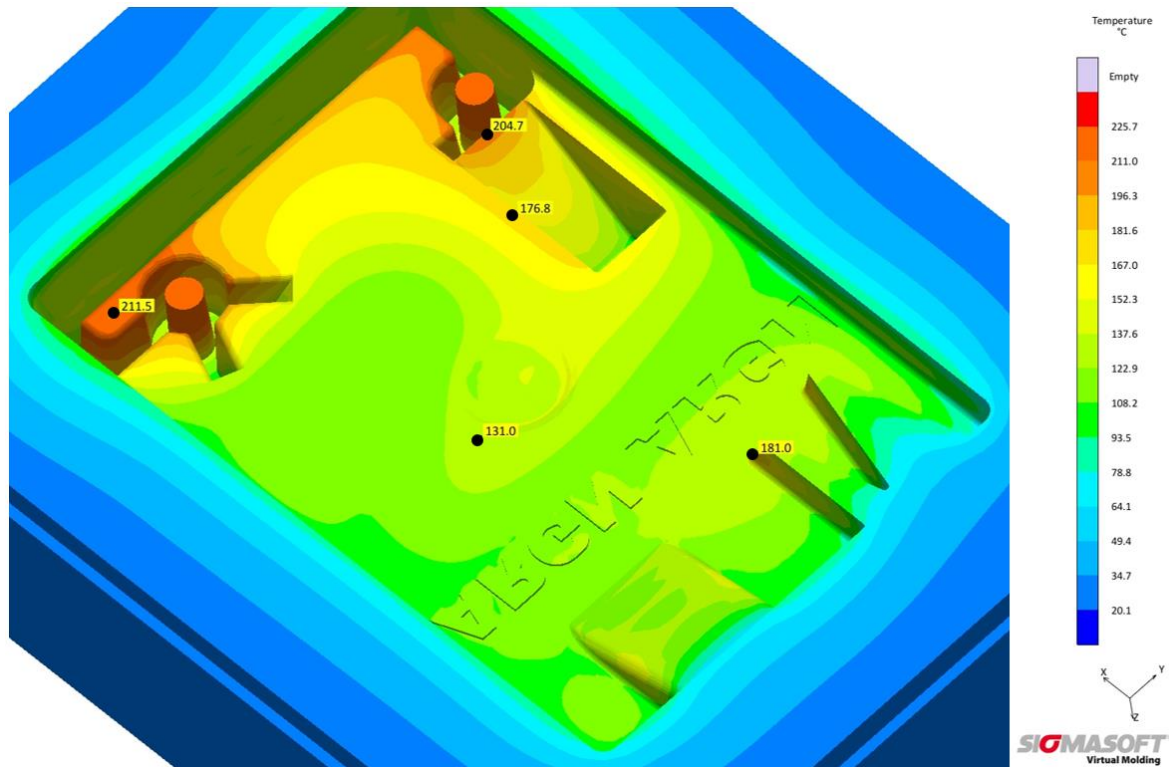


Figure 4.65 Temperatures of the moving half Alumide® insert using ABS after the 20th IM cycle, according to SIGMASOFT® virtual moulding software.

Measurements of the insert feature shown in Figure 4.64 A were taken from the IM parts with a Vernier calliper to determine the wear progression. Figure 4.66 shows a sectional view of the CAD model indicating how the measured value was obtained from the IM part. The wear value of an IM part was obtained by subtracting the measured value from the value the feature had before wear occurred (reference value).

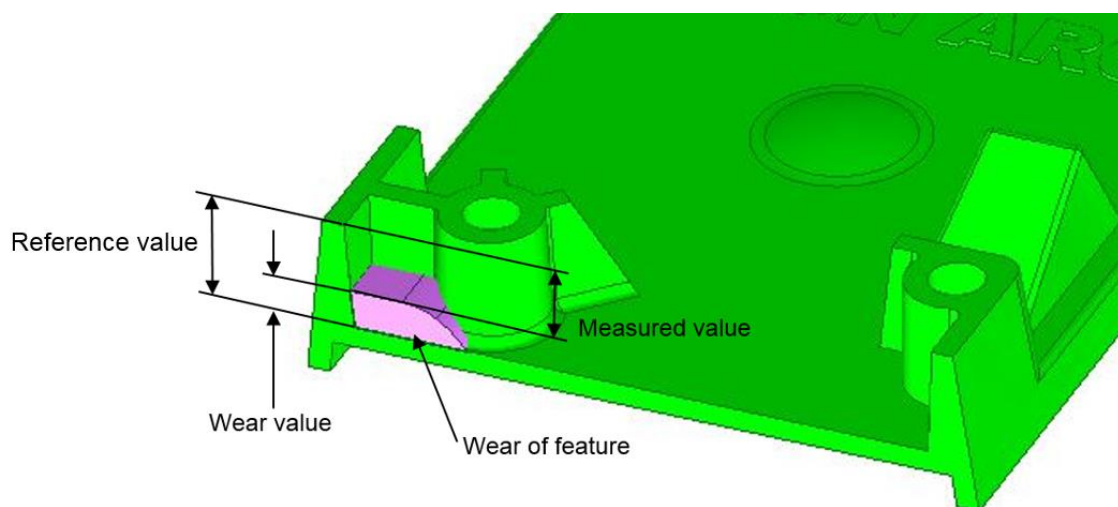


Figure 4.66 Sectioned view of a CAD model showing the wear of the mould feature as well as the location of the measured, reference and wear values of the IM part.

Measurements of the insert feature shown in Figure 4.64 A are graphically presented in Figure 4.67, indicating the wear progression of the feature during the IM trial.

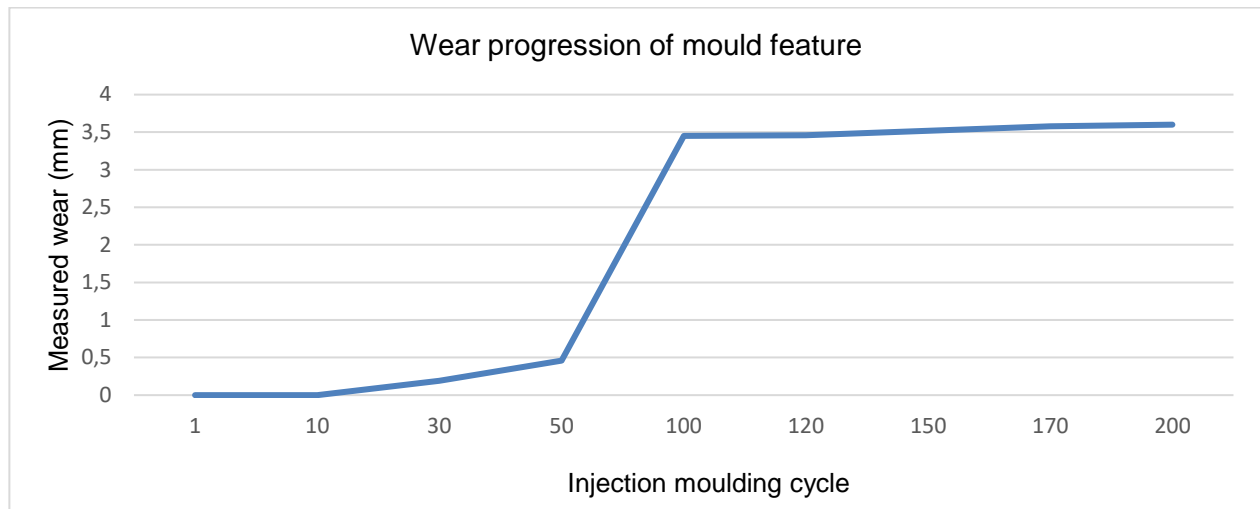


Figure 4.67 Wear of the uncooled insert feature from the first to the 200th IM cycle.

SIGMASOFT® simulation results shown in Figure 4.68 indicated maximum insert temperatures of 173.1 °C for the uncooled feature during the sixth IM cycle and 187.1 °C for the seventh IM cycle. The increase in temperature between the sixth and seventh IM cycle is more than the melting temperature of Alumide®, initiating wear. Wear of the feature slowly continued to increase until the 10th IM cycle when noticeable wear could be measured. As the feature continued to wear, more material was added to this region of the part during each IM cycle, increasing the temperature and wear at this region. This could explain the sudden increase in wear between the 50th and the 100th IM cycle, as shown in Figure 4.67. After the 100th IM cycle, the worn feature was closer to a section of the Alumide® insert where the cooling channels were able to cool down the feature between IM cycles. This reduced the temperature of the insert feature between IM cycles, decreasing the rate of wear.

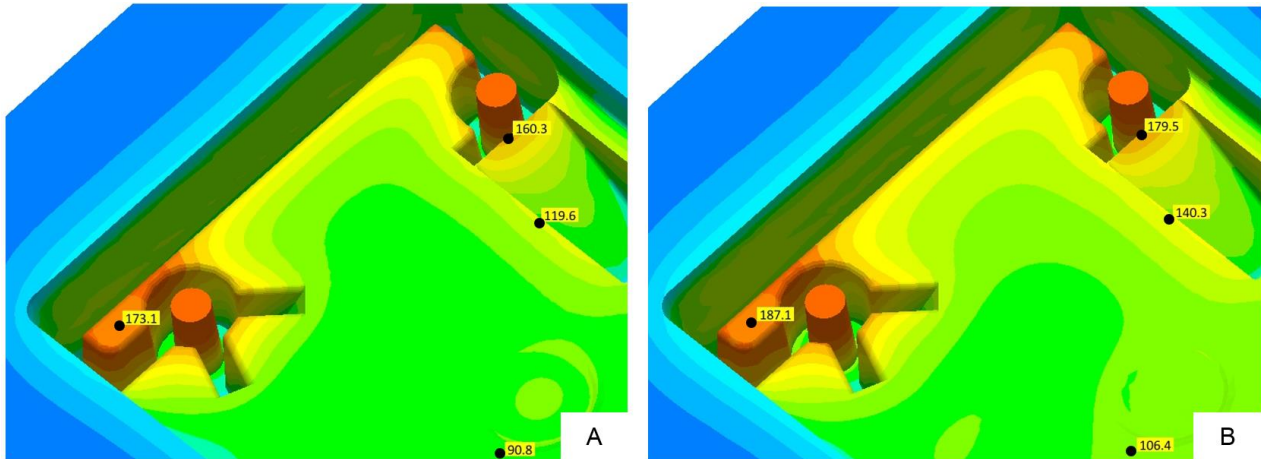


Figure 4.68 Insert temperatures of the moving half Alumide[®] insert during the 6th (A) and 7th (B) IM cycle, according to SIGMASOFT[®] virtual moulding software.

No noticeable wear was observed after the IM trials on the text features and the knife-edge corners shown in Figure 4.69.

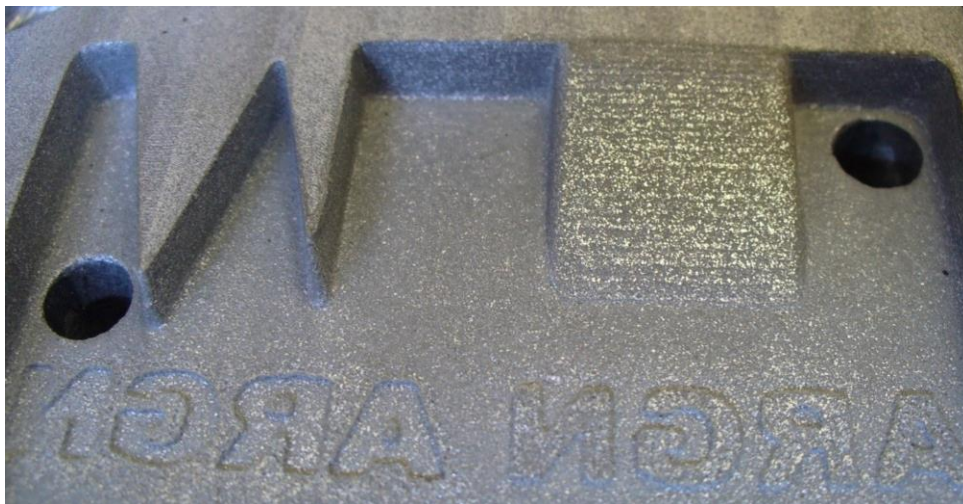


Figure 4.69 Text features and knife-edge corners without any wear after 200 IM cycles using ABS.

The Alumide[®] inserts were scanned after 200 IM cycles and compared to the CAD data. The deviation between the scan and CAD data was between 0.2 – 0.3 mm. Due to budget constraints, it was not possible to scan and compare the inserts to the CAD data before the IM trials commenced, therefore this deviation could be from material removed during the polishing of the inserts. From the scan results shown in Figure 4.70, there were no geometrical features (apart from the isolated feature shown in Figure 4.64 A) with a deviation larger than 0.5 mm.

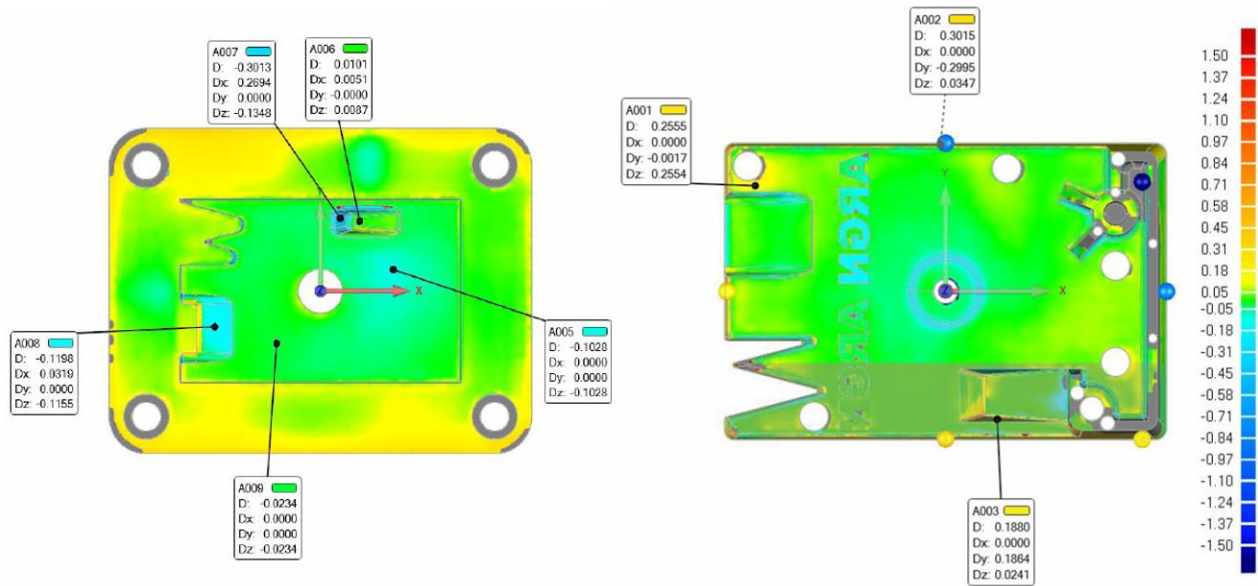


Figure 4.70 Scan results of the moving and fixed Alumide[®] inserts after 200 IM cycles using ABS.

iii. Geometrical mould trial with PC

The process parameters used during the trial with PC are summarised in Table 4.11.

Table 4.11 Injection moulding process parameters used during the manufacturing of geometrical parts from PC.

Material preparation	Material dried for 3 hours at 120 °C
Injection pressure	4 MPa
Nozzle temperature	300 °C
Cycle time	63 seconds
Mould cooling	Controlled by a tool temperature controller set at 30 °C

A total of 180 IM cycles were completed before the trial was ended. At the start of the trial, the tool temperature controller was initially set at 20 °C. At this temperature setting, the PC material flowing from the nozzle solidified before the cavity was completely filled. The temperature was gradually increased until the cavity completely filled at a temperature setting of 30 °C.

Within the first couple of IM cycles, wear was detected on the geometrical features of the Alumide[®] inserts. Figure 4.71 shows the fixed half of the Alumide[®] insert after 180 IM cycles.

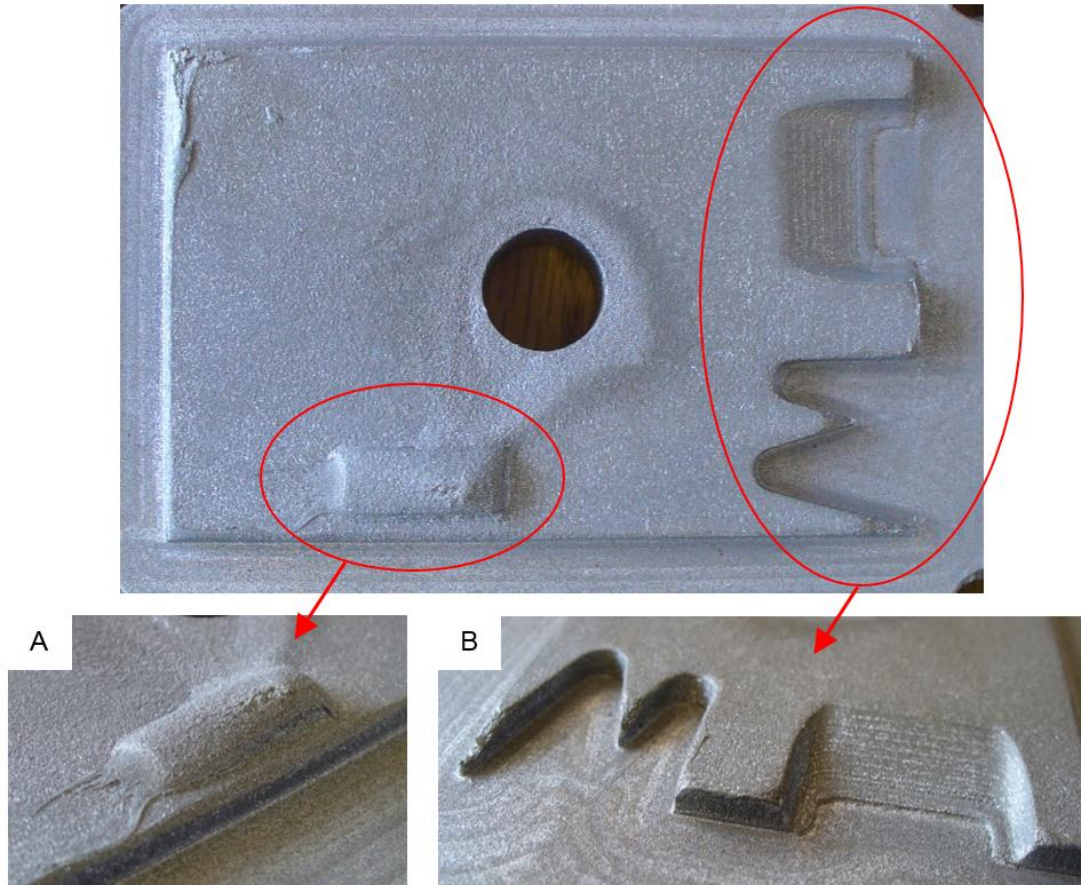


Figure 4.71 Fixed half of the Alumide® insert after 180 IM cycles using PC. Figures A and B are enlargements of the encircled regions of the insert.

SIGMASOFT® simulation results shown in Figure 4.72 indicated insert temperatures that exceeded the melting temperature of Alumide® after the 5th IM cycle resulting in the melting and wear of the features shown in Figure 4.71.

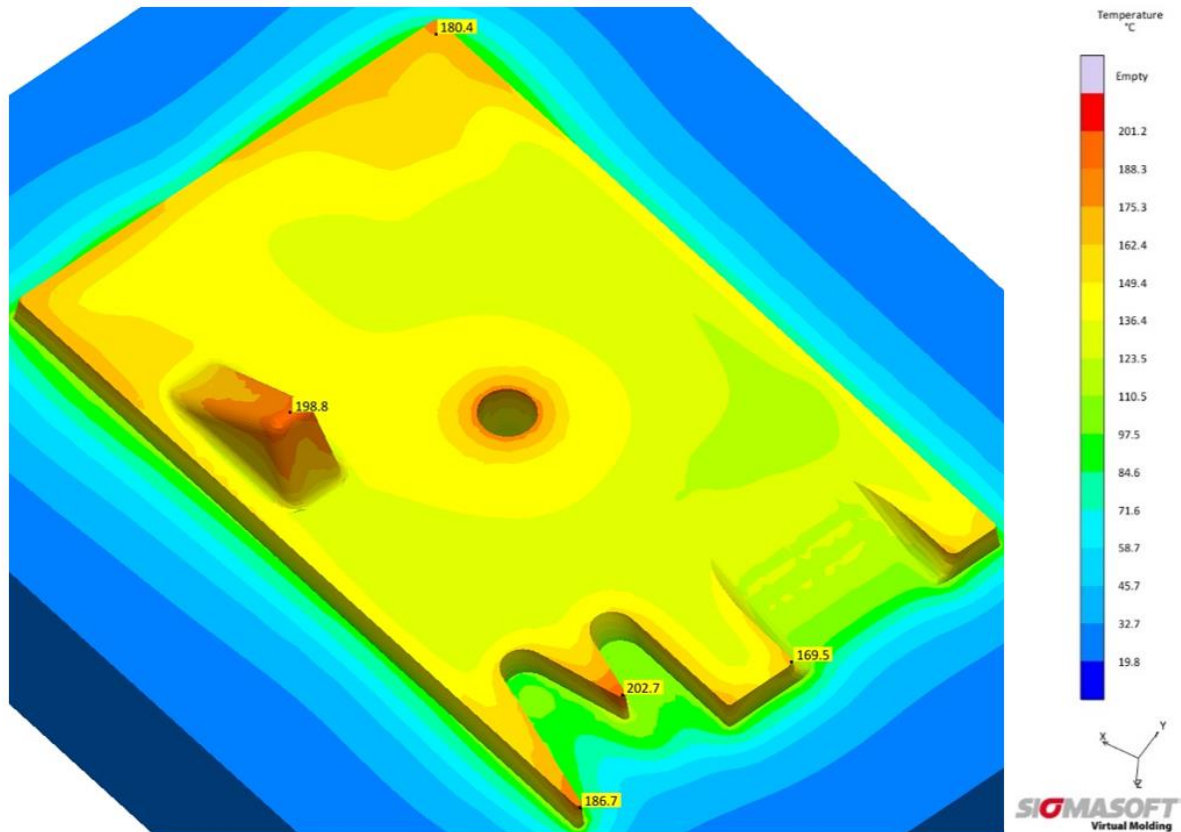


Figure 4.72 Temperatures of the fixed half Alumide[®] insert using PC after the 5th IM cycle, according to SIGMASOFT[®] virtual moulding software.

Because it was not practical to remove and scan the Alumide[®] inserts after a number of IM cycles to determine the wear, the geometrical accuracy of the IM parts were determined at certain intervals using the Kreon scanning arm. During the IM trial, parts produced from the Alumide[®] inserts were numbered in the sequence that they were manufactured. The first part produced was used as a reference for the subsequent parts to be compared to using Geomagic[®] Qualify software. This procedure was used to determine the progression of the wear for the Alumide[®] inserts. The wear of features that could not be scanned was measured on the parts with measuring equipment such as a micrometer or a digital Vernier calliper.

Figure 4.73 shows a graphical comparison in Geomagic[®] Qualify between the reference part and subsequent parts indicating the wear progression at a section from the fixed half of the Alumide[®] insert.

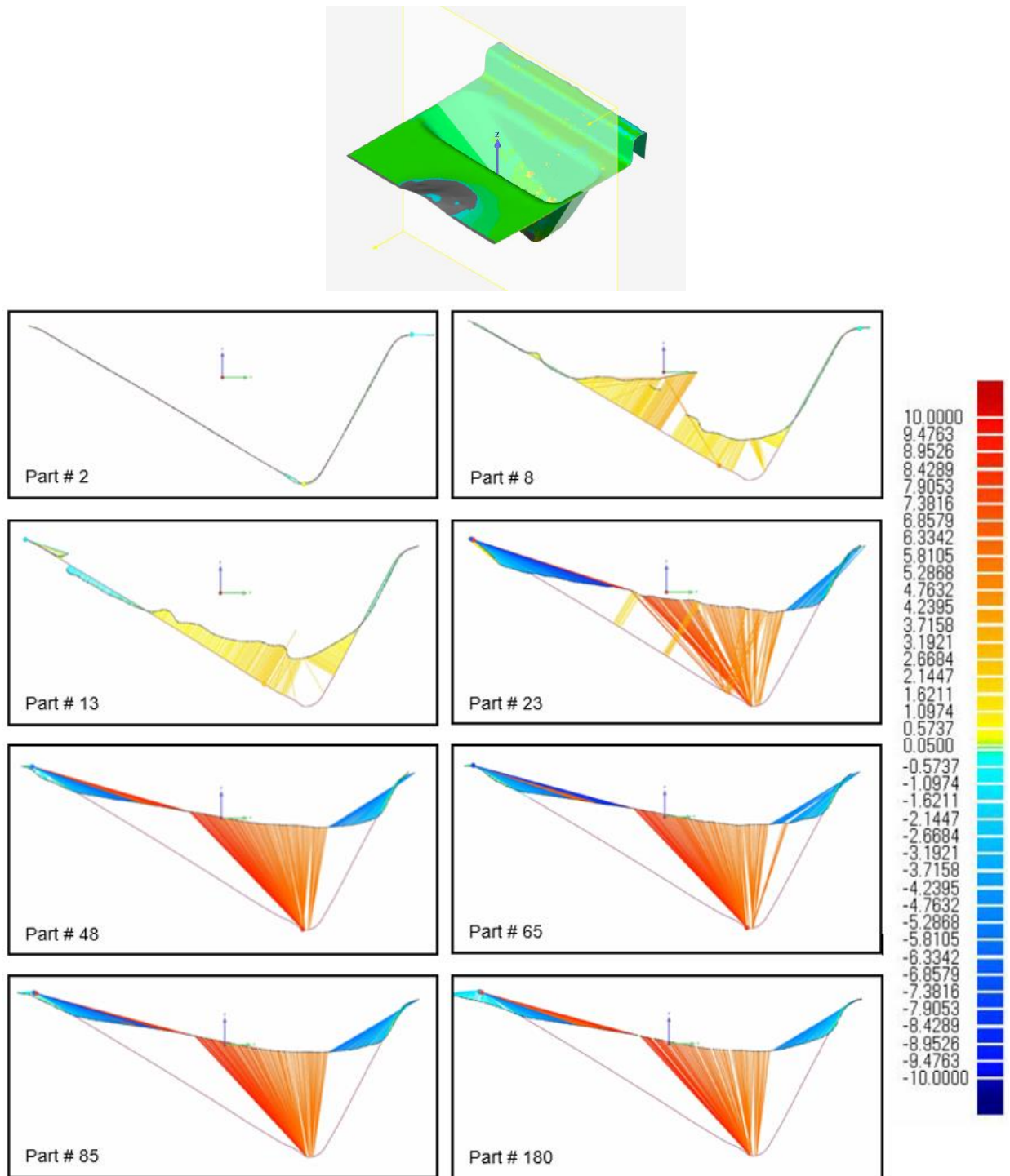


Figure 4.73 Graphical representation of the wear progression of a geometrical feature from the fixed half of the Alumide[®] insert from an IM trial with PC material.

Figure 4.74 shows the moving half after 180 IM cycles. Excessive wear occurred on the geometrical features of the insert, as shown in Figure 4.74 A and B.

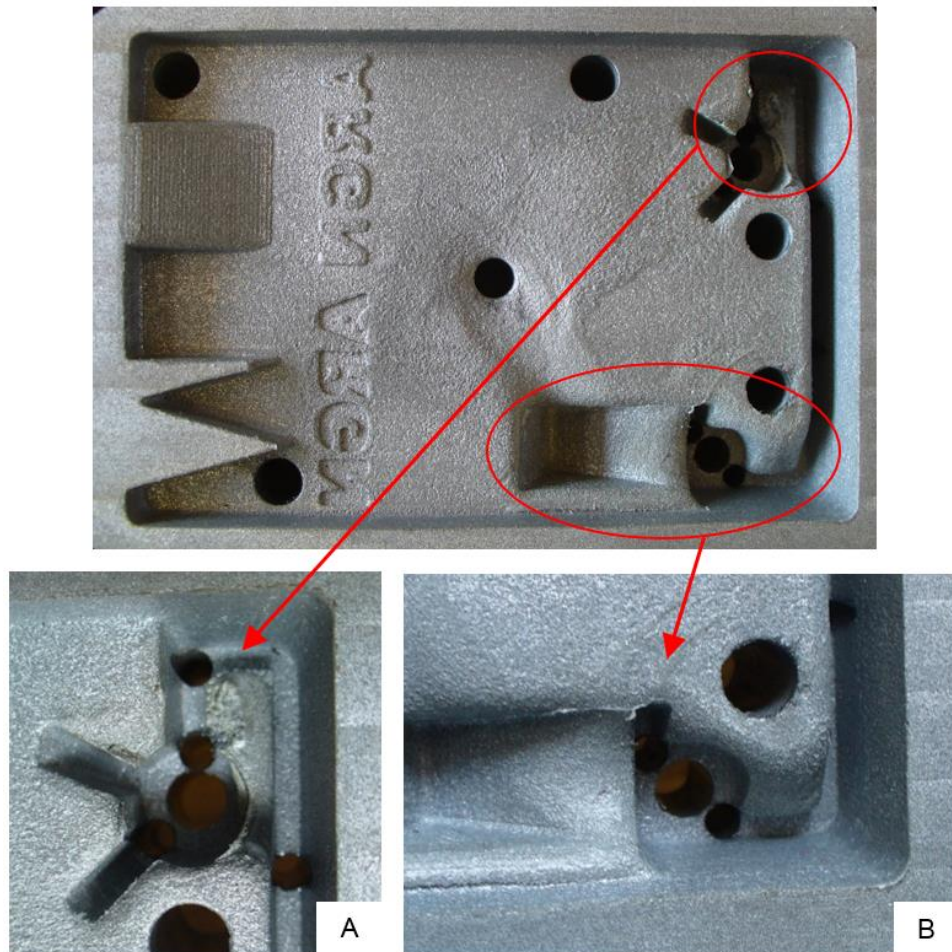


Figure 4.74 Moving half of the Alumide® insert after 180 IM cycles using PC. Figures A and B are enlargements of the encircled regions of the insert.

SIGMASOFT® simulation results shown in Figure 4.75, indicated insert temperatures exceeding 198.8 °C after the 5th IM cycle for the features shown in Figure 4.74. These high temperatures resulted in the melting of insert features causing the excessive wear shown in Figure 4.74.

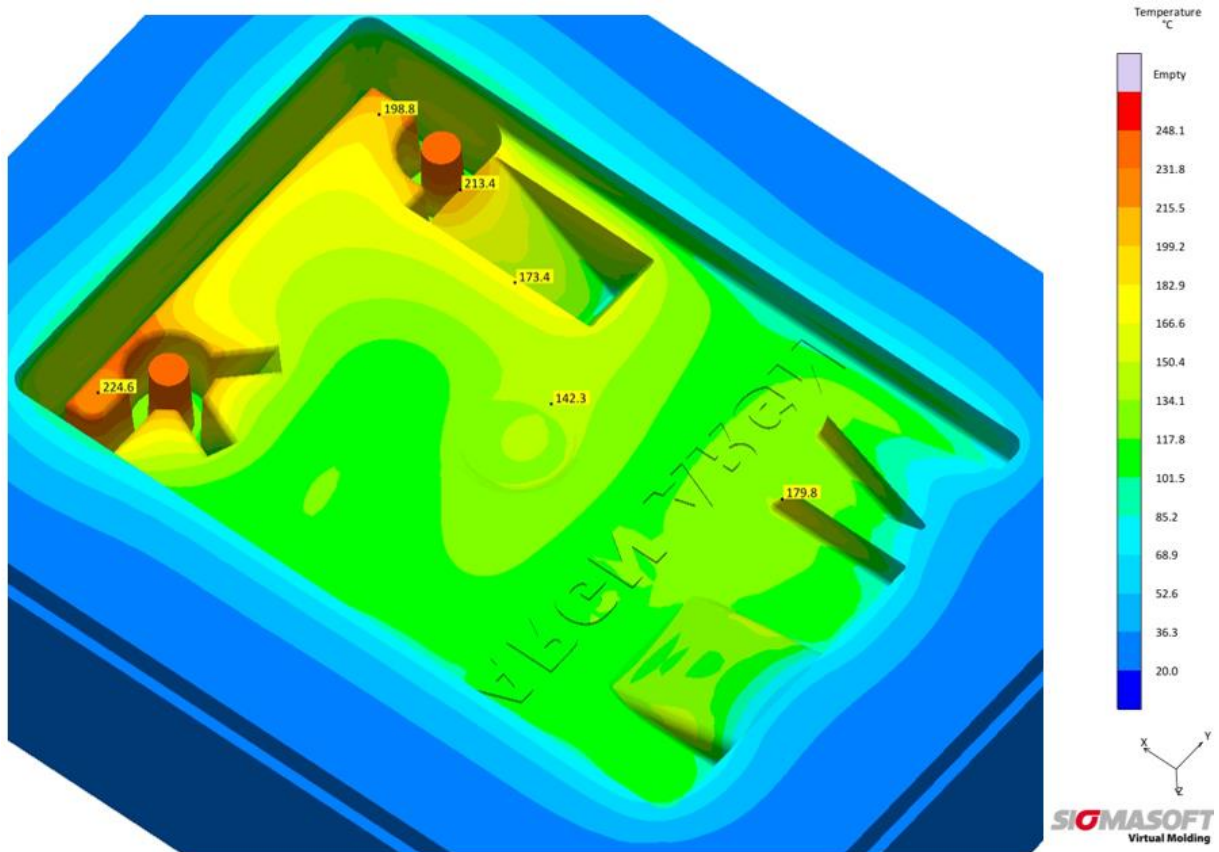


Figure 4.75 Temperatures of the moving half Alumide[®] insert using PC after the 5th IM cycle, according to SIGMASOFT[®] virtual moulding software.

Figure 4.76 shows a graphical comparison in Geomagic[®] Qualify, indicating the progression of the wear between the reference part and the subsequent parts at a section taken of the moving half of the Alumide[®] insert.

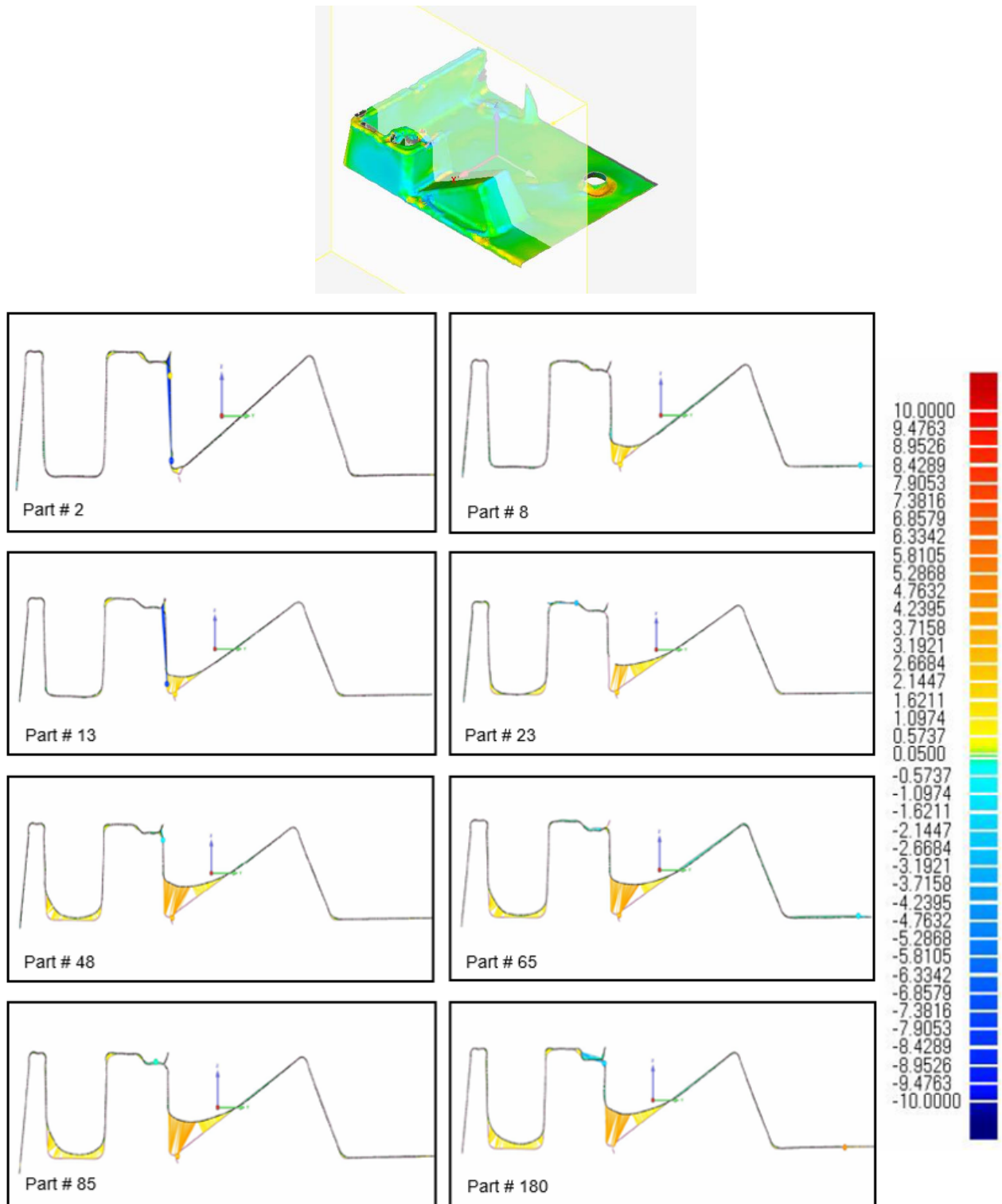


Figure 4.76 Graphical representation of the wear progression of geometrical features from the moving half of the Alumide® insert from an IM trial with PC material.

From Figures 4.73 and 4.76 it can be seen that after the eighth IM cycle geometrical features of the Alumide® insert wore to such extent that the manufactured part would no longer be acceptable. From these figures, it is also observed that insert features rapidly

wore until the 48th IM cycle after which the wear remained relatively unchanged. The reason for this could be that the features were closer to a section of the Alumide[®] insert where cooling channels were able to cool down these features between IM cycles, preventing the insert temperature from increasing above the melting temperature of Alumide[®].

Wear also occurred on the text features and knife-edge corners of the Alumide[®] insert, as shown in Figure 4.77, due to the high temperatures of the Alumide[®] insert.

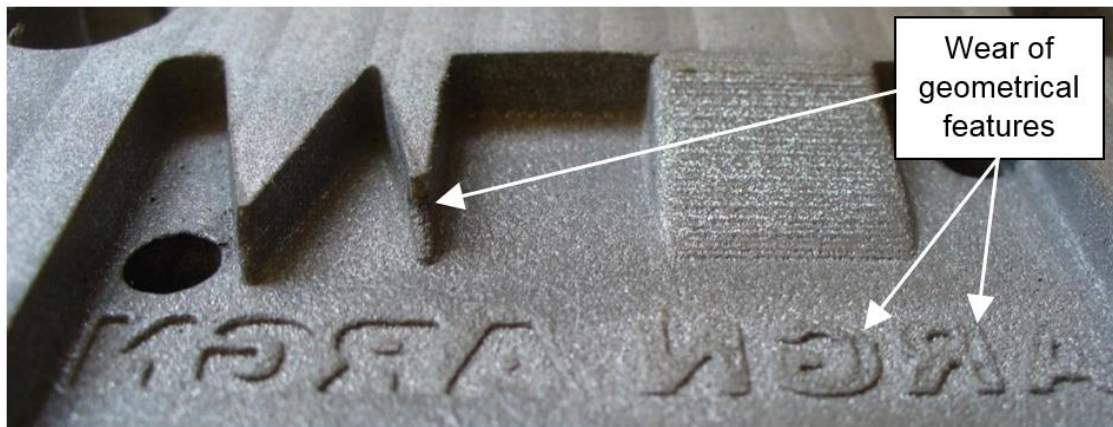


Figure 4.77 Wear occurring on text features and knife-edge corners after 180 IM cycles with PC material.

iv. Geometrical mould trial with PA 6

The process parameters used during the trial with PA 6 are summarised in Table 4.12.

Table 4.12 Injection moulding process parameters used during the manufacturing of geometrical parts from PA 6.

Material preparation	Material dried for 8 hours at 82 °C
Injection pressure	4 MPa
Nozzle temperature	240 °C
Cycle time	65 seconds
Mould cooling	Controlled by a mould temperature controller set at 20 °C

A total of 150 IM cycles were completed before the trial was ended. Within the first couple of IM cycles, wear was detected on the geometrical features of the Alumide[®] inserts. Figure 4.78 shows the fixed half of the Alumide[®] insert after 150 IM cycles.

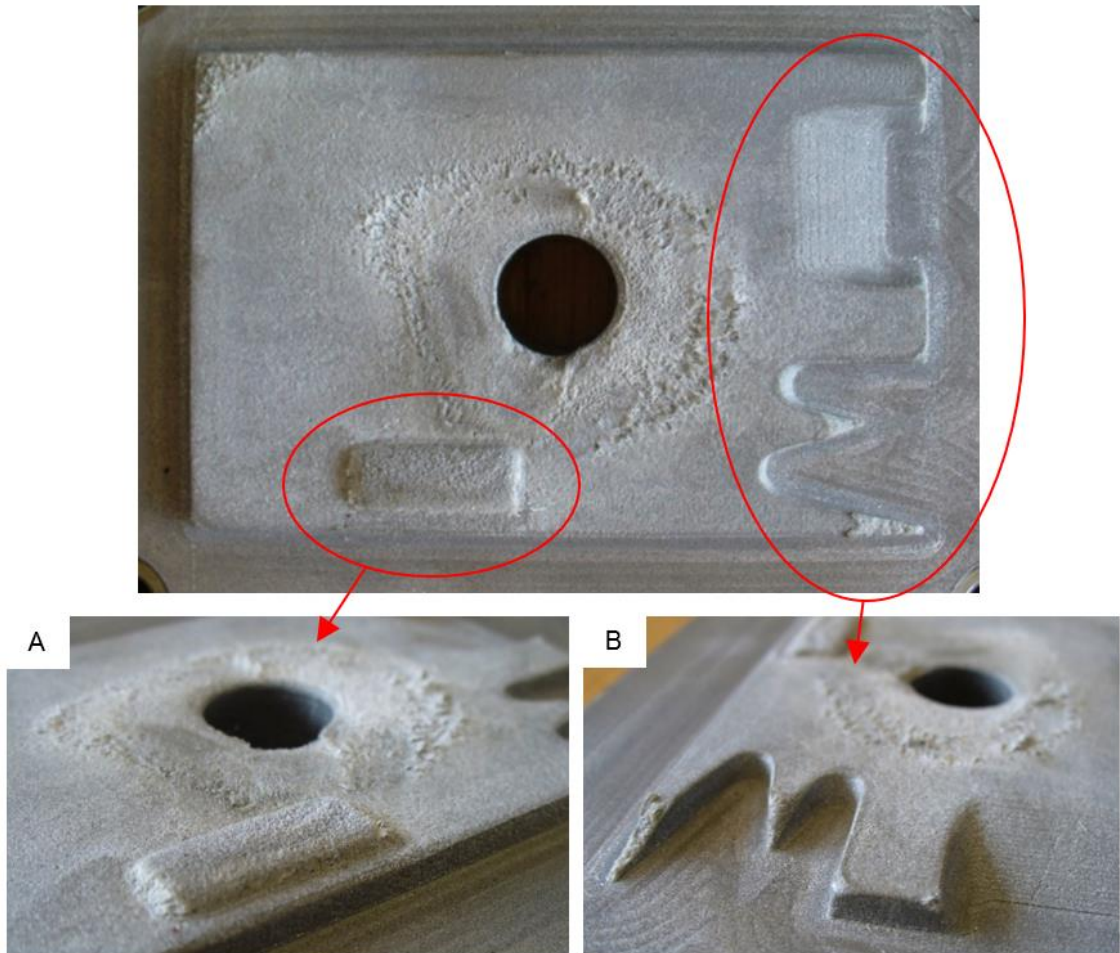


Figure 4.78 Fixed half of the Alumide[®] insert after 150 IM cycles using PA 6. Figures A and B are enlargements of the encircled regions of the insert.

SIGMASOFT[®] simulation results shown in Figure 4.79 indicated insert temperatures which exceeded the melting temperature of Alumide[®] after the 10th IM cycle. These insert temperatures were less than those predicted for the PC material.

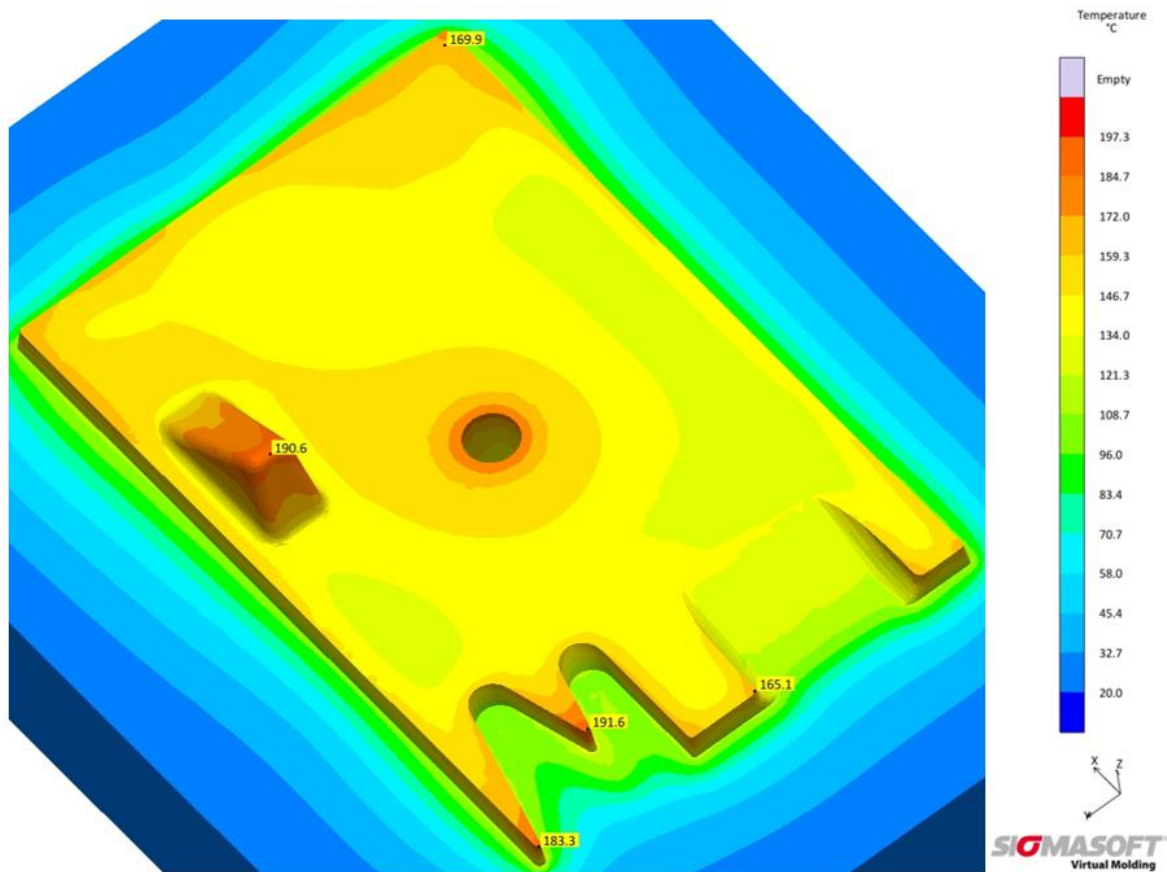


Figure 4.79 Temperatures of the fixed half Alumide[®] insert using PA6 after the 10th IM cycle, according to SIGMASOFT[®] virtual moulding software.

The significant wear on the features could be due to the melting and bonding of the polyamide particles in the Alumide[®] mixture with the injected PA 6 material, and removed with the part from the cavity during the ejection phase of an IM cycle. Fragments of Alumide[®] material were visible on the parts manufactured from polyamide throughout the trial, as shown in Figure 4.80.

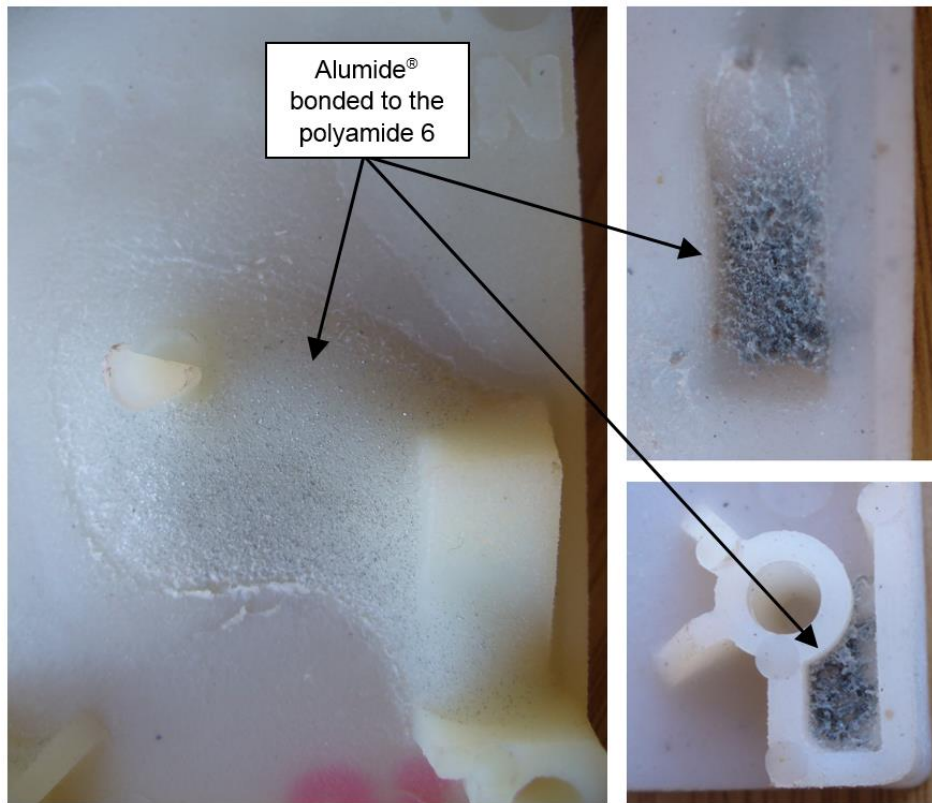


Figure 4.80 Alumide® material bonded to the polyamide 6 and torn from the Alumide® insert during the ejection of the part.

Figure 4.81 shows a graphical comparison in Geomagic® Qualify between the reference part and subsequent parts, indicating the wear progression at a section from the fixed half of the Alumide® insert.

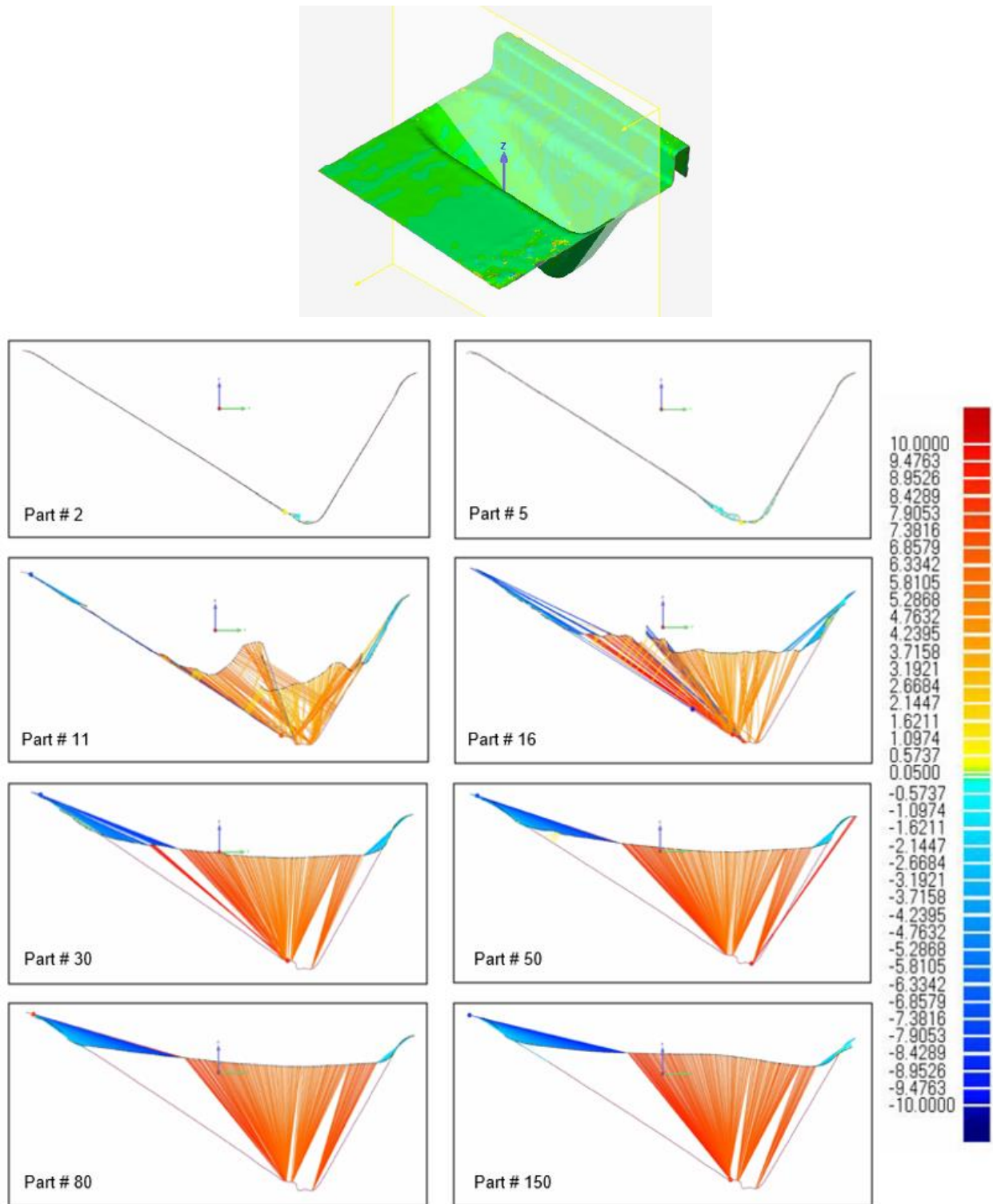


Figure 4.81 Graphical representation of the wear progression of a geometrical feature from the fixed half of the Alumide[®] insert from an IM trial with PA 6 material.

Figure 4.82 shows the moving half after 150 IM cycles with excessive wear to the geometrical features of the Alumide[®] insert.

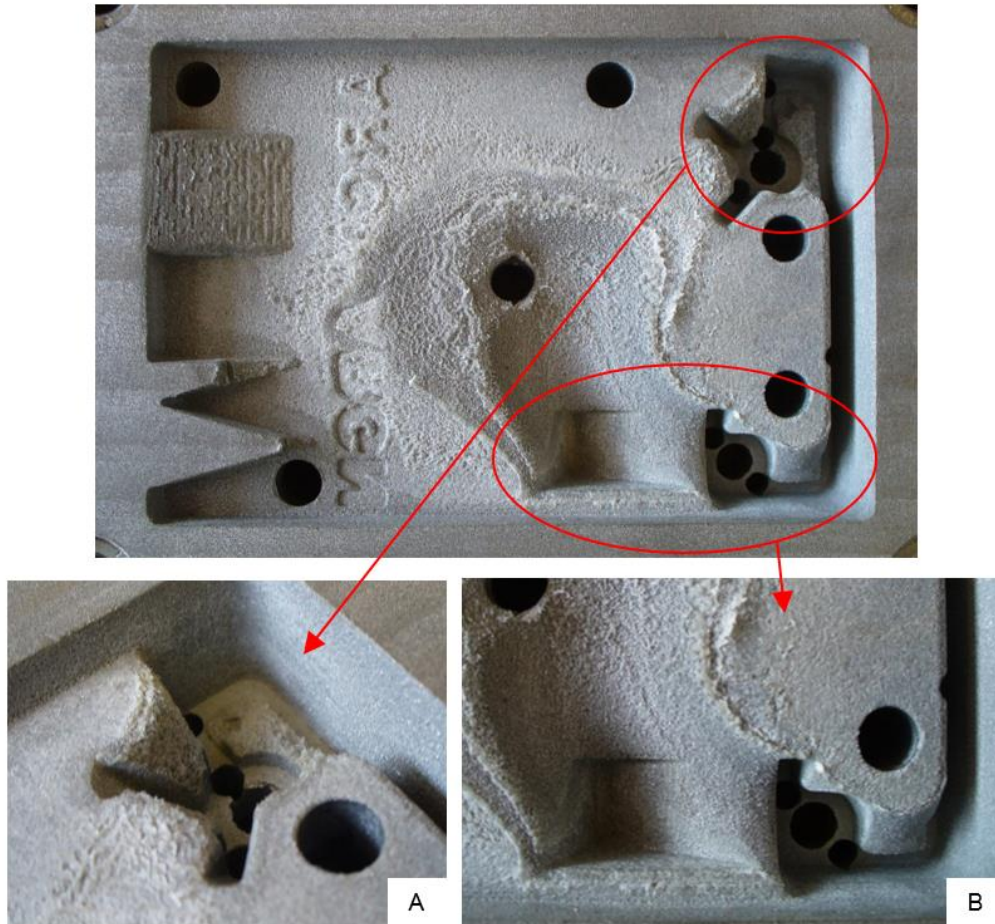


Figure 4.82 Moving half of the Alumide[®] insert after 150 IM cycles using PA 6. Figures A and B are enlargements of the encircled regions of the insert.

SIGMASOFT[®] simulation results shown in Figure 4.83 indicate insert temperatures which exceeded the melting temperature of Alumide[®], after the 10th IM cycle. The significant wear to the features shown in Figure 4.82 A and B could be due to the melting and bonding of the polyamide particles in the Alumide[®] mixture with the injected PA 6 that were removed with the part from the cavity during the ejection phase.

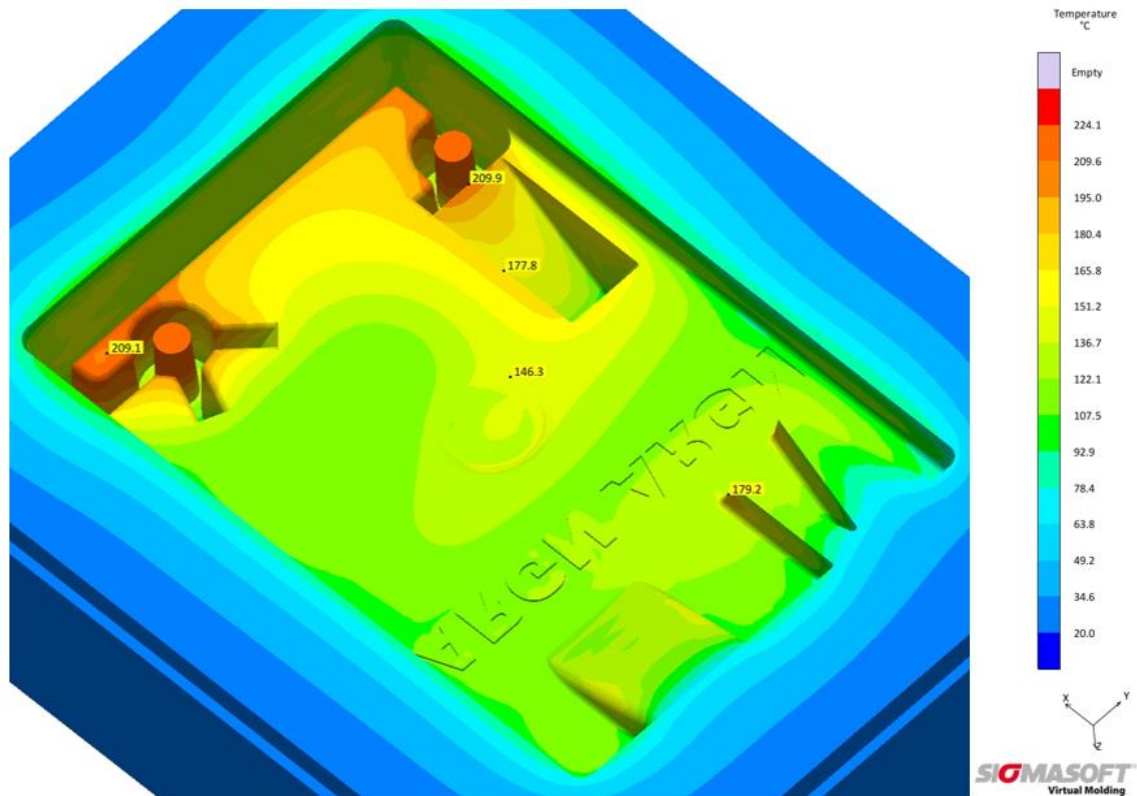


Figure 4.83 Temperatures of the moving half Alumide[®] insert using PA6 after the 10th IM cycle, according to SIGMASOFT[®] virtual moulding software.

Figure 4.84 shows a graphical comparison in Geomagic[®] Qualify between the reference part and the subsequent parts indicating the progression of the wear at a section taken from the moving half of the Alumide[®] insert.

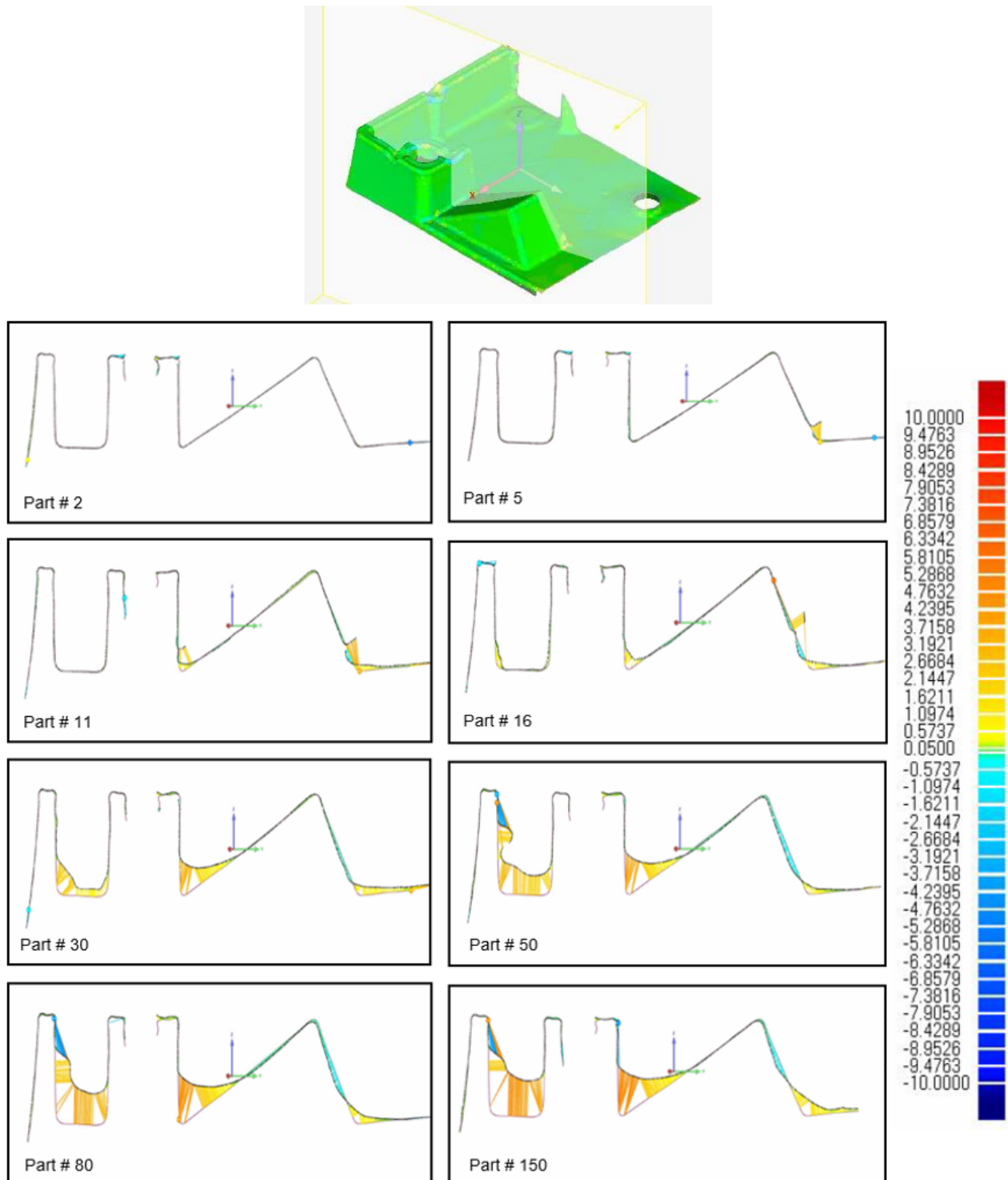


Figure 4.84 Graphical representation of the wear progression of a geometrical feature from the moving half of the Alumide® insert from an IM trial with PA 6 material.

Wear of the text features and knife-edge corners of the Alumide® insert are shown in Figure 4.85.



Figure 4.85 Wear of text features and knife-edge corners after 150 IM cycles with PA 6 material.

Discussion

Geometrical features close to the injection point tended to wear more quickly due to the continuous flow of molten polymer over these features. Redesigning of the geometrical part by moving features further from the injection point (shown in Figure 4.50), overcame this issue. A total of 200 IM cycles with PP did not cause any wear to the Alumide® inserts. From these results it can be concluded that PP is a suitable material for use with Alumide® inserts.

IM trials with ABS did not cause any wear to the Alumide® inserts in regions where effective cooling was present. Regions that could not be cooled effectively, due to mould constraints, resulted in wear as shown in Figure 4.64 A. This indicates that ABS can be successfully used with Alumide® inserts if effective cooling can be applied, particularly to regions with large volumes where molten polymer material can accumulate.

Due to the high processing temperature of PC (300 °C), the Alumide® material exceeded its melting point of 177 °C, causing rapid wear of the geometrical features, as shown in Figures 4.71, 4.74 and 4.77. Due to the rapid wear of geometrical features (within eight injection moulding cycles), PC is not suitable or feasible for use with Alumide® inserts.

Because polyamide is one of the constituents of Alumide®, it resulted in the bonding of the injected polyamide to the Alumide® during the cooling phase of the IM cycle. The Alumide®

material that bonded to the injected polyamide was torn from the insert during the ejection of the part from the mould as shown in Figure 4.80. From the scan data it can be seen that the wear on the insert continued to increase during the trial due to the bonding of the polyamide material. This indicates that polyamide is not suitable for use with Alumide[®] inserts.

From the results it can be concluded that polymer materials with a processing temperature of about 230 °C can be used for limited production runs with Alumide[®] if the insert features can be cooled to a temperature less than the melting temperature of Alumide[®].

5 CASE STUDY: INDUSTRIAL APPLICATION OF ALUMIDE® INSERTS

During Phase 4 of the research, an industry-specific product was identified that was suitable to be produced through Alumide® inserts. The results obtained from Phase 3 were implemented during the design of the inserts used during Phase 4. During the IM trial, a short production run was performed to determine the number of products that can be successfully manufactured with Alumide® inserts.

A cost and manufacturing time comparison between Alumide®, DMLS, PolyJet and conventionally manufactured inserts, as well as Rapid Manufacturing (RM) through AM processes was conducted. The aim of the comparison was to determine the feasibility of Alumide® inserts for limited run IM applications. The layout of Phase 4 is schematically illustrated in Figure 5.1.

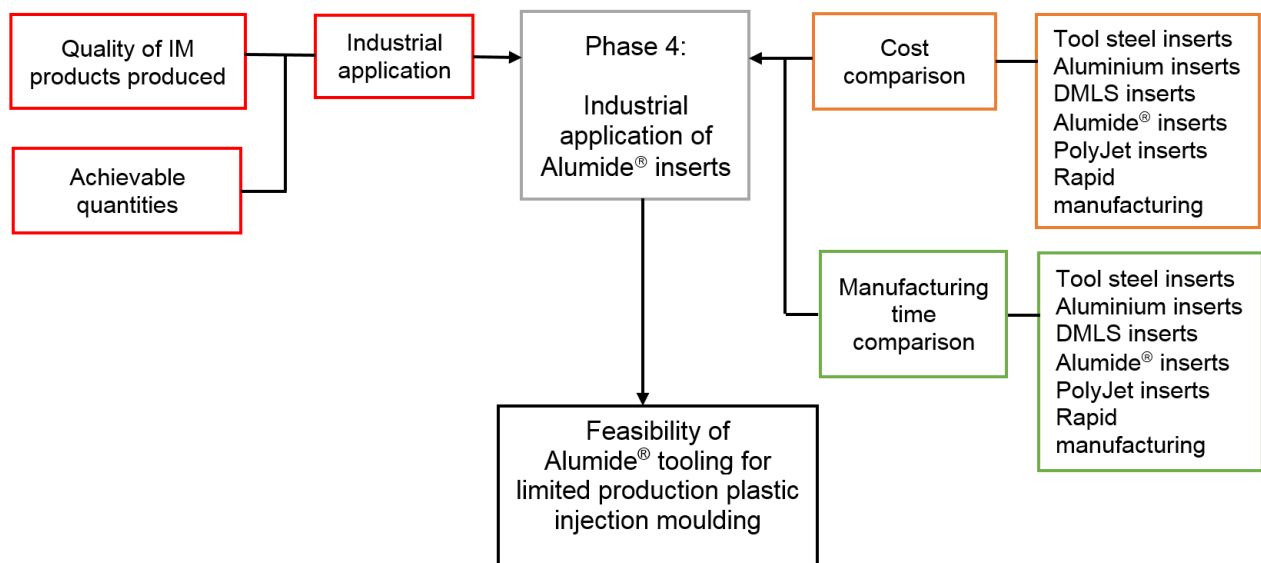


Figure 5.1 Schematic representation of Phase 4.

5.1 Enclosure mould

An ABS enclosure for a medical product was required for verification processes. Two hundred parts were required and due to the limited quantity, Alumide® inserts were used to manufacture the parts. It was also decided to do a trial run using PP. Figure 5.2 shows

a CAD model and a product drawing of the enclosure part including the dimensions and the geometrical features of the part.

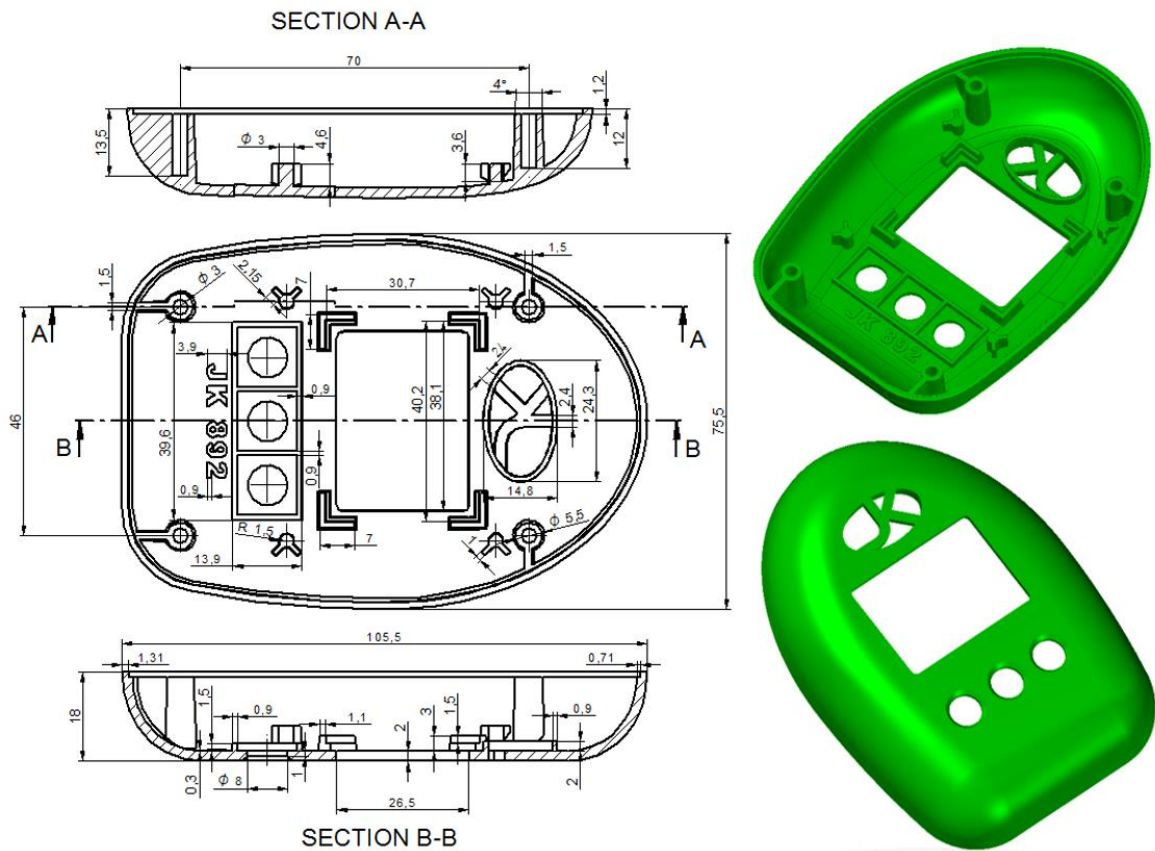


Figure 5.2 Dimensions and CAD model of the enclosure part.

5.1.1 Procedure

Alumide® inserts consisting of a single cavity were designed for the enclosure, as shown in Figure 5.3.

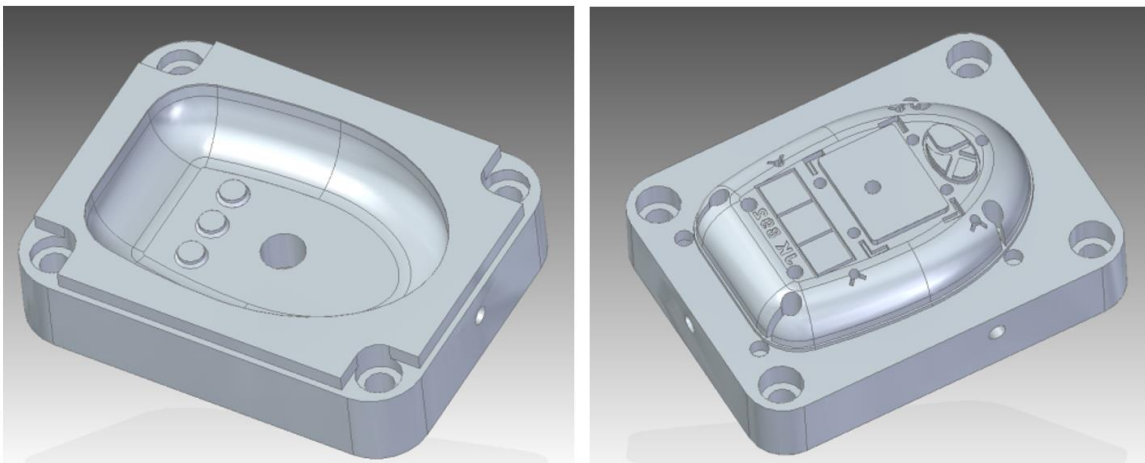


Figure 5.3 CAD models of the Alumide® inserts consisting of a single part cavity.

Oval conformal cooling channels, 5 mm from the cavity surface, were included into the Alumide[®] insert design. This channel geometry and placement was based on the results of experimental work described previously in the thesis. The conformal cooling channels were positioned along the cavity surfaces to obtain the best possible cooling while avoiding mould features such as screw and ejector pin holes, as shown in Figure 5.4. The inlet and outlet positions of the conformal cooling channels were placed at locations matching the cooling channel holes of the steel bolster.

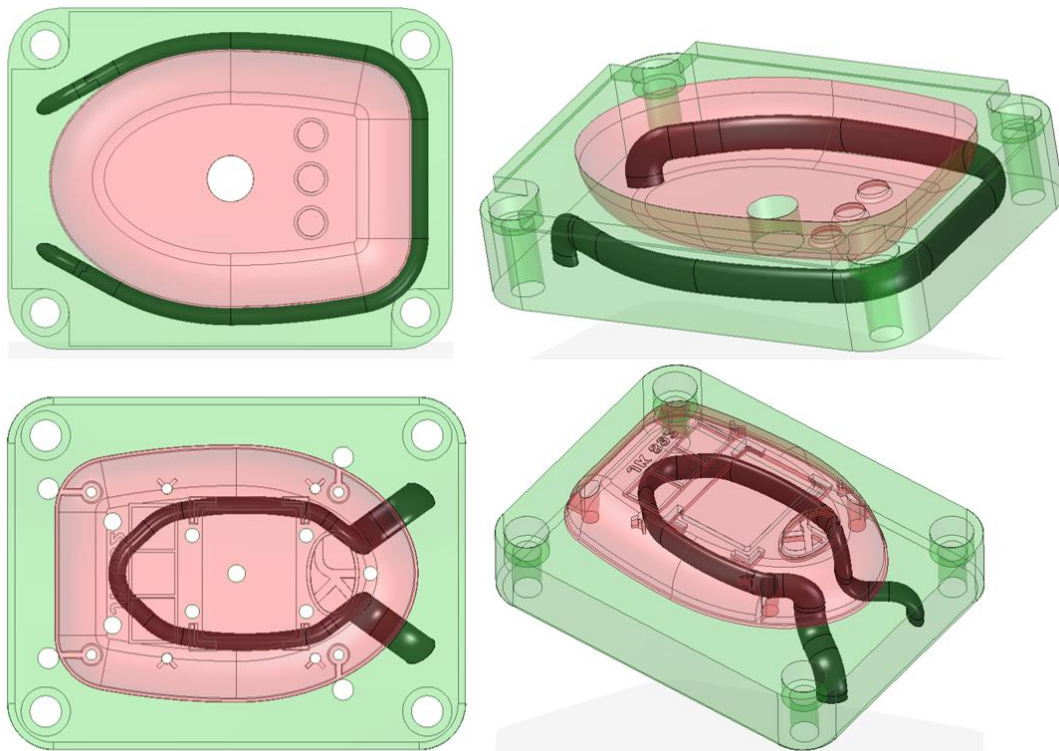


Figure 5.4 Conformal cooling channel design for the enclosure inserts avoiding mould features such as screw and ejector pin holes.

SIGMASOFT[®] IM simulation software was used to predict the temperatures of the Alumide[®] inserts, using PP and ABS. The software showed that geometrical features of the inserts with a temperature more than the melting temperature of Alumide[®] would occur only on the moving half, using PP and ABS, as shown in Figure 5.5.

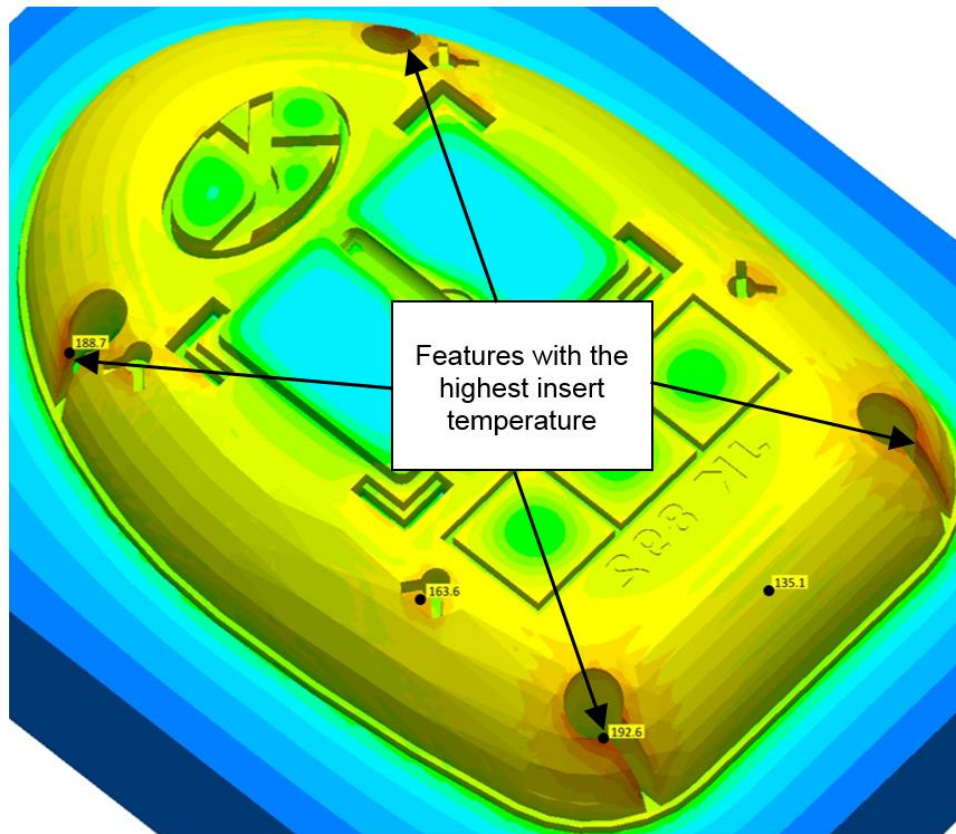


Figure 5.5 Geometrical features of the moving half insert with temperatures more than the melting temperature of Alumide®.

It would not be possible to cool the insert features shown in Figure 5.5 sufficiently due to their size and insert constraints, and the enclosure part could not be modified due to product specifications. A higher wear rate at these geometrical features was expected during the IM trials. IM trials with Alumide® inserts were continued because wear to these features would not influence the function of the part.

Figure 5.6 shows the AM inserts in the as-manufactured form. Figure 5.6 A and B show the fixed insert, and Figure 5.6 C and D the moving insert with the stair step effect visible on the insert features. Extra material was added to the cavity surfaces of the fixed insert for machining operations to obtain a polished-like outer surface on the parts. The surfaces of the moving inserts were polished by sanding using 320 and 400 grit sandpaper to remove the stair step effect.

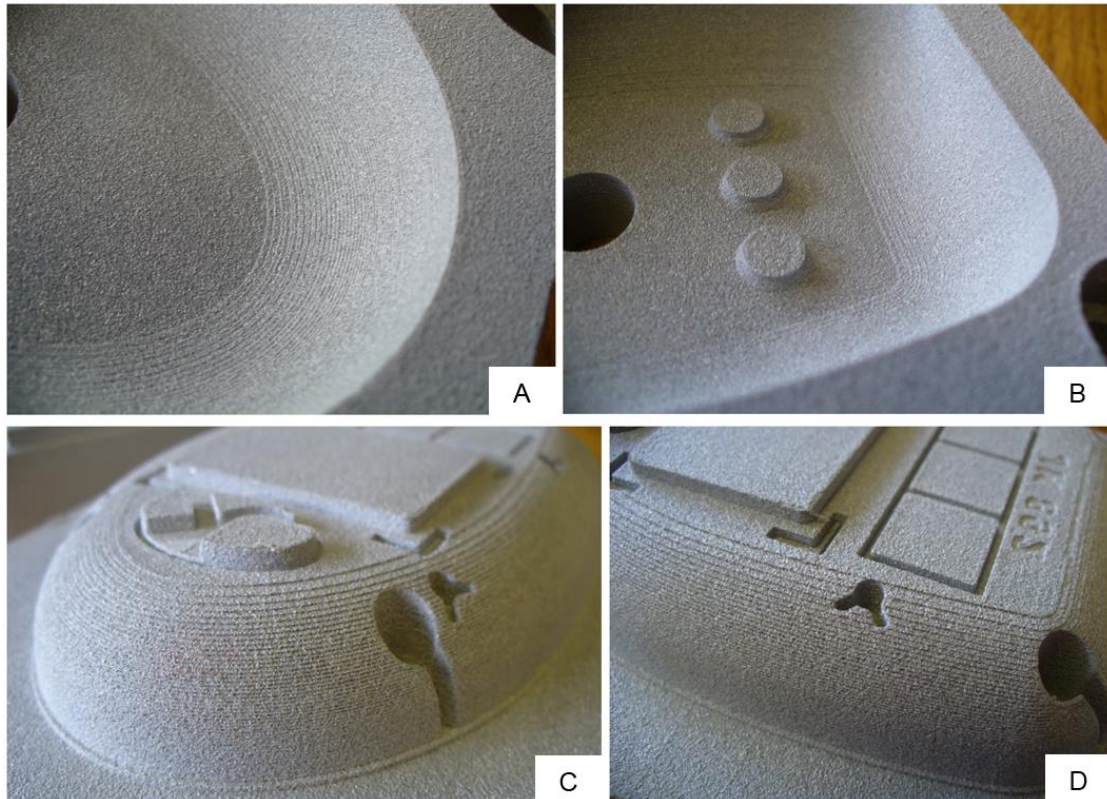


Figure 5.6 Stair step effect visible on features of enclosure insert in the as-manufactured form. A and B show the stair step effect on the fixed insert and C and D on the moving inserts.

Steel pins were inserted into the moving insert for the manufacturing of hole features, as shown in Figure 5.7. This post-processing procedure was repeated for both sets of inserts.

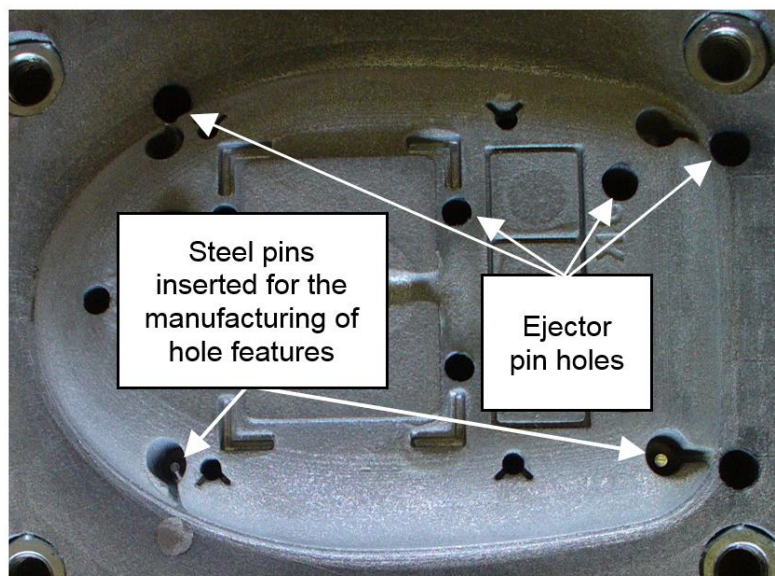


Figure 5.7 Machined and polished enclosure insert with ejector pin holes and steel pins inserted for the manufacturing of hole features.

The wall thickness of the manufactured parts at certain intervals was measured at four points (shown in Figure 5.8) with a micrometer to determine the wear of the inserts during the IM trial.

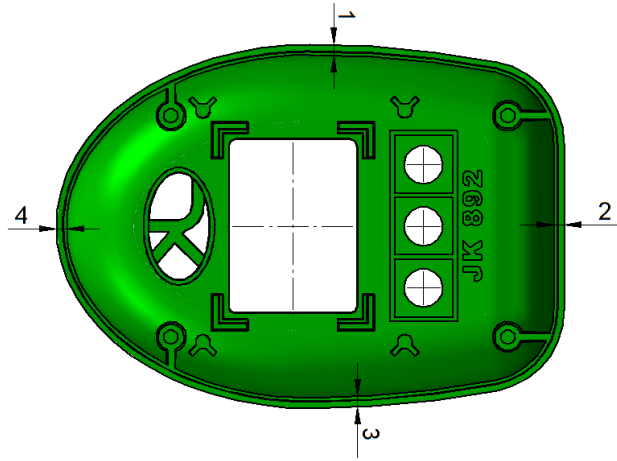


Figure 5.8 Positions of the four points where measurements were taken on the enclosure parts.

5.1.2 Results

Enclosure mould trial with PP

The process parameters used during the enclosure trial with PP, are summarised in Table 5.1.

Table 5.1 Injection moulding process parameters used during the manufacturing of enclosure parts from PP.

Material preparation	None
Injection pressure	4 MPa
Nozzle temperature	220 °C
Cycle time	45 seconds
Mould cooling	Water temperature controlled by a chiller unit set at 7 °C

After 200 IM cycles wear was noticed at the gate as well as geometrical features close to the injection position, as shown in Figure 5.9 C. The knife-edge corners of the geometrical feature shown in Figure 5.9 D started to delaminate due to the high heat retained in the boss feature. Apart from these features, no significant wear was observed on the Alumide[®] inserts, as shown in Figure 5.9 A and B.

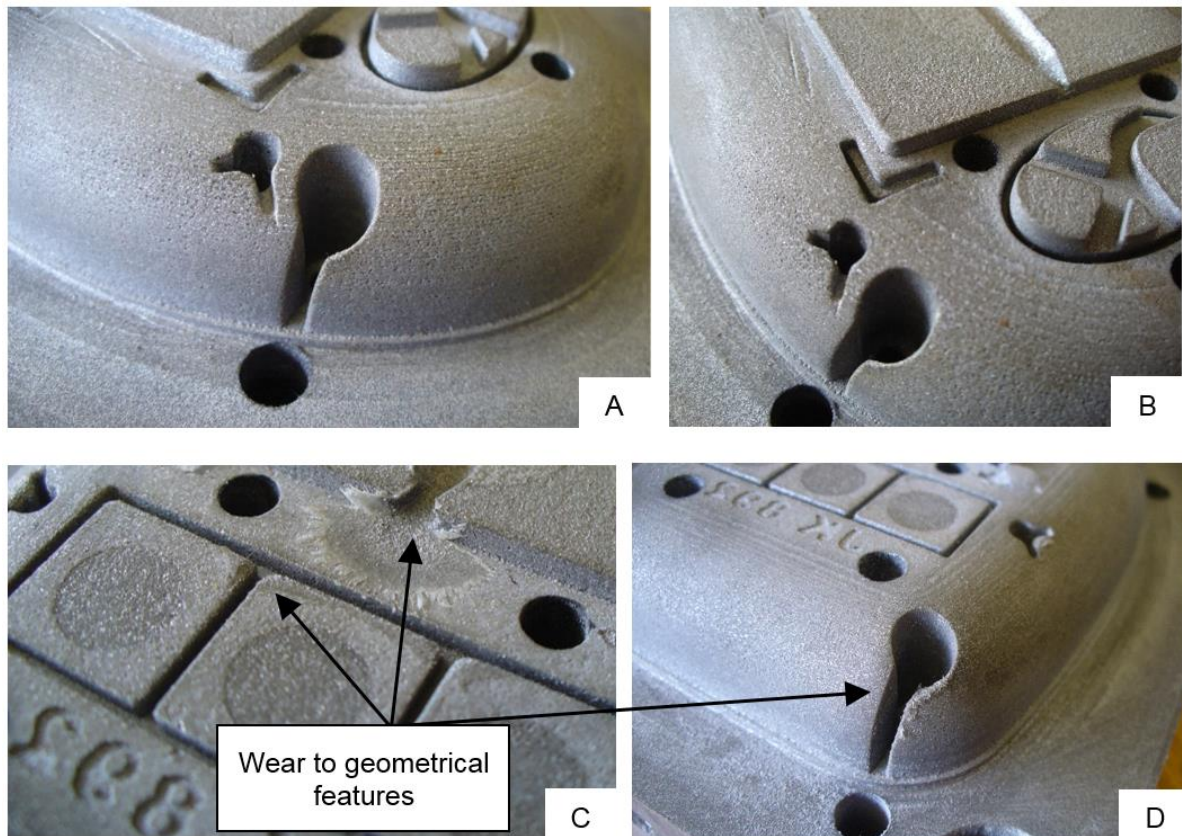


Figure 5.9 Alumide® inserts after 200 IM cycles using PP. C and D show the features where wear occurred.

Results from SIGMASOFT® virtual moulding software indicate that the insert features shown in Figure 5.9 A and D, have temperatures of 182.7 °C and 184.3 °C respectively after the 20th IM cycle, as shown in Figure 5.10. Because these temperatures are more than the melt temperature of Alumide®, wear to these features occurred. Although the temperature at the gate region is indicated as 123.4 °C, excessive wear (shown in Figure 5.9 C) occurred due to the high shear rate and subsequent viscous heating induced at the gate during the filling of the cavity.

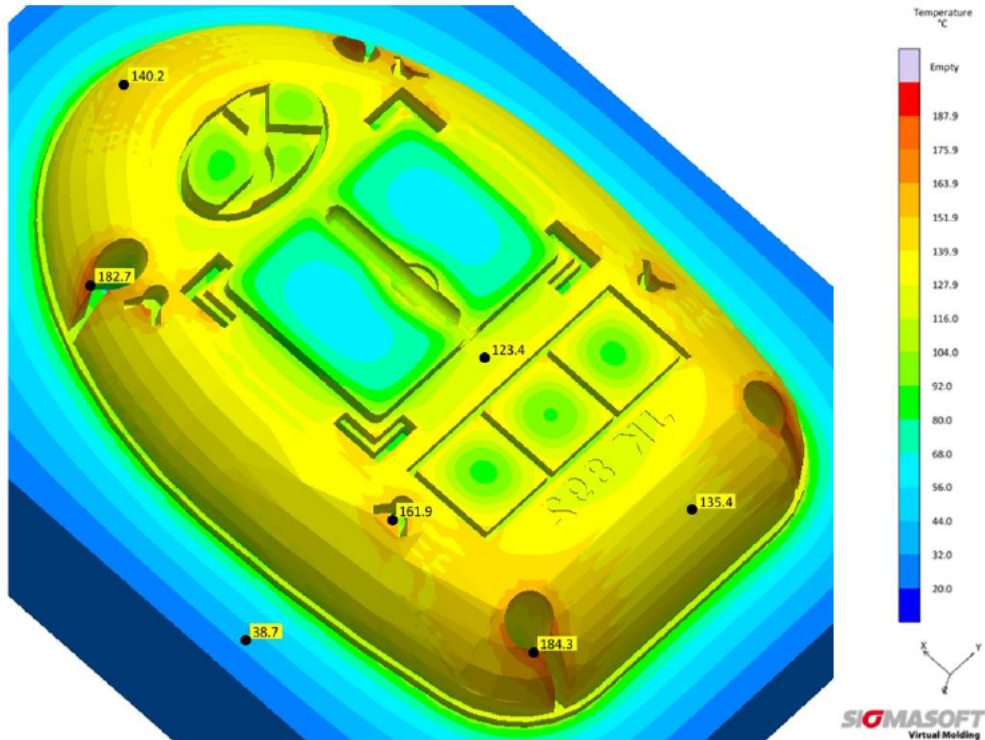


Figure 5.10 Temperatures of the moving half enclosure insert using PP material after the 20th IM cycle, according to SIGMASOFT® virtual moulding software.

The results from the measured wall thickness of the parts at the points shown in Figure 5.8 are shown in Figure 5.11. From the results it is seen that a small deviation occurred (less than 0.1 mm) from the 1st to the 200th injection-moulded part, which indicates that no significant wear occurred on the walls during the trial.

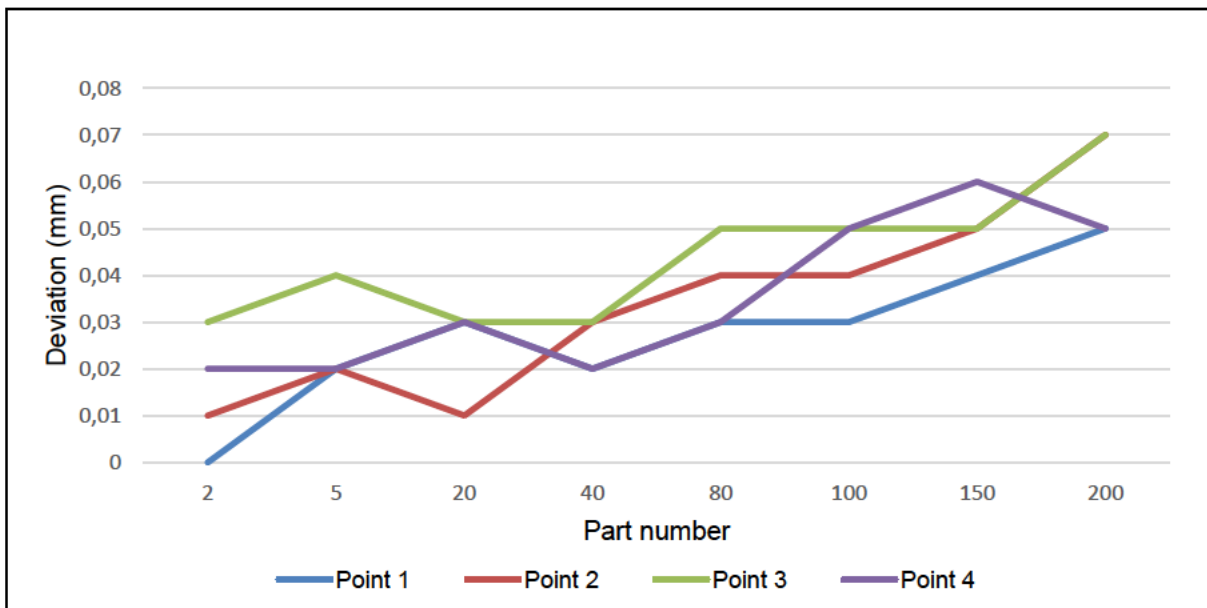


Figure 5.11 Wall thickness deviation of enclosure parts manufactured from Alumide® inserts using PP.

SIGMASOFT® simulation results indicated a maximum insert temperature of 121.9 °C for the fixed half Alumide® insert after the 20th IM cycle, as shown in Figure 5.12. This temperature is less than the melt temperature of Alumide® and resulted in minor wear, as shown in Figure 5.11.

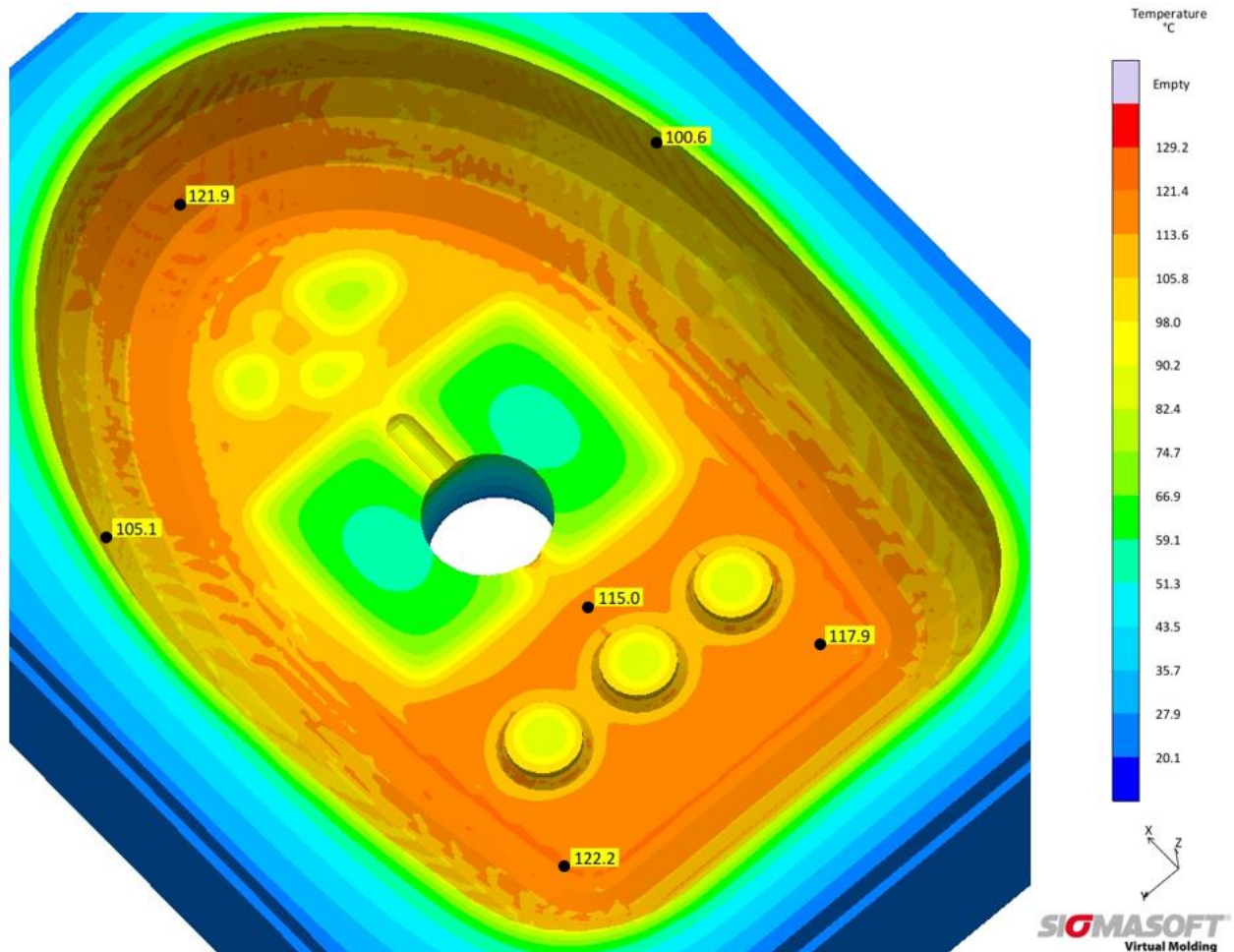


Figure 5.12 Temperatures of the fixed half enclosure insert using PP material after the 20th IM cycle, according to SIGMASOFT® virtual moulding software.

The Alumide® inserts were scanned after 200 IM cycles and compared to the CAD data of the inserts, as shown in Figure 5.13. The deviation between the scan and the CAD data was about 0.2 to 0.3 mm. This deviation could be from material removed during the polishing of the inserts.

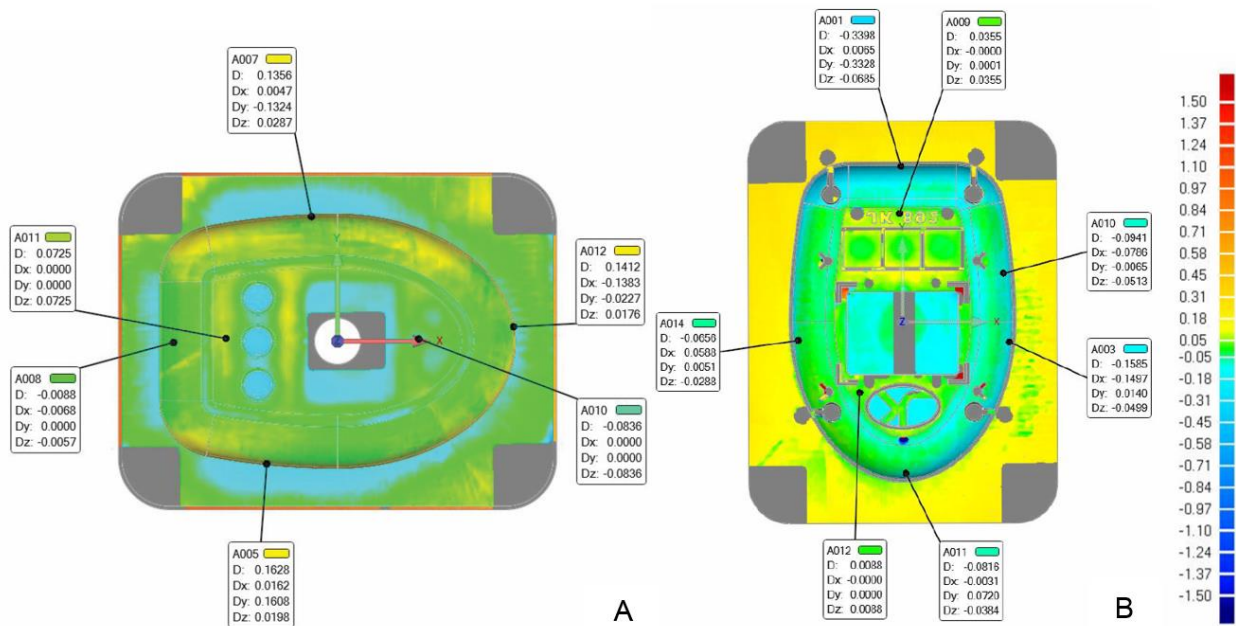


Figure 5.13 Scan results of the fixed (A) and moving (B) Alumide® inserts after 200 IM cycles using PP.

Enclosure mould trial with ABS

The process parameters used during the enclosure trial with ABS are summarised in Table 5.2.

Table 5.2 Injection moulding process parameters used during the manufacturing of enclosure parts from ABS.

Material preparation	Material dried for 2 hours at 82 °C
Injection pressure	4 MPa
Nozzle temperature	230 °C
Cycle time	52 seconds
Mould cooling	Water temperature controlled by a chiller unit set at 7 °C

After 200 IM cycles wear was noticed at the gate as well as geometrical features close to the injection position, as shown in Figure 5.14 C. The knife-edge corners of the geometrical feature shown in Figure 5.14 B and D wore due to the high heat retained by the boss features. Apart from these features, no significant wear was observed on the Alumide® inserts.

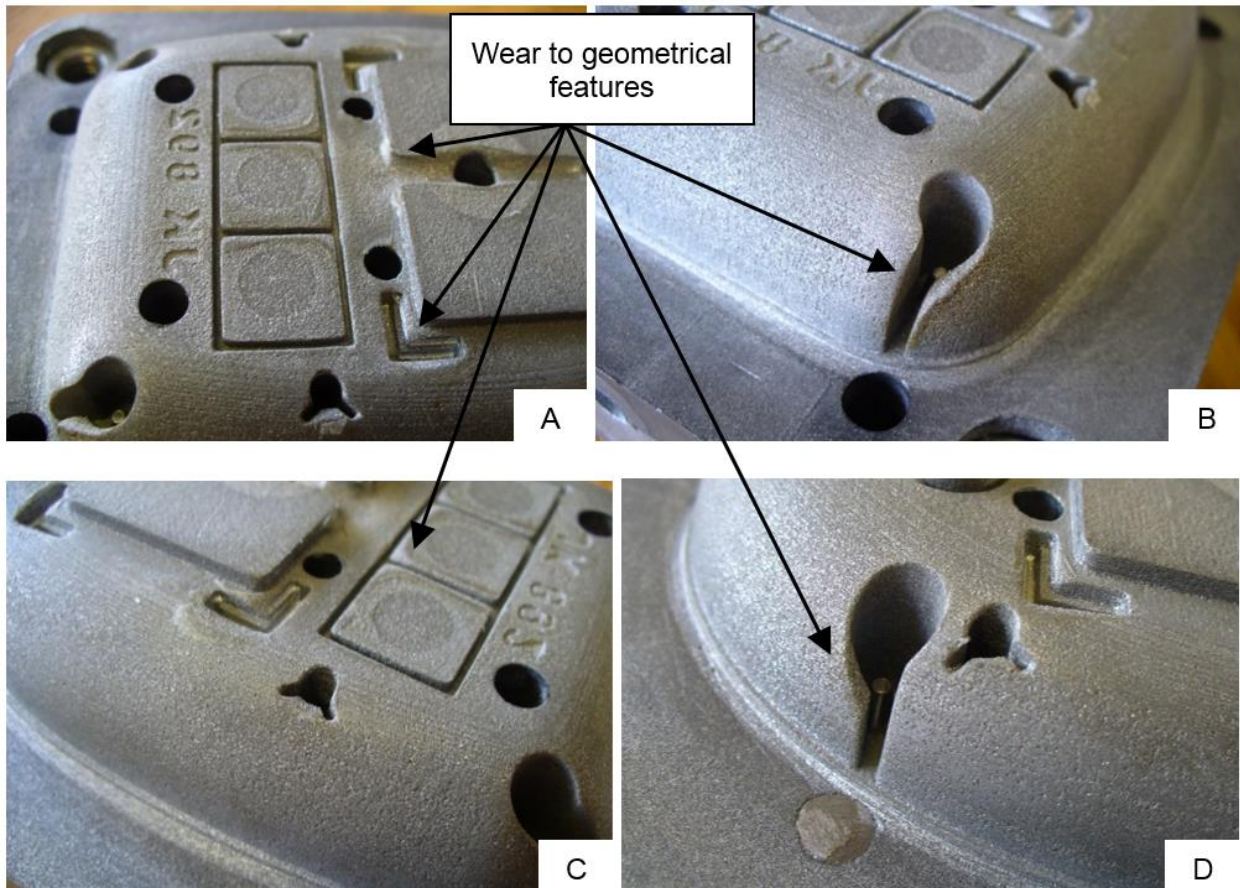


Figure 5.14 Alumide® inserts after 200 IM cycles using ABS. Figures A to D show the features where wear occurred.

Results from SIGMASOFT® virtual moulding software indicated that the insert features shown in Figure 5.14 B and D, have temperatures of 192.6 °C and 188.7 °C respectively, after the 20th IM cycle, as shown in Figure 5.15. Because these temperatures are more than the melt temperature of Alumide®, it resulted in wear to these features. Although the temperature at the gate region is indicated as 120.1 °C, excessive wear (shown in Figure 5.14 A) occurred due to the high shear rate induced at the gate during the filling of the cavity.

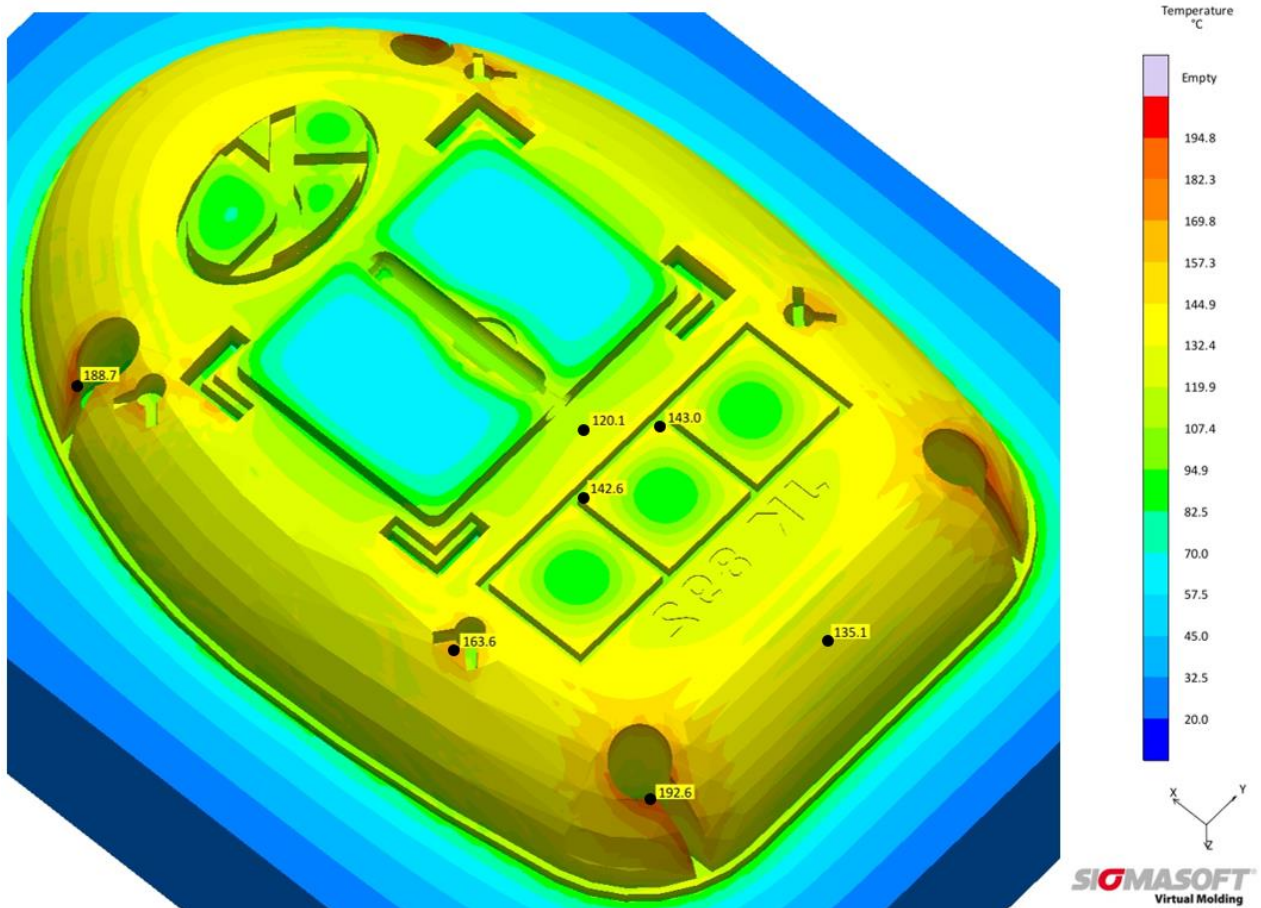


Figure 5.15 Temperatures of the moving half enclosure insert using ABS material after the 20th IM cycle, according to SIGMASOFT[®] virtual moulding software.

Figure 5.16 shows a graphical comparison in Geomagics[®] Quality between the reference part and the 200th part showing that no significant wear occurred during these IM cycles.

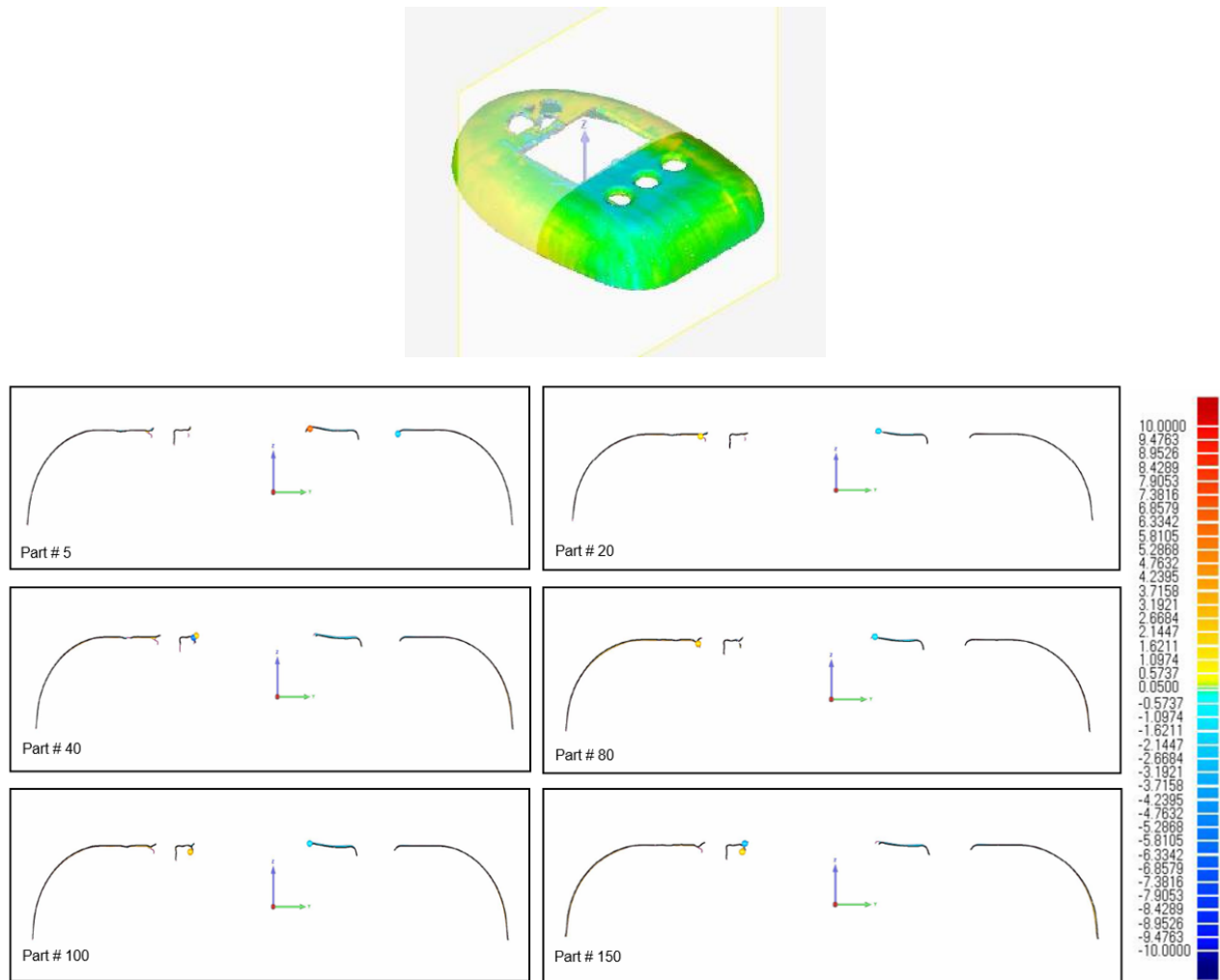


Figure 5.16 Graphical representation of the wear progression from 5th to the 200th IM cycle.

After 200 IM cycles it was decided to continue the trial to determine the useful life cycle of an Alumide[®] insert. The trial was continued until 2500 IM cycles were completed.

Figure 5.17 shows the fixed half after 2500 IM cycles. The cavity surface of the insert started to delaminate after about the 700th IM cycle and continued until the 2500th cycle. No further significant wear from the 200th cycle was observed on the moving insert.

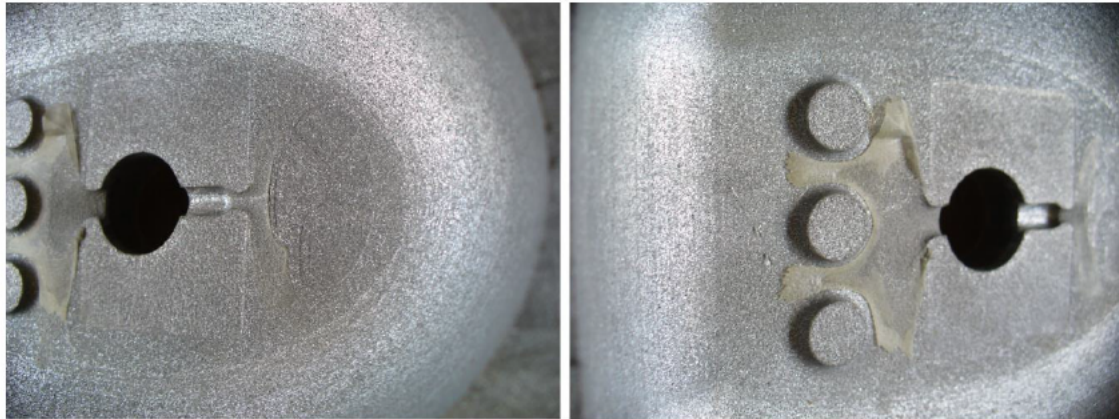


Figure 5.17 Fixed half of the Alumide insert showing the delamination of the cavity surface after 2500 IM cycles using ABS.

The results from the measured wall thickness of the parts at the points seen in Figure 5.8 are shown in Figure 5.18. From the results it can be seen that the deviation continuously increased during the trial. Significant deviation (larger than 0.3 mm) started to occur from about the 400th IM cycle.

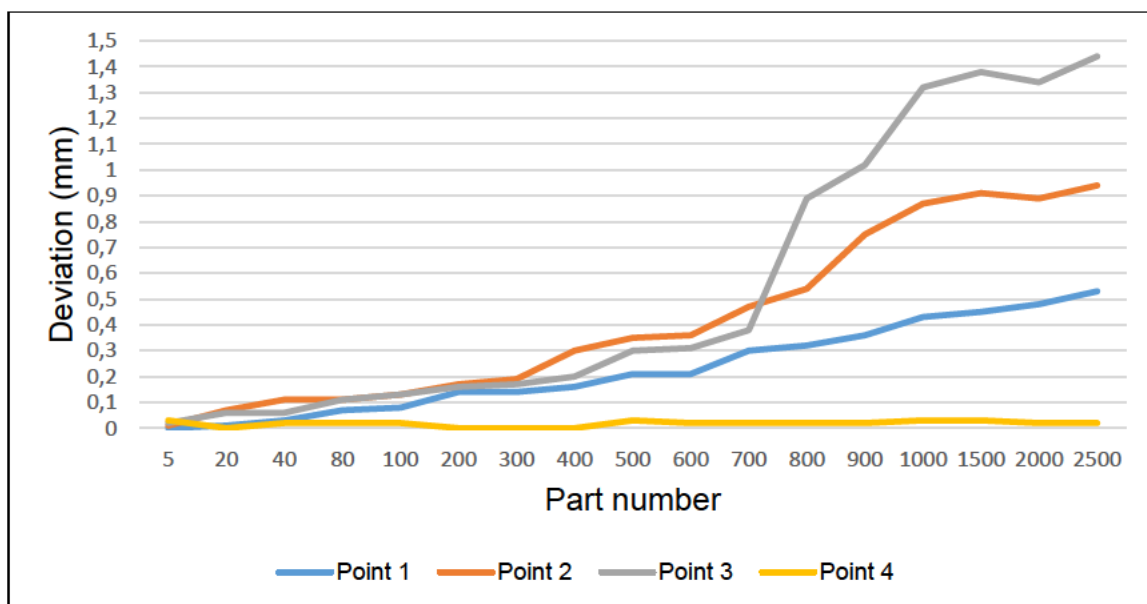


Figure 5.18 Wall thickness deviation of enclosure parts manufactured from Alumide[®] inserts using ABS.

Considering that the allowable manufacturing tolerance for industrial IM products is (0.6 %) [23], the deviation in the length and width of the part should not exceed 0.63 mm and 0.45 mm respectively. The deviation of the enclosure parts during the production trial run can be obtained by adding the deviation values of points 1 and 3 for the width and points 2 and 4 for the length. From the results of Figure 5.18 it can be seen that after about 400 IM

cycles, the allowable deviation for the enclosure part has been reached for the width, while the deviation for the length is still within the allowable tolerance. From these results it can be concluded that about 400 enclosure parts can be manufactured from Alumide[®] inserts within the allowable tolerance.

SIGMASOFT[®] simulation results indicated a maximum insert temperature of 125.2 °C for the fixed half Alumide[®] insert after the 20th IM cycle, as shown in Figure 5.19. This temperature is less than the melt temperature of Alumide[®], which should not result in significant wear to the insert. About 320 of the ABS enclosure parts could be manufactured during an eight-hour workday. The sudden increase in wall thickness of the manufactured parts after 300 and 700 IM cycles, as shown in Figure 5.18, could be due to over-packing of the molten material inside the Alumide[®] inserts during start-up procedures at the beginning of a workday, resulting in the deformation of the cavity.

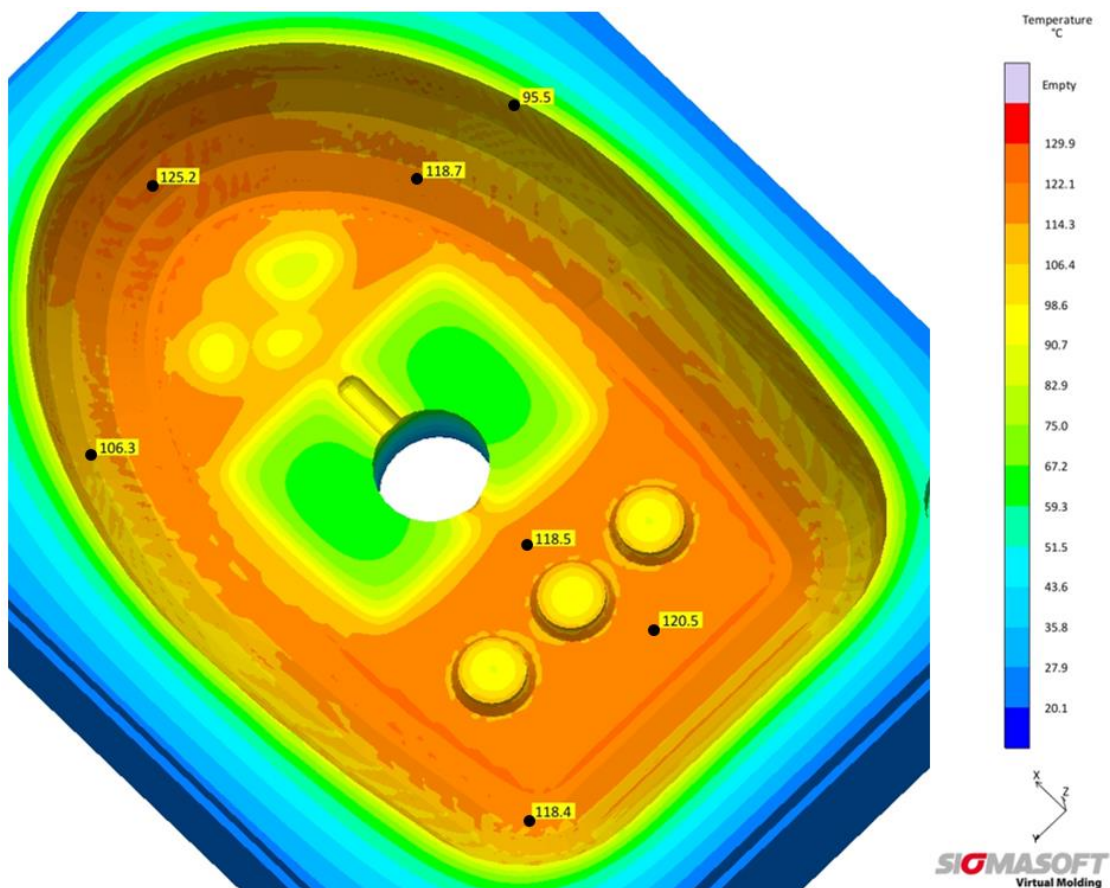


Figure 5.19 Temperatures of the fixed half enclosure insert using ABS material after the 20th IM cycle, according to SIGMASOFT[®] virtual moulding software.

To determine the wear of the Alumide® inserts during the IM trial, the manufactured parts at certain intervals were scanned and measured. The first part produced was used as a reference for the subsequent parts to be compared to. Figure 5.20 shows graphically in Geomagics® Qualify, the progression of the wear between the reference part and subsequent parts from the 200th cycle until the 2500th cycle.

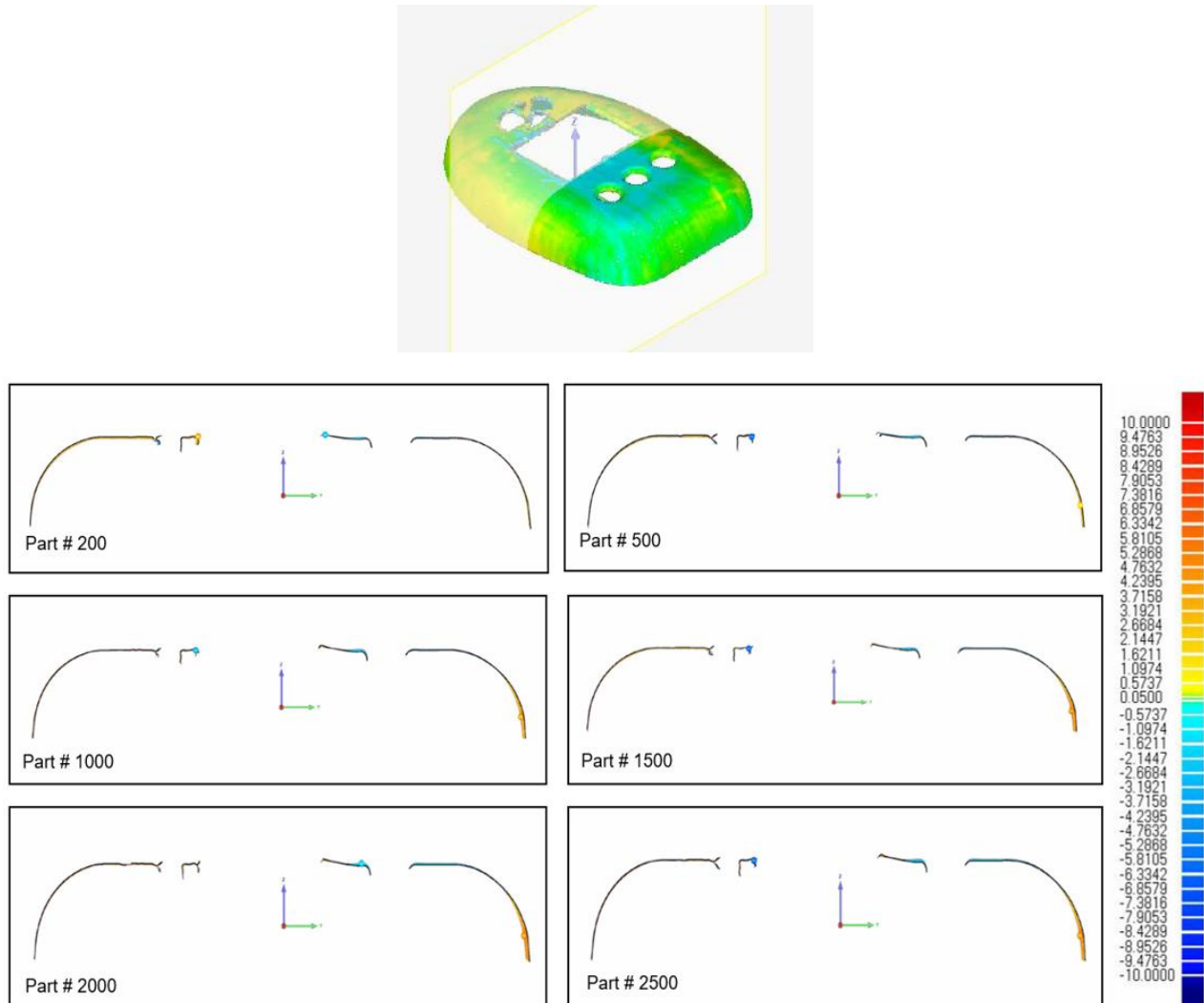


Figure 5.20 Graphical representation of the wear progression from 200th to the 2500th IM cycle.

The Alumide® inserts were scanned after 2500 IM cycles and compared to the CAD data of the inserts shown in Figure 5.21. The deviation between the scan and CAD data of the moving insert was about 0.2 mm. This deviation could be from material removed during the polishing of the insert. This small deviation indicates that this insert did not wear or deform during the trial.

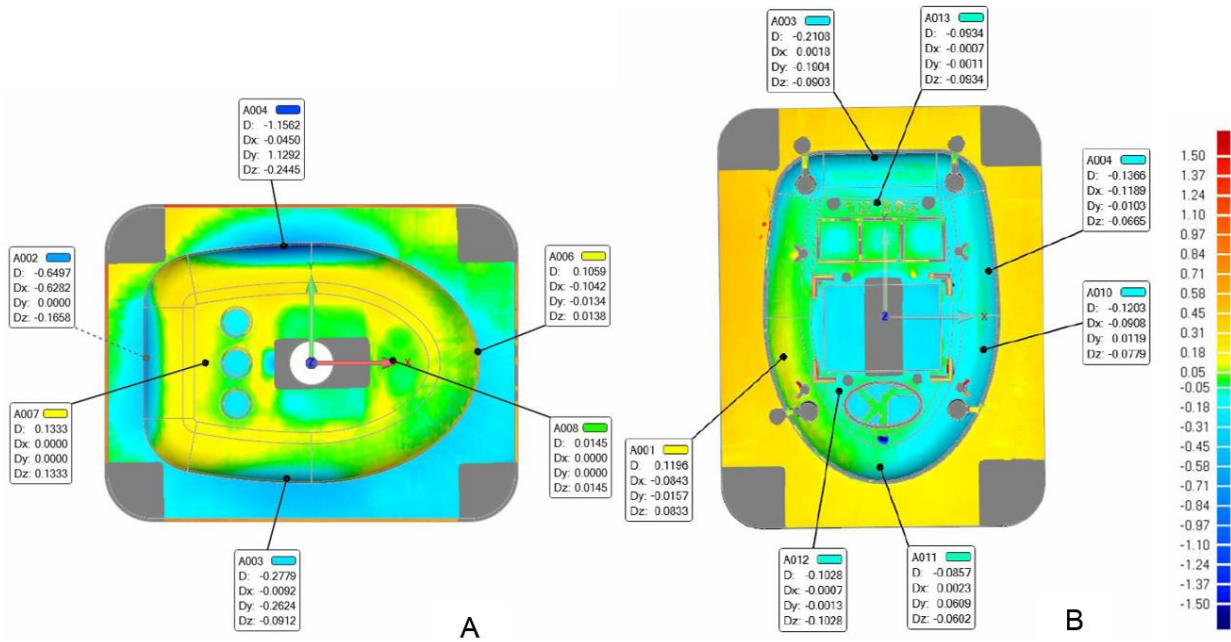


Figure 5.21 Scan results of the fixed (A) and moving (B) Alumide® inserts after 2500 IM cycles using ABS.

5.1.3 Discussion

IM trials with PP did not cause any significant wear to the geometrical features of the Alumide® inserts after 200 IM cycles. A gate machined into a steel insert can be inserted into the Alumide® insert to prevent wear of this feature.

IM trials with ABS did not cause any significant wear to the geometrical features of the Alumide® inserts after 200 IM cycles. A gate manufactured from a steel insert will prevent wear to this feature. Wear to the features, as shown in Figure 5.14 B and D, was due to the high heat volume of molten polymer from the boss feature. Improved cooling in these regions (if possible within the layout of mould features), could reduce the wear of these features.

From Figure 5.21 B it can be seen that after 2500 IM cycles no significant wear on the moving half insert occurred. The scan results of the fixed half insert indicated a large deviation of 0.65 to 1.16 mm, as shown in Figure 5.21 A. This indicates that the wall thickness deviation, as indicated in Figure 5.20, resulted from the wear and deformation of the fixed half insert.

During IM trials it was observed that the outer surface finish of the parts produced from PP and ABS was coarse within the first few IM cycles although the Alumide® cavity surfaces

were machined to a polished finish. It was noticed that there were small shallow holes on the cavity surface of the Alumide[®] insert causing a coarse surface finish, as shown in Figure 5.22.

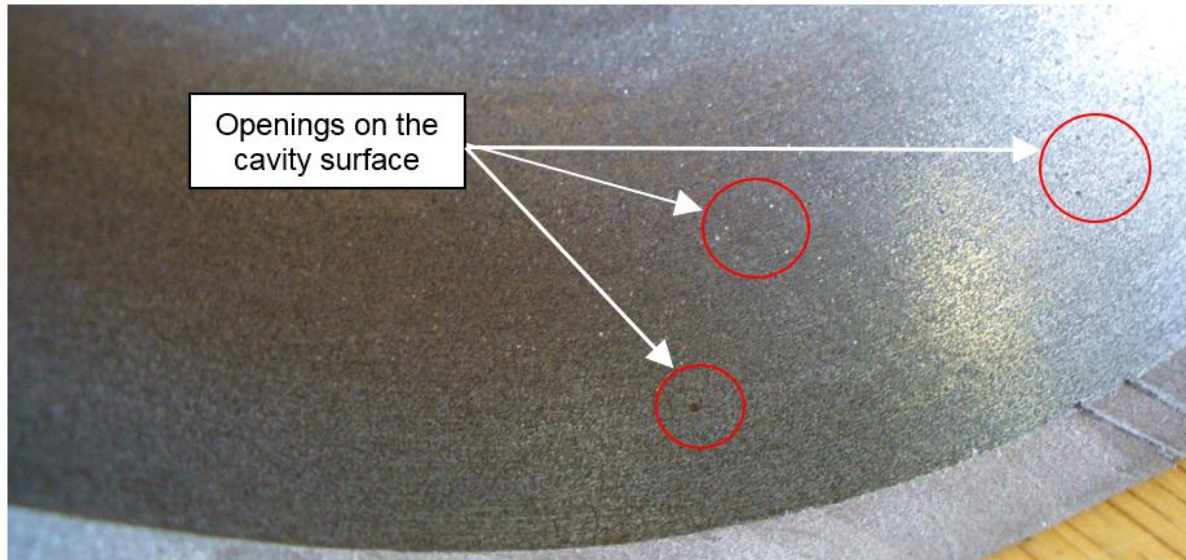


Figure 5.22 Holes on the cavity surface of the Alumide[®] insert causing a coarse surface finish on the parts manufactured from ABS and PP.

A possible cause for this occurrence could be that the aluminium particles at the machined surface of the cavity bonds with the injected polymer during an IM cycle and is removed from the surface when the moulded part is ejected from the cavity. Figure 5.23 shows a microscope image of laser-sintered Alumide[®], showing the polyamide material surrounding the aluminium particles.

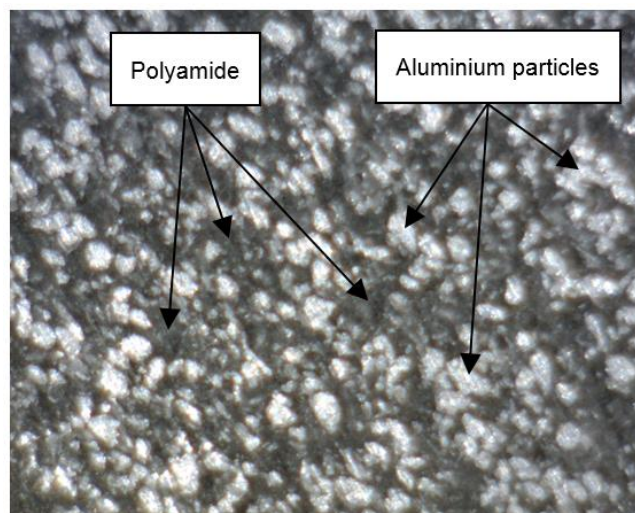


Figure 5.23 Magnified image (150 magnification) of laser-sintered Alumide[®] material showing the aluminium particles enclosed by the polyamide material.

After machining the AM-manufactured Alumide[®] cavity surface, the aluminium particles are exposed, as shown in Figure 5.24 B.

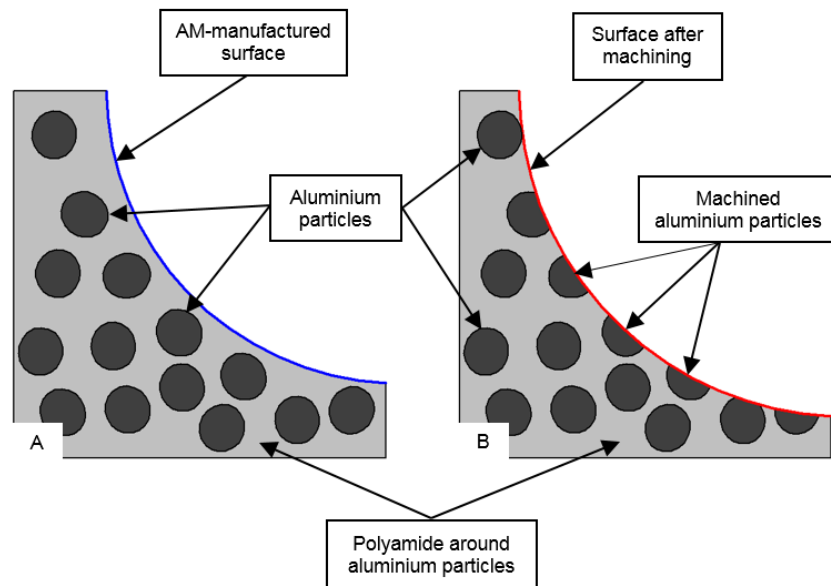


Figure 5.24 The aluminium particles and polyamide material, as manufactured by AM techniques (A), and after machining operations on the Alumide[®] surface (B).

When the machined aluminium particles bonded to the manufactured part are ejected from the cavity, this result in an opening for the molten polymer to flow into during the next IM cycle and continues during the IM cycles that follow, wearing the opening further. After a few IM cycles, the opening wears to such an extent that it results in a coarse surface. This coarse surface was visible on the IM parts, which will not be suitable for transparent parts or IM parts requiring a gloss surface finish.

5.2 Comparisons between different manufacturing processes

A comparison between the time and cost to manufacture inserts through different manufacturing processes was conducted to determine the feasibility of using Alumide[®] inserts for IM applications.

Manufacturing processes considered in the comparison include:

- **Tool steel inserts** manufactured through conventional manufacturing techniques such as CNC machining, EDM, drilling, etc.
- **Aluminium inserts** manufactured through conventional manufacturing techniques.
- **DMLS inserts** manufactured from MaragingSteel MS1 using an EOS M 280 AM machine. MaragingSteel MS1 is a DMLS metal powder, developed by EOS,

designed for tooling applications that is an ultra-high strength alloy, resistant to corrosion, has good thermal conductivity and can be hardened with a simple thermal age-hardening process.

- **PolyJet inserts** manufactured using Objet™ RGD 515 digital ABS through the material jetting process using an Objet™ Connex 350 AM machine.
- **Alumide® inserts** manufactured through the SLS process using an EOS P 380 AM machine.
- **RM**, which is the use of AM processes to construct parts that are used directly as finished products or components, and can be post-processed by techniques such as infiltration, bead blasting, painting, plating, etc. [6]. For the time and cost comparisons, RM parts were manufactured from polyamide 12 (PA 2200) material through the LS process using an EOS P 385 AM machine.

The cost and manufacturing times for all the different AM processes were obtained from the CRPM, an AM service provider. The cost per product is based on 200 parts manufactured from a single set of inserts for each manufacturing processes. The manufacturing time for the Alumide® and the PolyJet inserts includes the time required to backfill the inserts as well as the curing time of the backfill material (approximately 14 hours).

5.2.1 Time and cost comparison of geometrical parts

Table 5.3 shows the time and cost of the different manufacturing processes to produce 200 geometrical parts, as used in Section 4.4.5.

Table 5.3 Time and cost comparison of different manufacturing techniques and the cost per product for geometrical parts.

Manufacturing process	Manufacturing time (hours)	Manufacturing cost	Cost per product (after 200 IM cycles)
Tool steel inserts	30	R 18 550.00	R 92.75
Aluminium inserts	22	R 14 300.00	R 71.50
DMLS (MaragingSteel MS1) inserts	32	R 30 000.00	R 150.00
PolyJet inserts	25	R 16 540.00	R 82.70
Alumide® inserts	20	R 6 820.00	R 34.10
RM	22	R 25 663.00	R 128.32

Figure 5.25 shows a scatter plot of the cost comparison to manufacture one to two hundred geometrical parts for each of the manufacturing processes. Trend lines with a R^2 value between 0.997 and 1, were fitted to each of the plots.

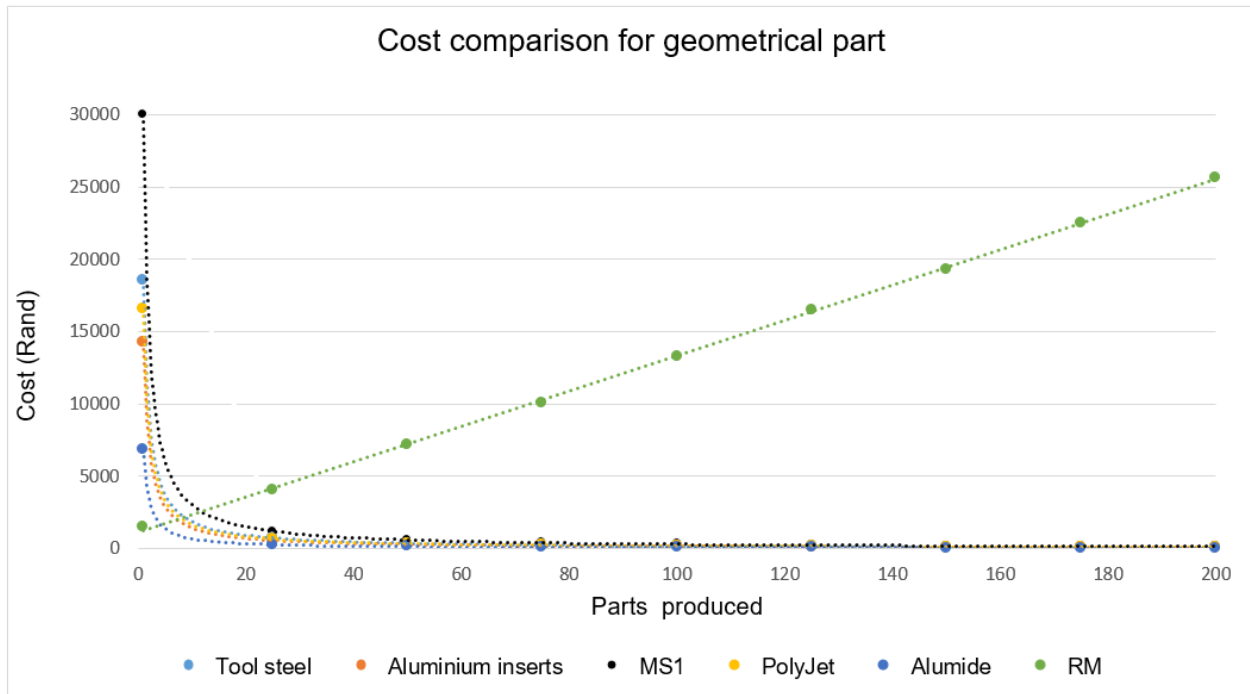


Figure 5.25 Cost comparison for the different manufacturing processes to manufacture one to two hundred geometrical parts.

Figure 5.26 shows an enlargement of the plot shown in Figure 5.25 with the intersection point between the Alumide[®] and RM processes. The intersection between the Alumide[®] inserts and the RM processes indicates the break-even point between the two manufacturing processes. The intersection point between the trend lines of the Alumide[®] and RM processes is 3.9. To verify the break-even point, the cost to produce four parts from Alumide[®] inserts and RM technologies was calculated. The cost per product to manufacture four parts from Alumide[®] inserts was R 1705.00 and to manufacture four parts from PA 2200 using AM technologies was R 1720.00. This resulted in an accurate comparison with only an R 15.00 difference between the two processes. From this plot it can be concluded that it was more economical to use Alumide[®] inserts to manufacture four to two hundred geometrical parts compared to the other manufacturing techniques considered in Figure 5.26.

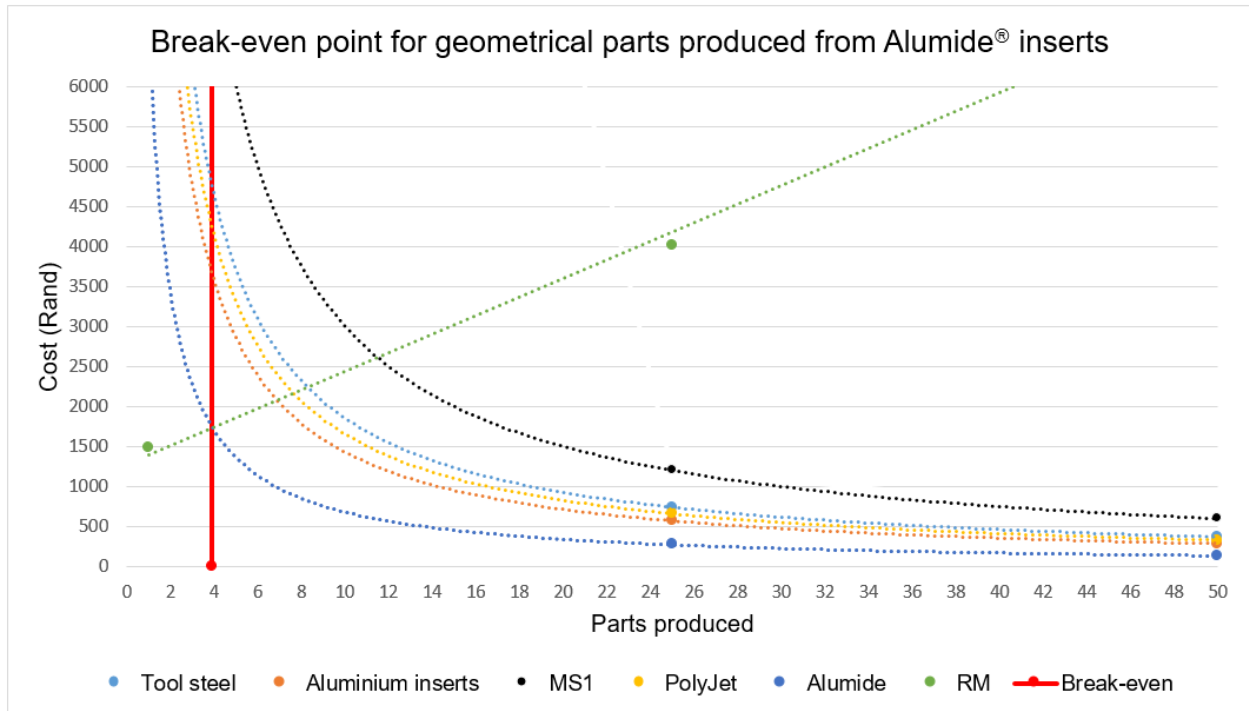


Figure 5.26 Break-even plot between Alumide® and RM manufacturing processes for the geometrical part.

5.2.2 Time and cost comparison of enclosure parts

Table 5.4 shows the time and cost of the different manufacturing processes to produce 200 enclosure parts, as described in Section 5.1.1.

Table 5.4 Time and cost comparison of different manufacturing techniques and the cost per product for the enclosure part.

Manufacturing process	Manufacturing time (hours)	Manufacturing cost	Cost per product (after 200 IM cycles)
Tool steel inserts	38	R 24 000.00	R 120.00
Aluminium inserts	30	R 17 950.00	R 89.75
DMLS (MaragingSteel MS1) inserts	46	R 45 000.00	R 225.00
PolyJet inserts	27	R 17 555.00	R 87.76
Alumide® inserts	20	R 6 820.00	R 34.10
RM	195	R 60 000.00	R 300.00

Figure 5.27 shows a scatter plot of a cost comparison to manufacture one to two hundred enclosure parts for each of the manufacturing processes. Trend lines with an R² value from 0.999 to 1 were fitted to each of the manufacturing process’s plot.

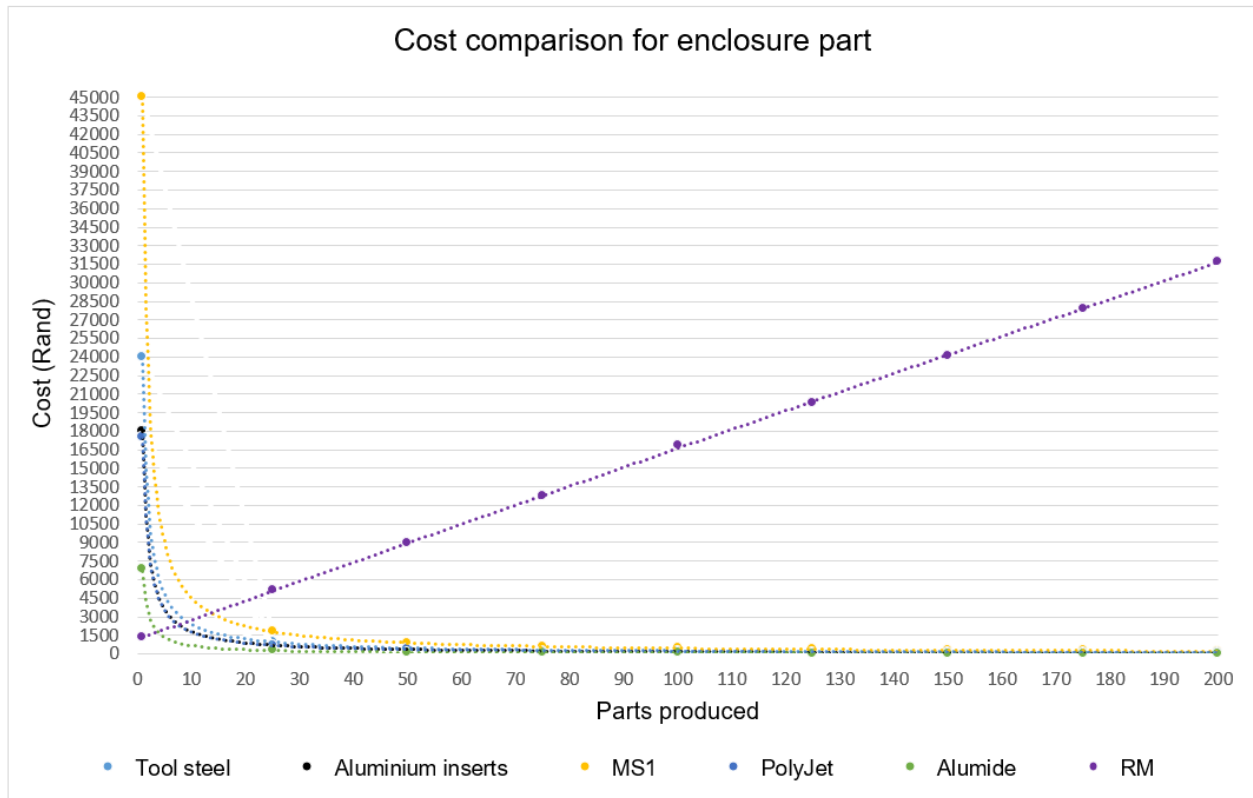


Figure 5.27 Cost comparison for the different manufacturing processes to manufacture one to two hundred enclosure parts.

Figure 5.28 shows an enlargement of the plot shown in Figure 5.27 with the intersection point between the Alumide[®] and RM processes. The intersection point between the trend lines of the Alumide[®] and RM processes is 3.6. To verify the break-even point, the cost per product to produce four parts from Alumide[®] inserts and RM technologies were calculated. The cost to manufacture four parts from Alumide[®] inserts was R 1705.00 and to manufacture four parts from PA2200 using AM technologies was R 1790.00. This resulted in an R 85.00 difference between the two processes. From this plot it can be concluded that it was more economical to use Alumide[®] inserts to manufacture four to two hundred enclosure parts compared to the other manufacturing techniques considered in Figure 5.28.

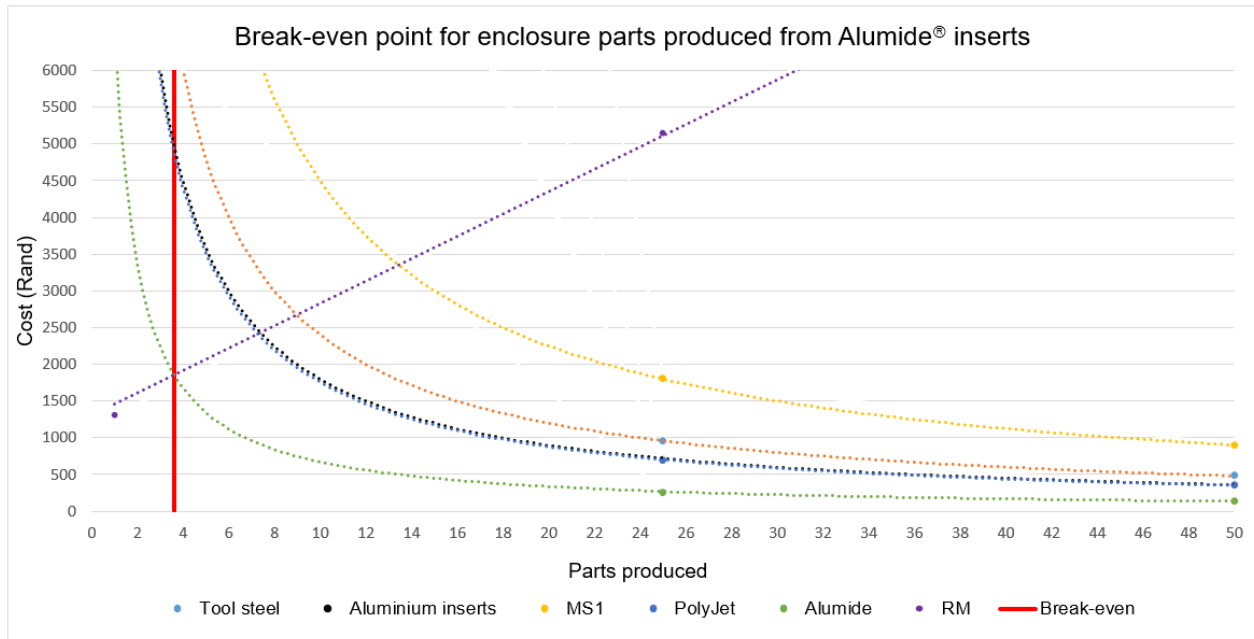


Figure 5.28 Break-even plot between Alumide® and RM manufacturing processes for the enclosure part.

5.2.3 Time and cost comparison of tractor wheel parts

A similar comparison was made for tractor wheels for toy cars. A set of wheels for a car consists of two large and two small wheels, both with wheel caps. Mould inserts produced through the DMLS process using MaragingSteel MS1, were used to manufacture the wheels and wheel caps.

Figure 5.29 shows product drawings of the tractor wheel parts used in the time and cost comparisons.

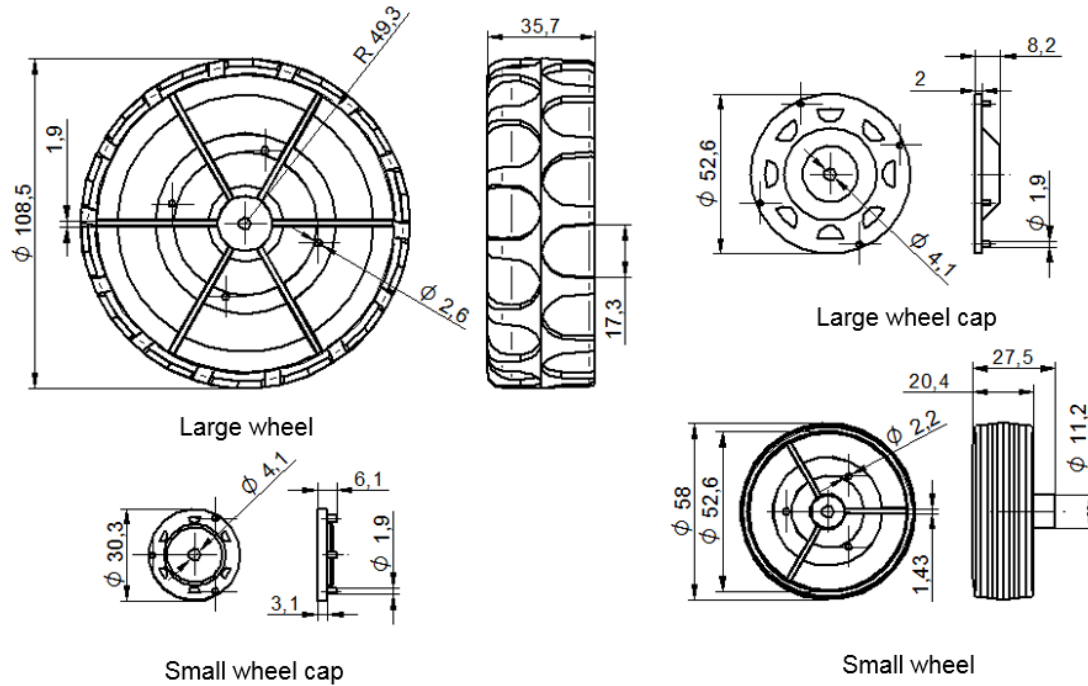


Figure 5.29 Dimensions and CAD model of the tractor wheel components used in the time and cost comparison.

Table 5.5 shows the time and manufacturing cost comparison for the four sets of tractor wheel inserts. The cost to manufacture 200 sets (consisting of two front and rear wheels as well as two front and rear wheel caps) was calculated for each manufacturing process.

Table 5.5 Time and cost comparison for different manufacturing techniques and the cost for 200 sets of the tractor wheel parts.

Manufacturing process	Manufacturing time (hours)	Manufacturing cost	Cost per 200 sets
Tool steel inserts	100	R 65 000.00	R 325.00
Aluminium inserts	80	R 52 000.00	R 260.00
DMLS (MaragingSteel MS1) inserts	78	R 97 820.00	R 489.10
PolyJet inserts	39	R 34 155.00	R 170.80
Alumide® inserts	26	R 9 900.00	R 49.50
RM	178	R 174 800.00	R 874.00

Figure 5.30 shows a scatter plot of a cost comparison to manufacture one to two hundred sets of tractor wheel parts for each of the manufacturing processes. Trend lines with an R² value from 0.999 to 1 were fitted to each of the manufacturing process's plot.

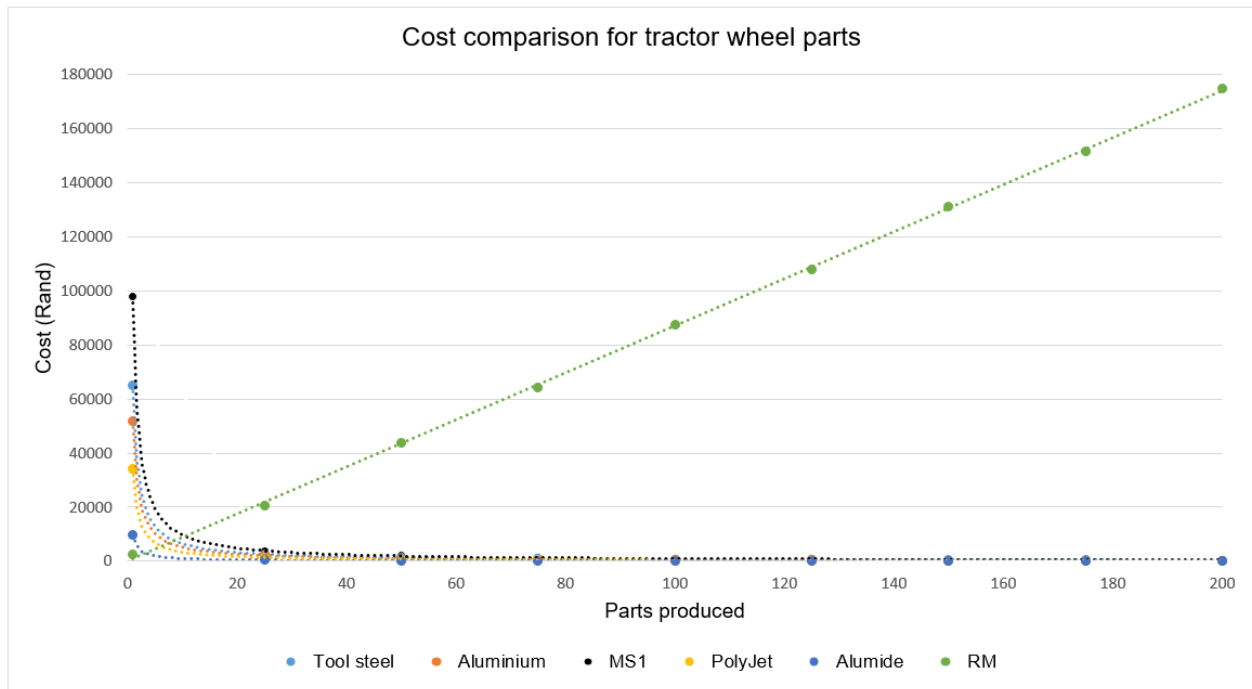


Figure 5.30 Cost comparison for the different manufacturing processes to manufacture one to two hundred sets of tractor wheel parts.

Figure 5.31 shows an enlargement of the plot shown in Figure 5.30 with the intersection point between the Alumide[®] and RM processes. The intersection point between the trend lines of the Alumide[®] and RM processes is 2.7.

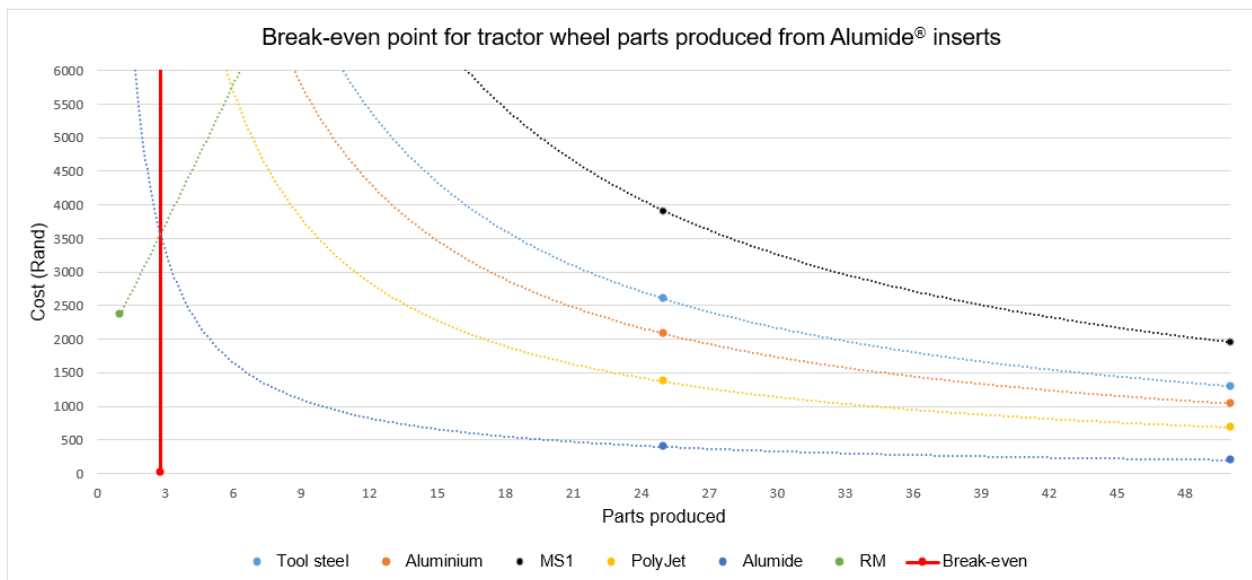


Figure 5.31 Break-even plot between Alumide[®] and RM manufacturing processes for the tractor wheel part.

To verify the break-even point, the cost per set to produce three sets of tractor wheel parts from Alumide® inserts and RM technologies was calculated. The cost to manufacture three sets from Alumide® inserts was R 3300.00 and to manufacture three sets from PA2200 using AM technologies was R 3535.00. This resulted in a R 235.00 difference between the two processes. From this plot it can be concluded that it was more economical to use Alumide® inserts to manufacture three to two hundred sets of tractor wheel parts compared to the other manufacturing techniques considered in Figure 5.30.

5.2.4 Discussion

From the cost comparisons it is evident that it is more economical to use Alumide® inserts to manufacture a few to two hundred parts. If the required quantities of the parts to be manufactured increase, it will become more cost-effective to use inserts manufactured through conventional manufacturing processes. Inserts produced from these processes are capable of manufacturing large quantities of parts before the inserts need to be replaced (in excess of 500 000 parts), as opposed to Alumide® and PolyJet inserts which have a limited lifespan before they need to be replaced. For a small production run up to 1000 parts, it becomes more cost-effective to use aluminium and tool steel inserts manufactured through conventional methods, as shown in Table 5.6.

Table 5.6 Cost comparison of the different manufacturing techniques to produce 1000 parts.

Manufacturing process	Sets of inserts required	Cost per product (after 1000 parts)		
		Geometrical part	Enclosure part	Tractor wheel part
Tool steel inserts	1	R 18.55	R 24.00	R 65.00
Aluminium inserts	1	R 14.30	R 17.95	R 52.00
DMLS (MaragingSteel MS1) inserts	1	R 30.00	R 45.00	R 97.82
PolyJet inserts	3	R 49.46	R 52.66	R 102.46
Alumide® inserts	3	R 20.46	R 20.46	R 29.70

Table 5.6 summarises the cost per product for the different manufacturing processes to produce 1000 parts. The costs for the Alumide® and PolyJet inserts are based on the assumption that one set of inserts would be able to manufacture about 350 parts before the inserts need to be replaced.

6 CONCLUSION AND FUTURE WORK

6.1 Conclusions and recommendations

In this study, the suitability of Alumide® processed through LS was investigated for producing IM tooling inserts for limited run plastic IM applications. To determine the suitability of Alumide® as a RT medium, the following were investigated during the study:

i. **Alumide® material properties and part properties**

Tensile tests conducted on test pieces manufactured in the *X*, *Y* and *Z* directions indicated that the build orientation has a significant influence on the UTS. Test pieces manufactured in the *Z* direction had the lowest UTS, while test pieces in the *X* direction had the largest UTS. This must be considered while orientating the Alumide® insert inside the AM machine's build envelope during the LS process, because mould features orientated in the *Z* direction will have a lower UTS than features orientated in the *X* direction.

Heat capacity plays an important role during the IM process because it determines how efficiently heat can be conducted from the cavity surface to the cooling channels. Heat capacity values for Alumide® were not specified by the supplier and tests were conducted at the CSIR to determine the heat capacity values of the material. The results indicated that Alumide® will start to soften at 169 °C and melt at 177 °C. In order to minimise wear, the mould temperature inside the Alumide® insert should be kept below these values.

For Alumide® to be used successfully as an RT medium, surface-finishing procedures such as polishing or machining are required. Without surface-finishing procedures, surfaces of Alumide® inserts often contain rough textures or stair steps on inclined surfaces. These surface textures can result in the bonding of a manufactured part to the Alumide® cavity, making it difficult to eject during the ejection phase of an IM cycle. If the part cannot be ejected or removed from the Alumide® insert, it will be ruined and a new insert has to be manufactured. For finishing procedures such as polishing and CNC machining, extra material must be designed onto the surfaces in order to retain the accuracy of the Alumide® insert after machining. A material thickness of 0.1 mm for polishing and 0.2 to 0.5 mm for machining should be added to the surfaces requiring finishing operations. Orientation of the insert inside the AM machine's build envelope

also influences the surface finish of the insert and should be considered during the manufacturing process of the Alumide[®] insert.

ii. **Suitable shelling thickness and backfill material for Alumide[®] inserts**

To reduce the internal stresses that occur inside Alumide[®] inserts during the LS process, the inserts need to be shelled. Backfilling of shelled Alumide[®] inserts is necessary to withstand the filling pressure of the molten polymer during an IM cycle. After evaluating locally available backfilling materials, Axson's EPO 4030 was found to be the most suitable backfilling material as it did not deform the Alumide[®] inserts during the casting and curing procedures. IM trials conducted with Alumide[®] inserts backfilled with EPO 4030 showed that the inserts did not deform under the pressures and temperatures experienced during IM cycles.

After experimentation, a shelling thickness of 5 mm was found to be the most suitable for Alumide[®] inserts because it will not result in deformation of the insert during the backfilling process and will provide sufficient strength and support to internal mould features during the AM manufacturing process.

The disadvantage of shelling Alumide[®] inserts is that the backfilling procedure results in additional manufacturing costs and time spent on the Alumide[®] inserts. The EPO 4030 material used to backfill a set of Alumide[®] inserts used during the IM trials resulted in an additional cost of about R 276.00. The time required for the casting and curing of the EPO 4030 material resulted in an additional 13 hours manufacturing time on a set of Alumide[®] inserts.

iii. **Effect of cooling channels inside an Alumide[®] insert**

IM trials conducted in Section 4.4.3 indicated that cooling channels inside an Alumide[®] insert do have an influence on the insert temperature, as shown in Figures 4.39 and 4.40. IM trials conducted with Alumide[®] inserts showed that features without cooling wear quicker due to the accumulation of heat at these mould features, as illustrated in Figures 4.64 and 4.65. Results from Section 4.4.3 also showed that cooling channels placed close to the surface of an Alumide[®] insert could result in the deformation of the cavity surface during an IM cycle. To prevent deformation, the cooling channels need to be positioned at an appropriate distance from the surface depending upon the injection pressure required to fill the cavity. The higher the injection temperature and pressure,

the further the cooling channels need to be positioned from the cavity surface. Results from Table 4.6 and 4.7 indicated that a cooling channel with an oval cross-section resulted in less deformation and was able to withstand higher injection pressures compared to a round cooling channel with the same cross-sectional area. SIGMASOFT® virtual moulding simulations have also shown that the heat removed from the cavity surface decreases when a cooling channel is positioned further from the cavity surface. To improve the heat transfer rate of cooling channels further from the cavity surface, the number of cooling channels can be increased.

iv. **Durability of Alumide® inserts in tooling applications**

IM trials conducted with Alumide® inserts showed that features close to the injection point wear quicker due to the continuous flow of molten material over these features, as shown in Figure 4.48. Moving these features further from the injection point did not result in any wear to the features, as shown in Section 4.4.5. To avoid wear at the injection point, a steel insert can be placed into the Alumide® insert, onto which molten material from the IM machine can be injected.

From the IM trials it was observed that Alumide® pin features are not able to withstand continuous IM cycles and broke off within a few cycles, as shown in Figure 4.47. Steel pins inserted into the Alumide® should be used instead, as shown in Figures 4.55 and 5.7.

Due to the high shear rates at the gates, these features also wear very quickly, as shown in Figures 4.28 and 5.9 C. A gate manufactured from a steel insert will prevent the wear of this feature.

SIGMASOFT® IM simulation results identified features of the Alumide® inserts with temperatures close to or more than the melting point of Alumide®. During IM trials, wear to these insert features was more than features with a lower temperature. To prevent excessive wear to Alumide® insert features due to high temperatures, sufficient cooling is necessary to cool the insert features to a temperature below the melting point of Alumide®. If features cannot be cooled sufficiently due to mould constraints, these features can be produced in metal and mounted into the Alumide® inserts. The metal inserts will prevent wear to these features, increasing the life span of the Alumide® insert. Regions where injected plastic can accumulate in the mould should be avoided. This will result in heat build-up in the area which will result in rapid wear to the insert.

During IM trials, 200 parts were successfully produced from Alumide® inserts using PP and ABS material. A production run in ABS, as described in Section 5.1.2, showed that about 400 parts can be manufactured within allowable tolerances and 2500 parts could be manufactured using Alumide® inserts. Scan data of the Alumide® inserts after 2500 IM cycles did not indicate any significant wear on the moving insert (core) while the fixed insert (cavity) had a deviation of 0.65 to 1.16 mm. The wear of the cavity could have been due to the over-packing of the molten material during the start-up procedure of the IM machine. This deviation is more than the allowable tolerance and not acceptable for IM applications. From these results it can be concluded that Alumide® inserts are more suitable for core applications, which typically has the most detail and geometrical features of a polymer part. The cavities which are usually easily machinable can be manufactured from a material such as aluminium. From the production run it can be concluded that Alumide® inserts can manufacture 2500 or more IM parts in a material with similar properties to PP and ABS.

During the production run it was also observed that parts manufactured from Alumide® inserts resulted in a coarse surface finish due to the removal of the aluminium particles from the Alumide® surfaces. This renders Alumide® inserts unsuitable to manufacture transparent parts or parts where a gloss surface finish is required.

v. **Suitability of Alumide® inserts for processing different polymers through IM**

From IM trials conducted in Section 4.4.5, it is evident that polymers with a high processing temperature, such as PC, are not suitable for use with Alumide® inserts. The high processing temperature increases the temperature of the insert beyond the melting point of the Alumide® material despite the conformal cooling system inside the insert. This causes excessive wear and deformation of the Alumide® insert. Results from Section 4.4.5 show that polyamide materials are also not suitable for use with Alumide® inserts in IM. The injected polyamide material bonds with the polyamide constituent of the Alumide® material resulting in excessive wear of the inserts. IM trials conducted with PP and ABS material produced quality parts without any significant wear to the Alumide® inserts. From the IM trials it can be concluded that materials with similar processing temperatures to PP and ABS should be suitable for use with Alumide® inserts.

vi. Cost and time comparisons

From the results of Section 5.2 it can be concluded that for 4 to 200 parts it is more economical to use Alumide[®] inserts for limited production runs. If the number of required parts increases to 1000, conventional manufactured IM inserts become more economical, although Alumide[®] inserts can still be very competitive, as shown in Table 5.6. Using Alumide[®] inserts for limited production is more feasible and economical than PolyJet inserts frequently used in industry for limited production runs.

From Section 5.2 it is evident that Alumide[®] inserts could result in a cost saving and a reduction in development time for limited run production. The part quantities obtainable from Alumide[®] inserts make it possible to test the market as well as receive feedback from the market before committing to the manufacturing of conventional production tools. Conventionally manufactured or DMLS manufactured MaragingSteel MS1 steel inserts can be placed into the same bolster that was used for the Alumide[®] inserts once production commences, resulting in further cost and time reductions. If more than one set of Alumide[®] inserts are manufactured simultaneously on an AM machine, it will result in a further reduction in the manufacturing costs of the inserts.

From these conclusions, it is evident that Alumide[®] inserts are feasible for an alternative RT process for limited production runs.

Design rules using Alumide[®] as a limited run tooling can be summarised from the study, as shown in Table 6.1.

Table 6.1 Alumide® design rules for limited IM production runs.

Product design considerations for Alumide® tooling	
Avoid geometrical features close to the planned injection point where possible	Continuous flow of molten polymer from the IM machine results in wear to the geometrical features of the Alumide® insert.
Alter draft angles of the part to at least 4°	Draft angles of at least 4° will assist in the successful demoulding of a part from an Alumide® insert during an IM cycle.
Avoid thick regions in the part	Thick regions results in more heat that will increase the temperature of the insert during an IM cycle, causing wear.
Fit tolerances	The AM process can achieve 0.15 mm accuracy. For features requiring a higher accuracy, machining operations need to be utilised.
Surface finish	Parts produced from Alumide® inserts will result in a coarse finish similar to EDM. It is not possible to achieve a gloss finish with Alumide® inserts.
Alumide® insert design considerations	
Mould-filling simulation	It is advised that mould-filling simulation is conducted after the insert design to identify regions with temperatures close to or more than the melting temperature of Alumide®. From the results, possibilities can be investigated to alter the part or insert design, if possible, to lower the temperature values. Insert temperatures close to or more than the melting point of Alumide® (177 °C), will result in excessive wear to insert features.
Insert build orientation	The build orientation of the insert during the AM process will influence the surface quality as well as the strength of mould features.
Post-processing operations	Additional material needs to be added to surfaces where post-processing operations such as machining are required to maintain the accuracy of the Alumide® inserts. A material thickness of 0.2 to 0.5 mm need to be added to the relevant surfaces.
Steel inserts for gate features	Gate features machined into steel inserts are required to reduce the wear of these features during IM cycles. Excessive wear of the gate features can result in additional finishing and trimming operations.
Steel inserts for core features	Pins required to manufacture hole features in an IM part need to be manufactured from steel inserts.
Cooling channels	Oval cooling channels will be able to withstand larger injection pressures than round channels. Oval cooling channels inside an Alumide® insert need to be at least 5 mm from the cavity surface to prevent deformation of the cavity surface.

6.2 Future work

Future work that can follow on from this study include:

- Investigate the possibility of using a lattice structure consisting of ribs manufactured from Alumide® to strengthen a shelled insert replacing the EPO 4030 material used to backfill the shelled insert. Backfilling of an Alumide® insert with EPO 4030 requires additional time and machining operations before the insert can be used in IM applications. The lattice structure must be able to withstand the injection pressures which typically occur during an IM cycle, while preventing the cavity surface from deforming. A lattice structure would reduce the manufacturing time and cost of an Alumide® insert.
- Investigate the influence cooling channels with different geometries and diameters would have during IM trials with Alumide® inserts. The heat extracted from the cavity and the distance the cooling channel needs to be from the cavity surface to prevent deformation can also be investigated.
- Investigate a procedure for the easy removal of un-sintered powder from the cooling channels. The removal of the un-sintered powder from cooling channels with sharp bends is problematic. This limits the path a conformal cooling channel can follow through an Alumide® insert to obtain optimal cooling.
- Investigate the injection pressures and speed that can be used to fill the cavities of Alumide® inserts without damaging the cavities. These parameters can be used to compile guidelines for IM machine setters using Alumide® inserts.
- Conduct IM trials with Alumide® inserts using polymer materials with similar processing temperatures as PP and ABS. Materials such as Polyvinyl chloride (PVC), High Impact Polystyrene (HIPS) and Acrylic-styrene-acrylonitrile (ASA) have processing temperatures of 240 °C and less, similar to PP and ABS.
- Test the suitability of using PA 2200 polyamide material to manufacture inserts for IM applications. The heat capacity values, melting point and Vicat softening temperature of PA 2200 is similar to the values obtained in Section 4.2.2 for Alumide®. The thermal properties of PA 2200 inserts would result in similar heat transfer and operating temperatures as Alumide® inserts during an IM cycle. Inserts manufactured from the PA 2200 material could improve the surface finish of the IM

part because there are no aluminium particles present in the mixture that can be removed from the surface, such as with Alumide[®] during an IM cycle, resulting in a coarse surface finish.

REFERENCES

1. **Johanson MD & Kirchain RE.** The importance of product development cycle time and cost in the development of product families. *Journal of Engineering Design*, vol. 22, no. 3, 2011, pp. 87–112.
2. **McDonald JA, Ryall CJ & Wimpenny DI.** Rapid Prototyping Casebook. London, Professional Engineering Publishing Limited, 2001, p. 36.
3. **Rees H & Catoen B.** Selecting Injection Molds: Weighing Cost versus Productivity. Cincinnati, Hanser Gardner Publications, Inc., 2006.
4. **Zhou ZD, Ai QS, Liu Q, Yang WZ & Xie SQ.** A STEP-compliant product data model for injection moulding products. *International Journal of Production Research*, vol. 47, no. 16, 2009, pp. 4497–4520.
5. **Osswald TA, Turng L & Gramann P.** Injection Molding Handbook, 2nd edition, Cincinnati, Hanser Gardner Publications, Inc., 2008.
6. **Hopkinson N, Hague RJM & Dickens PM.** Rapid Manufacturing: An Industrial Revolution for the Digital Age. West Sussex, John Wiley & Sons, Ltd, 2006.
7. **Rahmati S, Dickens PM.** Rapid tooling analysis of Stereolithography injection mould tooling. *International Journal of Machine Tools & Manufacture*, vol. 47, 2007, pp. 740–747.
8. **Yan C, Shi Y, Yang J, & Liu J.** Multiphase Polymeric Materials for Rapid Prototyping and Tooling and their Applications. *Composite Interfaces*, vol. 17, 2010, pp. 257–271.
9. **Emmatty FJ & Sarmah SP.** Modular Product Development through Platform-based Design and DFMA. *Journal of Engineering Design*, vol. 23, issue 9, 2012, pp. 696–714.
10. **Huang Y, Liu L & Ho J.** Decisions on New Product Development Under Uncertainties. *International Journal of Systems Science*, vol. 46, issue 6, 2013, pp. 1010–019.
11. **Hsu Y,** Relationships between Product Development Strategies and Product Design Issues. *Journal of Engineering Design*, vol. 22, issue 6, 2011, pp. 407–426.
12. **Cooper RG.** Winning at New Products: Accelerating the Process from Idea to Launch. 3rd edition, New York, Basic Books, 2001.

13. **Murthy DNP, Rausand M & Østerås T.** Product Reliability: Specification and Performance. London, Springer-Verlag, 2008.
14. **Roberts DL & Palmer R.** Developing a Visceral Market Learning Capability for New Product Development. *International Journal of Market Research*, vol. 54, issue 2, 2012, pp. 199–220.
15. **Kazmer DO.** Injection Mold Design Engineering. 2nd edition, Cincinnati, Hanser Gardner Publications, Inc., 2016.
16. **Özek C & Çelik YH,** Calculating Molding Parameters in Plastic Injection Molds with ANN and Developing Software. *Materials and Manufacturing Processes*, vol. 27, issue 2, 2012, pp. 160–168.
17. **Sancin U, Dobravc M & Dolšak B.** Human cognition as an intelligent decision support system for plastic products' design. *Expert Systems with Applications*, vol. 37, issue 10, 2010, pp. 7227–7233.
18. **Kutz M.** Applied Plastics Engineering Handbook: Processing and Materials. Oxford, Elsevier Inc., 2011.
19. The excellence of the plastics supply chain in relaunching manufacturing in Italy and Europe Executive summary. The European House Ambrosetti, February 2014, Available from: www.ambrosetti.eu [Accessed 15 October 2016].
20. The Plastics Industry: A strategic partner for economic recovery and sustainable growth in Europe Manifesto on the competitiveness of the plastics industry. The European plastics industry, Available from: www.plasticseurope.org [Accessed 18 October 2016].
21. Plastics – the Facts 2017: An analysis of European plastics production, demand and waste data. PlasticsEurope, Available from: www.plasticseurope.org [Accessed 16 August 2018].
22. Plastics SA Our Footprint: An annual review for the year 16/17. Plastics SA, Available from: www.plasticsinfo.co.za [Accessed 15 August 2018].
23. **Erhard G.** Designing with Plastics. Cincinnati, Hanser Gardner Publications, Inc., 2006.
24. **Sastri VR.** Plastics in Medical Devices: Properties, Requirements and Applications. Oxford, Elsevier Inc. 2014.
25. **Klein R.** Laser Welding of Plastics. 1st edition, Weinheim, Wiley-VCH Verlag GmbH & Co. KGaA, 2011.

26. **Biron M.** Thermosets and Composites Material Selection: Applications, Manufacturing and Cost Analysis. 2nd edition, Oxford, Elsevier Inc., 2014.
27. **Mckeen LW.** Permeability Properties of Plastics and Elastomers. 3rd edition, Oxford, Elsevier Inc., 2012.
28. **Wagner JR, Mount EM & Giles HF.** Extrusion: The Definitive Processing Guide and Handbook. 2nd edition, Oxford, Elsevier Inc. 2014.
29. **Rudin A & Choi P.** The Elements of Polymer Science and Engineering. 3rd edition, Oxford, Elsevier Inc. 2013.
30. **Rees H.** Understanding Product Design for Injection Molding. Cincinnati, Hanser Gardner Publications, Inc., 1996.
31. **McNally RC, Akdeniz MB, & Calantone RJ.** New product development processes and new product profitability: Exploring the mediating role of speed to market and product quality. *Journal of Product Innovation Management*, 2011, pp. 63–77.
32. **Malloy RA.** Plastic Part Design for Injection Molding: An Introduction. 2nd edition, Cincinnati, Hanser Gardner Publications, Inc., 2010.
33. **Twedell R.** Additive fabrication facilitates successful injection mold design and build. Available from: www.moldmakingtechnology.com [Accessed 7 January 2013].
34. **Shan Z, Yan Y, Zhang R, Lu Q & Guan L.** Rapid Manufacture of Metal Tooling by Rapid Prototyping. *International Journal of Advanced Manufacturing Technology*, vol. 21, 2003, pp. 469–475.
35. **Menges G & Mohren P.** How to Make Injection Molds. 3rd edition, Munich, Carl Hanser Verlag, 2001.
36. **Zhou H, Shi S & Ma B.** A virtual injection molding system based on numerical simulation. *International Journal of Advanced Manufacturing Technology*, vol. 40, issue 3-4, 2009, pp. 297–306.
37. **Fischer JM.** Handbook of Molded Part Shrinkage and Warpage. Oxford, Elsevier Inc. 2013.
38. **Gastrow H.** Injection Molds: 130 Proven Designs. 3rd edition, Cincinnati, Hanser Gardner Publications, Inc., 2002.
39. **Kamal MR, Isayev A & Liu S-J.** Injection Molding: Technology and Fundamentals. Cincinnati, Hanser Gardner Publications, Inc., 2009.

40. **Hassan H.** Heat Transfer During Injection Molding: Simulation, Analysis and Optimization. Saarbrucken, Lap Lambert Academic Publishing GmbH & Co. KG. 2010.
41. **Bralla JG.** Design for Manufacturability Handbook. 2nd edition, New York, The McGraw-Hill Companies, Inc. 1999.
42. **Stanek M, Manas M & Manas D.** Mold Cavity Roughness vs. Flow of Polymer: novel trends in Rheology III, Proceedings of International Conference: American Institute of Physics, 2009.
43. **Shayfull Z, Ghazali MF, Azaman M, Nasir SM & Faris NA.** Effect of Differences Core and Cavity Temperature on Injection Molded Part and Reducing the Warpage by Taguchi Method. *International Journal of Engineering & Technology*, vol. 10, no. 6, 2010, pp. 125–132.
44. **Rees H.** Mold Engineering. 2nd edition, Cincinnati, Hanser Gardner Publications, Inc., 2002.
45. **Shoemaker J.** Moldflow Design Guide: A Resource for Plastics Engineers. Cincinnati, Hanser Gardner Publications, Inc., 2006.
46. **Schwarz O, Ebeling FW & Lupke G.** Plastics Processing. Durban, Plastics Federation of South Africa, 2005, p. 168.
47. **Yang W, Peng A, Hsu DC, & Chang R.** True 3D Injection Molding CAE Tool for Practical Applications. AIP Conference Proceedings, volume 712, 2004, pp. 233–238.
48. **Mellor S, Hao L & Zhang D.** Additive manufacturing: A framework for implementation. *International Journal of Production Economics*, vol. 149, 2014, pp. 194–201.
49. **Monzón MD, Ortega Z, Martínez A & Ortega F.** Standardization in Additive Manufacturing: Activities carried out by international organizations and projects. *International Journal of Advanced Manufacturing Technologies*, vol. 76, 2015, pp. 1111–1121.
50. **Chang K.** e-Design: Computer-Aided Engineering Design. San Diego, Academic Press, 2015.
51. **Wohlert T.** Worldwide Review and Analysis of Additive Fabrication. Available from: www.moldmakingtechnology.com [Accessed 10 January 2014].
52. **Lokesh K & Jain PK.** Selection of Rapid Prototyping Technology. *Advances in Production Engineering & Management*, vol. 5, issue 2, 2010, pp. 75–84.

53. **Gebhardt A & Hötter JS.** Additive Manufacturing: 3D Printing for Prototyping and Manufacturing. Cincinnati, Hanser Gardner Publications, Inc., 2016.
54. **Byun HS & Lee KH.** Determination of optimal build direction in Rapid Prototyping with variable slicing. *International Journal of Advanced Manufacturing Technology*, vol. 28, 2006, pp. 307–313.
55. **Das P, Mhapsekar K, Chowdhury S, Samant R & Anand S.** Selection of build orientation for optimal support structures and minimum part errors in additive manufacturing. *Computer-Aided Design and Applications*, vol.14, sup 1, 2017, pp. 1–13.
56. **Gebhardt A.** Understanding Additive Manufacturing: Rapid Prototyping, Rapid Tooling, Rapid Manufacturing. Cincinnati, Hanser Gardner Publications, Inc., 2012.
57. **Thompson MK, Moroni G, Vaneker T, Fadel G, Campbell I, Gibson I, Bernard A, Schulz J, Graf P, Ahuja B & Martina F.** Design for Additive Manufacturing: Trends, opportunities, considerations, and constraints. *CIRP Annals – Manufacturing Technology*, vol. 65, 2016, pp. 737–760.
58. Quadrennial Technology Review 2015, Chapter 6: Innovating Clean Energy Technologies in Advanced Manufacturing Technology Assessments. U.S. Department of Energy, 2016.
59. **Gao W, Zhanga Y, Ramanujana D, Ramanian K, Chenc Y, Williams CB, Wange CCL, Shin YC, Zhanga S & Zavattieri PD.** The status, challenges, and future of additive manufacturing in engineering. *Computer-Aided Design*, vol. 69, 2015, pp. 65–89.
60. **Elwany BYA.** Making 3-D futures reality. *Industrial Engineer*, vol. 46, issue 9, 2014, pp. 32–35.
61. **Behrendt U.** Next generation technology for integrated production. e- Manufacturing, EOS, 2006.
62. **Gibson I, Rosen DW & Stucker B.** Additive Manufacturing Technologies: Rapid Prototyping to Direct Digital Manufacturing. New York, Springer, 2009.
63. **Mueller T.** The Impact of Rapid Prototyping on the Plastics Industry. Available from: www.mouldmakingtechnology.com [Accessed 14 February 2014].
64. **Mishek D.** Time and money saved with RP/RT strategy. Available from: www.mouldmakingtechnology.com [Accessed 7 December 2013].

65. **Wohlers T.** Rapid prototyping/rapid tooling: State of the industry. Available from: www.mouldmakingtechnology.com [Accessed 13 December 2013].
66. **Scaravetti D, Dubois P & Duchamp R.** Qualification of rapid prototyping tools: proposition of a procedure and a test part. *International Journal of Advanced Manufacturing Technologies*, vol. 38, 2008, pp. 683–690.
67. **Navrotsky V, Graichen A & Brodin H.** Industrialisation of 3D printing (additive manufacturing) for gas turbine components repair and manufacturing. VGB PowerTec, Available from: www.energy.siemens.com [Accessed 21 September 2016]
68. **Pilipović A, Raos P & Šercer M.** Experimental analysis of properties of materials for rapid prototyping. *International Journal of Advanced Manufacturing Technologies*, vol. 40, 2009, pp.105–115.
69. **Gibson I.** Rapid prototyping: A Review: Virtual Modeling and Rapid Manufacturing, Proceedings of the 2nd International Conference on Advanced Research and Rapid Prototyping, Leiria, Portugal, 28 September – 1 October, 2005, pp. 7–17.
70. **Zaragoza-Siqueiros J & Medellín-Castillo HI.** Design for Rapid Prototyping, Manufacturing and Tooling: Guidelines. *Proceedings of the ASME 2014 International Mechanical Engineering Congress and Exposition*, volume 2A: Advanced Manufacturing, Montreal, Quebec, Canada, November 14–20, 2014.
71. **Kamrani A & Nasr EA.** Rapid Prototyping: Theory and Practice, New York, Springer, 2006.
72. **Equbal A, Sood AK & Shamim M.** Rapid tooling: A major shift in tooling practice. *Journal of Manufacturing and Industrial Engineering*, vol. 14, no. 3-4, 2015, pp. 1– 9.
73. **Rahmati S, Dickens PM.** Stereolithography Rapid Tooling for Injection Moulding. Proceedings of the 2nd International Conference on Advanced Research and Rapid Prototyping, Leiria, Portugal, 28 September – 1 October, 2005, pp. 38–85.
74. **Noorani R.** Rapid Prototyping: Principles and Applications. New Jersey, John Wiley & Sons, Inc., 2006, p. 243.
75. **Bargelis A, Hoehne G, Šačkus A.** Integrated product and process development using rapid prototyping and rapid tooling technologies. *MECHANIKA*, no.1 (51), 2005, pp. 54–60.

76. **Pontes AJ, Queirós MP, Martinho PG, Bártole PJ & Pouzada AS.** Experimental assessment of hybrid mould performance. *International Journal of Advanced Manufacturing Technologies*, vol. 50, 2010, pp. 441–448.
77. **Nagahanumaiah, Subburaj K & Ravi B.** Computer aided rapid tooling process selection and manufacturability evaluation for injection mold development. *Computers in Industry*, vol. 59, issue 2-3, 2008, pp. 262–279.
78. **Yarlagadda PKDV & Lee LK.** Design, development and evaluation of 3D mold inserts using a rapid prototyping technique and powder-sintering process. *International Journal of Production Research*, vol. 44, no. 5, 2006, pp. 919–938.
79. **Nagahanumaiah & Ravi B.** Effects of injection molding parameters on shrinkage and weight of plastic part produced by DMLS mold. *Rapid Prototyping Journal* vol.15, no. 3, 2009, pp. 179–186.
80. **Zonder L & Sella N.** Precision Prototyping: The role of 3D printed molds in the injection molding industry, Stratasys, 2014.
81. **Pomager J.** 3D-Printed Injection Molding: The Future of Rapid Prototyping? Available from: www.meddeviceonline.com [Accessed 31 August 2017].
82. **Shellabear M & Weilhammer J.** Tooling Applications with EOSINT M. EOS Whitepaper, Krailling, September 2007.
83. **Cleveland B.** Prototyping: Matching the Method. Available from: www.appliancesdesign.com [Accessed 12 February 2010].
84. **Morris G.** Direct metal laser sintering and Tooling. Available from: www.moldmakingtechnology.com [Accessed 22 April 2014].
85. **Wu T, Jahan SA, Kumar P, Tovar A, El-Mounayri H, Zhang Y, Zhang J, Acheson D, Brand K & Nalim R.** A Framework for Optimizing the Design of Injection Molds with Conformal Cooling for Additive Manufacturing 43rd Proceedings of the North American Manufacturing Research Institution of SME, *Procedia Manufacturing*, vol. 1, 2015, pp. 404–415.
86. **Campanelli SL, Contuzzi N, Angelastro A & Ludovico AD.** Capabilities and Performances of the Selective Laser Melting Process. *New Trends in Technologies: Devices, Computer, Communication and Industrial Systems*, 2010, Available from: <https://www.intechopen.com/books/new-trends-in-technologies--devices--computer--communication-and-industrial-systems/capabilities-and-performances-of-the-selective-laser-melting-process>

87. **Siemer M.** Direct Versus Indirect Tooling and Beyond. Available from: www.mtadditive.com [Accessed 22 May 2014].
88. **Vasilash GS.** Rapid Tooling: Faster, Better, and Less Expensive. Available from: www.mtadditive.com [Accessed 20 May 2014].
89. **Zacharias M.** Direct Metal Laser Sintering vs. Conventional Tool, Part two. Available from: www.moldmakingtechnology.com [Accessed 14 May 2014].
90. **Zelinski P.** The Future of Manufacturing. Available from: www.additivemanufacturing.media [Accessed 14 May 2014].
91. Commercially available Indirect and Direct Tooling and Rapid manufacturing processes. Copyright Castle Island Co., All rights reserved, Available from: www.additive3d.com [Accessed 22 May 2014].
92. **Karunakaran KP, Suryakumar S, Pushpa V & Akula S.** Low cost integration of additive and subtractive processes for hybrid layered manufacturing. *Robotics and Computer-Integrated Manufacturing*, vol. 26, issue 5, 2010, pp. 490–499.
93. **Zhu Z, Dhokia V & Newman ST.** The development of a novel process planning algorithm for an unconstrained hybrid manufacturing process. *Journal of Manufacturing Processes*, vol. 15, Issue 4, 2013, pp. 404–413.
94. **Kerbrat O, Mognol P & Hascoët J-Y.** A new DFM Approach to Combine Machining and Additive Manufacturing. *Computers in Industry*, vol. 62, issue 7, 2011, pp. 687–692.
95. **Ponche R, Kerbrat O, Mognol P & Hascoët J.** A novel methodology of design for Additive Manufacturing applied to Additive Laser Manufacturing process. *Robotics and Computer-Integrated Manufacturing*, vol. 30, issue 4, 2014, pp. 389–398.
96. **Kerbrat O, Mognol P, Hascoët J-Y.** Manufacturing Criteria in Hybrid Modular Tools: How to combine Additive and Subtractive Processes. 3rd International Conference on Advanced Research in Virtual and Rapid Prototyping, 2007, pp. 419–424.
97. **Kerbrat O, Mognol P & Hascoët J-Y.** Manufacturing Complexity Evaluation at the Design Stage for both Machining and Layered Manufacturing. *CIRP Journal of Manufacturing Science and Technology*, vol. 2, issue 3, 2010, pp. 208–215.
98. **Boivie K, Karlsen R, Ystgaard P.** The Concept of Hybrid Manufacturing for High Performance Parts. *South African Journal of Industrial Engineering*, vol. 23, no. 2 2012, pp. 106–115.

99. **Booyesen G, de Beer DJ, Truscott M, Combrinck J, & Mosimanyane, D.** Combining Additive Fabrication and Conventional Machining Technologies to Develop a Hybrid Tooling Approach. iCAT 2010; Additive Layered Manufacturing: Education, Application and Business, Maribor, 2010.
100. **Martinho P, Bartolo PJ, Queiros MP, Pontes AJ, & Pouzada AS.** Hybrid Moulds: The use of combined techniques for the Rapid Manufacturing of Injection Moulds. Proceedings of the 2nd International Conference on Advanced Research and Rapid Prototyping, Leiria, Portugal, 28 September – 1 October, 2005, pp. 421–427.
101. **Mognol P, Jégou L, Rivette M & Furet B.** High Speed Milling, Electro Discharge Machining and Direct Metal Laser Sintering: A method to optimize these processes in Hybrid Rapid Tooling. *The International Journal of Advanced Manufacturing Technology*, vol. 29, issue 1-2, 2006, pp. 35–40.
102. **Miller B.** Bridging the Gap between Prototyping and Final Steel Production Tooling. Available from: www.moldmakingtechnology.com [Accessed 8 May 2014].
103. **Harris RA, Fouchal F, Hague RJM & Dickens PM.** Quantifying part irregularities and subsequent morphology manipulation in Stereolithography plastic injection moulding. *Plastics, Rubbers and Composites*, vol. 33, no. 2/3, 2004, pp. 92–98.
104. **Combrinck J, Booyesen GJ, van der Walt JG, & de Beer DJ.** Limited run production using Alumide[®] tooling for the plastic injection moulding process. *South African Journal of Industrial Engineering*, vol. 23, no. 2, 2012, pp.131–146.
105. **Booyesen GJ.** Bridge tooling through layered sintering of powder. Thesis (M Tech). Bloemfontein: Central University of Technology, Free State, 2006.
106. **Mosimanyane KD.** Validation of heat transfer simulation models for injection moulding of ABS in Alumide[®] tooling. Thesis (M Tech). Bloemfontein: Central University of Technology, Free State, 2015.
107. **de Beer DJ & Booyesen GJ.** Rapid Tooling using Alumide[®], Proceedings of the 2nd International Conference on Advanced Research and Rapid Prototyping, Leiria, Portugal, 28 September – 1 October, 2005, pp. 387–394.
108. Alumide[®] for EOSINT P, EOS material data sheet. Available from: www.eos.com

109. PA2200, EOS material data sheet. Available from: www.eos.com
110. **Brown ME.** Introduction to Thermal Analysis: Techniques and Applications. 2nd edition, Dordrecht, Kluwer Academic Publishers, 2001.
111. **Dastjerdi, AA, Movahhedy MR & Akbari J.** Optimization of process parameters for reducing warpage in selected laser sintering of polymer parts, *Additive Manufacturing*, vol. 18, 2017, pp. 285–294.